c2

NASA CR-54219

VON KARMAN CENTER

SNAP-8 DIVISION

SNAP-8 ELECTRICAL GENERATING SYSTEM DEVELOPMENT PROGRAM

CONTRACT NO. NAS 5-417

A REPORT TO

NATIONAL AERONAUTICS AND SPACE ADMINISTRATION

REPORT NO. 0390-04-17 (QUARTERLY) / OCTOBER 1964 / COPY NO. 26

AEROJET GENERAL TIRE GENERAL

NASA CR-54219

SNAP-8 ELECTRICAL GENERATING SYSTEM DEVELOPMENT PROGRAM

Contract No. NAS 5-417

a report to

NASA - LEWIS RESEARCH CENTER
SNAP-8 PROJECT OFFICE
H. O. SLONE, SNAP-8 PROJECT MANAGER

Report No. 0390-04-17 (Quarterly) October 1964

AEROJET-GENERAL CORPORATION
A SUBSIDIARY OF THE GENERAL TIRE & RUBBER COMPANY

ABSTRACT

33828

The objective of the SNAP-8 Program is to design and develop a 35-kw electrical generating system for use in various space missions. This report covers the progress during the seventeenth quarter of contract performance by the Aerojet-General Corporation. The status of the various necessary systems analyses is presented. Design and fabrication of components - turbine alternator assembly, NaK and mercury pump-motor assemblies, bearings, seals-to-space, mercury boiler and condenser, mercury injection system, electrical insulation, and electrical components - are reported. Testing the several component test loops is discussed. Materials evaluation of components exposed to mercury corrosion and erosion is presented.

Author

CONTRACT FULFILLMENT STATEMENT

This is the seventeenth in a series of quarterly progress reports submitted in partial fulfillment of NASA Contract No. NAS 5-417. It covers the period June - August 1964.

CONTENTS

CONTENTS (cont.)

CONTENTS (cont.)

CONTENTS (cont.)

CONTENTS (cont.)

CONTENTS (cont.)

CONTENTS (cont.)

GLOSSARY

Abbreviations commonly used in SNAP-8 Program reports are defined below.

AA	Alternator assembly
AEC	Atomic Energy Commission
AGC	Aerojet-General Corporation
AGN	Aerojet-General Nucleonics
AI	Atomics International
AOC	Award of contract
ATL	Acceptance test loop
AZFO	NASA - Azusa Field Office
BOD	Beneficial occupancy date
CGEST	Cold-gas electrical system test
CL	Corrosion loop (AGN)
CPC	Ceramic potting compounds
CTL	Component test loop (AGN)
DDAS	Digital data acquisition system
DWG	Drawing
EDM	Electrical-discharge machining
EFF	Efficiency
EGS	Electrical generating system
EM	Electromagnetic
EME	Electromagnetic equivalent
FPS	Flight prototype system
FPTF	Flight prototype test facility
FRA	Flight radiator assembly
GE	General Electric Company
GN_2S	Gaseous nitrogen stand
GPS	Ground prototype system
GPTF	Ground prototype test facility
HML	Heavy coating of ML (q.v.)
HR	Heat rejection
HRF	Heat rejection fluid
HRL	Heat rejection loop
HRS	Heat rejection system
HTL	Heat transfer loop
L/C	Lubricant-coolant
L/CL	Lubricant-coolant loop
LeRC	Lewis Research Center
LML	Liquid mercury loop
LMS	Liquid mercury stand
LNL	Liquid NaK loop
LOL	Liquid organic loop
LOS	Liquid organic stand
LPL	Low power loop
MECA	Mercury Evaporation and Condensing Analysis (Project at NASA LeRC)
MIS	Mercury injection system
ML	Pyre-ML, Du Pont polyimide organic resin; as employed in statorette serial numbers, indicates the use of this substance
MLA	Mercury loop assembly
MN_2S	Mercury-nitrogen system
MPMA	Mercury pump motor assembly
MSAR	Mine Safety Appliance Research Corporation
NaK	Sodium-potassium
NASA	National Aeronautics and Space Administration
NF	Nuclear facility
NHRA	NaK heat-rejection assembly
NPA	NaK pump assembly
NPMA	NaK pump motor assembly
NPS	Nuclear power system

GLOSSARY (cont.)

NPSH	Net positive suction head
NS	Nuclear system
ORNL	Oak Ridge National Laboratory
PBRF	Plum Brook Reactor Facility
PCS-1	Power Conversion System No. 1
PCS-2	Power Conversion System No. 2
PCS-3	Power Conversion System No. 3
PCS-4	Power Conversion System No. 4
PF	Power factor
PL	Primary loop
PLR	Parasitic load resistor
PMA	Pump motor assembly
PNLA	Primary NaK loop assembly
PO	Purchase order
PTAT	Preliminary type-approval test
PVT	Pressure-volume-temperature
R_B	Rockwell B (hardness)
RPL	Related power loop
SC	Speed control
S8DS	SNAP-8 development system
S8ER	SNAP-8 experimental reactor
SL-1	System Loop Test Facility No. 1
SI-2	System Loop Test Facility No. 2
SL-3	System Loop Test Facility No. 3
SL-4	System Loop Test Facility No. 4
SMU	Structural mockup
SNAP	Systems for Nuclear Auxiliary Power
SR	Saturable reactor
SS	Stainless steel
TA	Turbine assembly
TAA	Turbine alternator assembly
TAT	Type-approval test
TCL	Thermal convection loop (AGN)
TR	Transformer-reactor (assembly)
TS	Test section
TRW	Thompson Ramo Wooldridge
TSE	Test support equipment
VLB	Vehicle load breaker
VR	Voltage regulator-exciter
W/O	Without
WOO	Western Operations Office
-X, -1, -2, -3	Standing alone (i.e., not preceded by letters of the alphabet), these designations indicate design stages of SNAP-8 hardware

I. INTRODUCTION

The Aerojet-General Corporation is proceeding with the design and development of the SNAP-8 Power Conversion System, as authorized by National Aeronautics and Space Administration (NASA) Contract No. NAS 5-417. The effective starting date of the contract was 9 May 1960. This report covers the technical progress, the work accomplished, and the program status for the seventeenth quarterly period, from June through August 1964.

The ultimate objective of the SNAP-8 program is to design and develop a 35-kw electrical generating system for use in various space missions. The power source for this system will be a nuclear reactor furnished by the Atomic Energy Commission (AEC). The SNAP-8 system will use a eutectic mixture of sodium and potassium (NaK) as the reactor coolant and will operate on a Rankine cycle, with mercury as the working fluid for the turbogenerator. The SNAP-8 system will be launched from a ground base and will be capable of unattended full-power operation for a minimum of 10,000 hours. After the system is placed into orbit, activation and shutdown may be accomplished by ground command.

The nomenclature defined below is used in this series of reports.

Electrical generating system (EGS) - the complete SNAP-8 power plant, including all nuclear-system and power-conversion components, and the flight radiator assembly (FRA)

Power conversion system (PCS) - all components of the SNAP-8 system being developed by Aerojet-General

Nuclear system (NS) - all parts of the SNAP-8 system being developed by Atomics International.

Other pertinent abbreviations for the SNAP-8 program are listed in the Glossary. These abbreviations were established to aid in communications between the NASA Lewis Research Center and Aerojet-General.

As part of the SNAP-8 Contract materials work, a Mercury Corrosion Loop Program is in progress at Aerojet-General Nucleonics, San Ramon, California, under Aerojet-General Corporation subcontract. The purpose of the program is to provide information on the extent and nature of mercury corrosion in the SNAP-8 system by using dynamic loops that simulate, as closely as possible, actual SNAP-8 operating conditions. A discussion of the work performed during this report period was prepared by Aerojet-General Nucleonics personnel, and appears in Section VIII, B of this report.

II. SUMMARY

A. PROJECTS

Early in this report period the PCS-1 Project Office was formed to coordinate the PCS-1 and SL-1 tasks to ensure their technical compatibility, and to monitor budgets and schedules. The PCS-2 Project Office, established earlier, performs similar functions for PCS-2 and SL-2. The Ground Prototype System (GPS) Project Office coordinates GPs design and development work at Aerojet, and serves a liaison function with Atomics International.

B. SYSTEM ENGINEERING

Analysis by AGC and AI personnel supporting the SNAP-8 AGC/AI Design Point Working Group produced a definition of an area of compatibility for the NS and PCS. A major objective of this task was to determine the minimum changes required for the NS and PCS to achieve 10,000 hours of compatible operation.

Assembly of PCS-1, Phase I, Part 1 continued. The liquid-mercury lines were fitted and the instrumentation fittings were installed. The boiler outlet-turbine simulator inlet line was completed. The PCS-2 to SL-2 interface requirements were established and resolved. Conceptual layout drawings were completed for PCS-3 and GPS.

Startup and shutdown analyses continued using the analog computer. The analyses tended to confirm earlier computer results. A digital computer program has been prepared for conducting analyses involving SNAP-8 radiators. While the program is based on the tube-and-fin model it can, with slight modifications, be adapted to conical or flat configurations. An investigation made to determine the operating characteristics of the condenser NaK bypass flow control showed that the unit can satisfactorily regulate NaK exit temperature under all conditions likely to be imposed on the system, and the control system and loop will have satisfactory dynamic characteristics for all reasonable values of valve gains. Work began on modification of the reference system analog simulation to reflect the latest revisions in the system.

C. ROTATING MACHINERY

The third preprototype alternator was completed incorporating a slotted rotor-pole face, a thicker flux yoke, increased slinger radial clearance, and Teflon coating on the dynamic seals. Design and drawings for the prototype alternator are 95% complete, and some drawings have been released for fabrication of parts. The first test series of the turbine alternator assembly on the GN_2S-1 test stand were completed. Test objectives were to investigate the mechanical integrity of the TAA, the adequacy of the lubricant-coolant system, and the performance of the turbine and alternator using gaseous nitrogen as the working fluid. Test results are discussed at length in this report.

Phase I testing of the NaK pump motor in water was started. The first machined heat rejection loop motor housing was received and had an inorganic wound stator installed. Assembly of the first mercury pump-motor assembly was completed, and the unit was mounted on the LML-3 test stand. Test plans for this unit, and for a second unit completed later in the quarter, were prepared. The lubricant-coolant pump motor assembly was assembled and successfully operated at rated design conditions for 500 hours of the 1000-hour endurance test; the unit was then disassembled and inspected.

D. NONROTATING COMPONENTS

The analysis of mercury inventory fluction in the SNAP-8 boiler as a response to variation in NaK inlet temperature continued. Additional testing of the full-size boiler is necessary before the results of this analysis can be applied to the SNAP-8 system. Fabrication of -1 boilers A-3 and A-4 was completed. Planning for the extensive SNAP-8 condenser test series in RPL-2 was completed, and shakedown of the test loop was started. Satisfactory rolled and welded tube-to-header joints were developed for use in fabricating the -1 condensers for PCS-2 and NASA LeRC.

The preliminary design review for the expansion reservoirs was held. A final design review package containing design requirements, procurement specifications, and test program requirements is nearly complete. The mercury injection system final design review package was completed and issued.

The first preprototype voltage regulator assembly and exciter assembly passed acceptance tests at the vendor's plant, and were shipped to Aerojet. Long-term drift tests to ensure a stable speed-control sensing circuit continued, with no measurable drift recorded through the report period. The -1 design for the speed control module, the saturable reactor module, and the power transformer module were completed. Fabrication of the -X breadboard start programer was completed; during checkout tests the unit operated satisfactorily. The radiation effects test program continued, and reactor irradiations of the electrical controls components and subassemblies was completed.

E. MATERIALS

Materials evaluation and analysis supporting various areas of the SNAP-8 development program continued. The mercury corrosion loop test program continued at Aerojet-General Nucleonics, and the results are reported and discussed in this report.

III. PROJECTS

A. PCS-1 PROJECT OFFICE

Early in this report period the PCS-1 Project Office was formed to (1) coordinate the PCS-1 and SL-1 tasks so as to ensure their technical compatibility, and (2) monitor the respective budgets and schedules.

SL-1 Project coordination meetings were started with the various cognizant Operations personnel. Several PCS-1/SL-1 reviews were held for visiting NASA personnel. Both the status of the hardware and the techniques used in accomplishing the tasks were discussed.

The three PCS-1 Test Requirement Specifications for the three testing phases were issued. The PCS-1 design was completed, and the PCS is in the process of final welding and assembly.

Approximately 110 SL-1 drawings were released for fabrication. This represents about 90% of the number required for Phase I testing. All of the major components have been delivered and are positioned in the test facility. Both the primary and heat rejection loop piping are nearing completion in the test cell. The heat rejection system piping spools have been fabricated and are ready for installation. The required instrumentation wiring is near completion and considerable signal conditioning checkout has been accomplished. The facility controls wiring was completed.

B. PCS-2 PROJECT OFFICE

During this report period the configuration, pressure losses, and thermal stresses were established for the primary and heat rejection NaK piping. The configuration and pressure losses were also established for the lubrication and cooling system. The component and piping mounting structure was completed and ready for assembly of the PCS-2. The boiler handling and positioning fixtures used in PCS-1 were modified for use in the PCS-2. Boiler No. A3 was delivered to Aerojet on 3 June 1964. Flanges have been added and the unit is ready for PCS-2 assembly.

The testing requirements for the Phase I version, and the component requirements for the Phase II version of PCS-2 were combined to form a common requirement, thus reducing the number of phases from a total of 3 to 2. The PERT network and schedules were reworked to indicate the above change of phases.

Development-type (-1) mercury injection system, inverter, and start programer will be used rather than workhorse equipment as had been previously planned. The electrical harness will be of a workhorse type (not preassembled), but -1 installation techniques will be used.

Project coordination meetings were held to discuss and resolve problem areas and dissiminate information to all departments. NASA-LeRC personnel visited Aerojet several times during this report period to discuss status and schedules, and to coordinate information between NASA-LeRC and Aerojet.

C. GROUND PROTOTYPE SYSTEM PROJECT OFFICE

1. System Engineering

The conceptual design for the ground prototype system (GPS) was established during this report period; associated documentation which was prepared included the following:

a. GPS Schematic (Figure 1)

b. Conceptual Design Layout PCS for GPS (Figure 2)

c. GPS General Test Plan

d. Preliminary GPS Failure and Safety Analysis

e. GPS Instrumentation Requirements List

2. Design Reviews

Two design reviews were conducted, during the report period, on portions of the ground prototype system.

On 21 July, Atomics International presented the final S8DS reactor design for Aerojet review. The fuel, reactor vessel, and piping designs appeared to be firm and substantially unchanged from the Preliminary Design Review

held in January. The controller, temperature sensor system, drum-drive motor, and drum-drive gear train are undergoing some redesign as a result of the control dead-band and design-point revisions. Mechanical details of the gear train and bearing system for the control drum have been revised to meet the more stringent environmental requirements of NASA 417-2. These changes also reflected some of the Aerojet comments from the Preliminary Design Review.

On 29 July, Aerojet presented the conceptual GPS Power Conversion System and test support equipment design for review by Atomics International. Review of the AGC designs by AI is aimed at assuring (a) operating safety, (b) facility compatibility, and (c) system interface compatibility. The review focused attention on a number of coordinated work tasks. Foremost among these tasks are the following:

a. Definition of primary loop components including the need (if any) for workhorse pumps, the location of expansion reservoir connections, and the requirement for primary loop overpressure protection.

b. System analytical studies for use in the revised design point mentioned above (in the areas of startup sequence, normal shutdown procedures, and emergency shutdown requirements associated with a complete study of possible modes of failure).

IV. SYSTEM ENGINEERING

A. EGS DEVELOPMENT CONTROL

1. General Systems Engineering

a. Mass Properties Control and Reporting

Investigation was conducted and evaluation made of the existing standards, specifications, and original procedures and methods for compilation, control, and reporting of mass properties (weight control), including computer programs suitable for application to the SNAP-8 Program.

On the basis of the results of this investigation, a specification - including recording and reporting forms - was prepared. Meanwhile, current and projected weight data for the SNAP-8 are being compiled.

b. NS-PCS Design Point Selection

Analysis effort undertaken by Aerojet-General and Atomics International in support of the SNAP-8 AGC/AI Design Point Working Group resulted in the definition of an area of compatibility for the NS and PCS. A major objective of this task was to determine the minimum charges required to the NS and PCS to achieve compatibility for 10,000 hours of operation.

(1) Analysis of Reactor Outlet Temperature Transients

The Aerojet analog computer was used to simulate the primary NaK loop with various loop and reactor parameters. The simulation determined the effect of the parameters on the maximum reactor temperature transient resulting from a 35-kw vehicle load change.

Computer studies of many of the same parameters were also conducted by AI. The results of AI and AGC studies agreed very closely where comparisons were possible.

(2) Reactor Outlet Temperature Bandwidth

Based on the results of the temperature transient analysis, AI made a study of the reactor temperature bandwidths which would

result from various modifications in the temperature sensors and the reactor control system. This study led to the recommendation by the Design Point Working Group that the maximum reactor outlet temperature bend should be from 1282 to 1330°F. This can be achieved by the use of one sensor instead of two, plus improved accuracy in the sensor and a 50% reduction in the reflector drum step size.

(3) Boiler Pinch-Point and Inventory Variations

An analysis was made of the effects on boiler operation of the following parameters: boiler NaK inlet temperature bandwidth, boiler mercury pressure drop, NaK flow rate (or boiler NaK ΔT), and boiler outlet pressure.

The effects of varying the foregoing were investigated for the -1 boiler as presently designed, and for a modified -1 design which would have a reduced mercury pressure drop. The modified boiler was shown to be capable of operation with a minimum pinch point* ΔT of 30°F. This is considered adequate to minimize boiler inventory variation and outlet pressure fluctuation.

(4) System Studies

A series of calculations was made to determine the influence of NaK temperature drop across the boiler and reactor temperature band on the EGS operating parameters. System steady-state operating points were evaluated as functions of boiler NaK-ΔT from 200 to 140°F, and of reactor temperature bands from ±10°F to ±40°F.

The minimum power condition is the system operating point with boiler NaK inlet temperature at the lower limit of the band and with component tolerances at the limits which produce minimum power output. The system parameters are found for a vehicle load of 35.0 kw, plus 5.0 kw allowance for degradation.

---

*Pinch point ΔT is the difference between the NaK temperature and the mercury saturation temperature at the liquid-vapor interface.

The maximum power condition assumes a system designed to match the minimum power operating point, but operating at 1330°F boiler NaK inlet temperature and at the limits of tolerances which produce maximum power - including 5.0 kw allowance for degradation.

(5) Conclusions

A region of operating compatibility between the NS and PCS was found. This region is bounded by the required minimum boiler pinch point ΔT, minimum reactor temperature bandwidth, and performance curves of the modified boiler for various NaK ΔT at the boiler. This region is outside the capability of the -1 primary NaK PMA.

The NPS efficiency was found to increase with increasing boiler ΔT.

(6) Working Group Recommendations

The NS-PCS design point recommended was at boiler NaK ΔT equals 170°F, with a NaK inlet temperature range of 1282°F min to 1330°F max.

In order to meet this design point, the following changes are necessary:

(a) Modification of the -1 NaK primary PMA to meet the new flow rate

(b) Modification of the -1 boiler to reduce mercury pressure drop

(c) Reflector drum step size to be reduced 50%, single temperature sensor used, and accuracy increased.

c. EGS and PCS Model Specification

Recommended changes were incorporated in EGS Model Specification No. AGC-10151 and PCS Model Specification No. AGC-10152. The documents are being prepared for release.

d. Instrumentation

System instrumentation requirements for PCS-1, PCS-2, and GPS were formulated and tabulated for publication as a part of the appropriate

test specification. The requirements list included instrumentation necessary based upon the following criteria:

(1) Safety both to personnel and facilities

(2) System test requirements; instrumentation necessary to ascertain and record the degree of success attained in testing

(3) Component test requirements.

e. Start Programer

Preliminary studies were completed on the start-programer requirements. In the study the operational, performance, and physical requirements for the flight model of the start programer in the SNAP-8 EGS were detailed, including variations from the flight model necessary for ground prototype system.

2. Development Systems

a. PCS-1

The final test requirements specification for PCS-1, Phases I, II, and III were issued. NASA approval has been received on the Phase I portion of the document. The Test Requirements Specification (1) sets forth the requirements for support components and systems that are necessary to test the PCS, (2) describes the operating procedures to be used, (3) sets forth the desired tests to be made, and (4) specifies the PCS components that are furnished.

The intent of Phase I, Part 1 testing is to explore and verify boiler performance using a turbine-simulator heat exchanger, and to verify mercury pump operation. Phase I, Part 2 is to explore and verify turbine and condenser performance.

Phase II testing is to demonstrate PCS performance and short endurance capability.

Phase III testing is to demonstrate long-term endurance capabilities while subjected to sun-shade environments and variations of vehicle electrical load demands.

b. PCS-2

The test requirement specification, covering all phases of testing, was prepared and is ready for issue. The specification contains the component list, description of tests, test support equipment required, and a description of the data to be derived from the tests.

The primary purpose for PCS-2 testing, as described in the specification, is to develop the PCS starting procedure and to conduct a satisfactory endurance test.

The PCS-2 schematic was drawn and released during this report period.

c. GPS

A preliminary GPS schematic was drawn in preparation for an AI-AGC coordination meeting on GPS/GPTF. A study is in process to simplify the primary loop to increase the system endurance test reliability. Work on the test specification for GPS was initiated and is continuing.

d. Flight Reference System

The reference system schematic diagram was revised to incorporate the results of the analysis described in Reference 1.

The reference system was analyzed, based on a boiler NaK ΔT of 170°F, at 1282 to 1330°F inlet temperature. The analysis assumed a modified -1 primary loop pump, modified -1 boiler, and present -1 components in the remainder of the system. Allowances were made for system degradation and component performance tolerances. At minimum and maximum alternator output conditions the following items were determined for steady-state operation: flow rates, pressures, temperatures, TAA power, PMA power, PLR power, heat rejection from radiators, and reactor power. This analysis was issued as a technical memorandum (Reference 1).

B. SYSTEM DESIGN

Assembly is continuing on PCS-1, Phase I, Part 1. The liquid-mercury lines were fitted and the instrumentation fittings installed. The lines are

in the weld shop for final welding and stress relief. The boiler outlet-turbine simulator inlet line has been completed. The mercury flow control valve, the mercury pump, the temperature sensors, the pressure transducers, and the condenser instrumentation mounting installation are either incomplete or have not been delivered.

1. PCS-1, Phase I, Parts 1 and 2

A technical memorandum titled Flange Stress Analysis PCS-1, PCS-2 was released (Reference 2).

a. Design

The trace heaters for the boiler outlet-turbine inlet line were ordered. The turbine inlet line for PCS-1, Phase I, Part 2 was redesigned to incorporate the mercury vapor filter, and the turbine inlet and boiler mercury outlet line interface loads due to thermal expansion were calculated.

The PCS-1, Phase I, Parts 1 and 2 instrumentation installation drawings were completed. The PCS-1, Phase I, Part 1 drawing was revised to include the upgrading to PCS-1, Phase I, Part 2, and has been released. The insulation installation drawings for PCS-1, Phase I, Parts 1 and 2 are in the final stages of completion. Condenser instrumentation installation drawings are in process.

b. Assembly

The handling procedures for PCS-1, Phase I, Part 1 are completed and have been submitted to manufacturing for advance quotation request. Preliminary PCS-1 Phase I Part 1 installation procedures in SL-1 were completed and are being revised.

Instrumentation fittings were installed on all mercury lines and the boiler. The boiler inlet and outlet NaK circuit expansion joints and the condenser inlet and outlet NaK circuit expansion joints were fitted to the frame assembly. The mercury liquid lines, including the mercury flow venturi, were fitted and are in the weld shop for final welding and stress relief. The boiler outlet-turbine inlet line is about two-thirds complete and is awaiting completion of instrumentation welding. The turbine exhaust bellows has been received and is now installed in the PCS-1 assembly.

2. PCS-2

Revised lubricant-coolant loop and mercury loop inventories and volumes have been calculated. Pressure drop calculations for the lubricant-coolant loop, the primary NaK loop, and the HRL NaK loop were completed. The component fluid pressure at the lubricant-coolant circuit interfaces have been calculated. The one-quarter scale mockup has been completed.

Component interface loads and pipe stress levels that will result from piping thermal expansion have been calculated. The transformer reactor assembly, HRL NaK pump motor assembly, primary NaK pump motor assembly, and the parasitic load resistor mounting installation configurations have been resolved. The piping configurations incorporating the test support equipment flow control valves have been resolved, but exact valve mounting bracketry and pipe interface locations cannot be determined because the valve envelope limitations are unknown.

The PCS-2 to SL-2 interface requirements have been established and resolved.

3. PCS-3 and GPS

The conceptual layout drawings were completed. The materials-weight summary for the reactor environment activation studies was completed.

A PCS-3, GPS conceptual design was completed.

C. SYSTEMS ANALYSIS

1. Startup and Shutdown Analyses

a. Analog Computer Investigations

The results of the major portion of the analog computer startup analysis for reference system "B" have been reported in previous quarterly reports (References 3 and 4). Some additional computer runs were made to investigate two areas of the startup sequence to assure that reactor temperature criteria would be satisfied during all portions of the startup sequence. The complete reference system "B" analog computer simulation was used for these series of runs. The two areas investigated were (1) the effect

of the time to change the primary loop flow rate from 20 to 50% rated on the maximum rate of change of reactor coolant temperature and on the maximum coolant temperature at the reactor outlet; and (2) the effect of a speed mismatch between the inverter and the alternator, at the time of pump motor load transfer, on the maximum rate of change of reactor coolant temperature at the reactor outlet.

A series of runs was made for which the time to change the primary loop flow rate from 20 to 50% rated was varied between 30 and 120 sec. This series of runs was conducted to simulate the portion of the startup sequence when the inverter speed is changed so that NaK flow rates and the reactor power level are brought to required levels prior to mercury injection. The results of this series of runs are presented in Figure 3 which shows that the maximum rate of change of reactor coolant temperature did not exceed the 150°F/min limitation for inverter speed change ramp times that are greater than 50 sec. The maximum reactor outlet temperature did not approach the 1375°F limitation during any of the runs; the maximum value obtained was 1330°F.

An additional aspect of startup was also investigated with the aid of the analog computer simulation. During the initial mercury injection ramp period the turbine alternator assembly (TAA) will accelerate up to rated speed, and when the TAA speed reaches a nominal value of 50% rated speed, the PMA electrical loads will be automatically switched from the inverter to the alternator. The possibility of speed mismatches between the inverter and the TAA exists because of tolerances in the inverter speed and in the circuit which detects TAA speed. Any speed mismatches will result in small but rapid changes in NaK flow rate and will introduce temperature transients in the primary loop. Therefore, a series of runs was made with several combinations of inverter speed and TAA speed. The results of this series of runs indicated that, with the most adverse combination of inverter and TAA speed tolerances, the maximum rate of change of reactor coolant temperature would be increased by approximately 10% over similar startup runs in which no inverter or TAA speed tolerances were considered. No significant differences were noted in the maximum reactor outlet temperature for this series of computer runs.

b. Related Studies and Investigations

A study was undertaken to estimate certain condenser off-design conditions during the portions of PCS startup when mercury pump NPSH could be an important consideration. A digital computer program, originally written to provide condenser design data, was modified to perform off-design calculations for the -1 condenser. Since the digital program is suitable only for steady-state calculations, input data as a function of time were obtained from appropriate analog computer startup runs. The following input data as a function of time was required: mercury flow rate, NaK flow rate, NaK inlet temperature, mercury liquid interface location, and mercury inlet quality. The results of the digital computer analysis are presented in Figure 4 where the condenser inlet and condenser liquid interface pressures are presented as functions of time during startup. Figure 5 shows the condenser pressure drop during startup and indicates that actually a pressure rise is predicted during the portions of startup which were investigated. The fact that a pressure rise can exist in the condenser during startup indicates that mercury pump NPSH will not be a problem and that greater NPSH margin would exist during startup than was previously estimated.

An investigation was conducted to determine the possible effects of a condenser bypass control on system conditions during startup. Calculations indicate that, prior to mercury injection, system conditions will be essentially the same whether or not a condenser bypass control is contained in the heat rejection loop. However, during the latter stages of mercury injection and before rated mercury flow is obtained, a condenser bypass control would tend to maintain the condenser NaK outlet temperature at higher levels than for a system without a condenser control. As a result, the condenser bypass control would tend to override the operation of the temperature control valve. The resulting higher condensing temperatures and corresponding mercury saturation pressures would result in reduced turbine output power and it is possible that self-sustained system operation could not be maintained under these conditions. Therefore, if a condenser bypass control is incorporated in the heat rejection loop, provisions should be made to ensure that the control will not function during startup.

A review was made of proposed normal and emergency shutdown procedures for PCS-1 and PCS-2. An analysis was made which indicated that the proposed emergency shutdown procedure would be adequate for foreseeable emergency situations. The analysis indicated that, with a mercury dump valve located near the boiler inlet, the turbine inlet pressure would decay to 35 psia within 3 sec after the dump valve had been completely opened and after the mercury pump discharge trim valve has been completely closed. With the vehicle load on the alternator and with a 35 psia inlet pressure, the turbine speed would be negligible. As a result of the procedures review it was recommended that an isolation valve be incorporated in the mercury loop at the pump outlet for all phases of testing to eliminate the possibility of reverse flow through the mercury pump upon shutdown.

2. System Studies

a. Space Radiator Computer Programs

A digital computer program has been prepared for conducting analyses involving SNAP-8 radiators. The program is based on a tube-and-fin model with the tubes arranged in a cylindrical configuration (20 ft in dia) with no heat rejection occurring from the inside of the cylinder. With slight modifications, the program can be adapted to a conical configuration or a flat configuration. The model includes an inlet and outlet manifold with an approximately constant pressure drop per unit length in order to obtain a uniform flow distribution through all of the tubes. The armor thickness is calculated using the "NASA Standard Armor Criteria" (Reference 5). The armor thickness is based on the PCS vulnerable area which includes the lubricant-coolant (L/C) radiator and other PCS components as well as the HRL radiator.

The external heat load on the radiator due to solar, planetary thermal and planetary albedo radiation, is computed using the criteria in Reference 6. This accounts for the view factors that depend on the orientation with respect to the external heat source.

The program has provisions for varying the following parameters:

(1) Number of parallel flow circuits

(2) Number of tubes per circuit

(3) Fin dimensions

(4) Radiator cylindrical diameter

(5) Fluid inlet temperature and heat rejection required

(6) External heat flux

(7) Emissivity and absorptivity

Specifying the preceding parameters, the program calculates optimum tube and manifold diameters (with respect to weight) and the corresponding pressure drop. The program can also develop data for making a trade-off between pressure drop and radiator equivalent weight. The equivalent weight includes the added system weight necessary to provide the radiator pumping power. This program was initially developed to facilitate investigations for HRL system parameters. A modification of this program has more recently been prepared to facilitate investigations of the L/C loop parameters.

A third radiator program has been developed for evaluating off-design performance of space radiators. For a specified radiator configuration, specified external heat flux, and specified flow rate and inlet temperature, the program will compute heat rejection and the fluid outlet temperature. This program has been used to develop sun-to-shade off-design performance of a space radiator in an earth orbit as shown in Figures 6 and 7. The data compares closely with similar steady-state data previously developed on the thermal analyzer for both sun and shade operation.

b. HRL Investigation for a Venus Application

Investigations were made to evaluate the trade-off between system weight, radiator design, and heat rejection loop operating parameters. The analyses were made considering the use of the SNAP-8 ECS in a Venus mission, which is the most severe application with respect to external heat load described in environmental specification 417-2. The

radiation heat fluxes which would be experienced by space radiators in Venus and Earth orbits are indicated in the tabulation below which was taken from Reference 6.

	500-Mile Earth Orbit	1000-Mile Venus Orbit
Solar	442.4 Btu/hr-ft^2	846.3 Btu/hr-ft^2
Planetary albedo	154.8 Btu/hr-ft^2	402.6 Btu/hr-ft^2
Planetary thermal	59.3 Btu/hr-ft^2	33.2 Btu/hr-ft^2

The Venus radiator analysis was based on a cylindrical configuration (20 ft in dia) consisting of a number of tubes and fins with several parallel flow paths. The tube and fins were assumed to be insulated on the interior of the cylinder so that no heat rejection would take place within the interior of the cylinder. The interior surfaces of the radiator tubes will receive some micrometeorite protection from the fins and from radiation shields on the cylinder ends; therefore, these surfaces will not require as much armor as the externally exposed surfaces. It is not possible to define how much protection this will provide; hence, the interior armor thickness was arbitrarily assumed to be 0.1 in. thick or approximately 40% of the armor thickness on the exterior surfaces. The absorptivity and emissivity of the radiator surface were assumed to be 0.9 and 0.4, respectively.

The radiator digital computer programs described in a preceding discussion were used in making the Venus investigations. Two general cases were analyzed. In one instance, the radiator would be designed to provide the required heat rejection under the worst conditions of external heat flux in a 1000-mile Venus orbit with the cylindrical axis perpendicular to the solar radiation and in a high-noon position. The other case was one in which the cylindrical axis was maintained parallel to the solar radiation. Preliminary computer runs were made for the first case indicated above to determine the trade-off between radiator equivalent weight (including pumping power weight equivalent) and radiator design parameters (including the number of parallel flow paths, the number of tubes per flow path, and the pressure drop across the radiator and the connecting lines).

The HRL conditions for the preliminary runs were the same as those in the new nominal reference system operating in the sun which are as follows:

Condensing temperature	680°F
Radiator inlet temperature	665°F
HRL flow rate	39,300 lb/hr
Heat rejection rate	425 kw

The results of these runs are summarized in Figures 8 and 9. The results show that the optimum parameters are as follows: number of parallel flow paths = 130, number of tubes per flow path = 1, and pressure drop = approximately 19 psi.

Additional computer runs were made with varying condensing temperatures and HRL flow rates. In these runs the turbine inlet pressure, temperature, power output, and efficiency along with the number of radiator flow circuits and number of tubes per circuit, were assumed to be constant; hence, to obtain the required turbine output power with varying condensing temperatures (turbine back pressures), the mercury flow rate had to be varied accordingly. The variation of mercury flow rate and HRL heat rejection as a function of condensing temperature are indicated in Figure 10.

Figure 11 shows the trade-off between radiator equivalent weight and radiator pressure drop for a condensing temperature of 680°F, a radiator inlet temperature of 665°, and for various HRL flow rates.

Similar runs were made for condensing temperatures of 700 and 720°F. A summary of these runs is indicated in Figures 12 and 13 which show equivalent radiator weight as a function of HRL flow rate and nominal in-sun condensing temperature. Each of the radiator designs in this summary has an optimum pressure drop and pressure drop distribution between manifolds and tubes.

An additional analysis was made to determine the minimum NPSH provided to the mercury pump, with the worst accumulation of

tolerances and degradations in 10,000 hours, for the near-optimum designs in the preceding summary. The radiator off-design performance digital program was used in determining the shade operating temperatures in this analysis. The results of this analysis are indicated in Figure 14 which shows the minimum NPSH as a function of HRL flow rate and nominal in-sun condensing temperature.

Similar analyses were made for the second general case in which the radiator was oriented with the cylindrical axis parallel to the solar radiation. These results are summarized in Figures 15, 16, and 17.

The preliminary conclusions of these analyses are as follows:

(1) The near-optimum condensing temperature and flow rate are approximately 690°F and 60,000 lb/hr for the worst-orientation case. Present minimum NPSH criteria, however, may dictate a higher condensing temperature.

(2) The near-optimum condensing temperature and flow rate for the best orientation case are 680°F and 52,000 lb/hr, respectively. Present minimum NPSH criteria may dictate a higher condensing temperature.

(3) The sun-shade temperature variations are approximately -25°F for the worst orientation case and -5°F for the best orientation case.

(4) The weight saving achieved by favorable orientation is approximately 160* lb. It should be noted, however, that in order to obtain favorable orientation, some type of attitude control would be required. The additional weight required for such a control could exceed the radiator weight savings.

c. Primary Loop - Reactor Controller Deadband Investigation

An investigation was conducted to (1) define the areas of compatibility between the nuclear system and the EGS, (2) define the changes required in the reference flight system to assure compatibility between

*For "D" reference system conditions.

both systems, and (3) assure delivery of the required output power during 10,000 hours of system operation. As a part of this investigation, analyses were made to determine the influence of NaK temperature drop across the boiler as well as reactor control deadband on the selection of SNAP-8 system operating parameters. Several system power balances were performed for systems that would produce the required net output power under the most unfavorable accumulations of system tolerances, perturbations, and degradations leading to minimum power conditions. Similar power balances were also made for these systems assuming the most favorable accumulation of tolerances and degradations tending to produce maximum power. The criteria assumed for the minimum power condition were as follows:

(1) -1 component characteristics were considered (with the exception that in some cases a new primary PMA was required).

(2) System tolerances were as indicated in Reference 7, with some exceptions.

(3) Boiler pressure drop and performance were in accordance with estimates of boiler designers.

(4) Reactor outlet temperature was at the lower end of the deadband. (Upper end of deadband for all cases was 1330°F).

(5) A surplus allowance of 5 kw was assumed for 10,000 hours to accommodate degradation.

(6) System operation was in the sunlight.

(7) Boiler NaK ΔTs considered were 200, 180, 170, 160, and 140°F.

(8) Reactor controller deadbands (total temperature swing including transient) were 20, 40, 60, and 80°F.

The criteria assumed for the maximum power conditions were the same as in the preceding list except for the following: (1) reactor outlet temperature at the upper end of the reactor control band was 1330°F, (2) system operation was in the Earth's shadow, (3) turbine nozzle area was 10% greater than in the minimum power cases, and (4) loop flow rates were 6% higher than in the minimum power cases.

The effects of the reactor NaK outlet temperature deadband and the primary loop flow rate on other system parameters are indicated in Figures 18 to 23.

Figure 22 indicates a limitation in primary loop operating parameter due to maximum allowable power of 80 kva.

From boiler considerations a minimum of 30°F pinch point temperature represented another limitation to primary loop operating parameters. All points above the 30°F pinch point were not considered applicable.

3. Analog Computer Studies

a. Condenser Bypass Flow Control Study

An investigation was made to determine the steady-state and transient characteristics of the thermostatically operated condenser NaK bypass flow control, as shown in Figure 24, so that a component requirement document could be issued. Work is progressing toward the development of this valve for use in the system, if required during system testing. The flow control valve senses condenser NaK exit temperature and adjusts a bypass of the NaK flow around the condenser to minimize variations in condenser NaK exit temperature below the set point temperature of the valve. The purpose of this control is to prevent cavitation of the mercury pump by maintaining the mercury condensing pressure above the minimum consistent with the pump minimum inlet pressure requirement. The results of this study were published in a technical memorandum, Reference 8. A brief summary of the results is as follows:

The condenser bypass control can satisfactorily regulate NaK exit temperature (and therefore indirectly the mercury condensing pressure) under all conditions likely to be imposed on the system.

The control system and loop will have satisfactory dynamic characteristics for all reasonable values of valve gains up to 1 lb per sec (bypass flow) per degree Fahrenheit (below the valve set point), and for time constants up to 90 sec.

A description of the computer results is as follows.

(1) Figure 25 shows a sun-to-shade transient with a bypass control gain of 0.25 lb per sec per ^{o}F, and a 25-sec time constant. The trace shows that the condenser exit temperature is maintained within 4^{o}F of the valve reference temperature of 665^{o}F.

(2) Figure 26 shows that the same sun-to-shade transient without a control results in a 20^{o}F drop in condenser NaK exit temperature.

(3) Figure 27 shows the effect of a -10% step in mercury flow with a control gain of 0.25 and 25 sec time constant. The condenser NaK exit temperature is maintained within 8^{o}F of the reference temperature; without a control, the drop in temperature would have been 33^{o}F (see Figure 21).

(4) The steady-state regulation of the condenser NaK exit temperature for the minimum, nominal, and maximum system condensing temperature conditions are shown in Figure 28 by the intersection of the bypass control regulation and system curves. The minimum and maximum condensing conditions occur when system tolerances combine in the most unfavorable accumulation of parameter tolerances and component variations. These conditions are discussed in Reference 9. Figure 28 shows that the NaK condenser exit temperature is regulated as a function of the system conditions, the valve set point temperature, and the valve gain. The valve set point temperature defines the upper limit above which the temperature will not be regulated. The valve gain determines the variation in NaK temperature below the set point temperature and establishes the required bypass flow for a given system condition.

(5) Figure 29 shows the regulation of condenser NaK exit temperature following a sun-to-shade transient for different control gains. For a gain of 0.25, the temperature is regulated to within 4^{o}F of the sun temperature with a bypass flow of approximately 1 lb per sec. An increase in valve gain reduces the temperature change for a relatively small change in bypass flow. The same information can be obtained from Figure 28 by observing the nominal sun and shade system curve intersection with the appropriate control gain line.

(6) Figure 30 illustrates the effect of mercury flow rate variations on condenser NaK exit temperature for different control gains.

b. Reactor NaK Exit Temperature Transient Study

An investigation was made to determine the effects of individual design factors on the severity of the reactor NaK exit temperature transients following a full-load step change in parasitic load. The results of this investigation are reported in a technical memorandum, Reference 10, to be released shortly. This study, made with the use of the analog computer simulation of the primary loop, determined the significant factors which affect the reactor temperature transients.

Figure 31 shows a schematic of the primary loop simulation which was studied on the analog computer to determine the reactor outlet temperature transients following full-load step changes in parasitic power. This simulation was basically the same as previously used for the deadband study reported in Reference 11. For this series of test runs the boiler heat load is maintained constant at rated conditions of 450 kw while the reactor power varies from an initial power of 421 kw to a final power of 456 kw (6 kw of radiation heat loss in loop is assumed) after the parasitic load power is stepped off. For these series of runs the upper temperature deadband was removed so that the maximum possible temperature during the transient could be observed. Since a limit cycling of the controller is not possible if the upper limit is not reached during the transient, a deadband temperature limit above the maximum transient temperature allows for some stability margin.

Because of security classification, the results of this study are not contained in this report but will be available in a technical memorandum (Reference 10).

c. SNAP-8 Reference System

Work started on the modification of the reference system analog simulation to reflect the latest revisions to the system. The revisions are basically the result of a decision to produce a final flight system based on the -1 hardware designs rather than base the flight system on modifications to

the hardware. New system diagrams have been prepared and the system equations are being modified to reflect the new design conditions. System transient and steady-state studies will be made on the analog computer upon completion of the revised simulation. These studies will include PCS startup, shutdown, sun-to-shade variations, and vehicle load changes.

4. Miscellaneous

In view of the proposed changes to the reference system operating conditions resulting from the studies conducted by the AGC/AI design point working group, it was decided to re-evaluate the effects on the system of locating the parasitic load resistor in the heat rejection loop. The effects on the reference system were investigated for situations with the parasitic load resistor located between the condenser outlet and the radiator inlet (the HRL hot leg) and with the parasitic load resistor located between the radiator outlet and the condenser inlet (the HRL cold leg). The results for this investigation indicate that the turbine output power would be reduced by approximately 1 kw when the vehicle load is transferred to the parasitic load if the parasitic load were located in the hot leg of the HRL. Similarly, the turbine output power would be reduced by approximately 3 kw if the parasitic load were located in the cold leg. The turbine power reduction is a result of increased temperatures in the heat rejection loop which will cause an increase in the mercury condensing temperature and the turbine back pressure.

One method of overcoming the reduction in turbine power indicated in the paragraph above would be to increase the heat rejection loop flow rate so that condenser temperatures would not increase to the point where turbine power would be reduced when the parasitic load is required to dissipate the vehicle load power. If this method were used without increasing the radiator size, a substantial increase in heat rejection loop flow would be required and an increase in PMA power of approximately 2 kw would result. The increased PMA power requirement would entail an increase in system weight of approximately 360 lb. In addition, under conditions when tolerances and degradations are such that the mercury pump NPSH would be most severely affected, the available NPSH would be insufficient for satisfactory pump operation unless a condenser control were employed.

An additional method of overcoming the reduction in turbine power indicated previously would be to increase the radiator size without increasing the heat rejection loop flow rate. Thereby the condenser temperatures would not be permitted to increase to the point where turbine power would be reduced when the parasitic load is required to dissipate the vehicle load power. If this method were used, the resulting increase in radiator weight would be approximately 170 lb. In addition, under conditions when tolerances and degradations are such that the mercury pump NPSH would be most seriously affected, the available NPSH would be insufficient for satisfactory pump operation unless a condenser control were employed.

A PCS failure and safety analysis was initiated for the GPS design review which was held at Aerojet on 29 July. A suggested study program was outlined and preliminary results of the initial efforts towards a complete PCS failure and safety analysis were presented at the design review meeting.

D. NUCLEAR POWER SYSTEM COORDINATION

This section covers Aerojet activities in the integration of the nuclear system (NS), which is being developed by Atomics International under contract to the Atomic Energy Commission, and the Aerojet power conversion system (PCS) into a nuclear power system (NPS). The NPS forms a major portion of the SNAP-8 electrical generating system (EGS).

As the EGS Contractor, Aerojet-General is responsible to NASA for monitoring the NS contractor to evaluate compliance with specifications and delivery schedules, and must coordinate, monitor and review, for the purpose of control, the NS design and development to ensure the compatibility and operational stability of the NS and PCS in the EGS configuration. The contractor prepares a complete and acceptable integration plan covering the integration of the NS with the PCS and development of a reliable EGS.

Coordination with Atomics International is handled by EGS Project Office. Table 1 summarizes the AGC/AI coordination activities during the report period; some of these activities are discussed below, and others are covered in Section III,C under the GPS.

1. General Coordination Meetings

Project coordination meetings were held 22 May and 29 June. The Design Point Working Group report described below was given AI/AGC management approval at the latter meeting.

A CPS/GPTF Project Engineers meeting was held on 2 June. An action item list was generated to cover short-term group efforts.

2. Design-Point Coordination

On 29 June the joint AI/AGC Design Point Working Group presented coordinated design-point selection recommendation to the SNAP-8 Project Coordination Meeting. This report culminated three months of intensive analytical work, joint meetings, and data exchange. The details of the analysis and recommendations are found in Sections IV,A and IV,C.

3. Electrical Interface Coordination

Agreement was confirmed on the regulation of electrical power to be supplied by the PCS to the NS during startup and normal operation. It was agreed that

> All power supplied shall be 28 v,dc ±2.8 volts
>
> Where more closely regulated d-c power or closely regulated a-c power is required for operation of the NS control system, the power modification or regulation components will be supplied as a part of the NS control package.
>
> The suppression of short-term input voltage transients which could adversely affect the bistable digital counter circuits used in the AI controller will require joint solution when wiring and components become firm.

Aerojet and Atomics International have reached the following agreement regarding the mechanical configuration of the electrical wiring interface between the NS and PCS:

a. AI will terminate its harness in a flexible stainless-steel conduit like that employed by AGC. It will contain a flange which can be welded to a junction box supplied by AGC. This junction box will be located near the NS and PCS interface.

b. AGC will supply a flexible stainless-steel conduit between the junction box and the controls compartment located in the spacecraft. This conduit will be sized to house only the AI controls wiring.

c. The AI controls wiring will be Micatemp supplied by AGC. The size of the wires will be specified by AI.

4. NS/PCS Integration Plan

AI/AGC agreement has been reached on Section III,A of the plan draft, which covers the conduct and working rules for joint coordination meetings.

V. ROTATING MACHINERY

A. TURBINE ASSEMBLIES

The order of assembling the turbines was changed to meet program requirements. The turbine assembly with interstage pressure taps, which will be needed for detailed performance testing in RPL-2, was given priority. This completed assembly will be mated with an alternator assembly to form a turbine alternator assembly.

A turbine assembly is being reworked to incorporate concentric seals which do not rest on the shaft during operation as do the floating seals. This arrangement will be used only during cold gas testing where housing distortions are minor (see Section V,C TAA Test Results). This assembly will be part of a TAA that will be used for the electrical controls testing using cold gas. Only this assembly is scheduled to use the concentric seals. All other assemblies will use floating seals with the stronger antirotation pin.

The next scheduled assembly will be shipped to LeRC. Following this, the assembly of TAA, Serial No. 2, will be resumed. This assembly, intended for PCS-1, was suspended when labyrinth failures occurred on TAA, Serial No. 1, in GN_2S-1 tests.

Assembly of the remaining units will depend upon delivery of inlet and composite housing assemblies which are to be completed in September.

B. ALTERNATOR

1. Preprototype Alternator

The third preprototype alternator was completed. It incorporates the following changes: (a) slotted rotor pole face, (b) thicker flux yoke, (c) increased slinger radial clearance, and (d) Teflon coating of dynamic seals.

Slotting of the rotor pole faces (Figure 32) appeared to have decreased the rotor pole face losses by 13%. However, the test data were such that conclusive results have not yet been obtained.

The thicker flux yoke (Figure 33), a field coil having a very low thermal resistance, and secondary effects of the slotted rotor reduced the

field coil excitation current by 16.5% less than the first machine. Since a 6% decrease of excitation current was anticipated because of this change, the additional improvement was attributed largely to the effects of the low thermal resistance of the field coil itself. Therefore, in-process control was instigated for potting thickness, thickness of the copper can, solder fill, and coil concentricity. This control will reduce the variation in the field coil thermal performance and will ensure a uniform thermal performance on future units.

The increase of the slinger radial clearance from 0.010 to 0.017 in. appeared to reduce slinger losses by 25%, based on initial data. Test equipment and test procedures are being upgraded to obtain better data in future testing.

Teflon coating of the screw seals and stationary walls of the slinger seals resulted in improved seal performance; however, difficulty in bonding the Teflon to the parts (i.e., screw seal threads) has been a problem. A program to determine in-process quality control and end-item inspection of the Teflon coating has been started and should be completed by 1 September. The FEP coating applied to the third machine looks very favorable.

An aromatic polyimide base polymer material, SP (developed by the E.I. DuPont Company), which can be fabricated in heavy sheet form, is being considered to replace the present ceramic top sticks in the stator winding. The SP material has very impressive mechanical and chemical properties and will be most effective from the standpoint of reduction of installation labor and increased reliability without sacrifice of performance. This material will be incorporated on the fifth preprototype alternator for evaluation, and on prototype hardware pending the results of tests.

2. Prototype Alternator

Design and drawings are 95% complete and drawings are released for fabrication.

Development of weld joints and weld specifications is 85% complete. These welds involve welding heavy sections of Inconel-X to 304 SS end-shields and HY-80 to 1018 carbon-steel frame.

Ten design reviews were held at the manufacturer's plant. In attendance were engineering, manufacturing, materials, quality assurance, reliability, and drafting representatives. Two meetings were also held with Aerojet engineering personnel to ensure close coordination in the prototype alternator design.

A fully equipped clean room, with laminar flow wall and particle count control, is in operation at the manufacturer's plant.

C. TAA TEST RESULTS (COLD GAS TESTS, SERIAL NO. 1)

The first test series of the turbine-alternator assembly on the GN_2S-1 test stand was completed. Primarily, the test objectives were to investigate the mechanical integrity of the TAA, the adequacy of the lubricant-coolant system, and the performance of the turbine and alternator using gaseous nitrogen as the working fluid.

To accomplish these objectives, three significant tests were run. The first test (Test No. D-5-R-3) was run for startup and steady-state characteristics at the nominal operating speed of 12,000 rpm. The duration of the test was 1 hour, 16 min. The second test (D-5-R-5) repeated the previous one and, in addition, included various inlet temperatures of the Mix 4P3E to determine the effects on the lubricant-coolant system. The duration of this test was 2 hours. The third test (D-5-R-8) included a vibration survey for the range of speeds from 12,000 to 15,000 rpm and a peak alternator load of 53.4 kw at 12,000 rpm. The duration of the test was 1 hour, 50 min. The total accumulated test time on this TAA was 5 hours, 29 min.

Test No. D-5-R-3 was run with nitroger supplied to the turbine inlet at a pressure of 77 psia and a temperature of 333°F, and exhausting to the atmosphere at a temperature of 202°F. Under these conditions, the alternator load needed to produce 12,000 rpm was 13.5 kw. Calculated performances from the data, which takes into account the accuracy of the instrumentation, resulted in a turbine efficiency of 44 ±3%, compared to a predicted 47.5% and an alternator efficiency (unity power factor) of 86.6 ±7%.

By extrapolation of the alternator acceptance test data to 13.5 kw, the indicated efficiency would be 74%. This discrepancy between efficiency values of the alternator was due to the large influence which variations in bearing and slinger losses exert when the output power is low.

Bearing and heat exchanger data are given below.

Bearing	Inlet Flow lb/hr		Outer Race Temperature, °F		Bearing and Slinger Losses, kw	
	Nominal Design	Test	Nominal Design	Test	Nominal Design	Test
Turbine Antidrive	200	21	250	263	0.86	0.70
Turbine Drive	200	200	250	258	0.86	0.39
Alternator Drive	200	153	250	270	0.86	0.49
Alternator Antidrive	200	192	250	270	0.86	0.65

Unit Measured	Space Seal Heat Exchanger		Alternator Coolant System	
	Nominal Design	Test	Nominal Design	Test
$\dot{w}$, lb/hr	1600	1335	1600	1300
ΔP, psi	20	24	8.7	6
T Inlet, °F	210	230	219	230
ΔT, °F	9	-	5	4.0

During the test it was found that the test equipment lubricant-coolant cooler was unable to provide an inlet temperature below 230°F. Since the nominal temperature is 210°F, the excess temperature affected bearing outer race temperatures and bearing and seal losses, increasing the former and reducing the latter. The cooler flow paths were interchanged and satisfactory operation was obtained on subsequent tests.

The only deviation from nominal operating conditions was found in the space seal heat exchanger. When the recorded pressure drop was corrected to nominal flow and temperature, the pressure drop would be 34 psi instead of the 20 psi expected. This condition was felt to be unique to this assembly since a flow check of the TAA, space-seal heat exchanger with MIL-H-4606 oil, and corrected to Mix 4P3E conditions, resulted in a 17 psi drop.

Test No. D-5-R-5 was run under essentially the same conditions as before; but, during the test the lubricant-coolant inlet temperature was varied from 187 to 220°F. Calculated efficiencies for the turbine and alternator were 51 to 52% and 75 to 83%, respectively. From acceptance test data, the extrapolated value of the alternator electrical efficiency should be in the range of 88 to 91%. In calculating the test value, the temperature rise of the coolant across the alternator is used. In this test, the varying inlet temperature of the coolant coupled with the large heat sink of the alternator mass probably was responsible for inaccuracies in determining the temperature rise of the coolant. A small error in measuring the temperature rise has a significant effect on the efficiency calculation.

Bearing outer-race temperatures and bearing and slinger seal losses for Test No. D-5-R-5 were plotted as Figures 34 and 35, respectively.

Data reduction and analysis of Test No. D-5-R-8 is in process and a report will be issued in the next quarter. Preliminary analysis of raw data indicates no abnormalities for the high-speed or high-power run.

During the test series it was not possible to obtain indications of axial movement of the turbine by varying the pressure across the balance piston. The determination of balance-piston size will have to be done during mercury tests where a greater differential pressure exists than is true with the use of nitrogen.

The only mechanical discrepancy which occurred during the nitrogen tests was associated with the floating labyrinth seals. After Test No. D-5-R-5, a partial disassembly of the TA on the test stand showed that the antirotation pins (0.060 in. roll pins) which restrain the balance piston seal had been sheared. Also, the Spirolox retaining ring had been displaced from its groove, unwrapped,

and found to have rubbed the leading edge of the first-stage turbine blades. Wear had occurred on the balance piston seal inner diameter and the piston outer diameter (Figure 36). The TA was reassembled with solid pins instead of the roll pins, and testing was continued. Upon disassembly following Test No. D-5-R-8, all of the antirotation pins (roll pins) were found to be sheared. The solid pin replacements for the balance piston seal were intact.

Inspection of the hardware revealed that the contacting diameters of the seals and shafts were worn. The wear consisted of abrasion and tearing of the metal surfaces (Figures 37 and 38). The wear on the inner diameter of the seals was evenly distributed circumferentially. Discoloration of the metal indicated some high temperatures were obtained, which led to thermal cracking at the bottom of the antirotation slot (Figure 38). The degree of wear of the interstage seals was observed to be more severe as the overhang distance of the seal increased. In order of increasing overhang distance, measured wear of the fourth, third, and second interstage seals were 0, 0.006 and 0.012 in., respectively.

The high temperatures generated also affected the curvic couplings. Thermal expansion of the hubs from the frictional heat produced excessive axial loads which resulted in yielding of the tooth material along the line of contact. Functioning of the coupling was not impaired.

From the taped record of the vibration pickups mounted on the TAA, it was found that during startup and especially shutdown, a signal was generated (around 1000 to 1200 cps). During these transients there was little if any differential pressure across the turbine stages which would cause the seals to be pressed against the housings where frictional forces would tend to damp out motion of the seal. In the absence of this frictional damping force, the rings in contact with the rotating shaft are excited in such a way that the ring is picked up and whirled by the shaft. This motion appeared to be possible with or without the antirotation pins since the replaced balance piston seal exhibited wear evenly distributed circumferentially, and the solid pins were not sheared nor damaged.

The labyrinth seal test rig was run with a balance piston buildup to determine the effect of differential pressure. With no ΔP, an audible vibration was present which disappeared when the ΔP was increased to between 2 and 4 psi.

It was decided that this problem would not be severe in mercury testing where higher differential pressures obtain as contrasted to the nitrogen tests where lower pressures prevail and test termination is accomplished by suddenly terminating nitrogen flow. For all mercury test units, a design change was initiated to replace the roll pins with larger and stronger solid pins. In the case of the cold gas electrical test unit, where thermal and pressure distortions are small, the seal rings will be closely fitted into their housings and held concentric to the shaft to avoid any contact during operation.

Metallic particles held by magnetic attraction were found on the alternator assembly spline end of the quill shaft. Other small particles were found in the alternator interface cavity. These particles were identified as weld splatter, machining chips, and scale. Analysis of the particles gave their composition as iron with a small amount of nickel. It was concluded that these particles were from locations in the alternator which are difficult to clean, and were released during TAA testing.

D. BALL BEARING AND LUBRICATION SYSTEM

1. Material and Bearing Procurement

a. Material

A total of 394 lb of AISI M50 steel bar, 3-1/4 in. dia, was received from Latrobe Steel Co. The material was initially air melted, then vacuum-remelted three times using the consumable electrode process. Latrobe's test certificate qualifies the material for Type I, Class 3, M50 bearing steel in accordance with AGC Specification AGC-1037. This material is intended for PCS-1 and PCS-2 (-1 hardware) ball bearings.

b. Bearings

Requests for quotation were issued to six bearing suppliers for the manufacture of 20 bearings P/N 095355 Bearing Assembly, Ball-Angular Contact (-1 Model) to AGC Development Component Specification AGC-10206, Amendment 1, dated 1 July 1963. These bearings were intended for the Radiation Endurance Ball Bearing Test Program.

Also, requests for quotation were issued for the manufacture of 34 TAA bearings, P/N 095355, and 16 Hg PMA bearings, P/N 095306. These bearings are intended for use in -1 hardware, PCS-1 and PCS-2.

The Barden Corp., Industrial Tectonics Inc., and Marlin-Rockwell Corp. have submitted bids which are currently being evaluated. One of the six vendors requested additional time which could not be granted because of the schedule, and two vendors declined to bid.

2. Lubrication System Development

A series of lubrication system performance tests was conducted with the Model B Seal and Lubrication System Simulator. The objective of the tests was to determine lubricant and bearing performance characteristics under simulated SNAP-8 TA operating conditions, except for the nuclear radiation. The tests were run at 12,000 rpm with polyphenyl ether fluid (Dow Chemical ET-378).

The bearing installation, the spring preload arrangement, the lubricant injection components, and the oil slingers in the Model B Test Rig simulate the SNAP-8 TA configuration (Figure 39). Each bearing is axially preloaded to 60 lb, as in the turbine assembly. No additional thrust load was applied. Radial loads on the bearings were nominal, since the total weight of the rotor assembly is only about 17 lb, and dynamic imbalance was negligible. All tests were run with the shaft axis horizontal.

A schematic diagram of the test rig lubrication system and the primary instrumentation used in the tests is shown in Figure 40. All instrument sensors and recording devices were either calibrated or checked for calibration validity prior to testing. Each of the variable-area type flowmeters was calibrated with the ET-378 fluid at 175, 210, and 225°F.

The controlled variable parameters for the tests were as follows:

Lubricant inlet flow, per bearing: 120 to 400 lb/hr
Lubricant inlet temperature: 175, 210, and 225°F
Slinger discharge pressure: 2.5 to 20 psia

A total of 31 individual tests were performed. The majority of the tests were made at the TAA design values of 200 lb/hr inlet flow rate to each bearing, 210°F inlet temperature, and 5 psia slinger discharge pressure. A typical run consisted of establishing a specific inlet temperature and a discharge pressure, and then recording the following data over the specified inlet flow range:

Lubricant inlet pressures
Bearing outer race temperatures
Slinger discharge flow rates

Slinger discharge temperatures
Bearing cavity pressure
Deceleration rate of rotating assembly

Total inlet flow to each bearing was assumed to be the sum of the two corresponding slinger discharge flow rates. Three deceleration tests at zero inlet flow were also run to determine the fixed power losses in the rotating assembly.

The test data related to the "turbine-end" bearing was reduced and analyzed. The lubricant injector ring for this bearing is identical to the rings used in the TA (i.e., three 0.040-in.-dia jet nozzles, equally spaced, with a jet spray angle of 20° to the bearing axis).

Figure 41 shows total inlet flow rate vs absolute pressure measured just upstream of the lube injector ring. The bearing cavity pressure during these tests was less than 1mm mercury. At the design flow rate of 200 lb/hr, the data show an inlet pressure requirement of approximately 19 psia.

The lubricant through-flow of the bearing is plotted against the total inlet flow into the bearing shown in Figure 42. At design bearing inlet flow, nearly all the lubricant apparently passes through this bearing. In Figure 43, the same data is plotted as per cent bearing-through-flow vs total inlet flow. Here the data indicate some sensitivity to slinger discharge pressure, with a more clearly defined "optimum" inlet flow at discharge pressures just below the design value of 5 psia. However, because the flowmeters used cannot register extremely low values of flow, the data shown in Figures 42 and 43 should be interpreted as indicating a trend rather than as defining absolute values. Thus, it appears that the design inlet flow rate of 200 lb/hr is close to the optimum value in terms of proportion of flow through the bearing. When the limitations of the flowmeters are considered, a bearing-through-flow of 80 to 85% at design inlet flow appears to be a conservative estimate.

Figure 44 shows the outer-race temperature of the turbine-end bearing as a function of bearing-through-flow for three lubricant inlet temperatures. At the design values of 210°F and 200 lb/hr/bearing lubricant inlet, the race temperature was about 250°F. Figure 45 is a cross-plot of the same data, showing race temperature vs lubricant inlet temperature for three different inlet flow rates.

Several tests were performed to determine the relationship between slinger discharge and lubricant inlet pressure in terms of the point at which the bearing cavity becomes completely flooded. At a set value of inlet pressure, the slinger discharge pressure was progressively increased until full flooding in the bearing cavity was detected by sensing a sudden temperature rise in the normally void space between the two bearings. Figure 46 shows a relationship of the lubricant inlet pressure vs the slinger discharge pressure at which complete flooding of the bearing cavity occurs. At the lubricant inlet pressure of 19 psia (pressure required for flow of 200 lb/hr), the slinger discharge pressure, for complete flooding of the bearing cavity, is approximately 17 psia. Because of the prototype configuration of the bearing and seal assembly, no direct measurement of bearing cavity pressure was possible to determine precisely the points at which complete scavenging exists. However, previously reported data (Reference 3) shows that well-scavenged bearing operation occurs at slinger discharge pressures below 10 psia. Those tests were performed on the Model A Seal and Lubrication System Simulator, which contained a bearing and seal arrangement similar to that of the TA, except that the bearings were 35 mm. The data present relatively clear evidence that, at the design slinger discharge pressure of 5 psia, the bearing operates nonflooded over a wide range of lubricant inlet pressures.

The deceleration tests were performed over the test range of slinger discharge pressures to estimate bearing-and-slinger power loss by means of the inertia method. Total losses at zero inlet flow were subtracted from total losses measured with approximately the same flow rate to each bearing. The net power loss for two bearings and four slingers is plotted against slinger discharge pressure in Figure 47. The nominal lubricant temperature at the inlet was 210°F. At the design discharge pressure of 5 psia, the estimated net loss is about 2.3 kw. With no intermediate data points, the path of the curve between 10 and 20 psia is not defined. This is the transition region from svavenged to flooded bearing operation.

3. Bearing Test Programs

a. Ball-Bearing Endurance Test Program Using M-50 Bearing Material

Two 10-bearing groups of 309 bearings having inner rings of second and fifth consumable electrode vacuum remelted (CVM) M-50 steel,

respectively, were previously endurance-tested at the SKF Industries, Inc. Research Laboratory using circulating mineral oil lubrication. These tests were reported in Reference 4. Because of the relatively short lives of these two groups of bearings, SKF Industries completed additional endurance tests on bearings made of the first CVM remelt of the same heat of M-50 steel to verify the fatigue strength of the basic M-50 heat used in the manufacture of these bearings.

The tests were conducted at 9700 rpm under a radial load of 4240 lb (C/P = 2.15), and the test bearings were splash-lubricated with circulating Socony Mobil DTE extra-heavy oil supplied at a rate sufficient to maintain the operating temperature at 210°F. In these tests the bearing operating temperatures were recorded at 6-min intervals by an IBM 1710 data-logging system. During about one-third of this bearing testing, lubricant-out temperatures were also monitored by the IBM system while the lubricant-in temperatures and flow rates were manually recorded at 8-hour intervals.

Testing has been completed, and five inner ring fatigue failures were experienced at lives ranging from 24.2 to 122.2 million revolutions. Testing on one specimen was suspended at 39.5 million revolutions because of suspected interaction of a failure on a nontest element with a failure on the test specimen. The maximum likelihood technique yields an estimate of L_{10} = 29.3 million revolutions compared to the estimated L_{10} = 415 million revolutions for the first remelt M-50 bearings of another heat of steel tested previously under identical conditions. Also, another heat previously tested under slightly different test conditions had comparable endurance to this latter test. It is now apparent that the endurance life of the presently tested heat of M-50 steel is much lower than expected.

In an attempt to explain the relatively poor endurance lives of this heat of M-50 steel as exhibited by the above group and the two groups reported previously, alloying element analyses were conducted and compared with previously tested heats of M-50 steel. The results of these analyses are detailed in Table 2, together with the accuracy limits of determination given by the analytical laboratory. The only elements in which the poor heat showed a clear difference over the two previous heats are nickel and aluminum (both considerably higher).

It was previously determined that a trace element index involving aluminum, copper, vanadium, nickel, and molybdenum could be used as a quantitative measure for those elements found harmful to the fatigue life of 52100 steel. Since molybdenum and vanadium are intentionally added alloying elements in M-50 steel, a trace element index containing only aluminum, copper, and nickel could be used to measure harmful trace elements in these heats of M-50 steel. Table 3 shows the calculation of this index. It has a value approximating 7.0 for the "poor" heat and 4.0 for both "good" heats of M-50. If the material were 52100 steel, it would be reduced by a factor of approximately 3 compared to the "good" heats. Actually, the reduction factor found experimentally is closer to 5.

It must be borne in mind that the trace element results are not proven to be applicable to M-50 steel. Further, the life estimates for the groups of 10-bearings are not as reliable as for larger groups. Still, it appears reasonable to assume that the relatively high aluminum content and perhaps the nickel content of the "poor" M-50 heat is a causative factor in the reduced endurance life of this heat of steel.

In addition to evaluating the solid element contents, gas analyses were also performed on samples from the two first remelt M-50 "good" heats and the fifth remelt "poor" heat. The results of these determinations as given in Table 4 show there was no significant difference between the heats which could lead to a difference in inherent fatigue life.

Based on the additional tests and the analysis, this program is being redirected to perform further testing with bearings made of steel that has the alloying elements (especially the nickel and the aluminum) and the gas content of magnitude comparable to that of the "good" heat of steel as shown in Tables 2 and 4.

b. Endurance and Wear Ball-Bearing Test Program as a Function of Vacuum and Radiation

Two hundred and fifty pounds of test oil, Mix 4P3E was received from the Shell Oil Company.

Conceptual layouts were completed for a two-bearing tester and a four-bearing tester. Evaluation of the two layouts was made and the four bearing tester design was chosen for technical and economical considerations.

This program was stopped during the week of 29 June 1964.

E. PUMP PROJECTS

1. NaK Pump-Motor Assemblies

a. PMA Performance Evaluation in the NaK Simulation Loop (NSL)

(1) Motor

Phase I testing in water, as described in the preceding quarterly report (Reference 4), was started. No-load test results, shown in Figure 48 indicate the canning effect (can power loss) was lower than the calculated value. This loss reduction was attributed to the higher can resistance resulting from the stator can thickness being reduced when expanding the can into the stator slots. The electrical loss segregation, Figure 48, is based on the determination of the motor hydraulic and friction loss. The preliminary evaluation of the data indicates the determination of this loss may vary by $\pm 10\%$. A rotor deceleration test will help to establish a more exact motor hydraulic loss in water which will then be used to finalize the no-load saturation test results. The determination of the can losses in water is necessary to determine the motor performance in NaK, since can losses do not change with the fluid in the rotor gap.

The results of the torque-speed calculation in NaK based on in-air test results (Figure 49) indicate a maximum starting torque available of 23.6 in.-lb. Torque values from tests on a wet but nonwater filled unit were approximately 7 to 10 in.-lb, indicating sufficient margin for full voltage line starting.

The in-air reduced voltage and frequency test results, Table 5, indicate that motor torque may be as low as 3.7 in.-lb at a rotor temperature of 50°C or 5.25 in.-lb at a rotor temperature of 200°C. The corresponding torque in NaK may be as high as 7.25 in.-lb. The high starting torque of the PMA was expected to be reduced with the bearing modification discussed later; therefore, reduced voltage and frequency testing in water and NaK will be performed to determine the minimum starting power requirement of the PMA.

(2) Recirculation Pump

Phase I testing of the HRL NaK PMA recirculation system is nearly complete. Test objectives for Phase I testing were to determine the head-capacity performance of the pump, the minimum NPSH requirement, motor rotor thrust vs through flow, motor hydraulic losses, the effects of canning the motor, and the segregation of electrical losses.

Preliminary evaluation of Phase I test results indicate that the recriculation pump can supply to the motor the required flow at the design point pressure rise. Figure 50 shows the head-capacity curve. An orifice will be installed to match the recirculation pump and system at the primary and HRL PMA design flow rates.

The NPSH tests performed on the recirculation system show 45 ft NPSH required for the motor to avoid cavitation and associated instability. The results of these tests are not considered to be final until they can be compared to the results of the NPSH tests on the main impeller.

The motor rotor gap pressure drop is shown on Figure 51. The curve shows the theoretical pressure drop for fluid flowing through two smooth concentric cylinders. The difference between calculated and tested values results from: (a) an increased flow area in the expansion slots from the canning operation, and (b) the disruption of the peripheral fluid velocity resulting from the slots.

(3) Bearings

Upon completion of the pump motor loop installation and filling, several unsuccessful attempts were made to start the HRL NaK motor. The problem lay in the bearing pads and thrust runner. The extremely fine surface finish (better than 1.5 rms) and surface conformity of these parts were "wringing" (gage block effect) to each other which caused the bearing pivots to act as wedges. This wedging condition, offering a high mechanical advantage, amplified the wringing load 10 to 20 times. This action caused a bearing starting torque that measured in excess of 150 in.-lb. Since this torque was greater than the 19 in.-lb available from the motor for cold starting, the motor would not start. It was determined that once rotation had been accomplished, the shaft rotated

and spun freely. The conclusion reached was that the assembly and handling loads caused the surfaces to "wring" together when in a clean dry state. Once the surfaces were separated and kept immersed in the lubricant, wringing did not occur.

In an attempt to reduce the wringing action, the thrust pads were liquid-honed with 100-grit Alundum to roughen the surface to 10 to 14 microin. rms. The liquid hone did not produce the desired surface condition, but did reduce the wringing action. The bearings were again cleaned and the surfaces were coated with cocoa butter for improved frictional characteristics. The test unit has since been started more than 50 times and operated for 40 hours with several long periods of inoperation between starts. Additional comments will be found in the design section.

b. Fabrication

(1) Motors

The first machined HRL motor housing was received and had an inorganic wound stator installed. The fabrication procedure was followed by potting, curing, and insulation burnoff of the stator prior to forming and connecting the power leads. The forming of the power leads after burnoff caused a problem where the power lead wire insulation, because of burnoff, was too brittle to form and flaked off when making connections. The fabrication procedure was changed to allow for connecting, forming, and welding of leads prior to burnoff while the insulation was still resilient. Terminals prepared in this way have been tested at furnace temperatures up to 1000°F for 500 hours to substantiate the ability of the terminals to withstand the burnoff procedure without detrimental effects.

The stator assembly was canned, welded (hermetically sealed), leak tested, and found acceptable. The first attempt to can the -X ML (organic) insulated stator resulted in the collapsing of the stator stock teeth because of excessive column loading due to the expansion process. The inorganic stator is considerably more rigid because the potting insulation compound with a higher compressive strength filled all voids and better supported the stator teeth. This eliminated can collapsing.

After a second attempt to can the -X stator failed, a decision was made to drop further canning attempts of the ML-insulated stator. The organic insulated stator was intended as a backup to the inorganic insulated stator.

A vendor was unsuccessful in two attempts to assemble the can to the rotor. The interference fit required the can to be heated and carefully guided during assembly to avoid contact with the rotor, because rapid heat transfer from the thin can would promote a "boot-strapping" effect and shrink the can prematurely, even during a momentary contact.

Aerojet as a parallel effort initiated a canning program. After the proper technique was worked out using radiant heating and proper tooling, two rotors were successfully canned. The first rotor (using a scrap core) was the development model for welding. The model was used to develop the welding technique for hermetic sealing of the rotor. The next rotor proceeded through this fabrication process without incident and was prepared for assembly.

Several canned rotors being prepared for leak testing were found to leak in the end ring to the sleeve weld. Dye penetrant check of all rotors showed five to contain penetrant indications. Instructions were given for weld repair.

(2) Pumps

Several primary PMA pump castings were weld repaired and radiographed. Five were determined to be salvageable by grinding and further welding. The first article inspection was completed and two castings were sent to the machining vendor for further fabrication. The casting vendors through weld repair and changes in casting technique have produced acceptable castings, thus eliminating the problem. The first primary pump housing assembly has been received and accepted. The remaining castings have been delivered for machining.

The HRL castings have been delivered for machining after weld repair of the castings.

c. Assembly

Assembly procedures, parts lists, and drawings for the HRL motor assembly were completed. The -X assembly instructions were completed and released for the assembly of the HPL -X Model for NSL testing.

The assembly of the -X HRL pump motor proceeded without difficulty after a few minor modifications to the procedure were made.

d. Design

(1) Motor

During the installation of the first primary winding, the lower end turn rubbed the stator housing wall in the area where the coils leave the stack. The primary PMA housing design was changed by machining a larger end turn annulus clearance.

(2) Bearings

A review was made of the bearing design. As a result of the starting difficulty covered in the PMA performance evaluation section, the thrust bearing was modified. Since the basic problem was the wringing of the thrust pads to the runner, it was decided to provide a unidirectional crown on the thrust bearing surface which would eliminate the wringing tendency by removal of surface conformity. As a matter of manufacturing expediency, the crowning effect will be accomplished by grinding a radial taper of 0.00015 in./in. on the face of the thrust runner. The thrust pads positioned on the coned runner will have line contact at the pad center and a crown of 15 to 20 microin. at the leading and trailing edges (Note: In effect, the shoe plane is tangent to a cone on one line.) The bearing design modification does not compromise the load-carrying capacity of the bearing. A design modification was made to the thrust bearing which consisted of adding an antirotation pin to the bearing housings to prevent rotation of the bearing back plates.

(3) Additional Design Modifications

Radial holes were located in the annulus between the outer sealing cans and the internal flow passages to facilitate draining of the PMA.

e. Test Planning

The fabrication of the NSL (water test loop) was completed. After leak testing of the loop, the -X HRL pump motor was installed, and Phase I testing - as covered in the last quarterly - was begun. Testing results are covered in the performance evaluation section. Upon completion of Phase I testing (95% complete), the -X unit will be removed from the NaK simulation loop. It will then be disassembled, inspected, and reassembled with the main pump. Phase II testing will then proceed.

2. Mercury Pump-Motor Assembly

a. Design

Assembly of the first mercury pump-motor assembly was completed on 19 June 1964; the unit was then delivered to LML-3 and mounted on the test stand.

This PMA is a fully instrumented version that includes pressure pickups in the pump housing, enabling pressure profiles and thrust loads to be determined.

No serious problems were encountered during assembly of the unit. Actual dimensions for runouts, eccentricity, etc. which were taken during assembly indicate the following clearances:

Impeller front vane:	0.012 in. during operation
Impeller front vane:	0.010/0.014 in. at rest
Impeller back vane:	0.008 in. during operation
Impeller back vane:	0.010/0.014 in. at rest
Molecular/visco pump:	0.002 in. minimum
Molecular/visco pump:	0.004 in. maximum
Motor air gap:	0.009 all around

Assembly of the second unit was completed on 14 August. This unit is presently scheduled for PCS-1. Clearances for this PMA were similar to those measured for the LML-3 unit.

Parts for the third assembly, scheduled for PCS-2, were started through the pre-assembly inspection for determining critical buildup dimensions.

All hardware necessary for completing the assembly of these units has been delivered, with the exception of two motors and one instrumented pump housing.

b. Motor

Modifications were made to provide a standard MS terminal block attached to the end cap of the motor. Power leads are welded to the stud on the hermetically sealed terminal, the other end being attached to the terminal block. Thus, the possibility of damage to the hermetic seal is minimized when making terminal connections.

c. Pump

The jet pump test report for cold mercury operation will be released by the end of August.

d. Seals

Delivery of the first mercury discharge pressure-actuated liftoff device was scheduled for mid August of 1964. This unit will be installed in the PMA for PCS-1, if convenient. The balance of five pieces will be delivered later in August.

A design has been completed for Teflon-coated elements for the 4P3E dynamic seals. The antiwetting effects with Teflon coating have been established by dynamic seal testing.

A modified seal housing design and analysis with an increased radial gap is in process. This design includes a helical groove in the stationary as well as the rotating members of both the molecular and visco pump seals. The net effect is expected to be the same leakage rate as without the stationary helical groove; however, the larger clearance would be advantageous from the standpoint of machining tolerances, eccentricities, ease of assembly, and likelihood of rubbing during operation.

e. Motor Scavenging

The detail drawings for the motor scavenging slingers and the sealing elements have been amended to include Teflon coating, as mentioned previously. This design is presently in the release cycle. This scavenging hardware will be included in later units.

b. Testing

Amendments have been made to the LML-3 Test Request to include a requirement for preheating the mercury PMA prior to rotation to assure adequate oil flow through the bearings for initial rotational testing. This and other minor amendments are included in Amendment A, of Test Request No. 395/64-0008. It is not intended to make this a standard system operating requirement.

3. Lubricant-Coolant (L/C) Pump-Motor Assembly

a. Test Planning and Evaluation

The L/C PMA development test unit was assembled in accordance with the required assembly and test procedures. The unit was operated successfully at rated design conditions for the first 500 hours of the 1000-hour endurance test and then was disassembled and inspected.

The results of the 500-hour test inspection revealed no measurable wear or unusual marks. A comparison of the "before" and "after" test dimensions indicated no measurable changes. The unit was reassembled, placed back on test, and left to complete the remaining 500 of the 1000 hours of operation at design conditions. The disassembly and inspection showed the unit to be free from any dimensional changes - a finding which substantiated the ability of the L/C PMA to operate for 10,000 hours.

The first deliverable L/C PMA was tested and found to be 1.5 psi below the design head at design flow rate. The development unit was also found to be slightly under the 55 psi pressure rise design point. It was decided the first unit would be accepted on an SDAR since the required system flow was far less than the PMA output and the cause of the deficiency, discussed later, was not detrimental to the integrity of the unit. Subsequent units would be modified to raise the head to meet the design criteria. The PMA performance results are shown on Figure 52.

The second deliverable unit, after volute housing modification, was assembled, tested and found to meet the required design performance. The unit was then delivered to AGC. The results of the second unit's performance are shown on Figure 53.

The third deliverable L/C PMA was assembled for acceptance tests and installed into the loop. The operation of the unit showed it to be running in the reverse direction due to improper internal motor lead connections. The unit will be removed and the condition corrected.

A tabulation of the performance results at rated conditions for the development mercury PMA and the first two deliverable PMAs is shown in Table 6.

b. Design

During the development unit testing, the recorded temperatures of the motor cavity thermocouples were low (60 to 70°F below expected). After several days of investigation it was determined that the suction temperature thermocouple was reading approximately 50 to 60°F low. The thermocouple was replaced but the temperatures within the motor were still not up to the expected temperatures. A review of the thermocouple circuit revealed a large temperature drop (70 to 80°F) across the nickel pins of the connector. The error introduced by the temperature gradient in the pins resulted from the use of Chromel-Alumel thermocouples with a third material (nickel) as the connector. The correct temperature was determined by adding the temperature drop of the pins to the thermocouple readout. An independent thermocouple was installed in the upper motor cavity pressure tap to confirm the motor temperature. An external or surface type thermocouple was used to correlate the motor surface temperature with the internal steady-state temperature. This arrangement was used on subsequent tests.

The basic thermocouple problem is one in which both the measuring junction and the reference junction are inside the motor. The emf measured at the connector is the potential difference between the two junctions. Thermocouple data referenced to a fixed junction are not applicable. The testing performed on subsequent units used the emf readouts and the external surface thermocouple to determine the units' true temperatures.

The head rise of the development and first deliverable PMAs were below the minimum design criteria as covered in the test section. A drawing review of the pump revealed the pump housing, impeller contour tolerance was such that the impeller eye would have a smaller clearance than the impeller vane tips which caused a large impeller recirculation loss and lower head at rated flow. The drawings were corrected and the remaining pump housings were remachined.

The design of the bypass orifice in the PMA was modified to allow for O-ring sealing during AGC testing to facilitate the installation of various sized orifices for flow variation requirements.

c. Fabrication

The volute housing castings, which have been the most troublesome fabrication items of the L/C PMA, have been delivered and accepted.

All motor assemblies (rotors and stators) were completed and are ready for assembly into pump housings. The final three housings are presently being machined to correct suction passage deviations and to repair machining errors in the bypass orifice.

Several visits were made to TRW to witness assemblies, disassemblies, and to assist in problem solving.

The ET-378/ML immersion compatibility test motor has surpassed the 10,000-hour target operation time without revealing significant changes in dielectric strength. The total operating time at 250°F has been 11,190 hours. Chemical analysis indicates that fluid properties of ET-378 are within acceptable margins and the degradation of the ML insulation is within acceptable limits. The results of the dielectric testing are shown on Figure 54.

VI. NONROTATING COMPONENTS

A. HEAT EXCHANGERS

1. Boiler

a. Analysis

The analysis was continued of mercury inventory fluctuation in the SNAP-8 boiler as a response to variation in NaK inlet temperature. Figure 55 shows the boiler inventory as a function of the pinch-point temperature difference, ΔT_{pp}. The pinch-point temperature difference is the difference between the local NaK temperature and the mercury saturation temperature at the liquid-vapor interface and is related to the boiler inventory by

$$I_B = \frac{W_B Q_S \log_e (\Delta T_{in}/\Delta T_{pp})}{\pi D U_S \Delta T_{in}} + K$$

where

I_B = Boiler inventory

W_B = Inventory/unit length in sensible heating region

Q_S = Sensible heat transferred

ΔT_{in} = NaK exit temperature - mercury inlet temperature

D = Tube diameter

U_S = Overall coefficient in sensible heating region

K = Inventory in boiling and superheat regions.

Note that as the pinch-point temperature difference decreases, the inventory in the boiler increases. An analysis of allowable condenser inventory variations (Reference 12) has shown that a 10-lb change in mercury inventory can be tolerated without reducing the power available from the PCS below 35 kw at the end of 10,000 hours. Based on this, a minimum pinch-point temperature difference of $15^{\circ}F$ is required for the boiler, thereby permitting the $50^{\circ}F$ change in pinch point associated with the NaK inlet temperature variation.

Additional testing of the full-sized boiler is required prior to applying the results of this analysis to the SNAP-8 system. The tests to be conducted in the RPL-2 include a determination of inventory variation in the boiler which will be used to supplement this analysis.

b. Fabrication

The -1 boilers A-3 (for PCS-2) and A-4 (for NASA-LeRC) were completed at the Western Way Mfg Corp, Van Nuys, and delivered to the Aerojet-General Corporation, Azusa, on 3 June 1964 and 16 July 1964, respectively.

The -1 boilers A-3 and A-4 were both fabricated with little difficulty in meeting the stringent Class XV, AGC Specification AGC 13860 weld requirements. Only three repairs were required on the automatic internal tube-to-tube sheet weld joints for each of these two boilers; eleven such repairs were required during the fabrication of the previous -1 boiler A-2. The previous difficulties with the automatic internal welding process were resolved through a vendor development program which was initiated and guided by Aerojet-General Corporation SNAP-8 engineering personnel. The factors which resulted in success with the automatic internal welding process included optimization of the welding current and speed for each header "heat sink," and resolution of the proper bevel angle of 15° on the tubing.

The quality of the hand welding was also excellent on the fabrication of these two -1 boilers. The percentage of total (hand plus automatic weld) length on both -1 boilers which met drawing requirements was 100% and 98% after and before rework, respectively.

c. Stress Analysis

An approximate analysis of the transient temperature profiles across the boiler tube wall during startup has been completed. The analysis shows that the maximum thermal gradient, and hence the maximum stress, occurs at steady-state in the peak heat flux region of the boiler tube.

The analysis shows that film boiling will prevail until very near the end of the startup transient, effectively blanketing the tube wall to prevent a thermal shock. A Schmidt plot of the boiler tube wall covering

the transient from film to contact boiling was used to generate the curves shown in Figure 56. Although the analysis is only approximate, the thermal gradients are low enough so that a more detailed study is unwarranted.

2. Condenser

a. Testing

(1) RPL-2 Test Program

Planning for the extensive series of tests to be conducted in the RPL-2 has been completed and shakedown of the test loop has begun. Initial tests of the loop at reduced mercury flow rates show that condenser performance is stable and can be adequately controlled. An evaluation of condenser performance and demonstration of its adequacy for operation at SNAP-8 conditions will be completed following the test series of the -1 boiler.

(2) MECA Test Program

The single-tube condenser tests conducted at NASA-LeRC, in conjection with the MECA Program, have been extended. Off-design condenser pressure drop and condensing pressure measurements will be made on a single tube of the multi-tube condenser to determine the condenser performance during the startup phase of the SNAP-8 system. Data at mercury flow rates of 20 to 100% of rated flow will be taken for various combinations of coolant flow rate and inlet temperature with variable mercury liquid-vapor interface position. These data will be used in conjunction with the analog simulation of the SNAP-8 system to determine that sufficient NPSH is generated for the mercury pump during the startup transient.

b. Tube Sheet Development

Seven tube sample headers were fabricated which were representative of both headers of the -1 model condenser. Tapered tube ends were rolled into the sample headers and were welded using an automatic welder which had been used in the manufacture of the first two -1 condensers. Satisfactory joints were developed for the large diameter tube end. Additional work is required to achieve satisfactory small diameter tube joints.

The development of the 0.500-in.-dia (mercury inlet) end of the condenser proceeded smoothly. Rolling with lubricant provided a joint which completely filled the 0.005-in.-deep groove as evidenced by 100% photomicrographs of the joint. A second qualification sample was prepared, found acceptable, and used for welder certification.

The small-diameter end (0.250-in.-dia) rolling operation was more difficult to develop. Initial samples were unacceptable due to surface inclusions on the tube inner diameter after rolling. These defects appeared to be caused by over-rolling the tube in an effort to completely fill the groove. Additional samples were prepared which indicated that the depth of groove which could be filled, to prevent the localized spalling on the tube inner diameter, was 0.0020 to 0.0035 in. "Push" tests were performed on these upsets to determine their axial load carrying capacity. The allowable axial load was between 1850 and 2000 lb. The highest loading encountered on an individual condenser tube is 130 lb caused by the differential expansion between the tubes and shell; therefore, the 0.003 in. nominal extrusion into the groove was considered adequate. A sample is in preparation which will be used to qualify the joint.

c. Fabrication

All parts for the PCS-2 and IeRC condensers are complete with the exception of the tube bundle assemblies. The tube bundle assemblies were delayed pending the completion of the development of the rolled and welded tube header joint. Following acceptance of the final tube header qualification samples, fabrication of the tube bundle assemblies will be started.

3. Auxiliary Start Loop Heat Exchanger

The auxiliary start loop heat exchanger has been installed in the RFL-2 and is used to preheat the heat rejection loop in conjunction with startup tests for the boiler and condenser. Tests on the heat exchanger to determine performance will be conducted after loop shakedown is completed.

B. EXPANSION RESERVOIRS

During the past report period the preliminary design review for the expansion reservoirs was held. The observations made during that review have resulted in further examination of alternate means of satisfying the expansion reservoir requirements. A final design review package containing design requirements, procurement specifications, and test program requirements was initiated and is near completion.

The cooled gas expansion reservoir concept recommended in the Preliminary Design Review requires a relatively large volume of gas. This volume of gas acts on a bellows in such a way as to control the pressure of the liquid NaK on the other side of the bellows. A relatively large volume of gas is required to permit the required variations in NaK volume (and hence in bellows displacement) without encountering unsatisfactorily large variations in the stored gas pressure.

The large size of the resultant expansion reservoir was observed in the Preliminary Design Review and, as a result an analysis of alternate design concepts, has been initiated. While the evaluation of additional approaches is continuing, a summary of the conclusions regarding several alternate expansion reservoir concepts appears in Table 7. Most of these systems are heavier and/or more bulky than in the cool gas expansion reservoir concept. Many have additional liabilities which can adversely influence the component reliability. The cool gas expansion reservoir concept is still favored over any of the alternate concepts examined to date.

C. VALVES

1. Temperature Control Valve for ERL Start Transient

The temperature control valve is being designed and fabricated by Roylyn, Inc. A description is given below of their progress and present activity.

The (-1) design configuration arrived at for the temperature control valve features a 3-in.-dia bellows-actuated butterfly with 2-in.-dia inlet and outlet parts.

Detail drawings for all parts have been completed by Roylyn, Inc. (with the exception of the NaK chamber fill adaptor), and material procurement and fabrication has been initiated.

Flow checks utilizing water as the working fluid were conducted by Roylyn, Inc., with a 2-in.-dia butterfly mockup valve. Data from these tests will be used to determine the proper butterfly actuator linkage and any adaptations which might have to be made to obtain the desired valve characteristics.

2. Lubricant-Coolant Valves

The lubricant-coolant valves have been ordered from Valcor Corporation. Valcor is currently assembling and testing the valves. The valves are scheduled for shipment to AGC on 11 September 1964. These valves were described in the preceding quarterly report.

D. MERCURY INJECTION SYSTEM

The mercury injection system final design review package was assembled and issued. The design review resulted in the definition of a (-1) MIS system which is considered to be satisfactory for use in the SNAP-8 development program. Enough (-1) components for two complete MIS systems have been ordered. Complete sets of (-1) components sufficient for the assembly of two MIS systems will be available on or about 15 October 1964. A third set of components required to complete a MIS assembly is in the process of being ordered and will be available on or about 1 January 1965.

E. ELECTRICAL INSULATION DEVELOPMENT PROGRAM

1. High-Temperature Motor Test

Testing continued on an inorganic-insulated motor to determine the long-term electric strength of the insulation system. The motor stator was fabricated previously for the original 2-loop SNAP-8 system, and the insulation system used in the stator is essentially the same as now being employed in the new HRL and primary loop NaK motors. This 1000-cps motor has external bearings and operates at 450°F on a reduced 60-cps voltage to eliminate the need for a special power supply. The unit passed the 8000-hour mark during this period and has shown a slight but steady improvement in insulation resistance (Figure 57).

2. Evaluation of Organic Resins

The weight loss testing was discontinued at 1344 hours and showed that the higher-temperature-resistant organics are also high-strength, hard, brittle materials (Table 8). The silicone rubber materials Dow Corning 182 and 183, while showing high weight loss, retained their physical appearance and properties as well as the high-temperature epoxies and novalaks. The silicone rubber materials showed a tendency toward crack propagation that was not noted in the other materials.

3. Organic Insulated Statorettes

The statorettes ML-3, ML-4, ML-5 and ML-6 are still under test at 392°F. The ET-378 has evaporated, leaving the statorette exposed to air. This has resulted in an increased insulation resistance for this unit. The other units have shown little change, indicating that the systems are not materially affected by 392° temperature and OS-124 fluid.

4. HRL and Primary Loop NaK Motor Insulation Development

The first HRL inorganic unit was finished by the vendor and returned for the bakeout seal-off operation which was performed successfully. The temperature curves for this unit during processing are shown in Figure 58.

Winding assembly work continued on the next units.

5. Support Work

a. Organic Encapsulation of Inductors

Furane 17B organic resin was selected to encapsulate inductors for the Controls Group. This material was found to be unsatisfactory because of strains set up in the core material. The encapsulation material was changed to Epoxylite 813-9, and a coating of Dow Corning 183 was applied to the windings before encapsulation. This appeared to be successful. For further evaluation, see the Electrical Controls Section (Section VI,F).

b. Repair of General Electric Alternator Thermocouple Leads

During testing, some of the thermocouples on the first General Electrical alternator failed to register. Upon removing the flexible

potting compound around the terminals and thermocouple leads, electrical laboratory personnel noted that the joints were brazed and that incomplete removal of brazing flux resulted in rusting and corrosion. This rusting and corrosion caused the joints to fail. The use of brazing in the electrical systems, or in their housings, is contrary to the requirement that all SNAP-8 electrical joints be TIG welded.

F. ELECTRICAL CONTROLS AND COMPONENTS

1. Voltage Regulator-Exciter

The first preprototype voltage regulator assembly and exciter assembly passed acceptance test at Waynesboro, Virginia, and was shipped to AGC on 15 May 1964. Aerojet checkout procedure for the preprototype voltage regulator-exciter was issued, and provisions for checking out these assemblies was completed in the electrical laboratory. The checkout is not an acceptance test, but is used to determine whether the voltage regulator-exciter assemblies are operating properly after shipment. The first preprototype voltage regulator-exciter was received in the electrical laboratory and was installed in the checkout cabinet. After these two chassis were installed, the voltage regulator-exciter was qualified for test with the General Electric alternator in the electrical laboratory.

A GE alternator was received in the electrical laboratory, installed in the test bay, and made ready for electrical systems tests. A test outline was written for the systems test of the speed control, the voltage regulator, the alternator, and the necessary facility equipment.

Electrical controls systems tests were started in the electrical laboratory. This SNAP-8 system includes the preprototype voltage regulator-exciter (which controls the alternator output voltage), the alternator, and a simulated closed-loop speed control system using -X equipment. The facilities include a simulated parasitic load resistor, a vehicle load, a motor drive for the alternator, and a 400-cycle, 133 kva, motor-generator set that provides the electrical power to the motor. A control panel was installed to provide the instrumentation and switching control.

The first series of shakedown tests was completed successfully. The system has been operated at rated speed and voltage with an electrical load of 48 kw (unity pf). Thirty-six kilowatts were transferred from the simulated parasitic load resistor to the simulated vehicle load and back again.

Presently, complete detail testing is in progress. All tests conducted thus far have been successful. Data are now being obtained in such areas as voltage regulation, voltage transients, wave form, harmonic analysis, and stability, and for combinations of different power factors.

To date, preliminary information shows a total line-to-neutral harmonic content of 7.28% at 41 kw parasitic and at no vehicle load.

Wave forms at noted loads can be seen in Figure 59.

Speed control regulation is ±2.5 cps from no vehicle load to 34 kw vehicle load (unity pf). The total alternator load was 39.6 kw at 0.86 pf.

The system has been stable, but this is a motor-driven system. The CGEST will determine if stability is a problem.

The second GE preprototype voltage regulator-exciter has been acceptance-tested at the GE facilities in Waynesboro, Virginia, and has been received in the Aerojet electrical laboratory. This unit will be checked out in the same fashion as the first preprototype voltage regulator-exciter.

The TIG welding of the diodes in this unit was successful. Discussions with GE indicate that the original TIG welding problem areas for the diodes has been eliminated and the system worked out in the GE welding specification M1A-58.

Previously, subassembly drawings and materials for the prototype voltage regulator assembly had been reviewed and approved by AGC. The prototype voltage regulator-exciter enclosures drawings were received by AGC for review. The protective housings drawings were also received. After reviewing the drawings, AGC approved the voltage regulator-exciter enclosure drawings and the protective housings. With this approval, GE now has complete approval for the prototype voltage regulator-exciter design.

All process specifications, with the exception of the TIG welding specification M1A-58, have been approved. Additional information is required before specification M1A-58 can be approved. Conditional approval of M1A-58 was given and the specific areas that were not clear were pointed out to GE. When these areas are cleared up, complete approval will be given on the TIG welding specification.

To accomplish the ceramic terminal hermetic seal, GE has incorporated the coldweld process in their hermetic seal design. Their transition pieces for the ceramic terminal were reviewed by Kelsey-Hayes, the coldweld vendor. Some modifications were made in the original GE design to prevent material distortion at the time of coldwelding. GE has indicated that these modifications, as recommended by Kelsey-Hayes, do not present a problem. Modification of this design has been completed.

The coldweld tooling that was designed for AGC for the speed control housings will be used by GE to attach their ceramic terminals to their voltage regulator and static enclosures. GE has contacted Kelsey-Hayes, and they have been assured that their design will be compatible within the AGC tooling.

2. Speed Control

To ensure a stable speed sensing circuit, AGC is continuing its program to ensure stable performance under all environmental and operational conditions for a long period of time. The long period drift tests, started on 22 January 1964, continue. No measurable drift was recorded up to 14 August 1964. This test has been running continuously except for a few cases where there was power shut downs in the plant or the changing of some test equipment.

The fact that this circuit has not drifted is highly significant (see Figure 60). Aerojet is of the opinion that the primary success of this circuit is the combination of the silvered mica capacitors and the silicon iron conductors using alumina for the inductor gap material. Aerojet believes that these materials point out the value of using nonexotic materials for the core and extremely stable material for the gap. Silvered mica capacitors have had a long history of operation in tune circuits for extensive periods of time; this is why this particular type of capacitor was chosen.

Another area requiring investigation involves the question of how an inductor can be tuned, potted, and incorporated in a tuned circuit with the capacitor and yet not have the tuned circuit resonant frequency shift. This area was pointed out very dramatically during the first attempt at impregnating and potting the tuned circuit inductors. The first two inductors

were impregnated with Epocast 17A. This impregnation process was very successful, as reported in the preceding quarterly report (Reference 4). The inductor was then potted with Epoxolite 813-9; both inductors shifted 20 cycles. This shift is not acceptable in the speed control design because there are no potentiometers for adjustment.

The primary problem was believed to be the stress on the gap of the inductor. It was felt that if some resilient material could be used to cover the inductor before the potting process, the 20-cycle frequency shift could be reduced considerably.

Two more inductors were fabricated, impregnated, and tuned with a test capacitor. One inductor was covered with the resilient material Sylgard 183, and the other with a glass fiber material. The first inductor was heated to 400°F and dipped in the Sylgard 183 (a silicone resin). This process left a resilient material about 1/8-in. thick over the inductor, and also completely sealed the inductor. The inductor was then potted in Epoxolite 813-9.

In subsequent tests, the tuned inductor shifted only 0.8 cps. This improvement was much better than expected and is well within the trimming range. After this original test, the inductor was temperature-cycled to 200°F, and the inductor was returned to its tuned point with no mechanical failures in the potting materials. To further check the mechanical characteristics of the potting materials, the unit was then cycled to 400°F.

After one cycle, the silicone resin caused the potting compound to crack; the compound subsequently could be pulled off of the inductor. The inductor remained encased in the silicone resin and continued to operate satisfactorily. The 400°F temperature is twice the design operating temperature of the inductor because the inductor is located in the low-temperature package with an active heat sink at 150°F.

As a further check, the silicone-dipped inductor was repotted in the same epoxy material. Its shift was again less than 1 cps. The inductor was then cycled to 400°F - again resulting in the same fractured epoxy - but the performance of the inductor in the tuned circuit was not affected.

The combination of the Sylgard 183 and Epoxylite 813-9 has been highly satisfactory. The combination results in a rugged component which is not adversely affected by operating temperatures of 400°F and which will operate very well at the 200°F temperature. This potting system will be used in the fabrication of the -1 speed control amplifier (see Figure 61).

A parallel program which used a Fiberfrax covering over the inductor, and the subsequent identical potting materials, was not successful (see Figure 62). This method resulted in a 20-cps shift of the tuned circuit after potting and temperature test. The inductor was sectioned, revealing that the potting compound had penetrated the Fiberfrax material, resulting in unwanted pressure on the gap causing the 20-cps shift. It was noted that the 20-cps shift that occurred in this inductor was identical to the 20-cps shift that occurred in the inductors which were directly potted in Epoxylite 813-9. In all three inductors where the epoxy came into direct contact with the gap, the frequency shift was 20 cps. All work has been stopped on the Fiberfrax system.

The first delivery of the large and small ceramic terminals and the ceramic standoffs are expected to be made during the last week of August.

To attach the ceramic terminal to the aluminum housing, the coldweld process will be used. Coldweld samples and tooling were ordered. Sixteen sample copper flanges and aluminum cans were shipped to Kelsey-Hayes for coldwelding. The coldweld tooling has been designed and 12 of the samples (Figure 63) were returned to AGC for evaluation. (Kelsey-Hayes kept four coldwelds for their evaluation.)

The SNAP-8 Materials Department evaluated the coldweld samples by helium-leak testing and ultrasonic testing. The helium-leak tests were successful. None of the coldwelded samples failed any of these tests. The ultrasonic tests showed that a continuous bond was achieved on all of the tested samples. The Materials Department approved the coldweld bonding process as performed by Kelsey-Hayes.

As previously reported, coldweld joints degrade at elevated temperatures over a period of time. The first test performed on coldweld joints was conducted at 500°F for a period of 1600 hours. This particular joint did come apart in the tensile test. Since 500°F is a much higher

temperature than the ceramic terminal coldweld is likely to face, another test was run at 350°F for 1500 hours. The Materials Department then subjected this coldweld sample to a tensile strength test. The coldweld did not fail. Evaluation of the sample coldweld joints and the 1500-hour 350°F coldweld tensile tests shows that the coldweld joints will meet the environmental requirements of the SNAP-8 Program.

The prototype design (-1) of the speed control is packaged in three separate modules. The saturable reactor and the power transformer are installed in the TRA assembly, which is the high-temperature assembly. The third module (a speed control module) will be located in the low-temperature controls assembly. Another module, which may become part of the speed control assembly, is the stabilization transformer. Because the size of this transformer is a direct function of the stability of the system, no -1 work has been done on this unit. A -X design of this stabilization transformer has been completed and the fabrication of the unit has also been completed. Its actual size and shape will be determined during the cold gas electrical systems test.

During this report period, all -1 design drawings were released for the speed control module, the saturable reactor module, and the power transformer module. Fabrication orders were initiated.

One of the problem areas associated with the speed control module is the TIG welding of the diode assembly. To develop the TIG welding schedule and processes, a -1 diode assembly with "dummy" diodes were fabricated. TIG weld tests and evaluation are continuing. The major objective is to make successful TIG welds without exceeding the temperature limitations of the silicon diodes. Thermocouples were installed in this assembly for monitoring the temperature of the diode, and different types of heat sinks are being evaluated for their effectiveness in keeping the diode temperature as low as possible.

Before assembly, all speed-control module components must be matched. Because there are no potentiometers for setting the operational points of the speed control, and because the operational limitations are very stringent, the components of the speed control amplifier must be assembled on the precheckout board and tuned to the proper operating point. After this is done, the components are then removed from the precheckout board and installed in the -1 speed control module.

All SNAP-8 speed control modules contain ceramic terminals which project from the enclosure. To eliminate the possibility of breakage during assembly and checkout, these vulnerable ceramic te nals are shielded by protective housings during testing and handling module.

3. Saturable Reactors

The design of the -1 saturable reactor was completed, the drawings were released, and a fabrication order was issued.

To evaluate some of the problem areas in the -1 design (this design consists of three cores and one control winding), an experimental assembly of the -1 design, not including the housing, was fabricated.

One of the areas investigated was the welding of the braided leads to the weld clip which attaches to the terminals of the saturable reactors. These welds can be made with no problem, but the importance of the weld schedule must be considered because faulty weld settings will produce a substandard weld.

Further tests on the high-current copper feed-throughs were made using the TIG weld process to attach flexible leads to the -1 experimental saturable reactor. Considerable difficulty in techniques were encountered. Evaluation indicates that better heat sinks, closer engineering controls, and welding experience will eliminate the problem. Here again, the weld schedule and the implementation of the welding schedule is extremely important.

Because the configuration of the -1 saturable reactor is different from the -X saturable reactor, another series of time constants tests were conducted. The time constants of the experimental -1 design did not exceed 0.10 sec. Test results corresponded to design calculations.

4. Harness Assembly

In the conceptual harness design review, a cold welded copper to aluminum transition piece was proposed for use in the high-current bus system. Because of the separation of the coldweld after being exposed for 1600 hours at 500°F, a coldweld joint was retested at 350°F for 1500 hours. This particular piece is the same piece that is referred to in the coldweld tests for the ceramic terminals. A tensile-strength test of the sample showed that the coldweld joint

did not fail. The results of these tests indicate that the coldweld joints for use in the harness cannot be exposed to a temperature exceeding 350°F. Some of the original areas considered would be exposed to temperatures in excess of the 350°F level; therefore, in these areas copper will be used throughout. The coldweld joint may still be used in areas where the temperature cannot exceed 350°F.

The harness for PCS-2 basically will be a workhorse design. The -1 installation technique will be used where possible. Welding cable will be used for the high-current bus, and Teflon-insulated wire will be used in the low-current harness where the -1 design cannot be usefully employed. A schematic drawing of the PCS-2 harness was completed which incorporated all flight requirements currently known. After investigation of the electrical connections that must be made and the component location in PCS-2, it was possible to remove the distribution panel and the separate junction boxes from the harness design. The electrical connections formerly anticipated for the distribution panel and the junction boxes have been transferred to the transformer reactor assembly (TRA) and the start programer assembly.

The electrical schematic design of the PCS-2 harness is being used as a basis for the harness layout for the PCS-2 mockup. Layout of the PCS mockup has been started.

5. Start Programer

Fabrication of the -X breadboard start programer was completed. Fabrication of the checkout unit and its associated harness has also been completed. Checkout of the start programer with use of the checkout unit has been completed (see Figure 64). The breadboard assembly of the start programer operated correctly in accordance with the operational bar chart. This bar chart is not the final operating procedure, but it has been developed with the best information available. Some changes will probably be required in the sequence of operations, and some of the timing functions may change. In view of this, the Electrical Controls Department has recommended that a breadboard start programer be used in the first phase of the PCS-2 test. The timers on this breadboard are variable and are being fabricated in a breadboard style to allow modifications with minimum effort.

Timers purchased to AGC Specification 10209 were tested separately before being installed on the start programer breadboard. Test results agreed with the specification at ambient conditions; the timers operated electrically as specified and performed the proper timing functions when they were installed on the breadboard.

6. Vehicle Load Breaker and Protective System

In compliance with NASA Technical Direction No. 19, all work on the vehicle load breaker directed toward flight-type hardware was discontinued. Three Westinghouse Type AVB12A breakers were ordered.

NASA Technical Direction No. 19 also directed that no work be done on a flight-type protective system. Accordingly, a magnetic bistable circuit combined with available aircraft type components has been designed for use in ground system tests. This protective system will provide (a) short-circuit fault and overload protection by undervoltage sensing with time delay before breaker trip and before breaker close; and (b) overspeed protection by means of an under-over frequency relay. By use of two additional relays, lockout of the under-over frequency relay is provided until the speed of the TAA rises to near rated. After rated speed is attained, any increase in speed or decrease in speed to the under-over frequency relay trip joint will provide a contact opening which can be used to shut down the turbine.

7. Battery Assembly

All work on the battery assembly has been discontinued in accordance with NASA Technical Direction No. 17.

8. Parasitic Load Resistor

A purchase order was issued to Heat Engineering and Supply Company for the design and fabrication of four parasitic load resistors to meet the requirements of Specification AGC 10270.

Drawings and calculations were received from the vendor and reviewed. Design approval was granted with minor changes to be incorporated. The only physical design change was the specification of a discontinuous weld for the attachment of the mounting rings to the housing. This change was made

to reduce the possibility of a stress problem resulting from differential expansion of the rings and housing if a temperature gradient exists across the mounting rings. The other changes were for the addition of information to the drawings in the form of notes, dimensions, and tolerances.

The addition of a layer of INCO-82 weld material between the end of the resistor element sleeve, 316 stainless steel, and the nickel terminal flange was suggested to improve the weld and to eliminate brittleness and cracking. The SNAP-8 Materials Department has started checks on several test welds to determine if the addition of the INCO-82 material is necessary.

The three -X resistor elements are still operating at a temperature of approximately 1400°F. At the end of this report period, they had operated at this temperature for 3440 hours in addition to 2736 hours at a sheath temperature of 1100°F for a total operating time of 6176 hours.

9. Power Conditioner

No change has occurred in the requirements for the power conditioner. The output voltage will be 28 v,dc ±3 v.

10. Radiation Effects Program

Lockheed-Georgia Company continued this testing program and completed the reactor irradiations of the electrical controls components and subassemblies. Post-exposure testing of the samples which were subjected to the 200°C materials irradiation was also continued. All physical properties tests on these samples and exposure of the control statorettes to the temperature environment were completed. Electrical properties tests on the materials items are currently being conducted.

Preparations and checkout of instrumentation for the reactor runs for the electrical system control items were completed. The first of these runs were conducted on 7 and 8 July at a nominal heat sink temperature of 160°F.

The second run was conducted on 15 and 16 July at a temperature of 160°F. Cyclic, automatic data systems recorded parameter changes to both

the components and subassemblies prior to, during, and following these irradiations. Data were also taken manually. Similar reactor operating profiles were followed during these runs with a majority of the data being accumulated over the exposure range to about 1×10^{12} nvt. During the final few hours of the 160°F run, the LiH shield was raised to increase the neutron flux. A final exposure of about 6×10^{13} nvt was reached.

Although complete data from these tests are not yet available, the following observations were made:

a. No significant changes in the performance characteristics of any of the diodes occurred prior to an exposure of about 1×10^{12} nvt.

b. The performance of the high-current diodes which were tested appeared to be equal to, or better than, that of the low-current units. Both types were checked over their respective operating range, which included de-rating. This information on the high-current diodes is important to the SNAP-8 electrical control system because it essentially removes an area of concern about the use of the magnetic amplifier circuits which operate at a relatively high-power level. No information was found in the available radiation effects literature concerning high-current diodes. It was expected that these diodes would be more susceptible to a nuclear environment than would the relatively low-current units. Figures 65 and 66 show the range of observed values of forward voltage drop and of reverse leakage current for the irradiated units of both a high-current and a low-current diode as a function of neutron exposure.

c. Performance of the silicon-controlled rectifiers (SCR) which were tested was more affected by the accumulated exposure than was that of the diodes. They would be suitable, however, for use in SNAP-8 controls with the present radiation specification and possibly to somewhat higher exposures.

d. The specification for the acceptable radiation to the solid-state controls can probably be revised to increase the exposure levels.

With the presently assumed overall system configuration, the SNAP-8 LiH shield weight will be determined to a large extent by this allowable exposure. Any increase in the acceptable total dose that is on a technically sound basis could, therefore, reduce the required booster thrust with no sacrifice in required system performance. It appears that a recommendation to NASA for some increase in the specified levels could result from a detailed analysis of the test data. Additional increases in the specified exposures can probably be attained with added radiation testing and circuit design techniques.

Work is continuing on this program. This will involve completing the tests, reporting and analyzing the data, developing recommendations for the next series of radiation tests.

11. Inverter Startup System

A letter contract was issued to Westinghouse Electric Corporation on 21 May 1964 for 15 rotary inverters. Initial fabrication is limited to two units.

The development schedule received from Westinghouse shows the first unit scheduled to be delivered by 13 November 1964 and the second unit by 27 November 1964.

Preliminary inverter design reviews were conducted in June with Westinghouse. Westinghouse was requested to use a larger motor in the inverter so that the maximum hot-spot temperature of 205°C as specified in AGC-10281 would not be exceeded. Westinghouse was also requested to use redundant brushes as required by the specification. With these provisions, preliminary design approval was granted to allow completion of the detail design and design calculations.

A layout drawing and mechanical design calculations for the inverter were received from Westinghouse in July. Also received were motor performance calculations and alternator performance calculations.

The motor and alternator performance calculations were reviewed and judged to be satisfactory, except that it was thought that a higher grade steel than M-27 should be used in the motor armature.

The mechanical design calculations were reviewed. Because of lack of sufficient information on the calculations and the conclusions drawn from them, design approval was not given. Westinghouse was requested to supply additional specific information before approval could be given.

The definitive contract was completed, approved, and mailed to Westinghouse on 21 July 1964.

Proposals received from three vendors for inverter contactors were not considered satisfactory. It was decided to obtain four aircraft-type contactors, Hartman BH-138AKH, and inspect and test them to determine what modification is necessary to assure that they will meet the requirements of the SNAP-8 environment.

These contactors were ordered and are promised for delivery by 15 September 1964.

12. Transformer/Reactor Assembly (TRA)

The layout drawing of the TRA was completed, although complete information on the stabilization transformer, the motor transfer contactor, and the mounting of the ready relay is not available. Space for these components has been assigned in the overall layout of the assembly. The areas in which the layout is complete are the mounting configuration, the housing, the heat sink, structural, harness, and the junction box. Detail drawings have been made on the heat sink, the mounting provisions, the junction box, and portions of the housing and the structure.

Some changes in the design as presented in the design review manual for the TRA were made. The design review proposed a flexible high-current bus throughout the assembly of the TRA. Additional work in this area reveals that the insulation system for the flexible leads was too cumbersome. The flexible lead design was changed to one with a solid bus conductor, 0.375 in. square, terminating in the flexible lead as described in the design review manual.

Another change is in the connection of the aluminum heat sink to the stainless-steel lubricant and coolant loop. The design review proposed that a transition piece, made from aluminum and OFC copper, connected by the

coldweld process, be inserted between the aluminum heat sink and the stainless-steel tubing of the lubricant-coolant loop. This would enable the aluminum heat sink to be welded to the aluminum section of the coldweld, and the copper section of the coldweld could be welded to the stainless-steel tube. The coldweld transition piece will still be used, but further investigation by the Materials Department indicated that a problem area existed when welding copper to stainless steel because of brittleness in the joint. However, nickel appears to be a material that can be welded to copper and stainless steel. Hence, the TRA heat sink piping will be terminated in nickel so that the copper to aluminum coldweld transition piece can be welded on one end to the aluminum, and the copper end can be welded to the nickel section. The other end of the nickel will be welded to stainless-steel tube.

An area of investigation which was brought up in the TRA design review was the effect of ET-378 on copper. The ET-378 would come in contact in the copper portion of a coldweld transition piece.

Because of the potential copper corrosion problem, the Materials Department is investigating a protective metallic coating to be put over the copper to keep it from contacting the mix -4P3E. Coatings that appear most applicable are: (a) electroless deposition of copper, "Electroized" chromium (this method is a proprietary process of depositing crack-free hydrogen-free chromium, and (b) electrode-position of silver. A test program for exposure of candidate transition joints for the transformer/reactor assembly has been started and is scheduled to be completed in January of 1965. Because of the required delivery schedule of the TRA, it is necessary to design the transition joints into the assembly; therefore, the TRA design will continue under the assumption that one of the three proposed coating processes will be successful.

13. Cold Gas Electrical Systems Test

The Electrical Controls Department prepared and forwarded a test request to SNAP-8 Test Engineering for the cold gas test. The test request was modified in accordance with NASA-LeRC recommendations.

The cold gas electrical systems test operation has been prepared by Test Engineering. Work on the wiring installation for these tests is now under way. This series of tests will use -X electrical equipment. As previously mentioned, all of the electrical equipment provided by the Electrical Controls Department has been fabricated, accepted, tested, and is awaiting installation into the loop.

VII. TEST ENGINEERING

A. TEST FACILITIES AND EQUIPMENT DESIGN

1. LNL-3 Liquid NaK Loop (NaK PMA Test Facility)

a. Design

Because of the change of program needs, the LNL-3 system was modified to incorporate a simplified loop design. To simplify the loop, some versatility was sacrificed. The design objectives were devised in accordance with the following guidelines:

(1) The system pressure drop must accommodate the maximum flow and corresponding head rise of the primary loop NaK PMA (Figure 67). The system shall require a flow-limiting orifice under all conditions of flow.

(2) The system shall have heater capacity sufficient to raise the system NaK temperature from ambient to 1300°F in 2 hours and maintain that operating temperature for 3000 continuous hours of operation. Heater controls shall be capable of maintaining temperature constant within 5% of the design temperature.

(3) The system shall be capable of operating at 500°F by free convection cooling without auxiliary heat exchangers other than those provided with the PMA.

(4) The purity of the initial NaK charge will be introduced at a level less than 100 ppm of sodium oxide. The initial contamination combined with the sodium oxide resulting from the reduction of surface oxides will result in a total sodium oxide volume of less than 10% of the pump housing to motor shaft annulus.

(5) The instrumentation used will be direct-reading diaphragm pressure gages. Flow will be determined by the calibrated orifice described in paragraph VII,A,1,a,(1).

(6) If possible, a cooling system (ET-378) will be provided consisting of the L/C PMA (P/N 253800), the necessary piping, and heaters to maintain a coolant temperature from 100 to 230°F within 5% of the selected temperature.

(7) The whole system (including the cooling system) and the PMA (P/N 092949) will be housed on a single frame.

The design incorporating the objectives indicates that the system will have a NaK capacity less than 7 gallons, and the total NaK piping length involved will not exceed 26 ft.

b. Design Review

The LNL-3 design review meeting was held 23 July 1964 to present the conceptual design to interested personnel.

b. General Considerations

The analysis of the loop was completed. The hydraulic analysis resulted in the selection of an 0.847-in.-dia orifice for the HRL testing and an 1.113-in.-dia orifice for the primary loop testing. The resulting system curves are shown in Figure 67.

The design of the loop is virtually complete. The NaK loop will be constructed from 1-1/2-in.-dia Schedule 40 piping. The NaK expansion tank will be a bellows-type accumulator with an expansion capacity of 2 gallons. The ET-378 cooling system will also make use of an accumulator for thermal expansion compensation and pressure regulation. Detail drawings were initiated and vendor contacts have been made to ascertain the availability and delivery of necessary loop components. The NaK Loop Assembly (LNL-3) Drawing is complete.

2. Integrated Nonnuclear Test Complex

a. Digital Data Acquisition System (DDAS)

Final acceptance tests were performed on the DDAS, and the equipment was accepted by Aerojet.

b. Mechanical

A flanged, 2-in. manual shutoff valve and a flanged strainer suitable for 2200-psi service were installed by the Linde Company in the vertical riser which connects the upper bank of 15 nitrogen receivers to the 500-psi regulator. A 3/4-in. blowdown valve was added in the main 4-in. supply line downstream of the Annin regulator. This arrangement now enables the operator to shut off both banks of receivers for the performance of service work on the regulator and supply line.

A 6 in. burst diaphragm was installed in the main 4-in. line adjacent to the fenced area. This disk is set to burst at 720 psi and has a relieving capacity of 228,000 cu ft/min.

A 2-in. manual Grove gati valve was substituted for the 2-in. Nordstrom plug valve in the proving grounds gaseous nitrogen supply line to Building 180. This installation provides a leakproof connection to the high-pressure plant system which is acceptable to proving grounds management. This valve will be sealed shut and turned on only if the gaseous nitrogen supply to the SNAP-8 system should fail. The high-pressure gas will be regulated to 500 psi before entering the Building 180 and 187 distribution system. An additional rupture diaphragm will be installed at this point in the system.

Concrete socks will be cast around the base of each column supporting a piece of heavy equipment in the pad area to protect the metal structure and buy precious fire-fighting time in case of a serious NaK spill. The socks will be approximately 8 in. high with beveled tops. They will be painted to reduce moisture absorption to a minimum.

3. Building 156

Upgrading of the building for use as a data processing center with offices for SNAP-8 Test Operations was initiated by the removal of all equipment previously serving the six test cells in the south end of the building. The original ceiling was insulated with a 2-in. glass fiber mat. Air-conditioning ducts were installed for the data processing section, with the refrigeration unit mounted on the roof. Flush lighting fixtures were then mounted in a new suspended acoustical ceiling.

A solid wall was built to separate the data processing and office areas. A new floor tile was laid throughout the building.

Installation of a window air-conditioning unit in the west wall of the office area, the erection of several sections of partition, and the painting of all interior walls completed the scheduled building modifications.

The building is now occupied.

4. Building 156A

a. Mechanical

Erection of the new building was completed. Two-in. glass fiber insulation was installed on the three exposed walls, the two hinged doors, and the underside of the roof. The concrete ramp to the south side of the pad was modified to match the building door.

b. Electrical

Overhead fluorescent lighting fixtures, convenience outlets and the semi-automatic overhead door controls were installed. They are fed from a breaker panel on the east wall.

Light and convenience outlet services in all six cells were rerouted to feed from this panel. Power was furnished to several machine tools located in the open cell.

5. Building 180

a. Instrumentation

Installation was completed of all instrumentation, and of all signal conditioning and recording equipment. Additional recording equipment required by NASA Technical Directive No. 16 is presently being installed.

A single unit, 36-channel dynamic meter amplifier was installed for RPL-2.

All cell instrumentation for LML-3 in cell 3 was completed.

b. Mechanical

Repairs were completed on the Struthers-Wells gas-fired NaK heater behind cell 4. The heater is presently being connected into the primary NaK loop of RPL-2 to replace the recently failed electric heater.

The height of the fence at the south end of the equipment pad adjacent to Building 180 was increased by 9 ft for a distance of 12 ft from the edge of the building. This was done to protect personnel in the south walkway in case of a rupture in the high-NaK outlet line of the gas-fired heater.

c. Electrical

All electrical power services to cell 3 for the operation of LML-3 have been installed, including 220 v,ac 3-phase 60-cycle power for the Veeco vacuum station outside the cell in the high bay area. The control system to this loop was completed.

The installation of all electrical power services to cells 5 and 6 for the RPL-2 was completed including the 220-v,ac, 1-phase, 3-wire circuit, and secondary cords to the Veeco pump for this loop (installed in cell 4).

Work is continuing on the installation of the Sun load simulator for the TAA in RPL-2; this job is 75% completed. Installation of the load simulator for the TAA in GN_2S-1 was completed.

Services for 110, 220, and 440 v have been installed to junction boxes behind cell 4 for the RPL-2 NaK purification system now being set up at that location.

Fourteen emergency battery lights were installed in the Building 180 complex at locations where illumination was considered to be vital either to the safe evacuation of personnel or to loop shutdown if the main power should fail during an emergency.

The installation of warning and signal lights in Building 180 has been previously reported, but during this last report period it was found necessary to update the system in the following manner: "cell emergency" flashing red lights and "test in progress" amber warning lights were installed both inside and outside the building at all points of entry into potentially hazardous areas. Personnel signal lights were installed above each cell in the high bay area. In addition to the colors for the cell conditions listed above, these signals include a blue light for "personnel in cell," a white light for "liquid metal in cell" and a green light to indicate that the cell is "safe for personnel."

This system will be used in Building 180 and also in Building 187.

6. Building 187

a. Instrumentation

Instrumentation design is 85% complete. The remaining 15% will be completed as required for sound and noise, and vacuum signal conditioning. Documentation is 85% complete.

Installation of instrumentation wiring for SL-1 in cell 3B was completed as previously reported, and the balance of the signal conditioning wiring is now 40% complete.

Installation of the recorders in the control room on the mezzanine is continuing and is approximately 60% complete.

The functional checkout of cell 3B to patch panel input channels was started.

The chart drive selector system is 90% completed.

Installation of the two Honeywell "Electronik" recorders for SL-1 and SL-2 NaK-to-air fin-fan heat exchangers in racks R8 and R17 in the control room was requested.

b. Mechanical

Erection of the load simulator support structure on the equipment pad was started and is approximately 60% complete.

Mercoid high- and low-gas-pressure switches were installed in the lines to the two Struthers-Wells gas-fired NaK heaters in compliance with FIA requirements.

The control consoles for these heaters were set up in the mezzanine control room.

As a safety precaution, chain hangers on all lighting fixtures in the building were replaced with solid rod hangers.

c. Electrical

Installation of power to the SL-1 EM pump in cell 3B through the powerstat and capacitors in the equipment room was completed.

Connections to the pump through the wall junction box in the cell were run in solid without disconnects because of the anticipated current load of 370 amp.

The 400-cycle motor-generator set on the equipment pad south of Building 187 was checked out using a vehicle load simulator to absorb the output. Voltage and frequency recovery time from a shock test was found to be extremely short. Correction of a malfunctioning clutch coolant-pressure switch and alignment of the shafts and coupling between the magnetic clutch and the alternator was necessary before performance of the unit was considered to be satisfactory.

Bull's-eye indicator lights were added to all 400-cycle breaker boxes in the cells and high bay area to warn personnel when the breakers are hot.

Four No. 4 conductors were installed to supply Building 180 with 208-v,ac, 3-phase, 400-cycle power from the Building 187 distribution system. The cables tie into the system at the junction box on the south wall of the Building 187 high-bay area through a breaker. The cables terminate at a panel on the west wall of the mazzanine power room in Building 180, and power is distributed to the cells through individual breakers and control relays.

The ten reference junction boxes in the high-bay area were provided with 110-v convenience outlets.

Red and amber warning lights were installed at all building entrances, and signal lights were located at the personnel doors of cells 3B and 4A for SL-1 and SL-2.

Installation of conduit and control wiring to the 110 v air inlet damper solenoid valves was completed in cells 1, 2, 3B, and 4A. Conduit and wiring was also installed above cells 3A, 3B, 4A and 4B for the fire blanket and smothering gas solenoid valve control. This wire was Rockbestos NEC, Type AIA, Table R high-temperature wire rated 300 v at 392°F.

The 28-v,dc power supply was located next to the central control complex in the equipment room and provided with 440 a-c power. This installation is approximately 70% completed.

The 110/208 v,ac, 220 v,ac, 3-phase and 440 v,ac, 3-phase power panels are being installed in the equipment room for distribution of cell power.

Control wiring for SL-1 in cell 3B was started and is approximately 30% completed.

Installation of electrical power services for SL-2 and SL-1 loop components in cells 3B and 4A is continuing.

Mechanical design of the emergency and auxiliary emergency control panels was completed and has been released for fabrication. Wiring diagrams are in documentation.

B. NUCLEAR SYSTEMS TESTING

1. Ground Prototype Test Facility

DDAS system design, fabrication, and programing activities are proceeding. Fabrication and assembly of the DDAS are estimated to be 70% complete.

Work continued on layouts of piping, control room, vault, equipment pad, vacuum equipment, electrical equipment, and instrumentation equipment. Work continued also on the electrical power system, control, instrumentation, sea vacuum system, and signal conditioning.

Primary loop and L/C loop hydraulic analyses were initiated.

AEC initiated the modification of the GPTF for reactor pit vacuum, control room expansion, cooling capacity expansion, and electrical system expansion.

Liaison with Atomics International was continued on the design and installation aspects of the GPTF and the Test Support Equipment.

GPTF Phase I (Excavation, Vacuum Room Construction, and Reactor Pit Restoration) and Phase II (Control Room, Cooling System and Electrical System Expansion) drawings have been received from AI.

AI drawings and specifications for the nuclear system shakedown system have been received and are being reviewed.

Work continued on the definition of the requirements for the Request for Proposal for the AI subcontract on the installation of AGC-supplied TSE in the GPTF.

The Fiscal Year 1965 work plans and budgets were estimated and discussed with NASA.

A preliminary design review of the AGC test support equipment (TSE) was conducted for AI, AEC, and NASA. Specific AI questions on TSE design concepts were answered.

2. Flight Prototype Test Facility

The Title I Report (Preliminary Services for SNAP-8 Flight Prototype Test Facility, Building 056, Santa Susana, California) dated August 1964, and Title I drawings have been received from AI and are being reviewed.

C. TEST SUPPORT SERVICES

1. Data Reduction Services

The modification of the control room of Building 156 to accommodate an advanced data processing center has been completed and occupied. Arrangements are currently being made to move the magnetic tape reader to this location and to establish the requirements of data storage in this area.

A purchase order for two analog data reduction systems (strip chart readers) for the data process center is now in progress.

In coordination with the Aerojet Computer Sciences Division, a basic program for the DDAS has been developed using the IBM 7094. This basic program will permit maximum use of the memory section and minimum time expenditure for program updating during test. This DDAS program is currently being verified for test use.

2. Chemical Support Services

a. Lubricant-Coolant Fluid

An order for Mix-4P3E has been purchased under AGC-10320 specification from Shell Oil Co., New York. The specification requires [illegible]

purity of 99%. Certified analyses supplied with the shipment stated the purity as 99.6%. On the basis of experience on this order, Shell Oil Co. has indicated some changes for improvement of the Aerojet specification. This is currently being resolved and will result in a modification of the specification.

Evaluation of methods for reclaiming used or contaminated Mix-4P3E in an effort to reduce time and costs has been completed. Briefly, the method developed entails (1) agitating a mixture of the Mix-4P3E with basic alumina under high vacuum at 90 to 100°C, and (2) separating the Mix-4P3E from the alumina by vacuum distillation. A high carbonaceous or solid content requires an initial filtration over Hyflo-Super-Gel Celite followed by the basic alumina treatment. This method of reclamation has resulted in a process that is approximately one-third the cost previously encountered, and yields a more pure product.

b. NaK

Coordination with SNAP-8 Materials and System Engineering Departments has resulted in the formulation of AGC-10340 specification for purchasing commercial grade NaK.

c. Mercury

Coordination with SNAP-8 Materials and System Engineering Departments has resulted in establishing AGC-10327 specification for the purchase of high-purity mercury.

3. Planning and Procedures

The following procedures have been written in first preliminary form, subject to approval before preparation in final form:

a. Procedure for Transducer Replacement or Installation, TAA/GN_2S-1 (TS-M-1001)

b. Pre-test Cleaning of Components, Equipment, and Raw Material (TS-M-1002)

c. Accelerometer Calibration Procedure, Charge Amplifier (TS-1-2001)

d. Calibration Procedure - Voltron, Voltage - Current - Power (TS-1-2002)

e. System Calibration Strain Gage Transducers Below 100 psia (TS-1-2003)

f. Calibration Procedure, Daytronic - LVDT (TS-1-2004)

g. System Calibration, Strain Gage Transducers 100 psia and Above (TS-1-2005)

h. System Calibration, Potentiometer Transducers (TS-1-2006)

i. Calibration Procedure, Dynamic Accelerometer, Portable Shaker System (TS-1-2007)

VIII. MATERIALS

A. STAFF SUPPORT

1. Component Design and Development Support (Task A.1)

a. Transformer/Reactor Assembly Heat Sink Joint

A tubular transition joint between aluminum and 304 SS is required for connecting the lubricant-coolant (L/C) loop (304 SS tubing) to the transformer-reactor heat sink (aluminum tubing). Direct joining of aluminum to stainless steel by welding is not an established state-of-the-art procedure. Several companies are working on the problem. One company - Nuclear Metals, Inc., Concord, Mass. - provided samples of a hot coextruded transition joint to Aerojet-General for evaluation. Another acceptable transition joint using state-of-the-art procedures was made by joining aluminum to copper using the coldweld (pressure welding) process, then joining copper to nickel by TIG welding, followed by joining nickel to 304 SS by TIG welding. Previously prepared lap and butt weld samples had indicated that the copper end of the coldwelded part should not be welded directly to the 304 SS. Metallographic examination of these samples indicated a TIG copper-brazed joint with some Cu-SS alloying occurring in the joints. A typical microstructure is shown in Figure 68. Microhardness traverse of the lap and butt weld samples indicated that the hardness of the fusion zone was not appreciably greater than that of the stainless steel (R_B 84 in the fusion zone vs R_B 78 in the 304 SS parent metal). However, two lap weld specimens developed cracks through the stainless steel (Figure 69) initiating in the fusion zone, one immediately following welding and the other during 355-hour exposure at 350°F. The probable reason for the cracks was the presence of a precipitation hardenable chromium-copper phase and a brittle iron-copper phase. It was concluded that a nickel transition piece between the Cu and 304 SS is necessary.

The compatibility of the copper portion of this joint with the Mix-4P3E, the L/C fluid, is questionable. There is evidence that copper is attacked in the presence of nuclear irradiation due to degradation of the Mix-4P3E. The degradation is not sufficient to detrimentally affect the properties of the

Mix-4P3E. Because of the potential copper corrosion problem, it is deemed necessary to apply a protective metallic coating over the copper to keep it from contacting the Mix-4P3E. A program was started to evaluate three selected candidate coatings: (1) electroless deposition of nickel; (2) "electrolyzed" chromium (the method is a proprietary process of depositing crack-free, hydrogen-free chromium); and (3) electrodeposition of silver. Tubular transition joint specimens of Al/Cu/Ni/304 SS were prepared for coating evaluation. The Cu/Ni joint was completed using Monel (70Ni/30Cu) filler metal and the Ni/304 SS joint was completed using Inco A filler metal. Figure 70 shows a sketch of the joint to be evaluated.

Evaluation of a coldweld transition piece (copper/6061 aluminum alloy) was continued. A specimen (Figure 71) which had been exposed at 350°F for 1500 hours showed a slight diffusion zone in the copper (0.00008 in.). For comparison, Figure 72 shows the as-received specimen. No diffusion was detected into the aluminum alloy side of the interface on the aged specimen. The fracture faces of a tensile specimen were metallic gray. A comparison of tensile properties of the joint in the as-received condition (Reference 13) and 350°F aged condition is shown below.

Tensile Properties of 6061-T6 Al/Cu Coldweld Joints

	Condition	
	As-Received	Aged 1500 hr at 350°F
Ultimate tensile strength, psi	35,800	36,000
Yield strength, psi	33,150	--
Elongation, % in 2 in.	21	2
Reduction of area, %	70.4	14.4

The 14% reduction in area of the aged specimen (Figure 73) is judged to indicate adequate ductility for the application. Thermal exposure at 350°F of a specimen for 3000 hours was started to determine if embrittling

reactions are taking place. Based upon data generated to date, it appears that the reaction is to strengthen the aluminum alloy by age hardening and thus move the failure area from the aluminum alloy to the joint interface.

A coextruded tubular transition joint specimen of aluminum bonded directly to 304 SS was furnished by Nuclear Metals, Inc., Concord, Mass This joint would provide the simplest transition between the transformer/reactor and the L/C loop. An aluminum to aluminum weld would be made on the transformer/reactor side and a 304 SS to 304 SS weld would be required on the L/C loop side. This specimen was examined metallographically in the as-received condition (Figure 74). Another specimen was examined after exposure in air at 275°F for 350 hours (Figure 75). There was no significant diffusion resulting from the elevated-temperature exposure.

b. Speed Control Terminal Leaders

Prototype 6061 aluminum alloy-copper ceramic terminal leaders to be used on the speed control were received at AGC for process qualification. All samples passed a helium leak test at an internal pressure of 5 psig. Preparations were made for ultrasonic inspection of the bond area to determine if any voids were present.

2. Fabrication Support (Task A.2)

a. Boiler Fabrication

The A-2 boiler surface (9Cr-1Mo alloy steel) was oxidized during final stress relieving because of an air-contaminated argon furnace atmosphere. An investigation into potential procedures for removal of the oxide was conducted. The possibilities considered were: (1) cleaning all internal surfaces with high-temperature NaK, (2) pickling using the applicable solutions of Specification AGC-10226, (3) cleaning with fused sodium hydride, (4) cleaning by hydrogen at elevated temperatures, and (5) leaving the metal in the received condition.

It was decided to use the boiler with the oxide layer for two reasons. First, the other alternatives presented various problems.

Second, the TS-2B boiler (9Cr-1Mo steel) had produced superheated mercury vapor after exposure of internal mercury tubes to flowing air for 1 hour at 1300°F. This exposure would have resulted in an oxide layer similar to that present on the A-2 boiler. A vacuum stress-relieving operation was used to avoid an oxidized surface on boilers A-3 and A-4.

Boilers A-3 and A-4 were degreased prior to stress relieving, using a procedure slightly modified from that used for boiler A-2 (Reference). The procedure modifications were as follows:

(1) With the boiler in the vertical position and the mercury inlet at the top, the tubes were individually power flushed by condensed, hot trichloroethylene (TCE).

(2) The tubes were then filled with TCE and gravity flushed.

(3) The tubes were dried by room temperature nitrogen purge.

(4) The boiler was inverted so that the mercury outlet end was on the top, and steps (1) through (3) were repeated.

(5) The boiler was inverted once more to the original position and only steps (1) and (3) were repeated. Each tube was capped to prevent inadvertent recontamination by either the TCE or the shop atmosphere.

Internal automatic tube welding was monitored at Western Way. Prior to welding of the A-3 and A-4 boilers, detail changes were recommended in the area of pre-weld cleaning and weld machine settings. Subsequent weld samples and additional boiler welds showed an improvement in radiographic quality and in weld contour.

b. Bellows Fabrication

Bellows assemblies are being fabricated by the Palmer Company. They will operate at 700°F with an internal pressure of 20 psi. This component contains weldments of AISI 4340 steel and 9Cr-1Mo steel. A final

closure weld of 9Cr-1Mo to itself is required. The standard SNAP-8 stress relieving temperature for 9Cr-1Mo weldments is 1350 ±25°F; however, the A_{C1} temperature for AISI 4340 may be 1300°F or slightly lower, depending on chemistry variations and fabrication history. If the temperature of AISI 4340 components during stress relief exceeds the A_{C1} temperature, martensite transformation occurs during cooling. The impact strength and ductility of the 4340 would be reduced and could lead to service failures. Although an extra stress relief at a lower temperature will temper the martensite and restore satisfactory material properties, it was decided instead that the stress relief of the final weldment on the bellows shall be performed at 1225 ±25°F - not 1350 ±25°F. The use of this temperature avoids possible martensite formation in the AISI 4340 and the necessity of a double stress relief.

To determine the effect of the 1225°F stress-relieving temperature on the 9Cr-1Mo and on the AISI 4340, a series of stress-relieving treatments was performed on welded 9Cr-1Mo tube (1 in. OD by 0.109 in. wall) and welded AISI 4340 plate stock, 3/4-in. thick. Table 9 presents the results of the tests. On the heat of AISI 4340 investigated, weld metal softening continued through 1350°F and hardening occurred at 1400°F. The one-point increase in hardness as measured on the 1275°F specimens, is considered to be within experimental error and not indicative of hardness. Definite hardening of the AISI 4340 parent metal occurred when the 1400°F stress-relieving temperature was employed.

c. Local Stress Relief of 9Cr-1Mo Joints

The connection joints of several components were locally stress relieved using the procedure described by Process Specification AGC-10338. The experience of performing the procedure on these additional components led to revision of the specification.

The thermocouples were repositioned on the part. It was found most practical to attach the thermocouples on the outer diameter of the weld joint by capacitance discharge welding rather than attaching them to the inner diameter of the weld joint. Greater accuracy in temperature measurements resulted.

Provision for additional cooling of the Conoseal flange through use of an internal cooling coil was added. The requirement for keeping the flange temperature below 500°F is difficult to meet when the weld joint is only 3/4 in. from the flange sealing surface. Temperatures of 495°F had been encountered on some flanges. In the event that for some configurations the 500°F maximum temperature could not be maintained, additional internal cooling would be necessary.

The 9Cr-1Mo Conoseal flange welded joints of the A-3 boiler and A-1 and A-2 mercury TMA were locally stress relieved in accordance with Specification AGC-10338 using induction heating. To avoid inductor overheating, which occurred occasionally in the past, valve and line restrictions in the incoming water coolant lines were removed.

Induction heating was also employed to stress relieve welded joints of 9Cr-1Mo to 316 nipples on two Chempump mercury inlet and outlet lines. The pump bodies were maintained below 150°F during the 1350°F stress relieving operation by flowing water through copper tubing wrapped around the base of the inlet and outlet mercury lines.

An electrical resistance clamshell heater was employed to locally stress relieve a welded 9Cr-1Mo to 316 joint at 1350°F for 1 hour on the mercury inlet line of RPL-2. Argon was flowed through the boiler inlet line during heating and cooling.

d. Electrical Components

Sample welds were prepared representative of two configurations of copper braid to copper terminal connections for the transformer-reactor assembly. These samples were sectioned and it was determined that the procedure used provided satisfactory weld penetration as shown in Figures 76 and 77.

Sample work was accomplished on joining of rectifier terminals (diodes) for the transformer-reactor assembly. The two terminal materials being joined were alloy 52 (52% Ni, 48% Fe) and oxygen-free copper. Metallographic samples (Figure 78) indicated satisfactory joints. They are primarily TIG brazed with a small amount of fusion occurring between the two materials. To facilitate assembly of the diodes, a dummy section of the -1 model speed control module was prepared. Using this dummy, it was possible to develop heat sinks and an assembly sequence for the module. Thermocouples were attached to several diodes to determine the temperatures reached at sensitive portions of the diodes during welding. The heat sinks satisfactorily maintained diode temperatures below 300°F, the permissible maximum.

3. Specifications

The following specifications were issued or modified during the report period:

AGC-10354 - "Development Material Specification, Steel, Bearing, AISI M50, Requirements for"

AGC-10319/2 - "Degreasing of Non-Precision SNAP-8 Components and Systems, Procedure for"

AGC-10319/3 - "Acid Pickling of Non-Precision SNAP-8 Components and Systems, Procedure for"

AGC-10227 - "Welding, Fusion, SNAP-8 Materials"

AGC-10331 - "Electrical Connections, Inert-Arc Welding of, Procedure for"

B. SYSTEM FLUIDS EVALUATION (Task A.4)

1. Fluid Analysis Procedures

Analytical methods for evaluating the Mix-4P3E were established through a laboratory program which was completed during the report period.

a. Gas Chromatographic Determination of Isomer Ratios and Volatile Impurities

A method was selected for identification and quantitative analysis of the isomer distribution in the fluid, and to establish the identity and quantitative distribution of volatiles and possible homologues.

Three potential partitioning fluids were evaluated. These were Dow Corning DC-710, Dow Corning High Vacuum Grease, and General Electric SE-52. The DC-710 fluid was unsatisfactory because it resulted in "bleeding," which is the emission of volatiles from the column fluid caused by thermal breakdown. These volatiles fog the results of the volatiles contained in the Mix-4P3E. The SE-52 fluid was selected because it gave better and sharper resolution of the isomers than the High Vacuum Grease. The developed procedure will be issued as part of Aerojet Standard AGC-STD-2003, "Chemicals and Materials, Sampling and Testing."

b. Halogen Analysis

A satisfactory analysis procedure for determination of total halogen content (allowable up to 0.05%) was established. The method is a modification of ASTM-D1317-57T, "Method of Test of Chlorine in New and Used Lubricants." In this method, a toluene solution of the sample is refluxed with sodium metal in the presence of a small amount of butanol. This converts the halogens to an easily ionizable sodium salt. Reproducible results were obtained during the test program. This method will be incorporated into AGC-STD-3003 as Method 5604, "Halogens in Organic Compounds, Determination of."

c. Phenol Analysis

Phenols and other acidic materials in the Mix-4P3E will be determined by nonaqueous titration. This method consists of dissolving the sample of Mix-4P3E in pyridine and titrating to a visual or potentiometric endpoint with a standard solution of potassium hydroxide in isopropyl alcohol (nonaqueous solution). The procedure is being incorporated into AGC-STD-3003 as Method 5106.1, "Acids, Very Weak, In Organic Compounds by Nonaqueous Titration, Determination of."

2. Materials Compatibility

A review of available literature on the compatibility of copper and polyphenyl ethers was made and a memorandum issued. The conclusions from the data were (a) in a nonradiation atmosphere, SNAP-8 conditions should not affect either the copper or the polyphenyl ether, and (b) in an irradiation atmosphere, copper is attacked.

3. Post-Test Fluid Analysis

The Mix-4P3E used during the modified endurance test of the lubricant-coolant pump motor (L/C PMA) was analyzed after 500 hours. A slight decrease in room-temperature viscosity (from 205.5 to 197.2 centistokes) and an increase in pour point (from 15 to 32°F) were observed. There was no change in isomer distribution or impurity content. The increase in pour point may be a manifestation of a change of the fluid away from supercooling towards crystallization.

C. BOILER MATERIALS AND FABRICATION DEVELOPMENT

1. 9Cr-1Mo Weld (Task D.1.a)

The objective of this task is to establish the gross strength efficiency of 9Cr-1Mo steel welds by elevated-temperature, tensile and creep-rupture tests at 1325°F, the approximate maximum operating temperature of the boiler.

Eight sheet specimens of 9Cr-1Mo material are being tested in air at 1325°F, as described in the preceding quarterly report (Reference 4).

Calibration of the furnaces in the creep machines was completed and four tests were started.

Creep Tests on 9Cr-1Mo Alloy Steel

Specimen No.	Condition	Stress, psi
1	Transverse weld at the center of the gage section	2300
6	As-received	2300
2	Transverse weld at the center of the gage section	1600
5	As-received	1600

Specimen No. 6 ruptured after 1070 hours of testing and the remaining specimens have accumulated 1290 hours of time at their respective test conditions.

2. 9Cr-1Mo/316 SS Bimetal Tube (Task D.1.d)

The objective of this task is to establish the availability of a bimetal tube comprised of nonrefractory, conventional materials. This tubing will be evaluated to establish its utility as a backup material to the 9Cr-1Mo steel mercury-containment tube for boiler service.

A capsule corrosion task was initiated during the report period to determine the mercury corrosion resistance of welded joints in bimetallic 9Cr-1Mo/Type 316 stainless steel and Cb/Type 316 stainless steel tubing. The tubing was supplied by Nuclear Metals, Concord, Mass., and it was fabricated using the hot extrusion cold drawing process. The refluxing capsules (Figure 79) will be operated so that one welded joint is below the mercury boiling interface and the second welded joint is in the area where mercury vapor is condensing.

Eight capsules will be tested as outlined below. A set of capsules will be removed and evaluated after 1000 and 2000 hours of exposure at 1150°F. One extra capsule body of each item listed will be made so that unexposed welds can be evaluated and compared to welds exposed to mercury in the capsule welded joints.

Mercury Reflux Capsules

Item	Number of Capsules	Material	Fabricated by	Method of Welding
1	2	9Cr-1Mo/316SS Bimetallic tubing	SNAP-8 Division, Von Karman Center	TIG (Tungsten inert gas)
2	2	9Cr-1Mo/316SS Bimetallic tubing	AGN	TIG
3	2	Cb/316SS Bimetallic tubing	Airite Products, Los Angeles, Calif.	Electron beam
4	2	9Cr-1Mo Unclad	AGN	TIG

The capsules fabricated from unclad 9Cr-1Mo tubing will be used for control samples when evaluating the 9Cr-1Mo/316/SS clad tubing welded joints. All capsules will be heated in the SNAP-8 capsule test furnaces described in Reference 14.

During this report period the eight capsules and the extra capsule bodies were fabricated. Eight capsules were filled with mercury to the level indicated in Figure 79 and evacuated to a vacuum of less than 1 micron. The fill tubes on the capsules were pinched while the capsules were under vacuum and seal welded. The capsules were loaded into one furnace and 218 hours of exposure at 1150°F were completed at the end of the report period.

3. 9Cr-1Mo/316 Transition Joint Development (Task D.1.e)

The objective of this task is to evaluate welded transition joints connecting 9Cr-1Mo steel and 316 SS using 310 SS weld-filler metal. Such a joint is required at various interfaces between the first three loops of the SNAP-8 system. The joint must withstand extended service at a maximum temperature of approximately 1325°F (at the mercury-superheated-vapor manifold of the boiler). The specimen and planned exposure test are described in (Reference 3).

The startup cycle phase of the evaluation was completed. Measurements made on the specimens after the simulated startup phase gave no indication of creep. The endurance testing phase was started and 1454 hours of exposure were accrued during the report period. The conditions of test are described in Figures 80 and 81.

4. Refractory Bimetal Tube Material Development (Task D.1.f)

The objective of this task is to establish the availability of refractory-bimetal tubing as a backup for mercury containment in the SNAP-8 system if experience indicates that 9Cr-1Mo steel (the present reference material) does not exhibit sufficient mercury-corrosion resistance for a life of 10,000 hours. If direct-bonded tubing (refractory to 316 SS) cannot be fabricated or proves to be unusable because of elevated-temperature diffusion effects, a source is to be developed for refractory-bimetal tubing fabricated using an interface material or materials between the refractory and the 316 SS.

Thermal exposure of multimetal bonded specimens from Nuclear Metals, Inc., Concord, Mass., and from Metals & Controls, Inc., Attleboro, Mass., was completed. The specimens were placed in storage for future evaluation. Included are bonded specimens of each of the following systems which were exposed at 1350 and 1450°F in a vacuum of 10^{-5} Torr for 500, 1000 and 2500 hours.

Cold-Bonded Flat-Sheet Specimens

Cb/316 SS
Cb/Fe/316 SS
Cb/V/Fe/316 SS
Cb/Mo/Ni/316 SS
Cb/Cu-1/4Zr/316 SS
Ta/Fe/316 SS
Ta/Mo/Ni/316 SS
Cb-1Zr/316 SS
Cb-1Zr/Fe/316 SS
Cb-1Zr/V/Fe/316 SS
Cb-1Zr/Mo/Ni/316 SS
Ta/316 SS
Ta/V/Fe/316 SS
Ta/Mo/Cr/316 SS

Coextruded Round Specimens

Cb/316 SS Tube
Cb/V/Fe/316 SS Bar

5. Refractory Bimetal Brazing Development (Task D.2.b)

The objective of this task is to develop a procedure for producing a welded and back-brazed tube-tube sheet joint. The tube and tube sheet are both constructed of a refractory/316 SS bimetal system. The joint must be so designed that mercury flowing in the tube shall be exposed only to the refractory. Pyromet Co., San Carlos, California, is developing a joining procedure under a SNAP-8 subcontract.

Flat Cb/316 SS bimetal tube sheet specimens were fabricated by Pyromet for back-brazing development. An intermediate layer of iron was used to provide a transition of thermal expansion coefficients across the bond area. This transition was deemed necessary because of previous unsuccessful attempts to produce a bond between the 0.050-in.-thick Cb and the 0.250-in.-thick 316 SS. A 97.2 Au-2.8 Pd braze alloy was used at the Cb/Fe interface and a 50 Au-50 Ni [illegible]

alloy at the Fe/316 SS interface. The layers were braze-bonded using the Horton-Clad Process.* A cooling rate of 100°F/hour from the bonding temperature, 2000°F, was used to further minimize the possibility of bond separation.

Four sets of machined tube-tube sheet joint specimens were prepared by Pyromet and shipped to the Aerojet Von Karman Center. These specimens consist of Cb/316 SS bimetal tubes and the multi-metal tube sheets described above. The joint configuration is shown in Figure 82. These specimens are to be seal welded on the Cb side by Aerojet-General and then returned to Pyromet for development of the back-brazing technique.

D. MERCURY CORROSION LOOP PROGRAM

The purpose of operating the dynamic corrosion loops (1/16th scale) is to determine corrosion and mass transfer patterns in the mercury and NaK loops of the SNAP-8 system. Corrosion Loops 1 and 2 were constructed of Haynes 25 alloy. Operation of the first loop has been completed (Reference 15), and the second loop has been converted into Component Test Loop 2 (CTL 2), which is being operated to check the performance of certain components to be used in subsequent loops. Corrosion Loops 3, 4, and 5 are constructed with 9Cr-1Mo as the mercury containment material. The NaK primary loop is constructed of AISI Type 316 stainless steel with a section of chromized Hastelloy N in the high-temperature area, and a section of Hastelloy C in the low-temperature area.

1. Corrosion Loops 3 and 4

a. Fabrication

(1) Components

The fabrication of the components for the NaK purification system for the primary and condensing loops of CL 4 was completed. The fabrication of the liquid corrosion product separator for CL 4, described in Reference 4, was completed. The material used in construction of the liquid separator was 9Cr-1Mo except for the columbium and iron wool.

*A proprietary process of Chicago Bridge and Iron Co. whereby two or more metals are bonded by exposing the assembly composite to a high temperature under vacuum. A braze alloy is utilized between the surfaces to be bonded.

(2) Assembly

The assembly of CL 4 continued throughout the quarter. The assembly and welding of the NaK primary and condensing system was completed and the assembly of the 9Cr-1Mo mercury system was 50% completed. The hot trap in the NaK purification system of CL 4 was not installed since the experience with CL 3 indicated that the oxide level in the NaK could be controlled with the cold trap. The turbine simulator valve between the blade mockup and the condenser inlet was not installed in the mercury system of CL 4 since operation of CL 3 showed the valve was not necessary.

The two mercury Chempumps scheduled for installation in CL 4 were shipped to the SNAP-8 Division at Von Karman Center for use as backup pumps for Rated Power Loop 2.

b. Operation

(1) NaK Systems

As reported in the previous quarterly report, the oxide level in the primary NaK system of CL 3 was reduced to 19 ppm by using the cold trap only. A plugging valve was used to determine the oxide level. The oxide level in the primary NaK system of CL 3 was determined three times during the report period.

Oxide Level in Primary Loop of CL 3

Operation Time (hours)	Oxide Level (ppm)	Remarks
100	38	Cold trapped (250°F) 4 hours oxide level reduced to 18 ppm
530	20	
1130	< 20	

The loop operated steadily at all times, and no problems were encountered in keeping the oxide level at 20 ppm or less. The oxide level determination made at 1130 hours was done while the mercury system was operating.

The condensing NaK system operated satisfactorily during the report period.

(2) Mercury System

The operating conditions of the mercury system of CL 3 are summarized in Table 10 and Figure 83. Table 10 shows selected state points around the system at various times from the start of mercury boiling. Figure 83 is a daily plot of the mercury boiler outlet temperature, the mercury saturation temperature that corresponds to the boiler outlet pressure, the mercury flow rate, and the effective flow area of the choked nozzle.

Mercury boiling in CL 3 was restarted on 17 May, but superheated mercury vapor was not obtained immediately. After a total of 195 hours of operation, a sudden increase in the mercury boiler outlet temperature (on 22 May) indicated that superheat conditions were achieved (Figure 83). The temperature increase occurred when the loop was operating stably. The adjustable choked nozzle was opened slowly to lower the boiler outlet pressure over an 8-hour period just prior to the first indication of improved boiler performance. The initial increase in the mercury boiler outlet temperature was accomplished in 1 hour followed by a gradual improvement in boiler performance.

The maximum boiler outlet temperature recorded was 1210°F with a boiler outlet pressure of 265 psia (1265°F, 265 psia are rated conditions). The loop operated at this condition until 29 May when a momentary electrical power failure caused the loop to shut down. Mercury boiling was resumed 10 hours later and superheat was not achieved until 3 hours after the boiling was started. The boiler output temperature did not reach the 1210°F temperature previously obtained (see Figure 83).

The loop was shut down on 1 June upon failure of the mercury flow control system. During the loop shutdown the mercury inventory was forced to the expansion tank and the loop was pressurized with argon. It was found that the mercury flow control problem was due to the rupture of the diaphragm in the differential pressure transducer that measures the pressure difference across the Venturi flow meter. Rupture of the diaphragm was caused by a line pressure surge

when the mercury pump was started. The differential pressure transducer was replaced and the operating procedure was modified so that the differential pressure transducer did not experience the initial pressure surge when the mercury pump was first started.

Mercury boiling was started on 19 June, following the procedure for loop startup given in the previous quarterly report. Superheated mercury vapor was obtained immediately with a mercury boiler outlet temperature of 1050°F at a saturation temperature of 960°F. During the initial operation, a low-pressure condition at the pump outlet caused the automatic switchover system to activate the standby pump, causing a pressure surge in the mercury line. This surge damaged the differential pressure transducer causing the mercury flow control system to fail. After this time the mercury flow rate was controlled manually and the mercury flow rate was calculated from a heat balance across the mercury preheater and the mercury boiler. The manual control of the mercury flow accounts for the changes in mercury flow shown in Figure 83. After stable operation was achieved, the mercury flow rate was increased gradually. This resulted in an increasing boiler outlet pressure, but the boiler outlet temperature did not increase. It was then necessary to open the choked nozzle to maintain some degree of superheat. This condition lasted for approximately 200 hours until 30 June when the flow rate was reduced intentionally to try to increase the degree of superheat. When this was done the degree of superheat increased from 50 to 200°F and it was necessary to close the choked nozzle to maintain boiler output pressure. This sequence can be followed on Figure 83 between the 19 June startup and 4 July.

The mercury flow rate and boiler outlet pressure were then adjusted until the rated boiler output pressure of 265 psia was obtained. The maximum boiler output temperature reached was 1210°F and the loop operated at these conditions throughout the remainder of the report period.

(3) Discussion

Boiler performance, showing the improvement that occurred during CL 3 operation, is plotted in Figures 84, 85, and 86. The data for these figures were taken before superheated mercury vapor was obtained (Figure 84 - 19 May) immediately after superheat conditions were obtained (Figure 85 - 23 May), and when the maximum mercury outlet temperature was first

reached (Figure 86 - 29 May). No explanation can be given for the sudden increase in boiler performance noted on 22 May nor for the constant improvement in performance with time. Previous experience with forced convection mercury boilers has indicated the need for a "run in" period for some boilers before superheated mercury vapor is produced.

During the operation of the mercury boiler in CL 3 there was no temperature drop in the NaK temperature in the last 3 or 4 ft of the boiler inlet plug section. The heat transfer in this plug region of the boiler is lower than was predicted in the original design by a factor of almost 2. The calculated heat flux in the plug region from Figure 86 is 18,110 Btu/hr-ft^2 while the predicted value was 35,000 Btu/hr-ft^2. It is possible that an increase in boiler performance could be achieved by changing the geometry of the inlet plug to give a higher mass flow rate in the plug region of the boiler.

As shown in Figure 83, it was necessary to open the choked nozzle between the 19 June startup and 25 June to keep the boiler outlet pressure from increasing. It was hypothesized that buildup of corrosion products started soon after the startup because the degree of superheat was small (approximately 50°F). When the boiler was operating in this condition the area in the boiler available for drying the mercury vapor was small, and apparently corrosion products were carried over with mercury droplets, depositing them in the nozzle.

When the mercury flow rate was decreased on 30 June, the degree of superheat increased to approximately 200°F. After this, it was necessary to close the nozzle gradually to maintain boiler outlet pressure even when the mercury flow rate was subsequently raised. Apparently when the superheat increased the area in the boiler for drying, the mercury vapor increased so that the mercury droplets did not carry over corrosion products that deposited in the nozzle. Instead, the corrosion products either deposited on the boiler tube wall before reaching the nozzle or were carried through the nozzle without sticking. Finally, when the corrosion product buildup stopped, the high-velocity vapor must have eroded away the deposits. This can be followed for the period 30 June to 7 July in Figure 83.

During operation of CL 3 to date the boiler has not achieved rated superheat temperature (1265°F). This is not expected to affect the total amount of mercury corrosion in the boiler since the rated mercury boiling temperature (1075°F) has been achieved and corrosion by superheated mercury vapor is considered negligible. However, the corrosion pattern in the boiler may be shifted because of the poor performance of the inlet plug region of the boiler.

c. Evaluation

The purpose of this task is to evaluate the NaK and mercury systems of the corrosion loops for mass transfer and corrosion patterns when loop operation is completed.

A metallurgical evaluation procedure was outlined in rough draft form. The preliminary metallurgical evaluation of as-received samples of materials used in the construction of the loop was started.

2. Corrosion Product Separator Studies

The leak on the NaK side of the boiler in CTL 2 was repaired and the boiler was refilled with NaK. When the boiler was started the NaK level system would not function properly, apparently because of an oxide plug in the line from the bottom of the boiler to the level tank. Attempts to dissolve the plug in the line so that the level system would operate were not successful. Since the boiler would not produce superheated mercury vapor during its last run, and because the problem with the NaK level system could not be corrected, it was decided to replace the boiler assembly. A spare Haynes 25 boiler was installed of design similar to the one in CTL 2.

The loop is scheduled to be started early in the next quarter so that testing of the vapor phase corrosion product separator, described in the previous quarterly report, can be completed.

IX. CLEAN ASSEMBLY AND OVERHAUL OPERATIONS

Upon completion, the Aerojet Von Karman Center new clean assembly and overhaul facility (Figure 87) will provide a completely integrated capability for the assembly and overhaul of precision components and complete SNAP-8 power conversion systems. The high-bay final assembly area in Building 179 is scheduled for completion during September 1964. Upon its completion in the spring of 1965, the new component assembly area in Building 179/112 will replace the interim clean assembly area now in use in Building 183.

The high-bay final assembly area consists of two 20 ft by 20 ft clean assembly cells with associated support area. High-efficiency filters are designed to provide the assembly cells with an environmental cleanliness equal to or cleaner than Class 100,000 of Federal Standard 209 (Level 5 of AGC-STD-1191, Figure 88), during final assembly operations. During preliminary assembly of power conversion systems (PCS-1, PCS-2, etc.), two of the plastic curtain sides may be rolled back to provide free access under normal, less restrictive operating conditions. A two-speed, two-ton capacity bridge crane in each assembly cell provides for precision lifting to a height of 21 ft.

The component assembly area of approximately 30 by 50 ft is being designed for an overall cleanliness level equivalent to Class 100,000 with Class 10,000 (Level 4 of AGC-STD-1191) or cleaner to be provided by the laminar flow work stations. Experience with the present interim clean assembly area in Building 183 has shown a consistent capability of achieving environmental particle concentrations up to 20 times lower than the above nominal design cleanliness levels.

The interim clean room (Figure 89) in Building 183 has been successfully operated for several months at cleanliness levels equivalent to, or cleaner than, Class 1000 of Federal Standard 209 (Level 3 of AGC-STD-1191, Figure 88) during assembly operations. Delays in receiving certified temperature and humidity measuring equipment delayed formal certification of the clean assembly area until September 1964. Operations are performed in accordance with specification AGC-10336, which was released on 4 June 1964.

Degreasing and ultrasonic cleaning equipment uses Freon PCA as the cleaning agent for immersible components. During September 1964 a 20-gpm system will be completed which will circulate filtered Freon for cleaning large items and piping systems such as the test loops and complete power conversion systems. In addition to complete precision assembly and measuring equipment, the clean assembly area is equipped with a helium leak detector, a halogen leak detector, and a Gisholt balancing machine. Operators are certified for balancing of precision rotating components.

X. RELIABILITY

A. MANAGEMENT AND PLANNING

Meetings were held with Mr. F. Spiegl (NASA-LeRC) where such topics were discussed as (1) Reliability Program Plan (AGC Report No. 2406); (2) the coordination of activities between AGC and AI; (3) proposed revisions to NASA Specification 417-4; (4) planned FY 1965 Reliability Program; (5) Failure Analysis Reports 1146 and 1148, SNAP-8 Division Procedure VI-A6, "Deviation/Waiver" (Second Draft); and (6) the NS Reliability Program Requirements. A preliminary revised draft of the Nuclear System Reliability Program Requirements (343:R-64-0120) was coordinated with W. Brown (NASA-LeRC), the EGS Project Office, and SNAP-8 Quality Assurance and Program Control Departments. This was done to assure the reflection of informal NASA suggestions in making the document compatible with the unreleased Revision A of NASA Specification 417-4A, current concepts of the SNAP-8 EGS Project Office, and possible interfaces with SNAP-8 Quality Assurance. This draft was finalized on 16 August 1964, and will be submitted to NASA-Lewis for approval during the next report period.

Reliability documentation requirements pertaining to testing were presented at the Weekly Test Engineering Seminar. Reliability considerations were discussed with cognizant personnel on the development of an optimum component checkout test program. Coordination meetings were held to improve the correlation between test reports and test requests. It was recommended that those test requests and test reports issued after February 1964 be reviewed to assure conformance with SNAP-8 Division Procedure VI-B1, "Test Plans, Specifications, Procedures, and Reports," issued 24 February 1964.

An investigation was made of the NASA QA audit results pertaining to reliability. Results of this investigation were submitted to SNAP-8 Program Control. The recommended revision to Division Procedure VI-B4, "Test Equipment Fabrication Requirements," was coordinated with Program Control.

B. RELIABILITY SYSTEM STATISTICAL ANALYSIS

Technical Memorandum No. TM:343:64-3-232, "SNAP-8 EGS Reliability Apportionment Methodology and Meteoroid Survivability," was upgraded and published. Coordination efforts in relation to GPTF NS/PCS integration were continued. Design

review studies of the NS/PCS integration were conducted. Analysis of the NS/PCS/GPS test sequencing continued, including NS interface and related safety considerations. The NS/PCS apportionment was reviewed regarding failure rate apportionment and reapportionment upgrading. An investigation was conducted relative to the impact of changes to the NS and PCS reliability requirements in relationship to the specified NPS reliability requirement of 0.90 (NASA Specification 417-1A, preliminary draft). The analyses indicated that although the revised specifications did not change the overall reliability requirement for the EGS, a specific reliability requirement for the NPS (0.90) was imposed. This constraint causes a significant change in the reliability values previously apportioned to the NS, PCS, and FRA.

The reliability analysis of the parasitic load resistor was upgraded and coordinated with cognizant personnel. Reliability Action Request No. 199 was issued requesting specific review of welded structures, potential elimination of half of the tube weldments to space, and reduction of the number of elements per leg. A statistical review of the parasitic load resistor design presented by Heat Engineering and Supply Company was performed; recommendations were directed to the responsible design engineer.

The reliability failure mode and effects analysis procedure including general format, detailed instructions, logic diagram, numerical allotment, and minimum reliability component requirements was upgraded; finalization will be completed during the next report period.

A reliability data search was initiated on several hardware components pertaining to their use in the EGS. A feasibility study of using Weibull distribution for bearing design and life requirements was initiated. Particular emphasis was placed on the development of techniques that are applicable to reliabilities greater than 99.9.

The preliminary draft of the upgraded reliability procedure for specifying required safety margins and design life was completed and distributed for review. Applicable recommendations integrated into this procedure included nominal values for the case of normally distributed stresses and normally distributed failure distributions.

C. RELIABILITY DESIGN ENGINEERING

The PCS design review check lists for systems-loops and components were issued for design review use.

Reliability personnel attended the final design review meeting on the mercury injection system, as well as the preliminary design review meeting on the expansion reservoir. The design review of the condenser rolled taper tube program and subsequent presentation to NASA was also attended.

Specific design review questions pertaining to the S8DS final design review were prepared and submitted to the EGS Project Office.

The parasitic load resistor design review was held with cognizant SNAP-8 personnel and the vendor to review the current design status.

The insulating tape used on the 450-kw electric heater element connection repair was reviewed and approved. The bearing cavity test results were reviewed with the design engineer. PCS-2 condenser drawings were reviewed and applicable reliability recommendations were made. These recommendations were scheduled to be incorporated as "A" changes. Previously issued reliability recommendations pertaining to the detail prints of the turbine were reviewed to check the coordination between Reliability and Design Engineering. Reliability liaison on NS/PCS integration was continued.

Reliability's participation in the RPL-2 Task Force activities included (1) RPL-2 NaK primary and HRL system installation checkout and engineering review; (2) review of piping flexibility analysis on spools (374-64-206-216, and -226), piping stress analysis, instrumentation, piping layout, and design prints (including the analysis received from AETRON and C. F. Braun Corporation's analysis for lines 1, 3, and 6); (3) line 1 hanger analysis review (by type and location); (4) pipe hanger and support installation; (5) review of the L/C system, using GN_2S-1 experience [specific corrective action (ET-378 and water piping) was requested; this RPL-2 L/C system was subsequently approved for system checkouts]; (6) engineering surveillance during dry and wet checkout of the NaK primary system; (7) review of the mercury cover gas system and liquid mercury lines; (8) addition of a direct vent valve to the HRL NaK expansion tank; (9) installation of insulation, hangers, and restraints to the HRL and mercury piping; (10) task force follow-up during loop operation; and (11) definition of RPL-2 rework requirements necessary prior to further operations.

Requirements for the pressure gage indicating NaK level in the primary and HRL expansion tanks were coordinated with test personnel. The design of the 3-position electric contact pole level indicators for the primary NaK tank and HRL expansion tank was reviewed. The modification of the control console to include dynamic gages for improvement of loop operational control was reviewed.

A coordination meeting on AGC Specification 10356 ["Motor Assembly, HRL (-X Model) Design Configuration 095367-1, Assembly and Inspection of"] was attended, and reliability requirements were included for publication.

Three-hundred and ninety-nine design drawings were reviewed, and reliability recommendations were coordinated with cognizant personnel. Twenty-two specifications were reviewed, including development component specifications AGC 10281 ("Inverter, Rotary, Hermetically-Sealed"), and AGC-10264 ("Contactor, SNAP-8"). Applicable reliability recommendations concerning all specifications were coordinated with the cognizant engineers.

D. OPERATIONS EVALUATION AND FAILURE ANALYSIS

Three-hundred and forty-one test equipment drawings and one-hundred and five inspection documents were reviewed, and reliability requirements coordinated with cognizant engineers. Reliability personnel participated in the engineering review of the PCS-2 expansion reservoir test request. Specific reliability requirements and comments were discussed and were included in the test request as applicable.

The RPL-2 loop operation and checkout procedure, RPL-2-005 through -011, -022, -023, and -024, was reviewed and approved. The cold-gas electrical system test procedure (Rev 0) was reviewed. The test procedures for the auxiliary start loop heat exchanger and the -1 boiler assembly to be tested in the RPL-2 were reviewed. Reliability personnel participated in the preliminary design review on the LNL-3 redesign, and presented reliability considerations. The NASA audit of QA activities regarding interface with reliability requirements was assessed and preliminary recommendations submitted to management. The -1 model boiler test procedure and six RPL-2 shakedown procedures were reviewed.

Three Reliability Failure Reports (RFR) were issued and distributed to NASA concerning incidental equipment failures at AGN on the mercury corrosion loop No. 3.

The test request and test procedure for the GN_2S-1 test loop, including TAA No. 1, were approved. Two failure reports (RFR 1084 and RFR 1085) were processed concerning GE-installed alternator thermocouples which failed during the first TAA test. Investigation by the Reliability Department of RFR 1084 revealed that the turbine thrust seal (Spirolox) retaining ring had worked out and was rubbing against the first-stage turbine wheel and the antirotation pin had also worked out and was missing. The turbine inlet housing was reworked by the SNAP-8 Assembly Department. Following reassembly of the housing to the TAA assembly in the GN_2S-1 loop, Test Run D-5-R-8 was performed on 18 June 1964. The TAA overspeed trip switch caused an automatic test shutdown when the d-c converter for the visual data recorder failed (RFR 1085). Disassembly and inspection of TAA No. 1 in the SNAP-8 assembly area was monitored. The static and startup testing of this loop was monitored. During startup, the normally opened solenoid valve delta 44 and delta 45 (Reference P and I drawing E-100914) failed (RFR 1083). Failure of this valve was investigated at AGC, and an investigation was also performed by the vendor on a similar valve. These test support equipment valves were removed and replaced with the same type of valve.

Test activities in Buildings 180, 183, 187, and 194 were monitored. These activities included (1) rework of RPL-2; (2) adequacy of equipment installation, and installation of RPL-2 piping (lines 1 through 3, and 5 through 9) including fitting and wet shakedown; (3) dry checkout of the RPL-2 L/C system; (4) RPL-2 build-up and instrumentation installation; (5) wet shakedown checkout of the L/C system; (6) dry operational checkout of RPL-2, wet checkout of the RPL-2 primary NaK loop, and dry checkout of the HRL; and (7) RPL-2 fabrication activities (including replacement of faulty valve controllers, replacing primary NaK tank and HRL tank level indicators, repairing the replacement gas heater, and performing a wet shakedown of the primary and HRL NaK loops during which mercury super-heat was achieved).

The line heater on the supply tank return line (RPL-2 L/C system) shorted to the tubing, burning a hole in the tube and causing the heating element

to burn out (RFR 1198). The damaged section of line was replaced and reinstalled so as to eliminate a bend in the line where the new clam-shell heater was installed. Wet shakedown and checkout of this system was continued following these repairs.

Malfunction of the 420-kw electric heater in the RPL-2 primary NaK loop during wet checkout (RFR 1176) was investigated and classified as incidental. Faulty heater elements were eliminated and all necessary rework was completed before operational checkout. A subsequent primary NaK heater failure (RFR 1170) was investigated, indicating that a catastrophic failure occurred in the heater's center section when NaK leaked to the atmosphere and a spontaneous fire occurred, causing extensive damage to the heater. The vendor was requested to help determine the cause of the failure. Preliminary corrective action was to remove the heater from the RPL-2 NaK loop and replumb the loop. Final corrective action will include installation of a second "gas-fired" heater prior to completion of wet checkout.

During preliminary checkout of the RPL-2 mercury loop and dry checkout of the RPL-2, it was determined that the cover gas and vacuum systems were not in accordance with issued loop schematics. Corrective action was implemented by the RPL-2 task force, including definition of the cover gas and vacuum system and revision of associated test procedures.

RPL-2 mercury Chempump, Model 10, S/N-1 failed during wet checkout (RFR 0860) and was replaced with Chempump Model 10, S/N-2A, which also failed during wet checkout (RFR 1168). Investigation of these failures indicated the same basic failure modes (failed journal bearings and stator-rotor cans severely scored or ruptured) of which photographs were taken. Further investigation of S/N-1 and S/N-2A Chempump failures was deferred pending a complete damage analysis by the vendor. Chempump CFHT-7-1/2-6S (S/N-12878-2) was installed in the mercury loop with supplementary instrumentation which was expected to help define the primary cause of failure of the Chempump which it replaced. During preparation of the RPL-2 loop before startup, the Chempump was accidentally started dry and without the Dowtherm coolant system in operation. The Chempump overheated sufficiently to create a high oil pressure in the stator, causing collapse and rupture. Oil from the failed Chempump contaminated the mercury system. This failure was classified as incidental (RFR 0861), and a positive lockout of the electrical circuit was implemented as corrective action. A second CFHT-7-1/2-6S Chempump was installed and is currently being used during the completion of wet checkout.

E. RELIABILITY CONTROL AND LIAISON

Reliability analysis of the TAA bearing lubricant development program (Test D-1-B) test data was started. Reliability personnel participated in a meeting on LOL-1 (bearings) test data correlation and continued to assist the cognizant engineer. Reliability personnel also participated in the bearing wear life data analysis review meeting.

Reliability criteria that are pertinent to the selection of an alternate L/C fluid were coordinated with the Materials Department.

It was requested by Reliability that the parasitic load resistor reliability program plan be upgraded by the subcontractor.

A coordination meeting was held with the supplier regarding reliability requirements on the turbine inlet filter.

Hardware documentation from Westinghouse, TRW, GE (Erie and Waynesboro) and AGN was reviewed, including engineering design prints on the alternator and voltage regulator.

The log book for the preprototype alternator (AGC P/N 094162, S/N-481486), submitted by GE, was reviewed. The revised GE (Erie) equipment log was rejected and corrective action initiated and coordinated with cognizant engineers. Data were gathered from various reports and discussed with cognizant engineering personnel regarding the TAA failure on the first alternator. The equipment log book on voltage regulator (No. 2) submitted by GE (Waynesboro) was reviewed.

The GPS startup demonstration testing requirements were reviewed and analyzed to determine the minimum number of starts required. The preliminary GPS test plan was completed and submitted to cognizant personnel for review.

Reliability requirements for the inverter were further clarified for Westinghouse, and coordinated through AGC Procurement. Westinghouse is to submit the required subcontractor's reliability program by 31 August 1964.

Review of AGN progress and interpretation of corrosion loop 3 operational performance was coordinated with cognizant VKC personnel.

REFERENCES

1. C. L. Svoboda, Analysis of the Operating Range of the SNAP-8 Reference System, (U) Aerojet-General Corp. Technical Memorandum No. TM 340:64-1-238, 10 August 1964 (Confidential RD).

2. A. Levitsky, Flange Stress Analysis - PCS-1, PCS-2, Aerojet-General Corp. Technical Memorandum No. TM 340:64-1-186, 30 June 1964.

3. SNAP-8 Electrical Generating System Development Program (U), Aerojet-General Report No. 0390-04-15 (Quarterly), March 1964 (Confidential).

4. SNAP-8 Electrical Generating System Development Program, Aerojet-General Corp. Report No. 0390-04-16, June 1964.

5. I. J. Loeffler, S. Lieblein, and N. Clough, Meteoroid Protection for Space Radiators, ARS Paper 2543-62.

6. J. A. Stevenson and J. C. Grafton, Radiation Heat Transfer Analysis for Space Vehicles, ASD Technical Report 61-119, Part I.

7. R. G. Geimer, R. L. Sheffer, W. W. Tingle, Evaluation of the Effects of System Tolerances and Degradations on Condensing Temperature and Power Output, Aerojet-General Corp. Technical Memorandum No. TM 340:64-1-226, 21 April 1964.

8. I. P. Wishney, A Dynamic Study of the Condenser Bypass Flow Control As Proposed for SNAP-8, Aerojet-General Corp. Technical Memorandum No. TM 340:64-1-237, 24 July 1964.

9. E. F. Perez, W. W. Tingle, Evaluation of HRL Condensing Temperature Controls, Aerojet-General Corp. Technical Memorandum No. TM 340:64-1-234, 19 June 1964.

10. I. P. Wishney, Additional Investigation of the SNAP-8 Reactor Outlet Temperature Transients (U), Aerojet-General Corp. Technical Memorandum No. 340:64-1-236, 17 August 1964 (Confidential RD).

11. I. P. Wishney, Preliminary Investigation of the SNAP-8 Reactor Outlet Temperature Deadband (U), Aerojet-General Corp. Technical Memorandum No. TM 340:64-1-235, 1 July 1964 (Confidential RD).

12. R. L. Sheffer, Evaluation of SNAP-8 Condensing Temperature Variations, Aerojet-General Corp. Technical Memorandum No. TM 340:64-1-214, 5 March 1964.

13. R. A. Mendelson, Evaluation of Coldwelded Butt Joint Transition Piece, Aerojet-General Corp. Technical Memorandum No. TM 340:64-4-183, 21 January 1964.

14. SNAP-8 Topical Materials Report for 1962, Vol. III - SNAP-8 Mercury Corrosion Materials Research, Aerojet-General Corp. Report No. 2517, August 1963.

15. Mercury Corrosion Loop Testing Program, Aerojet-General Corp. Report No. 0584 (Final), August 1963.

TABLE 1

AEROJET/ATOMICS INTERNATIONAL SYSTEM INTEGRATION ACTIVITIES

Activity	Status
Project Coordinating Committee	Continuing Monthly Meetings
Working Groups	Four Currently Active
Project Engr Groups	GPS/GPTF Group Established
Informal Data Exchanges	Intensified
Resident Offices	Established and Active
Formal Design Reviews	S8DS Compl Prel GPS 29 July
PERT Networks	Joint Master NPS PERT Established
Interface Control	Established; First Joint Drawing Pending
NS/PCS Integration Plan	AI/AEC Review; AGC/NASA Draft

NPS System Design Studies (e.g., Reference System Design Point)

GPS and PCS Support Equipment Design

TABLE 2

SPECTROSCOPIC ANALYSES OF ALLOYING ELEMENTS, %

Elements	1st Remelt M-50 Heat No. 1	1st Remelt M-50 Heat No. 2	5th Remelt M-50	Percent Accuracy of Determination
Ti	0.015	0.015	0.013	±10
Al	0.026	0.027	0.051	±10
As	<0.01	<0.01	<0.01	±10
Co	<0.005	<0.005	<0.005	±10
Cu	0.087	0.086	0.084	±10
Ni	0.061	0.063	0.15	±10
Pb	<0.005	<0.005	<0.005	±10
Si	0.23	0.22	0.23	±10
Sn	0.051	0.017	0.024	±10
Mn	0.17	0.17	0.038	±5*
Mo	4.26	4.32	4.27	±5
V	1.05	1.00	1.00	±2
Cr	4.06	4.00	3.81	±2
Mg	Trace <0.01	Trace <0.01	Trace <0.01	±10
Cb	0.01 to 0.1	0.01 to 0.1	0.01 to 0.1	±10

The following elements were not detected:

Bi, Zr, Ag, Sb, B, Zn, W, Ca

*This is the latest accuracy figure received from National Spectrographic Laboratories.

TABLE 3

DETERMINATION OF TRACE ELEMENT INDICES

$$\Theta = \frac{Al}{\overline{Al}} + \frac{Cu}{\overline{Cu}} + \frac{Ni}{\overline{Ni}}$$

where:

Al, Cu, and Ni = percent content of each element

$\overline{Al}$, $\overline{Cu}$, and $\overline{Ni}$ = mean percent content of each element found in a large number of 52100 samples.

First Remelt M-50,
"Good" Heat No. 1

$$\Theta = \frac{0.026}{0.015} + \frac{0.089}{0.060} + \frac{0.061}{0.070}$$

$$= 4.0$$

First Remelt M-50
"Good" Heat No. 2

$$\Theta = \frac{0.027}{0.015} + \frac{0.086}{0.060} + \frac{0.063}{0.070}$$

$$= 4.0$$

Fifth Remelt M-50
"Poor" Heat

$$\Theta = \frac{0.051}{0.015} + \frac{0.084}{0.060} + \frac{0.150}{0.070}$$

$$= 7.0$$

TABLE 4

GAS CONTENTS OF CONSUMABLE VACUUM-MELTED M-50 STEEL

	1st Remelt M-50		
Gas	Heat No. 1	Heat No. 2	5th Remelt M-50
N_2	0.0040	0.0045	0.0040 ±15%
O_2	0.004	0.003	0.004 ±15%
H_2	0.0007	0.0007	0.0008 ±15%

TABLE 5

HOT STARTING TORQUE EXTRAPOLATIONS IN NaK

Torque (in.-lb)	Volts (L-L)	Frequency (cps)	Volts/Frequency Ratio
In-Air Tests (200°C Winding and Rotor Temperatures)			
23.6*	208	400	0.52
17.1*	88	220	0.40
28.9	114.5	220	0.52
7.25*	19.0	95	0.20
29.0	38.0	95	0.40
49.0	49.4	95	0.52
In-Air Tests (50°C Rotor Temperature)			
19.4**	208	400	0.52
11.7**	88	220	0.40
3.7**	19	95	0.2
In-Air Test (200°C Rotor Temperature)			
21.5	208	400	0.52

*Design voltage and frequency (all values calculated).

**Minimum torque position.

TABLE 6

L/C PMA PERFORMANCE CHARACTERISTICS COMPARISON

Unit	Capacity (gpm)	Head Rise (psi)	Power Input (watts)	Current (amperes)
Development S/N 481501	17	54.6	1498	6.52
First Deliverable S/N 481502	17	53.6	1370	6.3
Second Deliverable S/N 481503	17	65	1494	6.53

TABLE 7

SUMMARY OF ALTERNATE EXPANSION RESERVOIR CONCEPTS

Type	Reliability	Complexity	Weight, lb	Space, cu ft
Cooled gas	Positive action maximum cycle life	Bellow tank 300°F L/C temp rise - 3°F maximum	43.3	5.17
Heated gas	Cycle life reduced 32% at 1100°F	Electric heat for launch and metal heat conductor required	50.0	5.25
Metal springs	Heavier walls for pressure and temperature reduce cycle life	Spring rate difficult to control	885	8.4
Hydraulic force	Same as for metal springs force	Three sets of bellows	356	9.7
High-pressure gas source	Valve performance and leakage reduce reliability	Pressure control range difficult without leakage	41.7	4.55
Pressure relief to tank	Valve performance reduces reliability	Additional valves and lines	52.7	5.52
Pump pressure valve controlled	Valves and pump reduce reliability	Additional valves, pump, and lines	41.7	3.66
Liquid dumped to diaphragm chamber	Valve performance reduces reliability	Additional valves and two reservoirs	106	4.70
Liquid dumped to sphere	Valve performance and gas temperature control	Additional valves and two reservoirs	24.4	2.85

TABLE 8

ORGANIC RESIN WEIGHT LOSS AT 392°F

Material	Type	%Loss* Following 168 hr at 392°F	Following 336 hr at 392°F	Following 504 hr at 392°F	Following 1176 hr at 392°F	Following 1344 hr at 392°F
3M Scotchcast 292	Epoxy impregnant	5.33	6.20	6 93	8.43	8.71
3M Scotchcast 241	Epoxy encapsulant	2.19	2.44	2.70	3.67	3.98
3M Scotchcast 235	-	4.63	5.00	5.32	6.06	6.20
Epoxylite 813-9	-	0.25	0.36	0.51	0.99	1.12
Epoxylite 8793	-	0.28	0.44	0.63	1.09	1.21
Epoxylite 8794	-	0.31	0.52	0.74	1.39	1.54
Epoxylite 2154	-	4.84	6.24	7.65	10.82	11.47
Furane Epocast 17-B	Epoxy encapsulant	0.58	0.78	0.97	1.44	1.54
Furane Epocast 17-A	Epoxy impregnant	0.35	0.51	0.74	1.50	1.68
Furane Epocast 3	Epoxy impregnant	0.51	0.76	1.09	2.06	2.30
Hysol 7-4252	Epoxy encapsulant	2.11	2.79	3.30	4.60	4.92
GE Novalak Epoxy	-	0.22	0.32	0.41	0.66	0.73
GE Bisphenyl A Epoxy	Epoxy encapsulant	0.62	0.80	1.00	1.51	1.63
Dow Corning Sylgard 182	Silicone encapsulant	1.42	1.75	2.03	2.88	3.13
Dow Corning Sylgard 183	Silicone encapsulant	1.49	1.78	1.98	2.49	2.60
Dow Corning Sylgard 7521	Silicone impregnating resin	1.74	2.24	2.65	3.95	4.25

*All percentages are referred to the organic base.

TABLE 9

STRESS RELIEVING TEMPERATURE EFFECTS ON
WELDED 9Cr-1Mo AND WELDED AISI 4340

Material	Stress Relief Treatment	Weld Hardness, Rockwell C	Parent Metal Hardness, Rockwell B	Flattening Distance Between Plates at Failure, in.*	
				Weld Bead On	Weld Bead Removed
9Cr-1Mo	None (as welded)	45	81	0.5	0.688
9Cr-1Mo	400°F - 16 hr	43	-	-	-
9Cr-1Mo	1225°F - 1 hr	25	77	0.375	0.437
9Cr-1Mo	1350°F - 1 hr	21	77	0.375	0.312
AISI 4340	None (as welded)	55	100	-	-
AISI 4340	1225°F - 1 hr	32	90	-	-
AISI 4340	1275°F - 1 hr	31	91	-	-
AISI 4340	1350°F - 1 hr	28	91		-
AISI 4340	1400°F - 1 hr	34	101	-	-

*Flattening test performed in accordance with ASTM A-450, with weld located 90° from application of load. This specification dictates that failure may not occur before a distance of 0.623 in. is reached for ferritic steels.

TABLE 10

TYPICAL OPERATION DATA-CORROSION LOOP 3

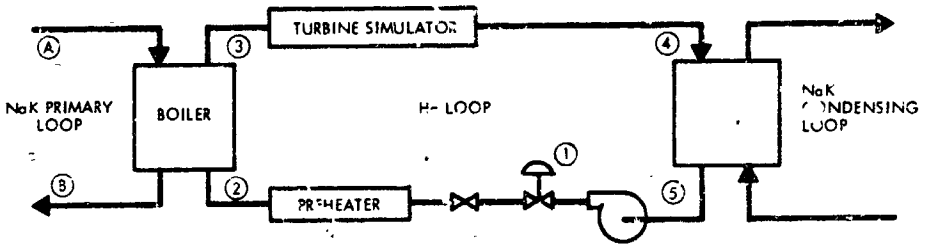

Accumulated Time of Hg Boiling hr	Primary NaK loop				Mercury loop -									Remarks
	Flow Rate lb/hr	(A) °F	(B) °F	Flow Rate lb/hr	(1) °F	(1) psia	(2) °F	(2) psia	(3) °F	(3) psia	(4) °F	(4) psia	(5) °F	
2	1800	1205	1070	595	460	613	430	160	950	11[illegible]	425	6.8	250	4/21/64
	(Loop shut down because of electrical power modification)													4/21/64
3	1800	1300	1185	600	410	560	440	270	1050	250	380		280	4/25/64
14	1800	1280	1089	600	470	560	470	284	1085	256	380	3[illegible]	280	
38	1800	1325	1150	500	470	560	470	290	1075	265	720	27.5	260	
59	1800	1310	1200	450	445	580	450	288	1060	258	770	31	200	
70	(Loop shut down because of high condenser inlet pressure)													4/28/64
73		1270	1175	300	380	560	450	125	890	90	545	3	390	5/17/64
97	1800	1210	1125	300	400	560	600	125	890	95	570	4.5	375	
146	1800	1300	1210	300	390	540	840	168	955	145	600	6.0	395	
188	1800	1300	1200	300	400	532	800	175	950	140	600	6.5	385	
193	1800	1320	1190	300	405	540	825	165	1105	130	605	6.6	410	Superheated Hg obtained 5/22/64
195	1800	1300	1190	300	400	532	760[illegible]	170	1130	130	610	7.0	420	
266	1800	1320	1150	410	430	530	730	190	1150	150	640	10.0	470	
295	1800	1320	1150	470	460	530	720	165	1175	210	680	14.0	510	
319	1800	1320	1120	590	460	546	680	190	1200	240	680	15.0	520	
340	1800	1320	1130	590	490	525	675	300	1200	270	680	16.0	505	
	(Loop shut down due to electric power interruption)													5/29/64
352		1310	1170	310	40[illegible]	546	800	155	930	122	640	11	350	5/29/64
354	1800	1310	170	340	4[illegible]0	540	770	168	1070	135	650	11	390	Superheated Hg obtained 6/1/64
378	1800	1310	1150	340	418	540	772	165	1100	33	655	12	420	
406	1800	1310	1120	500	460	530	690	220	1050	80	670	14	510	
430	(Loop shut down due to Hg flow instability)													6.1/64
450	1790	1[illegible]0	1175	330	470	588	680	135	1030	100	505	4	465	6/19/64 Start; superheated Hg
500	1790	1300	1180	324	450	588	610	237	1050	207	580	4	440	obtained immediately
600	1950	1310	1150	421	490	560	620	220	1060	190	650	10	495	
700	1830	1320	1210	321	490	560	755	162	1120	127	640	10	485	
800	2170	1310	1150	549	490	553	720	185	1180	140	630	8	510	
900	1680	1310	1150	507	490	546	715	2[illegible]	1190	240	620	8	475	
1000	1950	1310	1150	520	490	546	595	280	1185	255	618	8	500	
1100	1950	1310	1130	569	490	553	520	305	1205	270	630	9	515	
1300	1950	1310	1150	507	490	553	518	300	1200	265	670	9	505	
1500	1950	1310	1130	503	500	560	520	310	1190	267	635	9	490	8/3/64

NOTES:
1. INTERPRET DRAWING PER STANDARDS PRESCRIBED IN MIL-D-70327
2. FOR P&I DIAGRAM, CPTS TEST EQUIPMENT SEE DRAWING 101213
3. STATE POINT CONDITIONS BASED ONLY ON ZERO 'G' REFERENCE CONDITIONS
4. DEFINITION OF SYMBOLS
   - ○ MINIMUM POWER CONDITION BASED ON MINIMUM REACTOR OUTLET TEMPERATURE, MAXIMUN SOLAR FLUX IN EARTH ORBIT, AND MINIMUM COMPONENT PERFORMANCE
   - ● MAXIMUM POWER CONDITION BASED ON MAXIMUM REACTOR OUTLET TEMPERATURE, ZERO SOLAR FLUX AND MAXIMUM COMPONENT PERFORMANCE

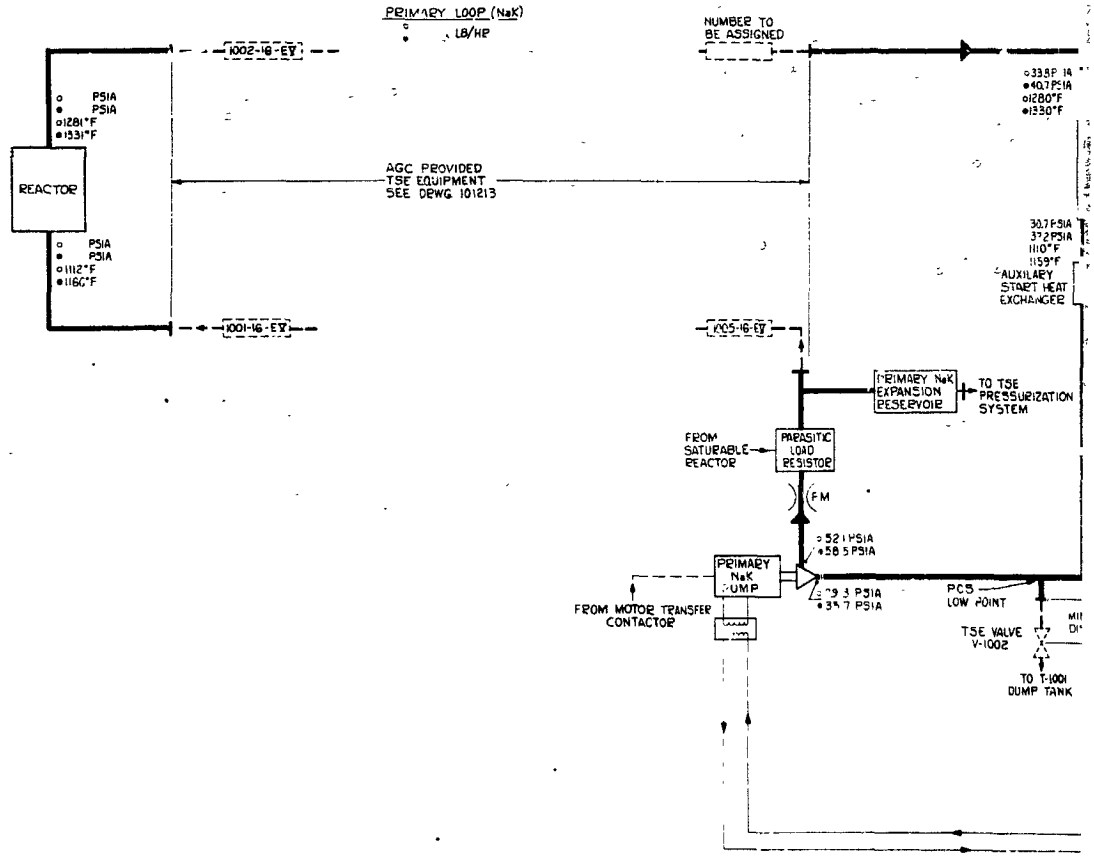

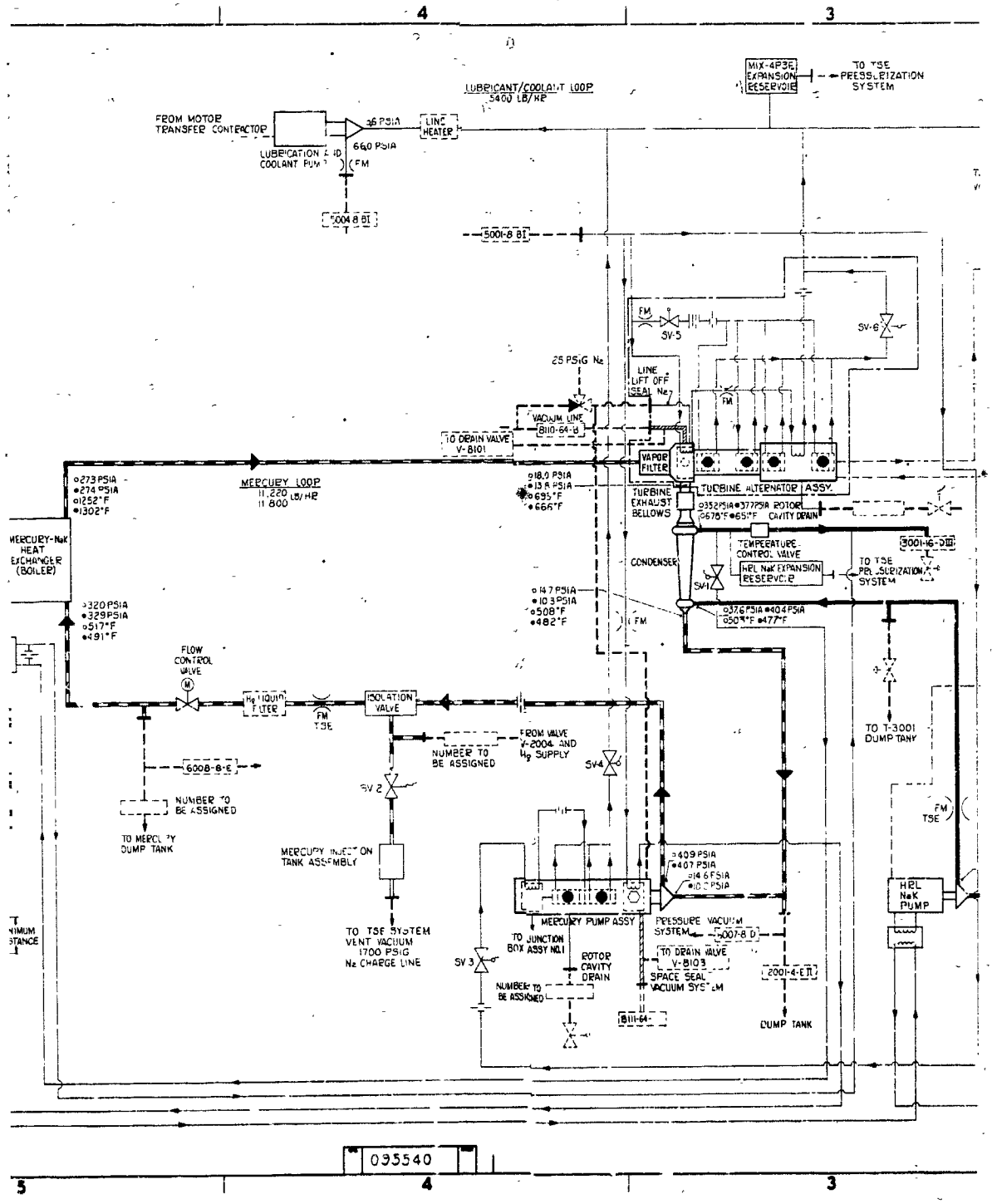
4
3
MIX-4P3E EXPANSION RESERVOIR
TO TSE PRESSURIZATION SYSTEM
LUBRICANT/COOLANT LOOP 5400 LB/HR
FROM MOTOR TRANSFER CONTACTOR
36 PSIA
640 PSIA
LINE HEATER
LUBRICATION & COOLANT PUMP
FM
5004-8 BI
5001-8 BI
FM
SV-5
SV-6
25 PSIG N2
LINE LIFT OFF SEAL N2
FM
VACUUM LINE B110-64-B
TO DRAIN VALVE V-8101
VAPOR FILTER
TURBINE ALTERNATOR ASSY.
TURBINE EXHAUST BELLOWS
ROTOR CAVITY DRAIN
MERCURY LOOP 11,220 LB/HR 11,800
MERCURY-NaK HEAT EXCHANGER (BOILER)
CONDENSER
TEMPERATURE CONTROL VALVE
HRL NaK EXPANSION RESERVOIR
TO TSE PRESSURIZATION SYSTEM
3001-16-D III
SV-1
FM
FLOW CONTROL VALVE
Hg LIQUID FILTER
FM TSE
ISOLATION VALVE
FROM VALVE V-2004 AND Hg SUPPLY
NUMBER TO BE ASSIGNED
SV-4
6008-8-E
SV-2
NUMBER TO BE ASSIGNED
TO MERCURY DUMP TANK
TO T-3001 DUMP TANK
FM TSE
MERCURY INJECTION TANK ASSEMBLY
HRL NaK PUMP
MERCURY PUMP ASSY
PRESSURE VACUUM SYSTEM
5007-8 D
TO JUNCTION BOX ASSY NO.1
SV-3
ROTOR CAVITY DRAIN
TO DRAIN VALVE V-8103
SPACE SEAL VACUUM SYSTEM
NUMBER TO BE ASSIGNED
2001-4-E II
B111-64-
DUMP TANK
TO TSE SYSTEM VENT VACUUM 1700 PSIG N2 CHARGE LINE
095540
5
4
3

2

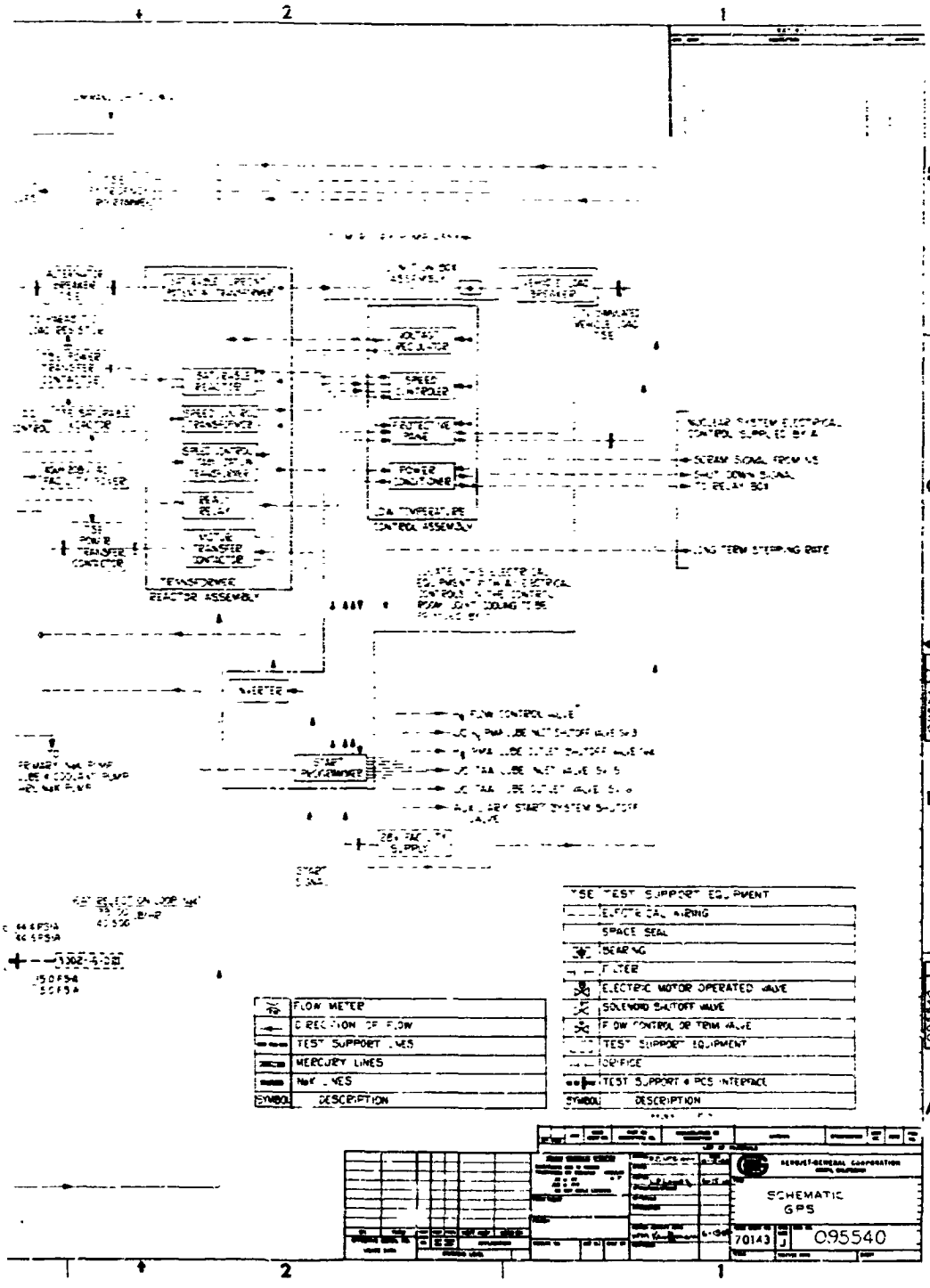

(dwg 095540)

3

Figure 1

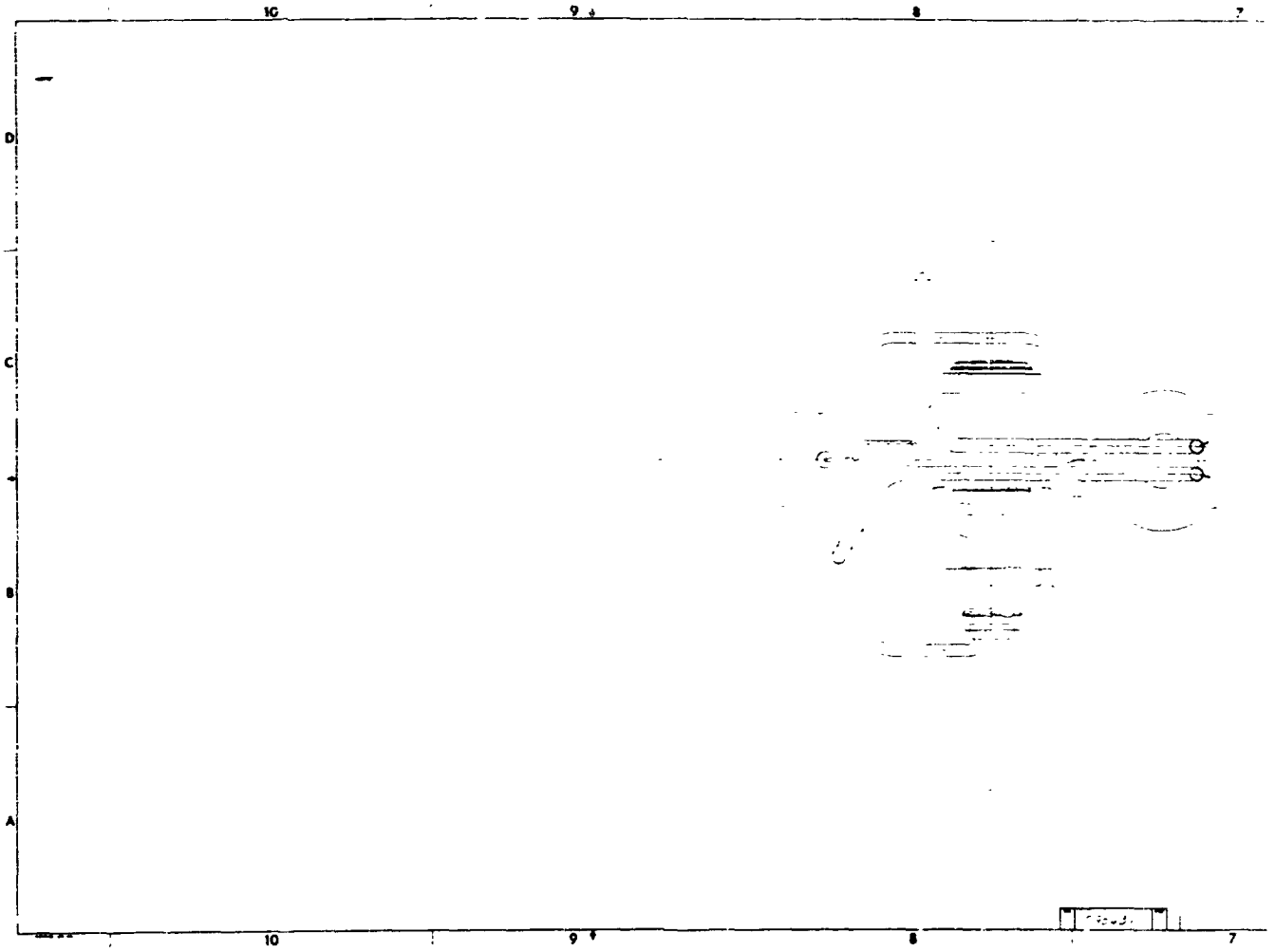
10
9
8
7
D
C
B
A

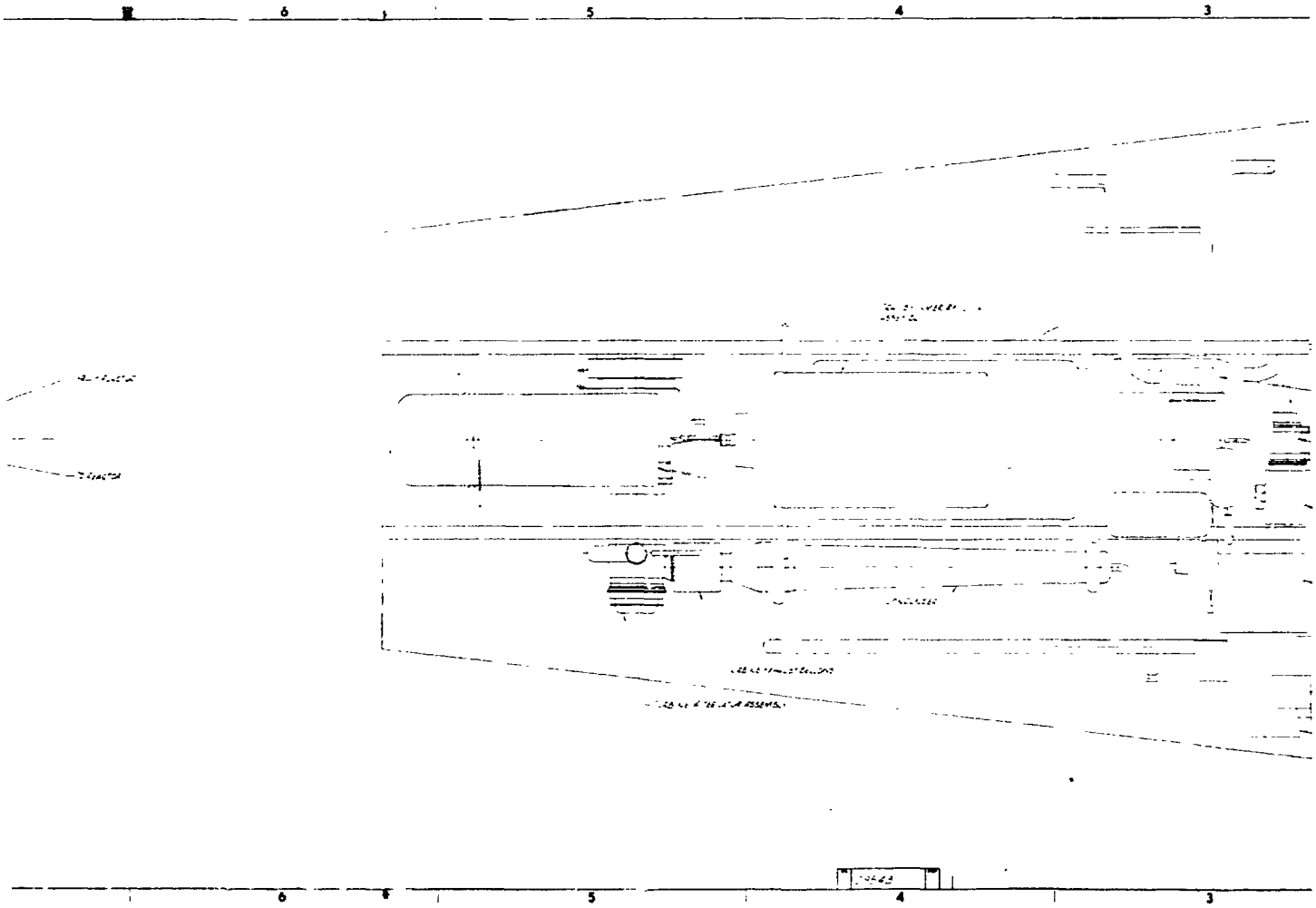

onceptual Design Layout of the Power Conversion System for the Ground Prototype System

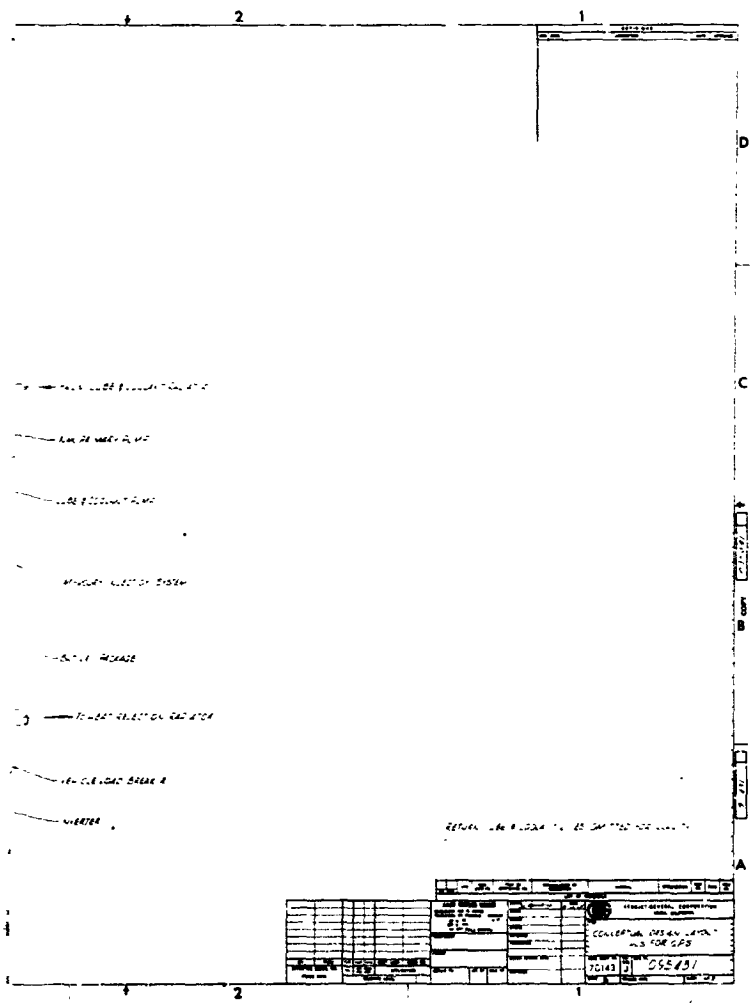

(dwg 095451-sht 1)

3

Figure 2
Sheet 1 of 2

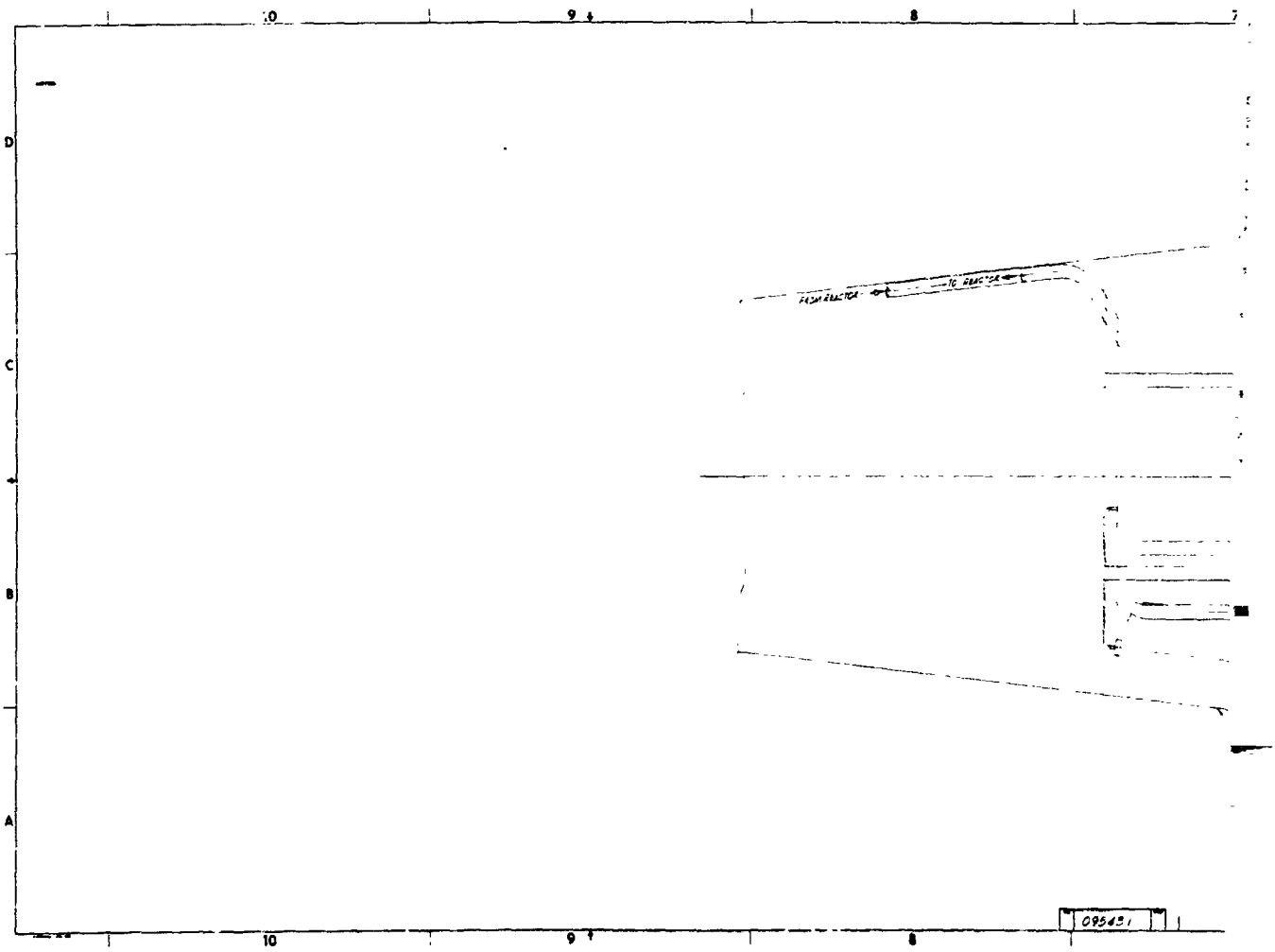
10
9
8
7
D
C
B
A
FROM REACTOR
TO REACTOR
095491

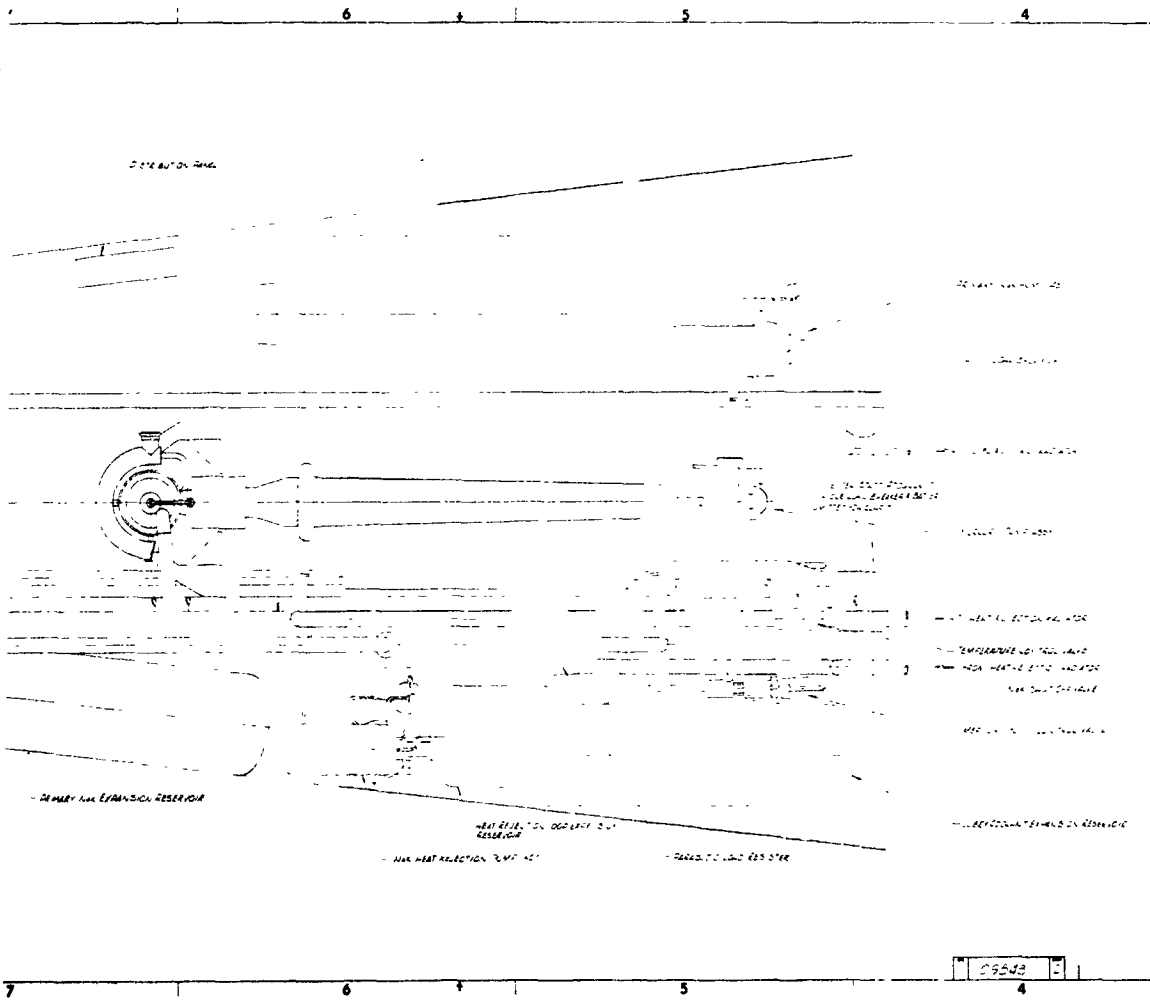

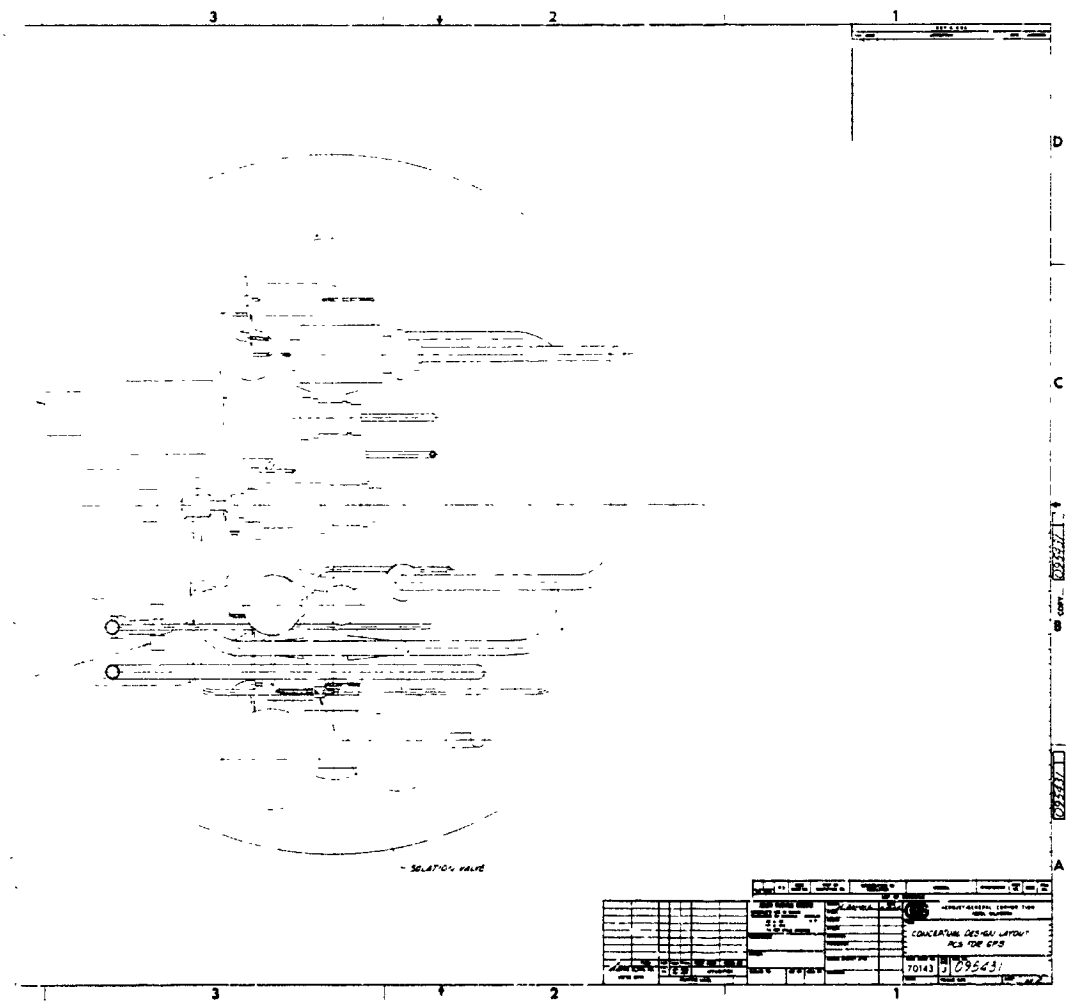

(dwg 095431-sht 2)

3

Figure 2
Sheet 2 of 2

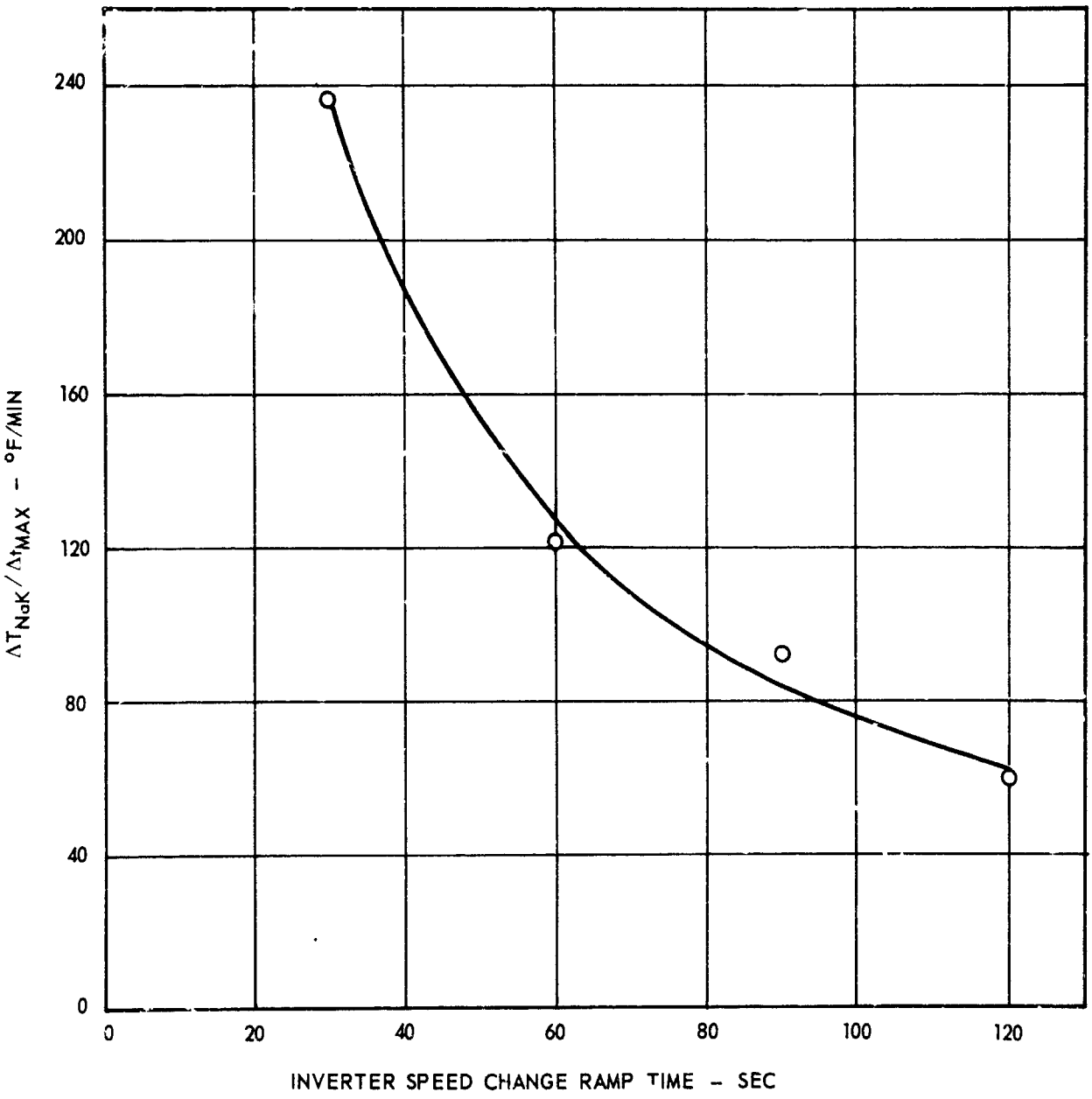

SNAP-8 PCS Startup - Reference System P Complete System Simulation.
Effect of Inverter Speed Change on Maximum Rate of Change of Reactor Coolant Temperature.

Figure 3

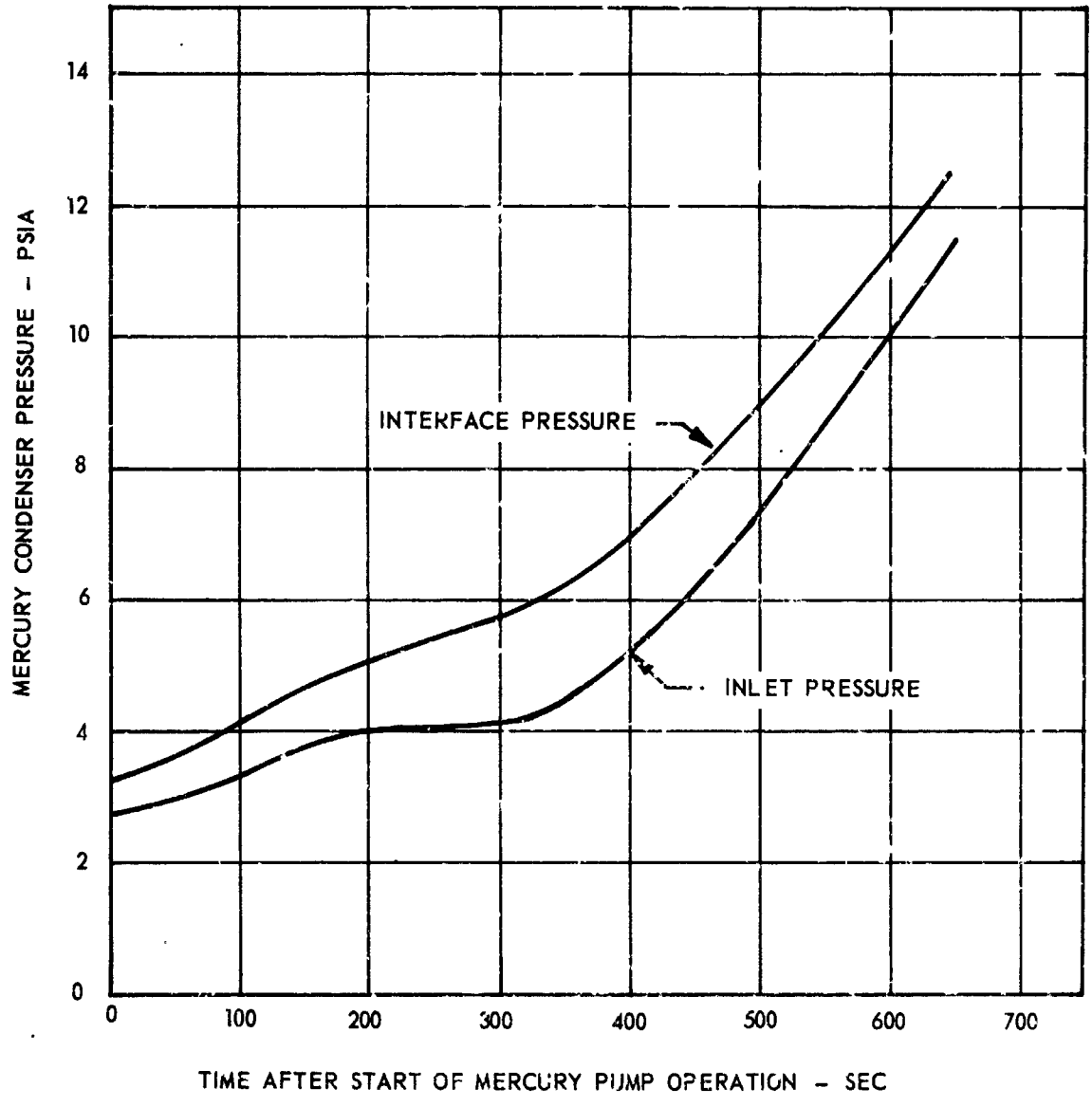

Mercury Condenser Inlet and Interface Pressure During Startup

Figure 4

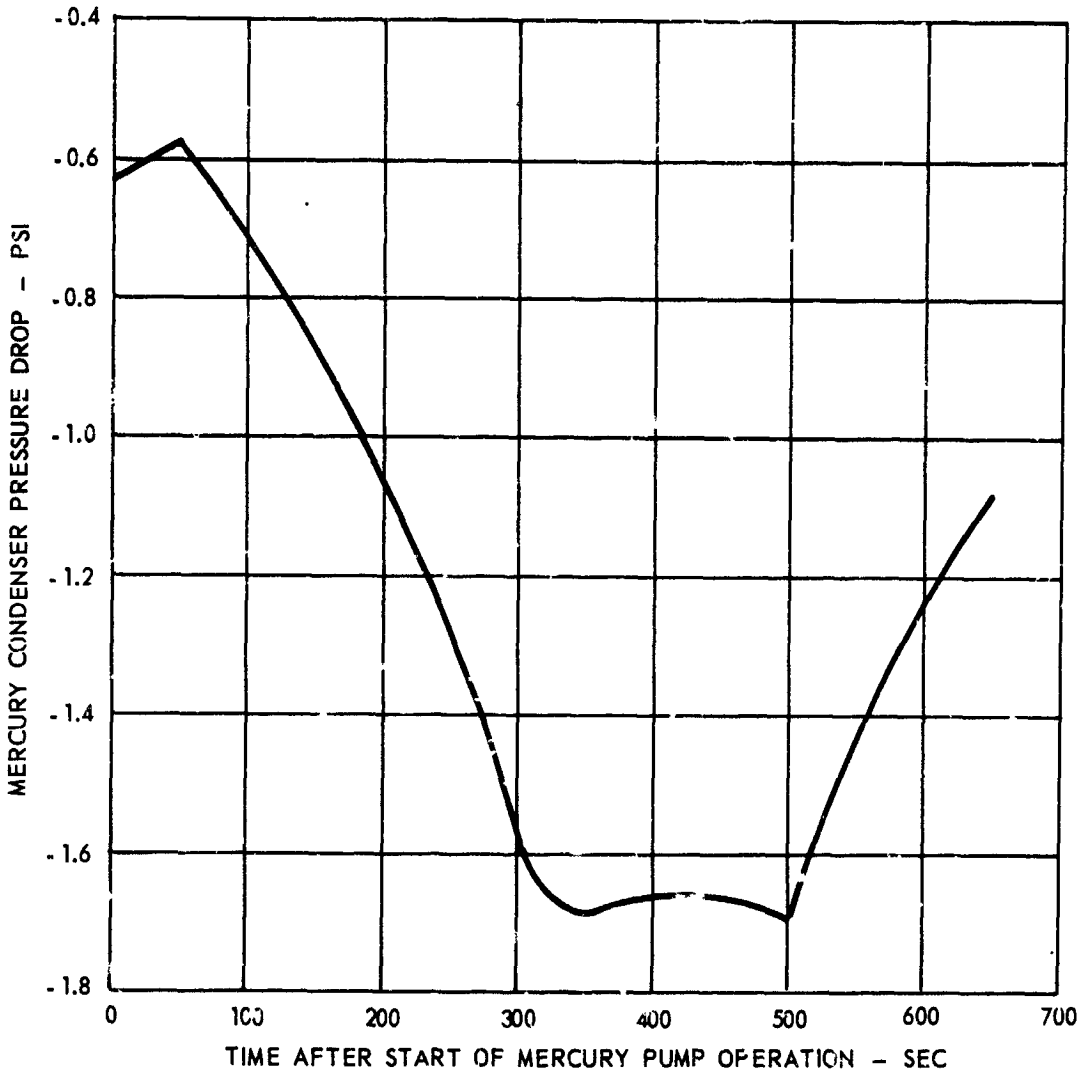

Mercury Condenser Pressure Drop During Startup

Figure 5

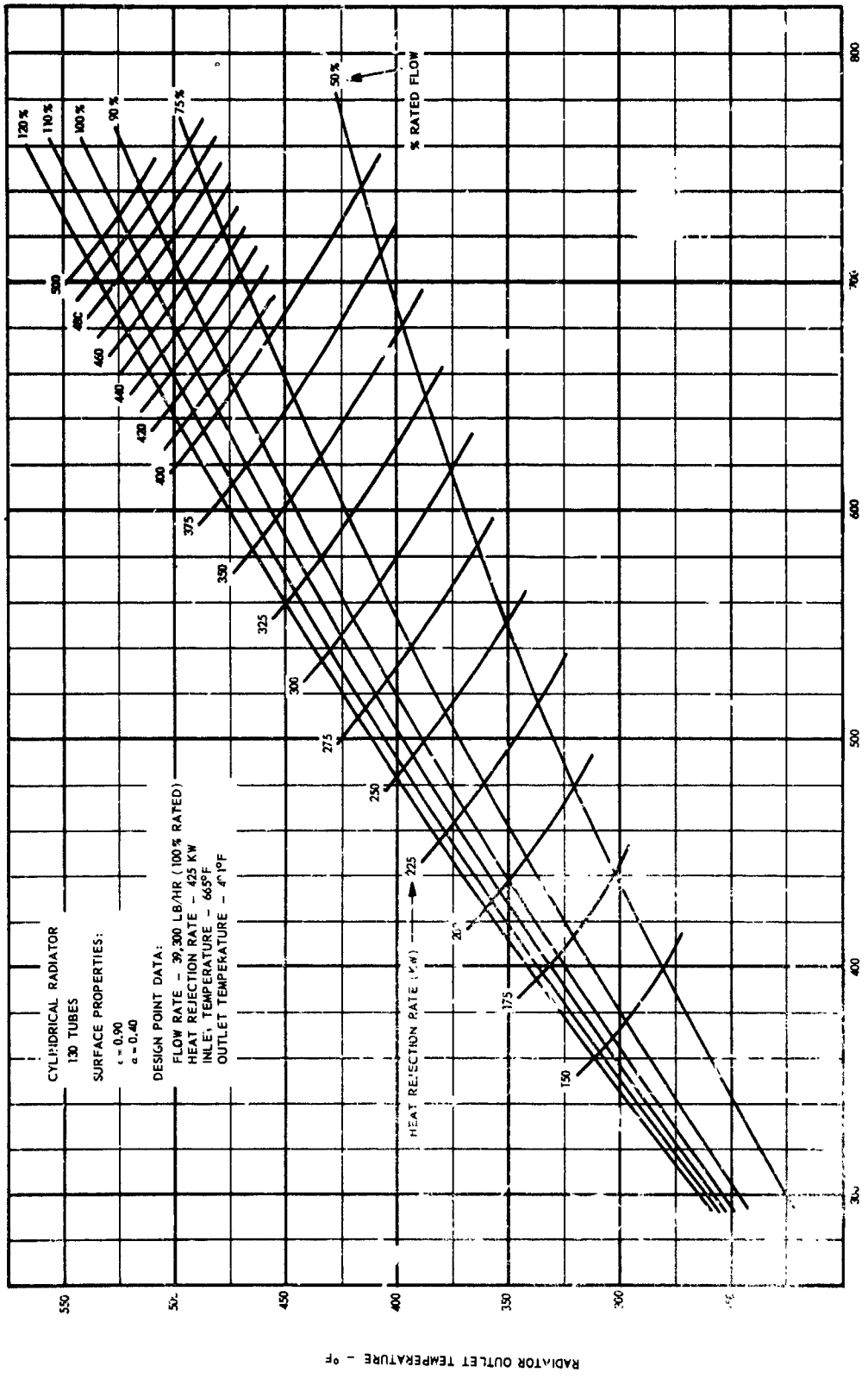

SNAP-8 Earth-Radiator Performance - Sun Operation

Figure 6

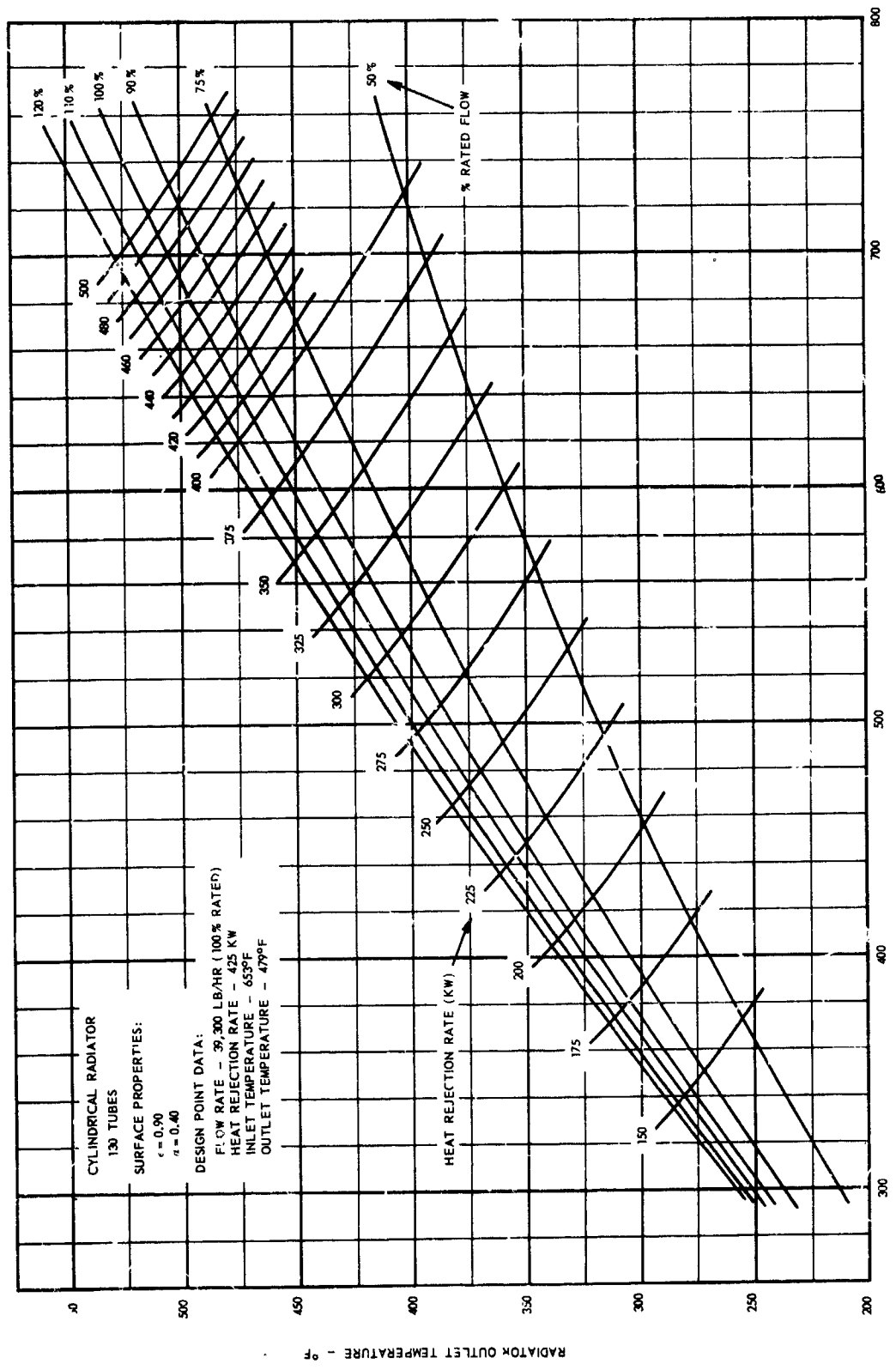

SNAP-8 Earth-Radiator Performance - Shade Operation

Figure 7

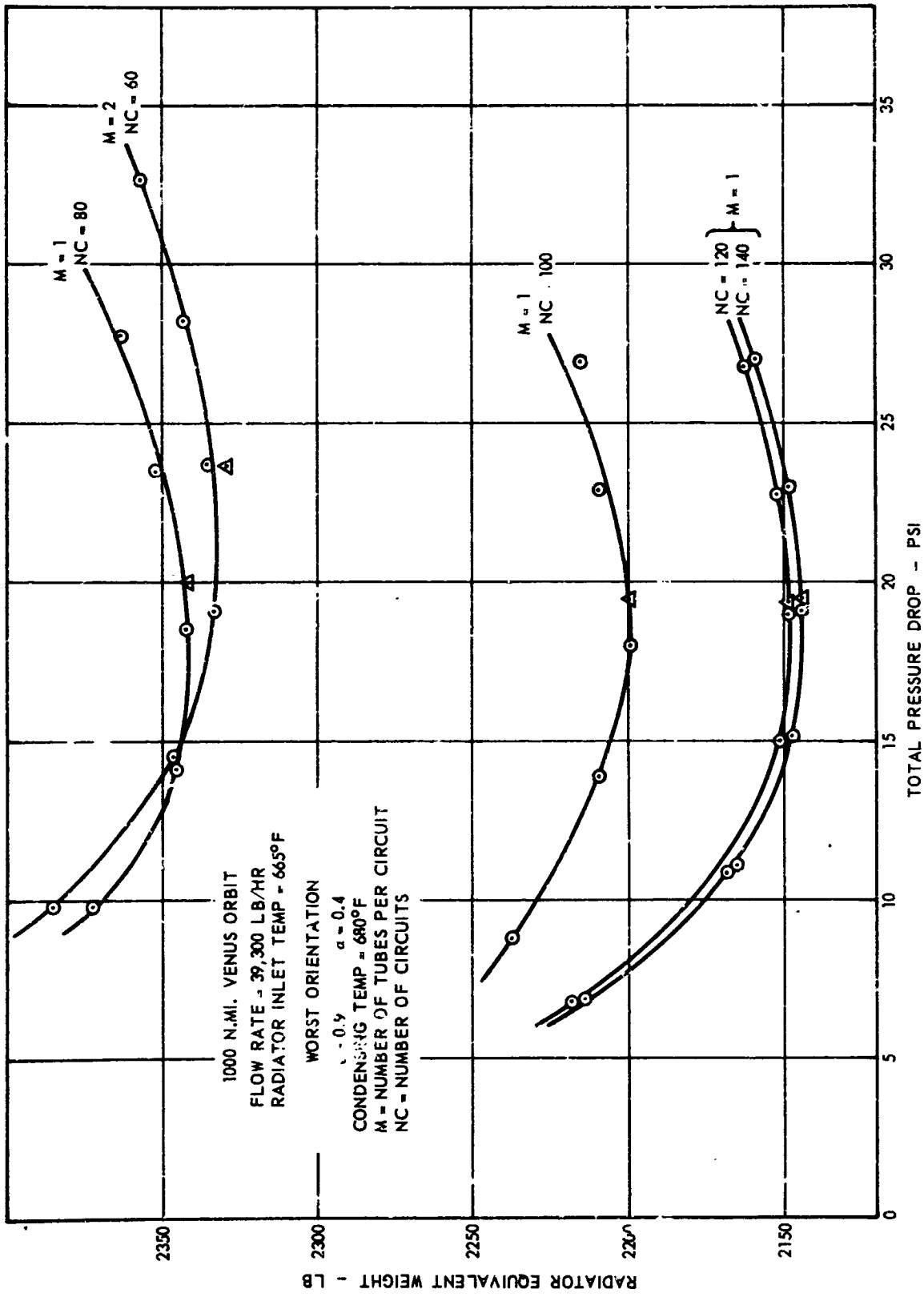

Radiator Weight-Pressure Drop Trade-Off - Radiator Equivalent Weight vs Total Pressure Drop

Figure 8

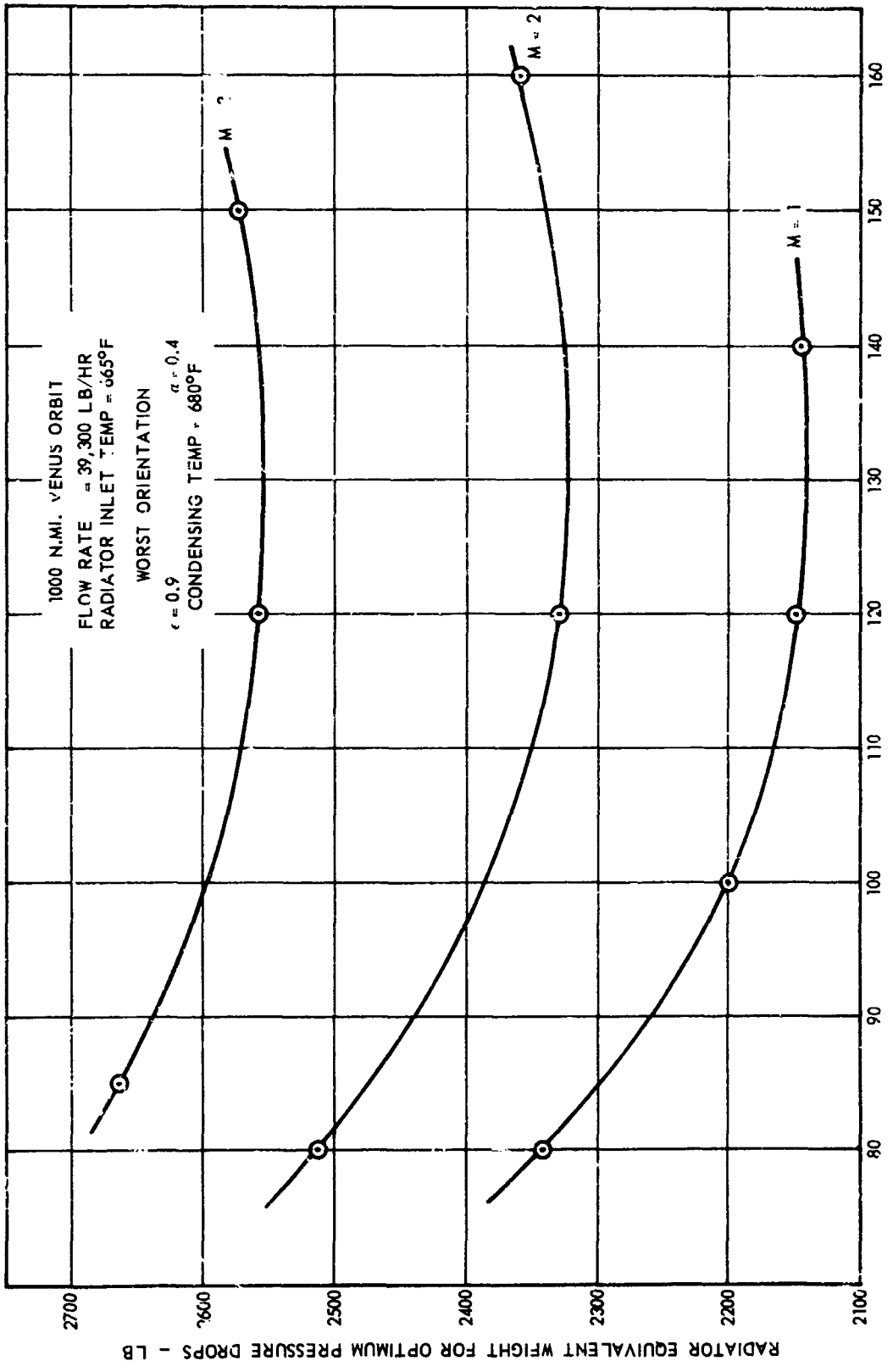

Radiator Weight Trade-Off - Number of Tubes vs Radiator Equivalent Weight

Figure 9

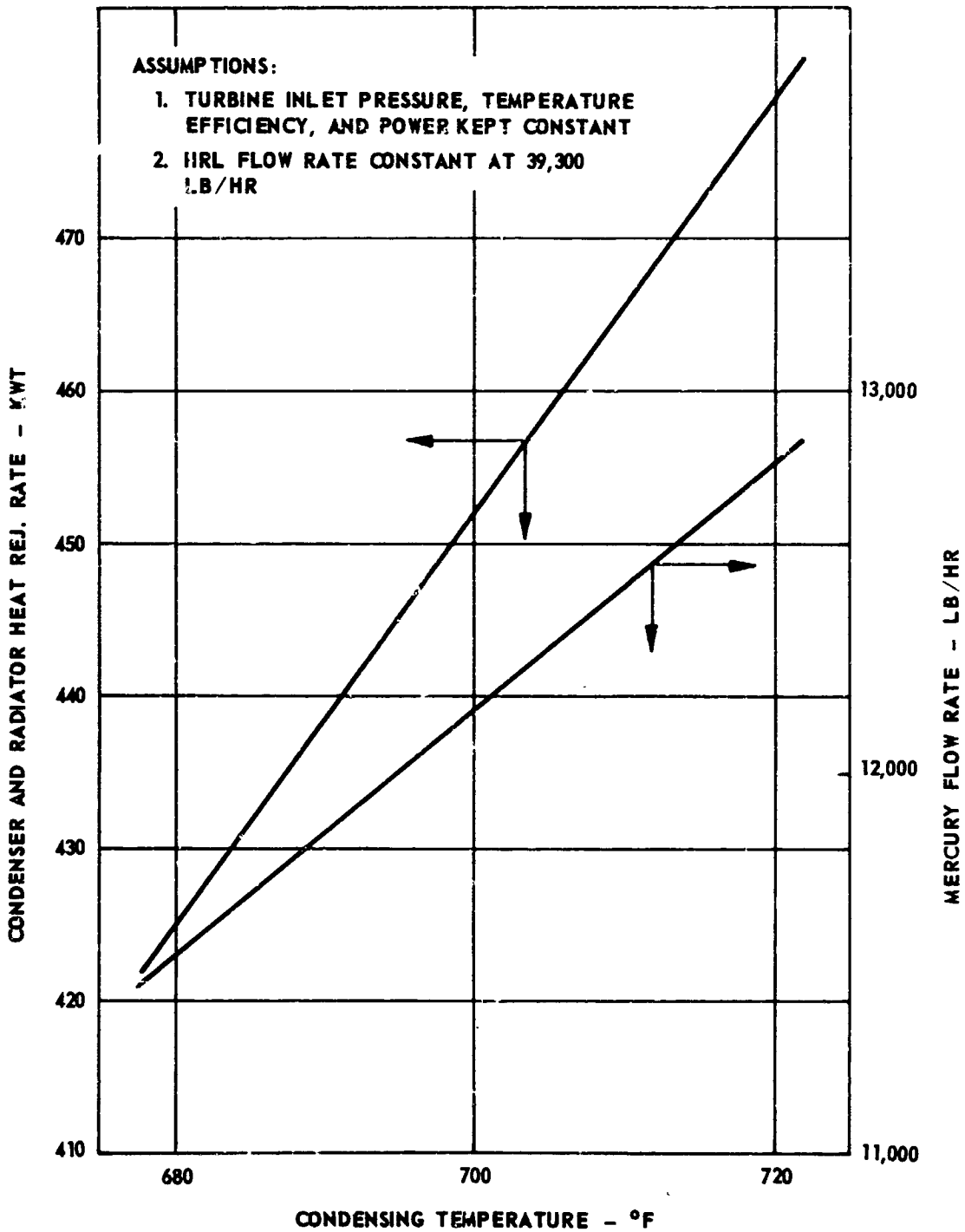

Condenser and Radiator Heat Rejection Rates and Mercury Flow Rates vs Nominal Design Condensing Temperatures

Figure 10

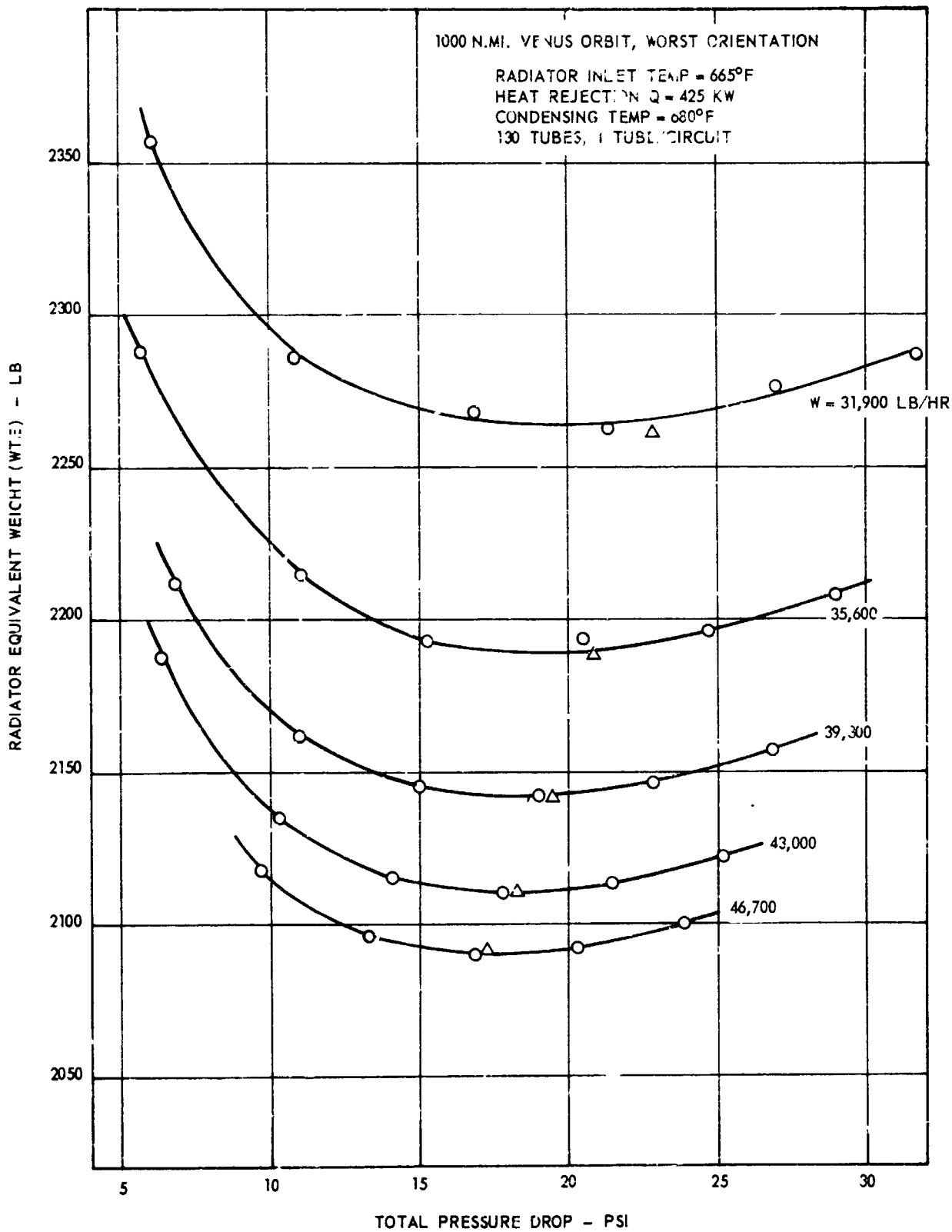

Radiator Weight Trade-Off - Total Pressure Drop vs Radiator Equivalent Weight

Figure 11

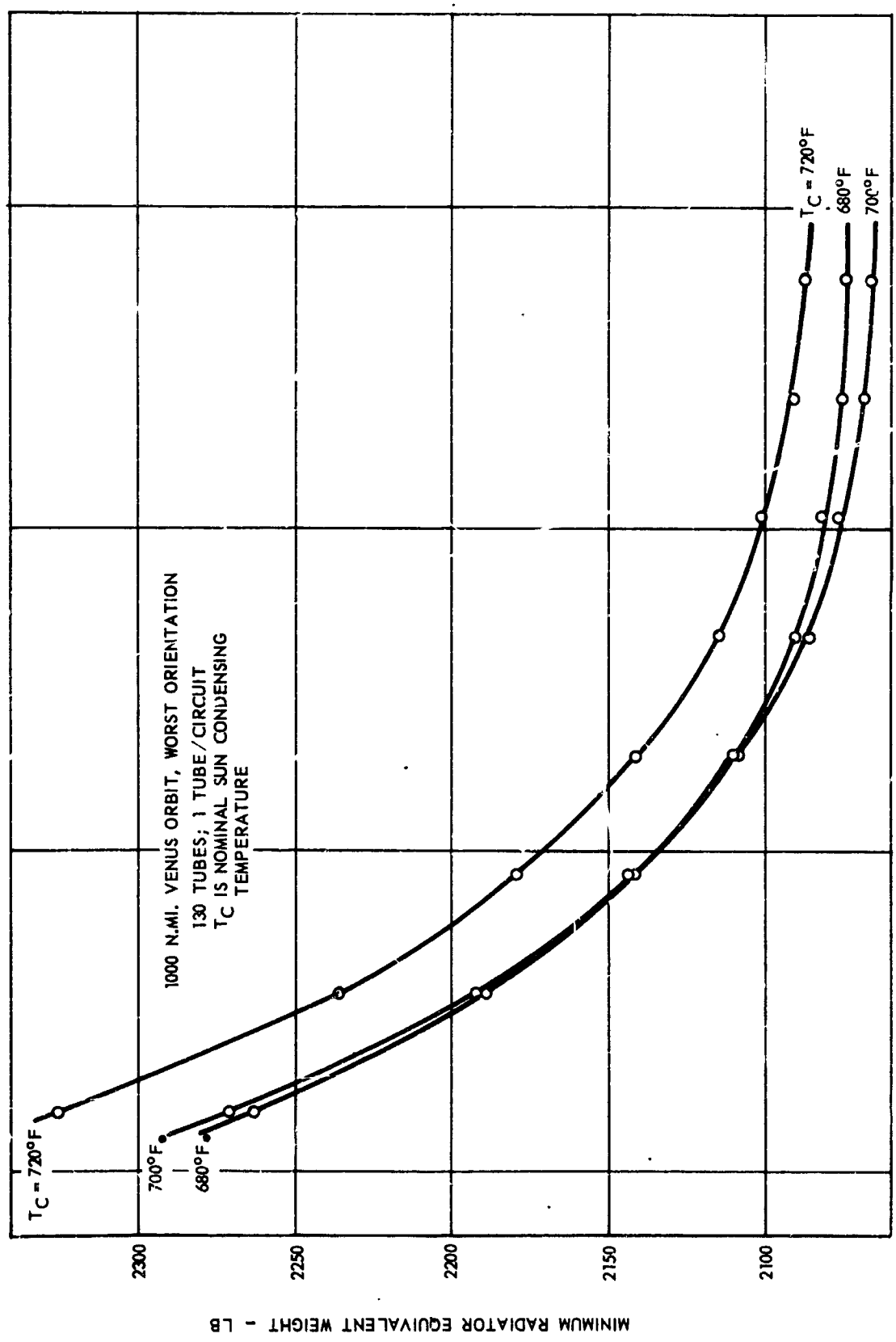

Radiator Weight Trade-Off - Minimum Equivalent Weight vs NaK Flow Rate

Figure 12

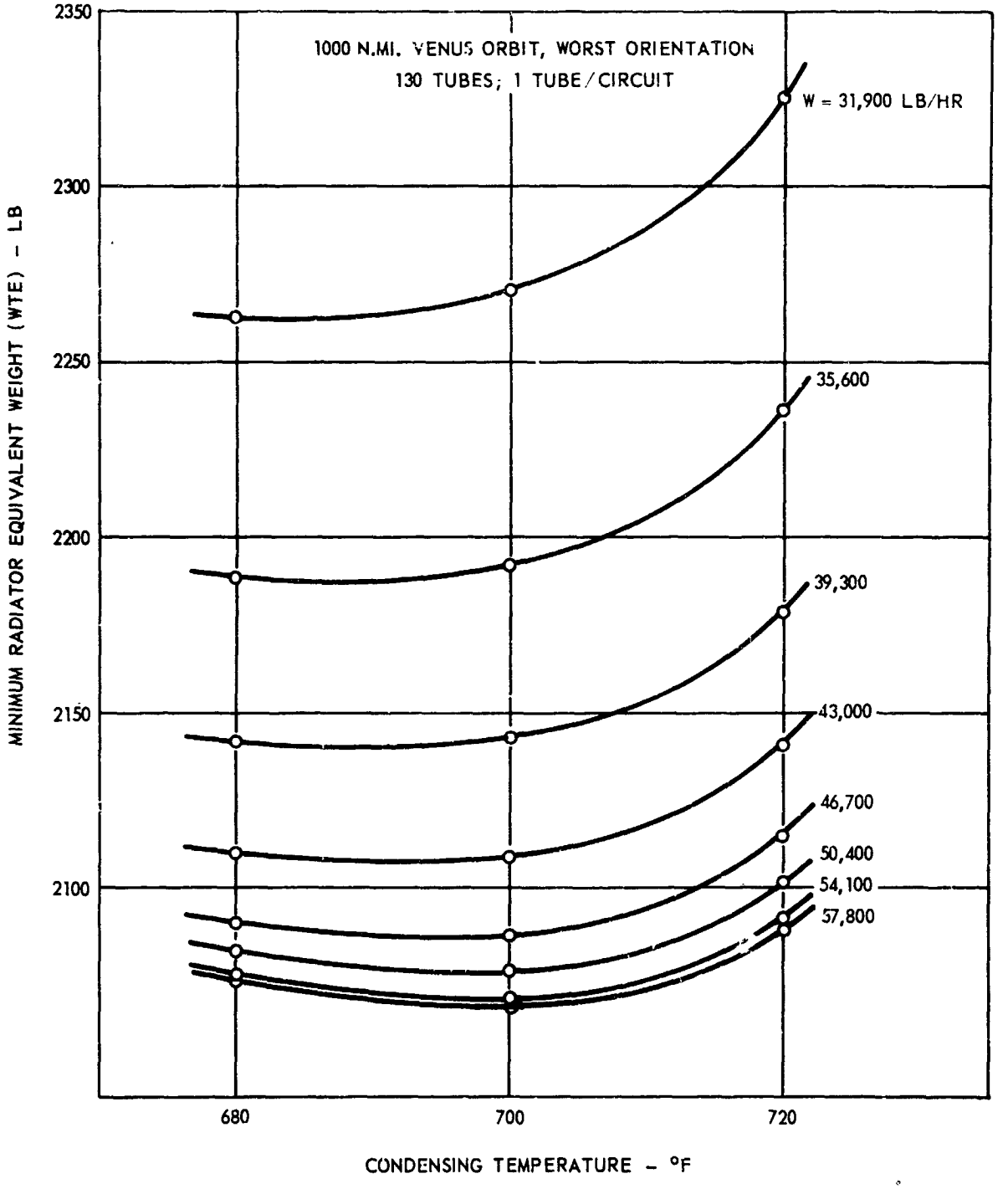

Radiator Weight Trade-Off - Minimum Equivalent Weight
vs Mercury Condensing Temperature

Figure 13

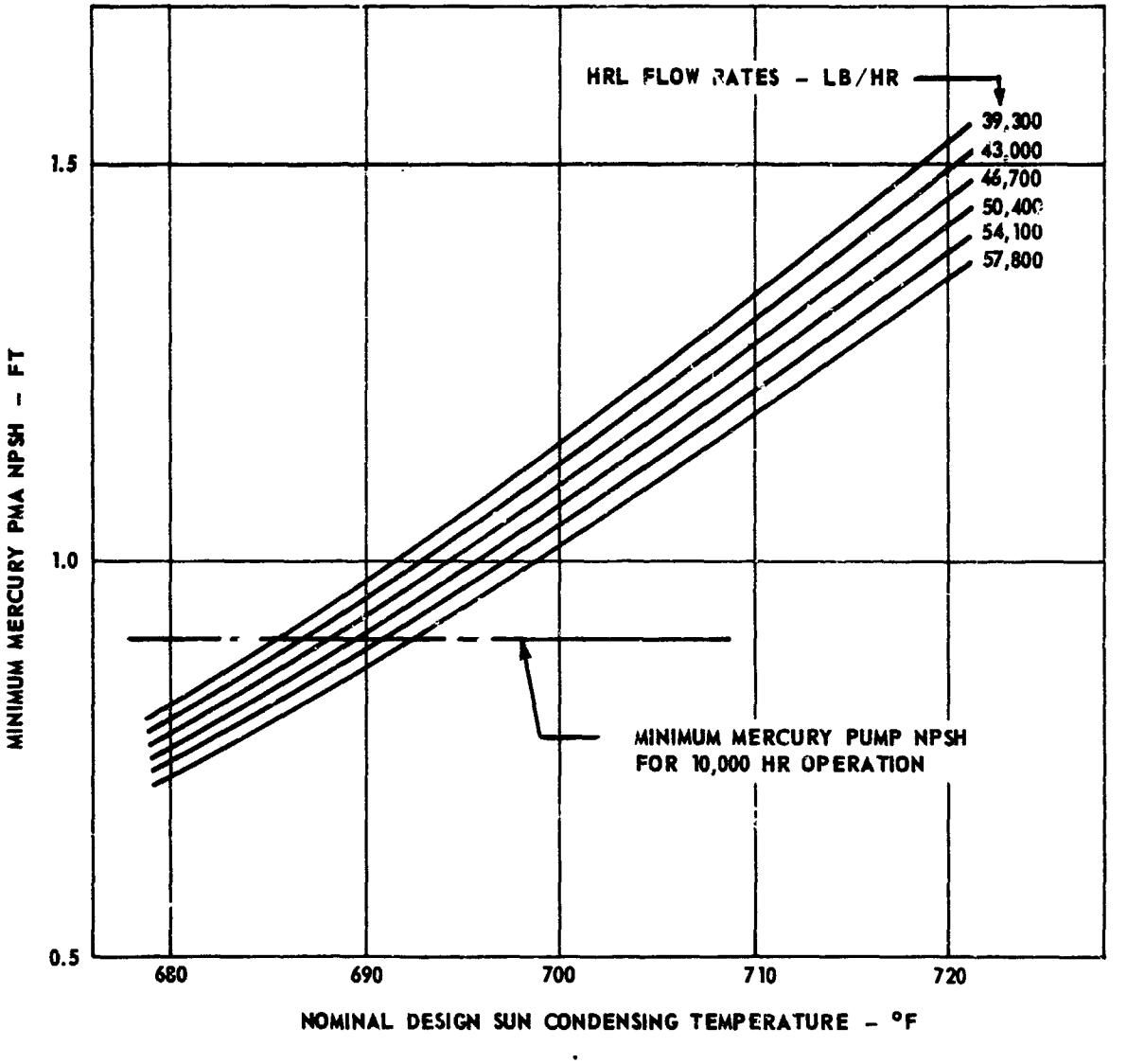

Mercury Pump Minimum NPSH vs Nominal Sun Condensing Temperature of Radiator Models Designed for Worst Orientation at a 1000 n.mi Venus Orbit (NPSH Calculated for Shade Operation with Maximum Accumulation of Tolerances and Degradations).

Figure 14

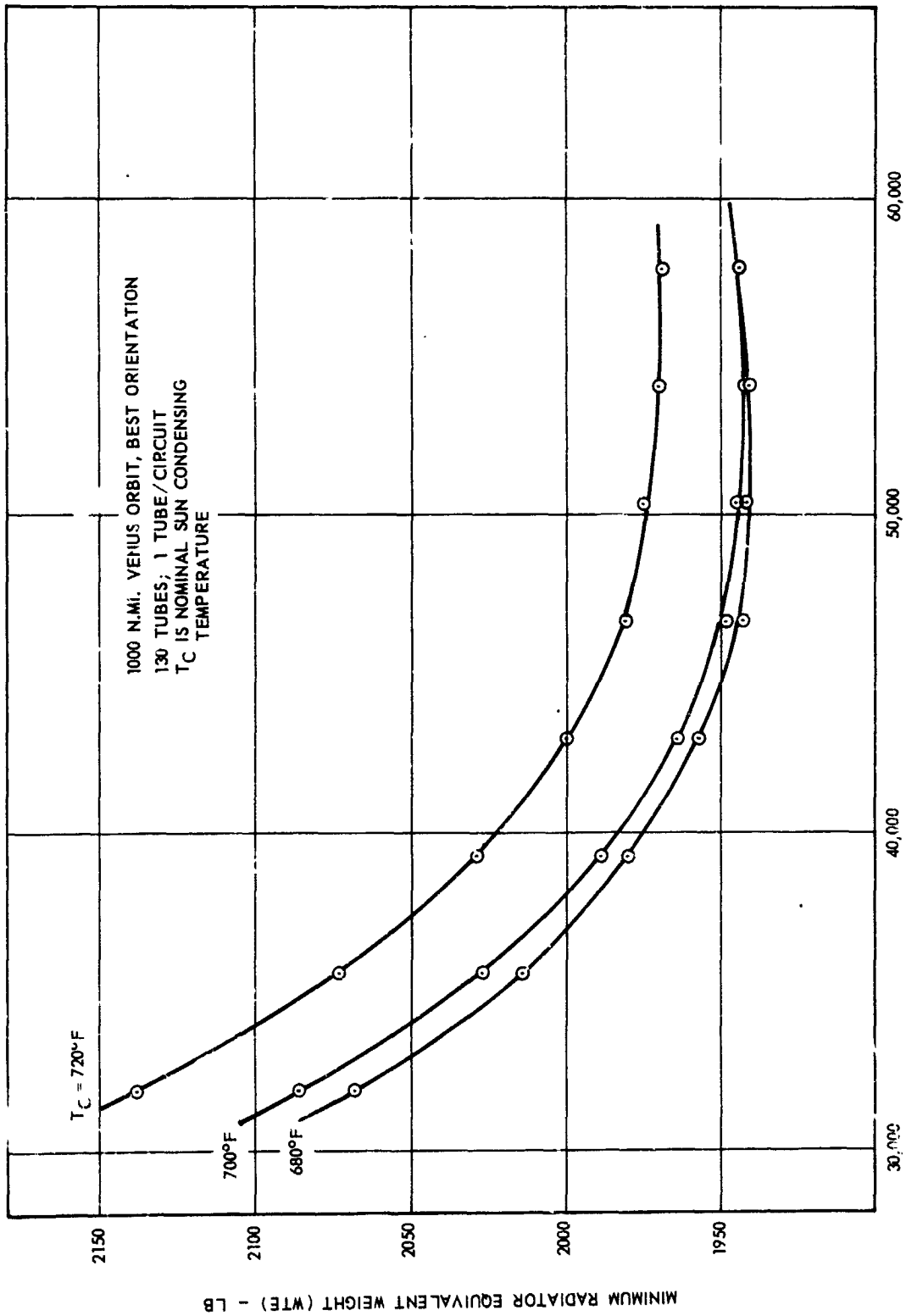

Minimum Radiator Equivalent Weight vs Nak Flow Rate

Figure 15

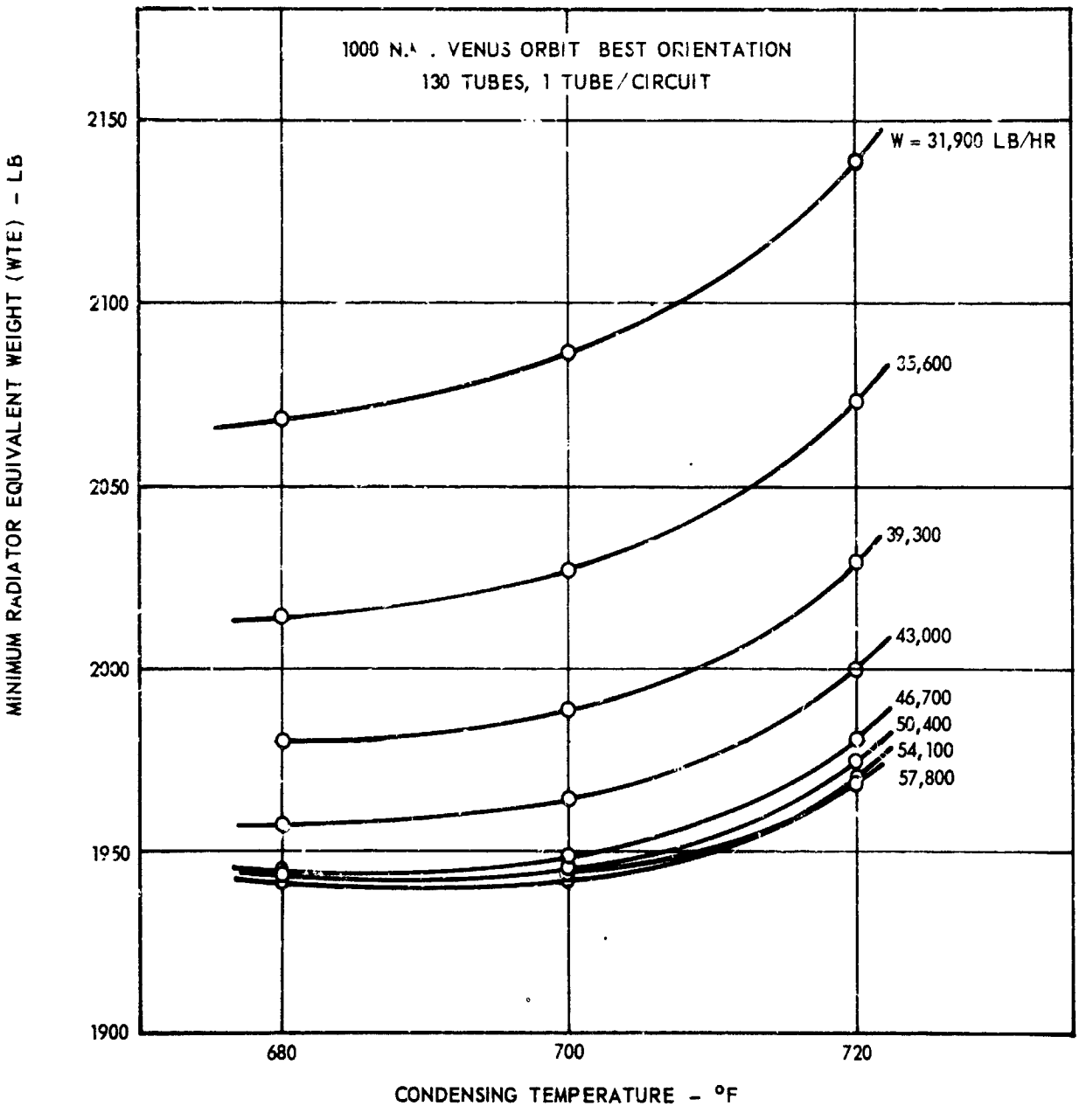

Minimum Radiator Equivalent Weight vs Mercury Condensing Temperature

Figure 16

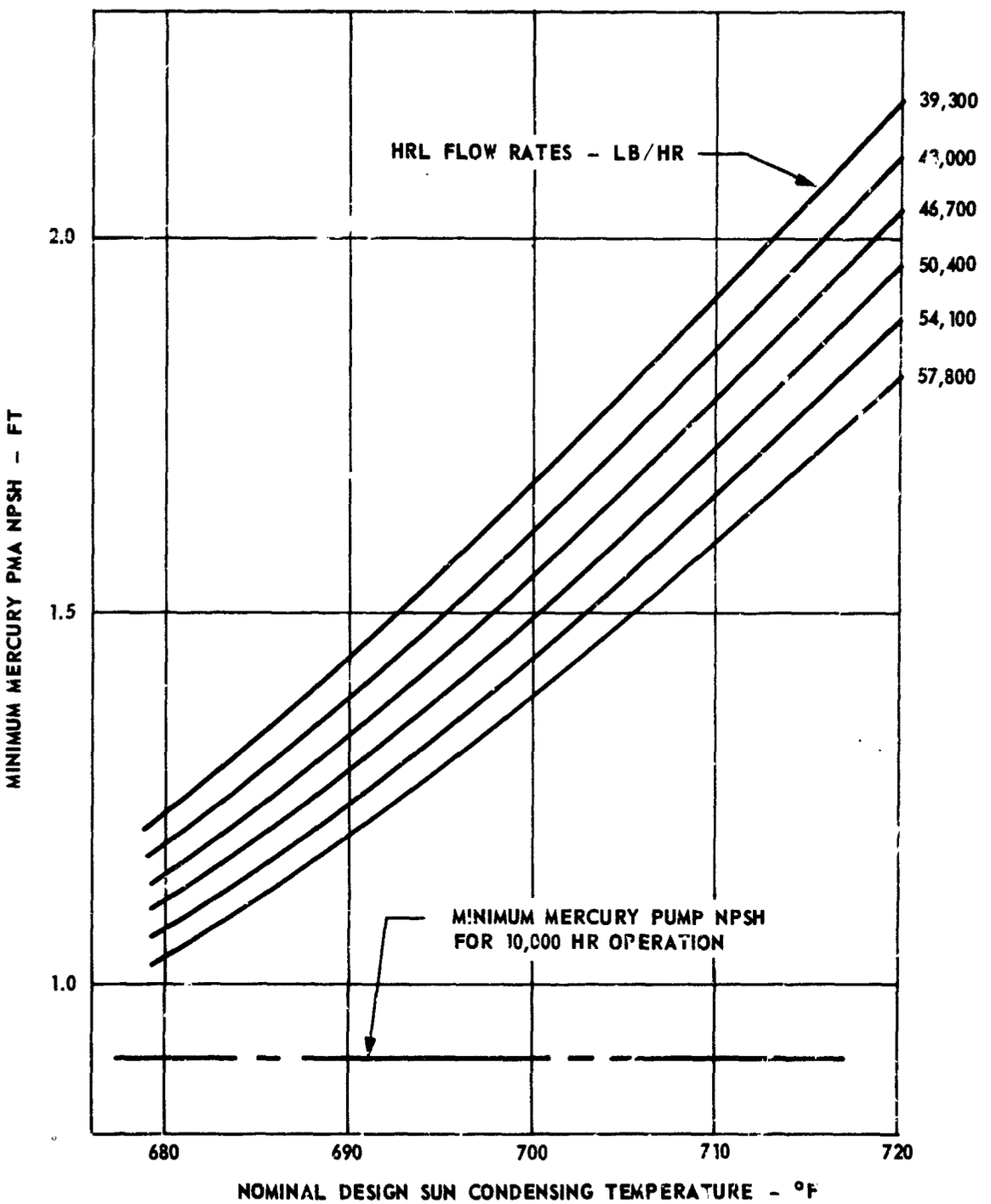

Mercury Pump Minimum NPSH vs Nominal Sun Condensing Temperature of Radiator Models Designed for Best Orientation (NPSH Calculated for Shade Operation with Maximum Accumulation of Tolerances and Degradations).

Figure 17

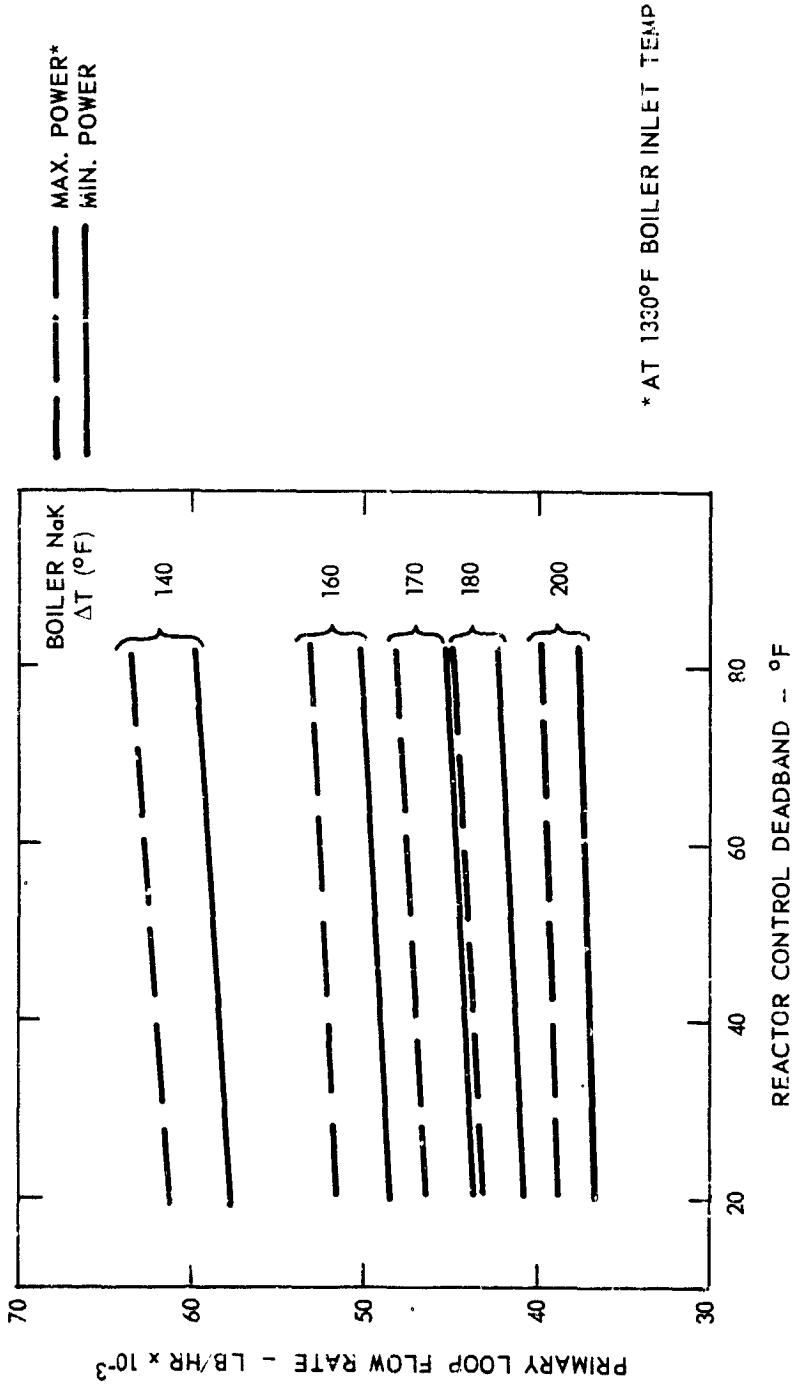

Primary Loop Flow Rate as a Function of Reactor Control Deadband and Boiler and NaK ΔT

Figure 18

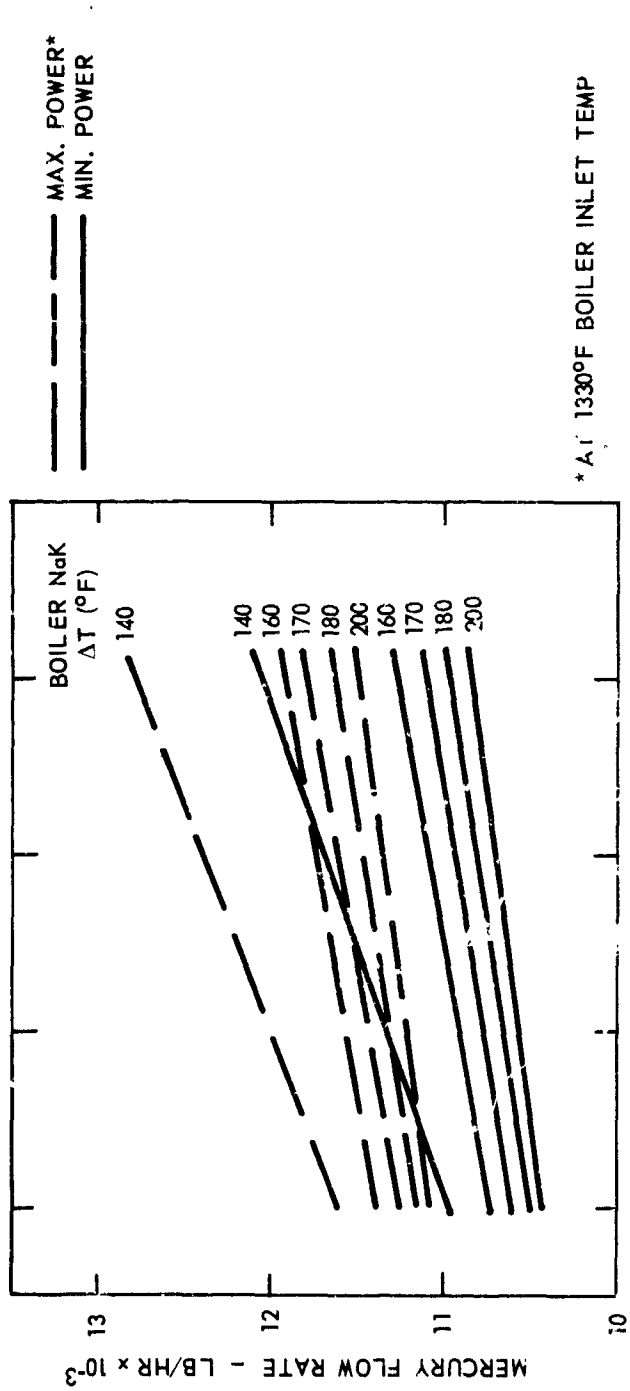

Mercury Flow Rate as a Function of Reactor Control Deadband and Boiler NaK ΔT

Figure 19

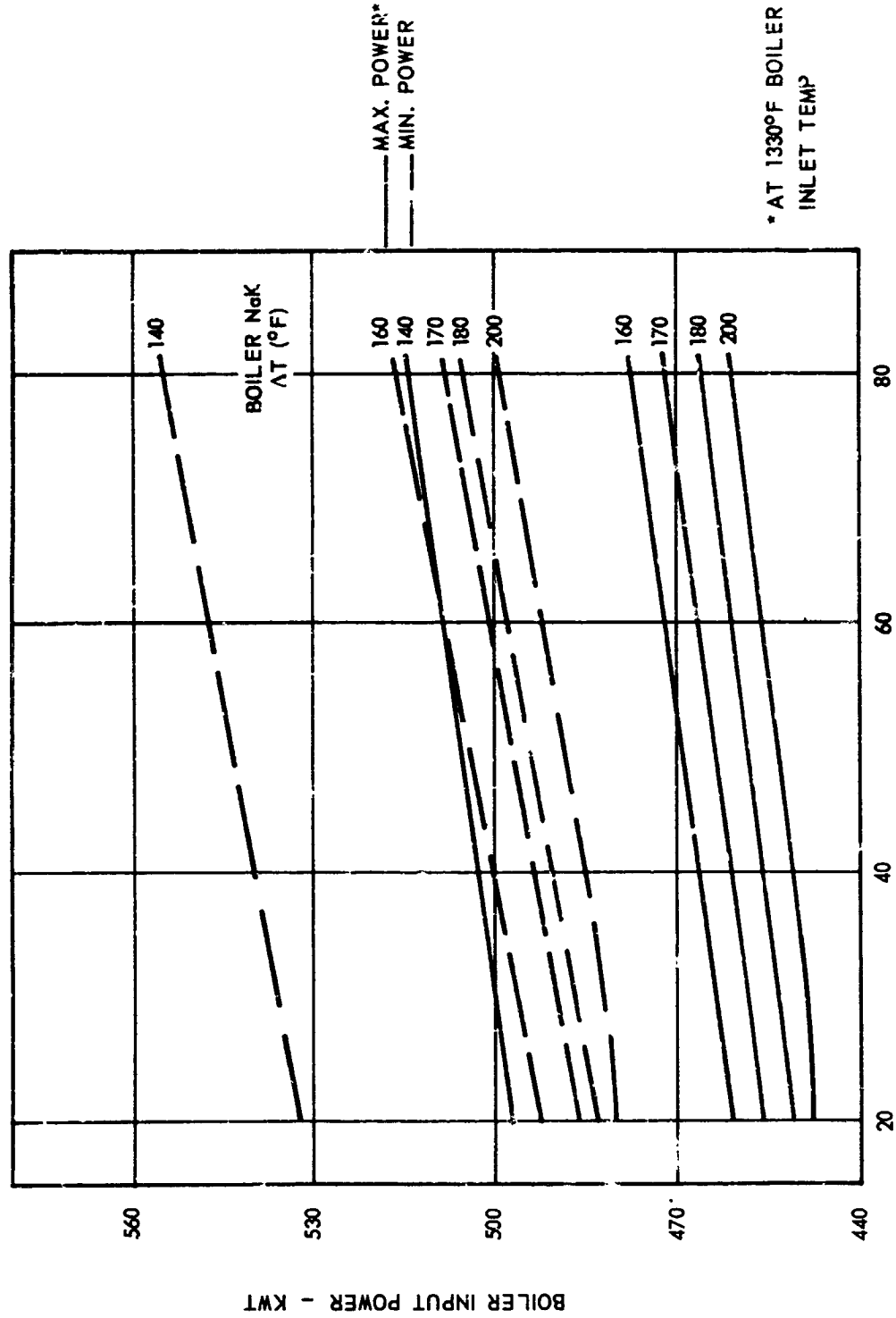

Boiler Input Power as a Function of Reactor Control Deadband and Boiler NaK ΔT

Figure 20

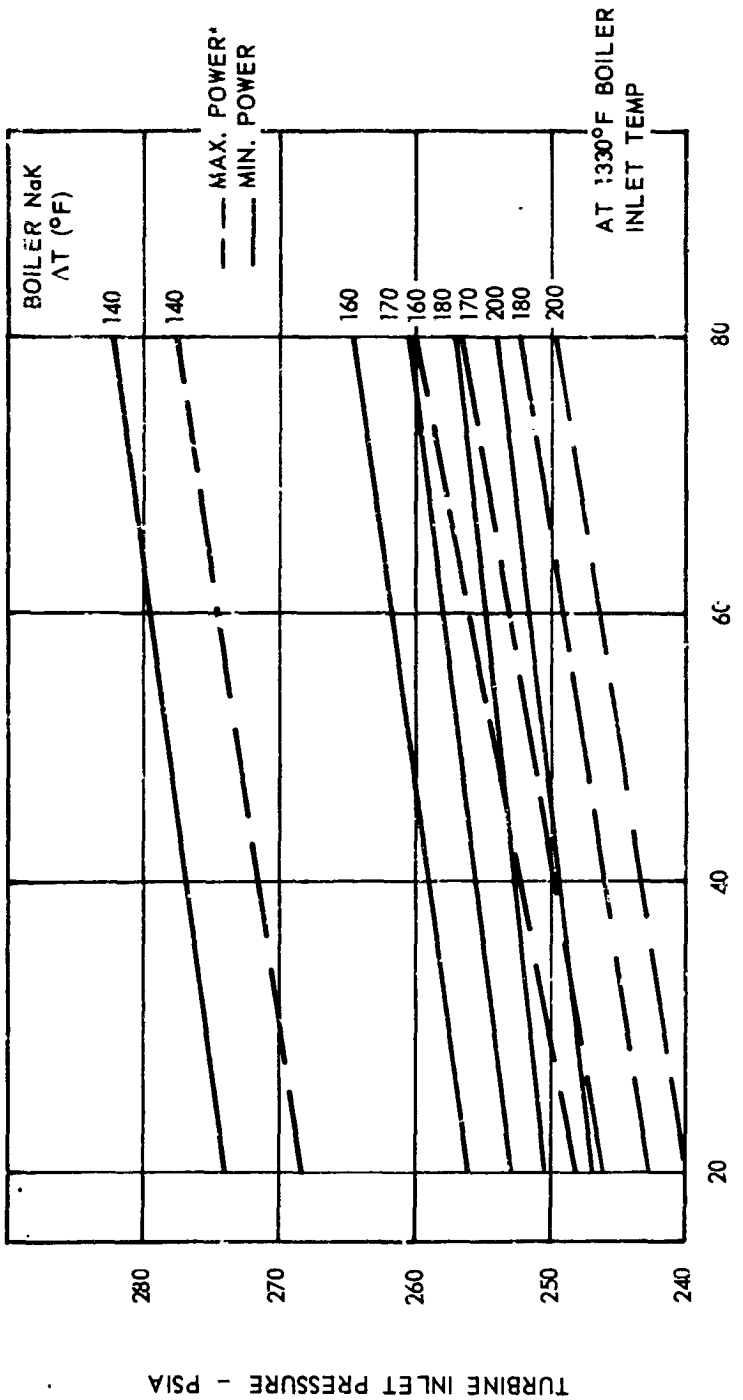

Turbine Inlet Pressure as a Function of Reactor Control Deadband and Boiler NaK ΔT

Figure 21

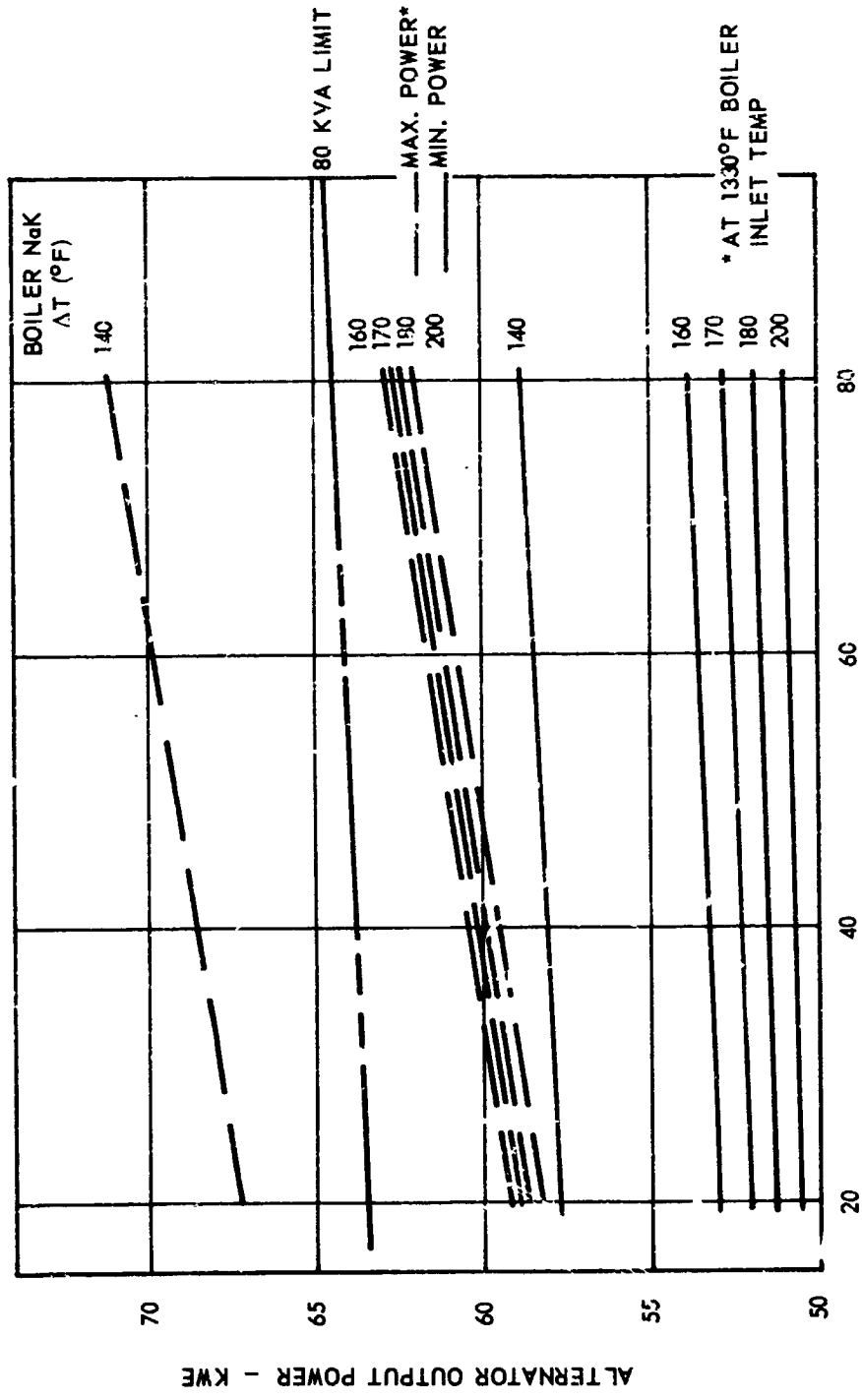

Alternator Output Power as a Function of Reactor Control Deadband and Boiler NaK ΔT

Figure 22

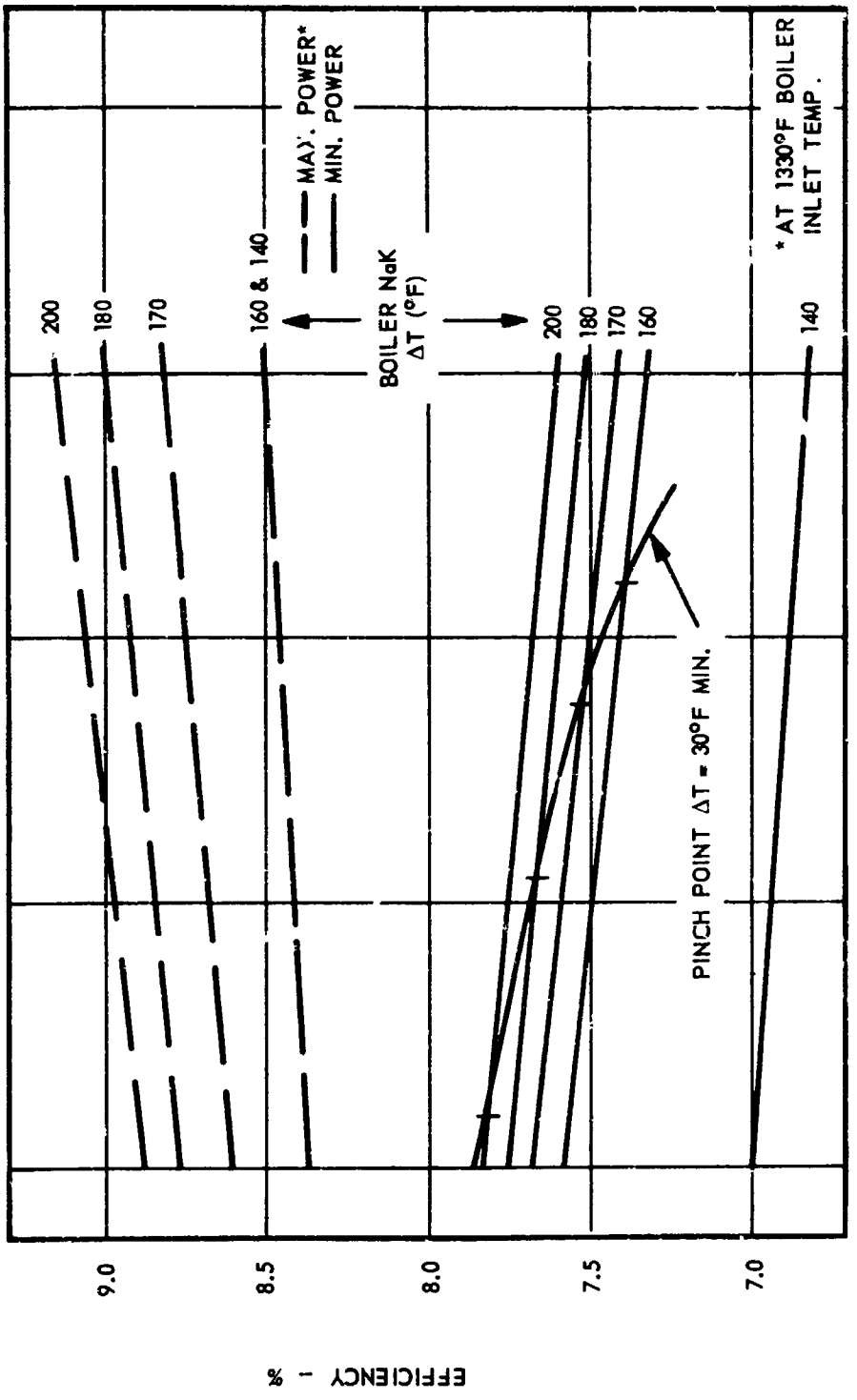

Overall Cycle Efficiency as a Function of Reactor Control Deadband and Boiler NaK ΔT at End of 10,000 Hours

Figure 25

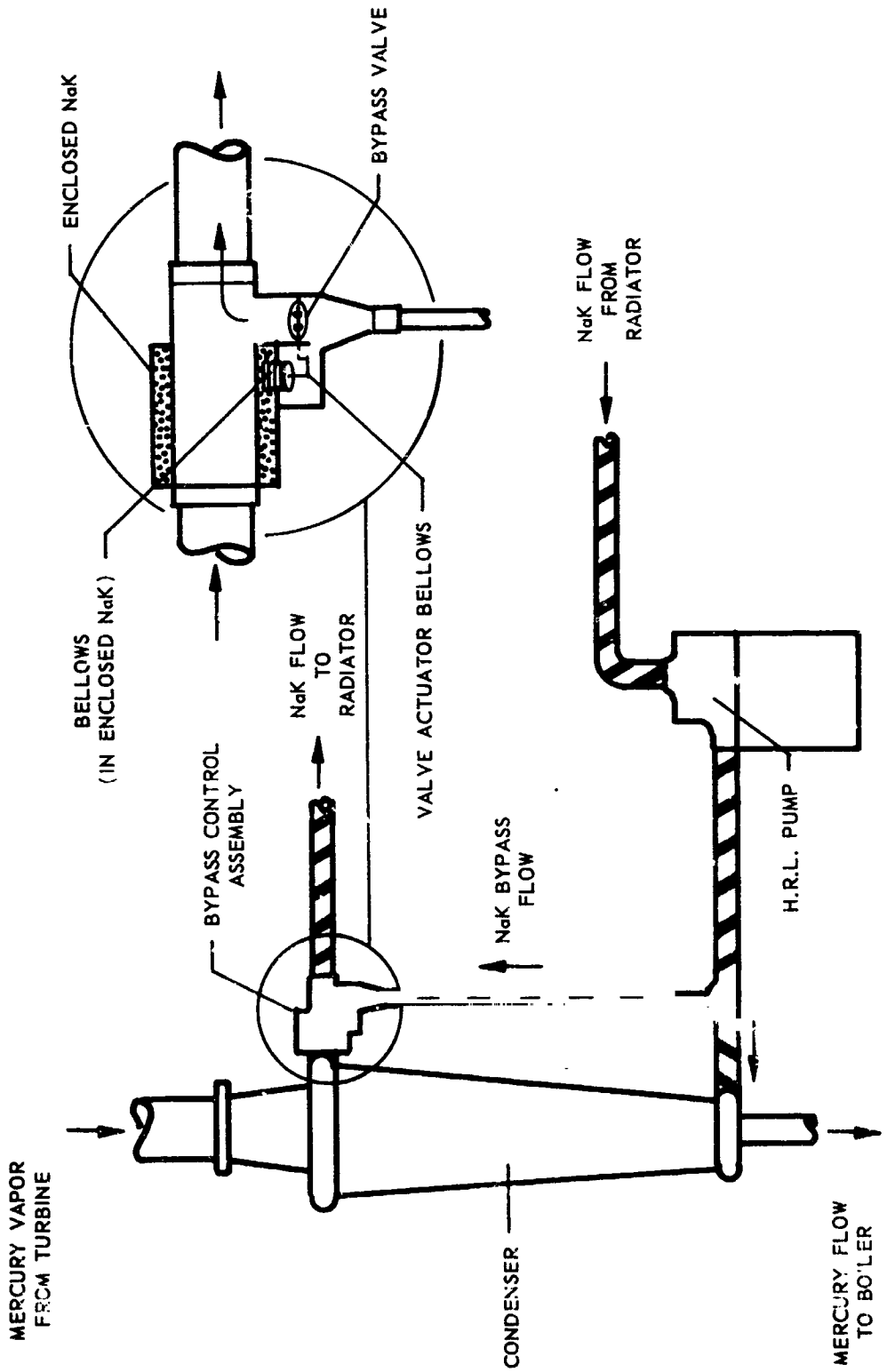

Condenser Bypass Flow Control

Figure 24

BLANK PAGE

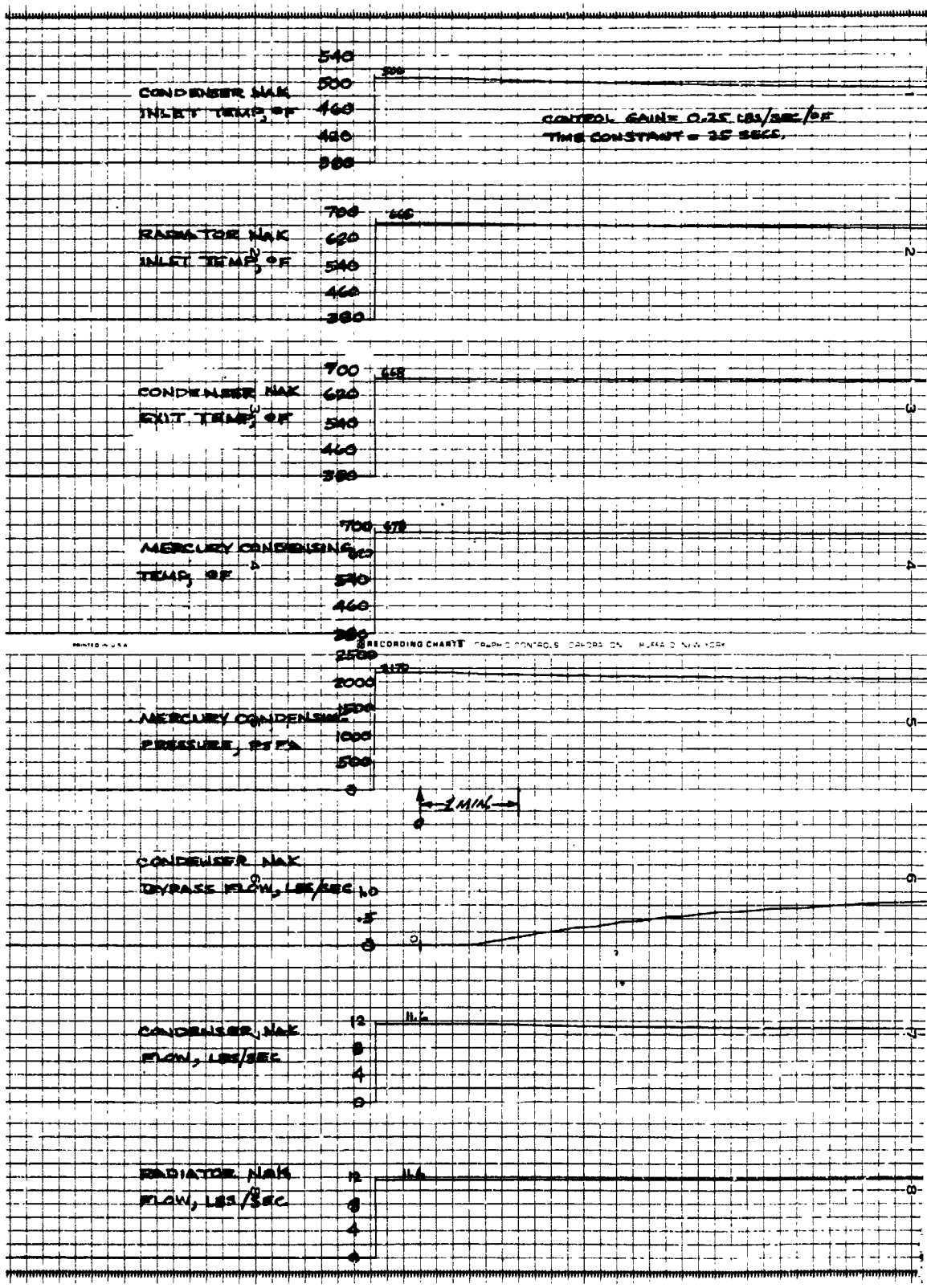

Condenser Bypass Control -

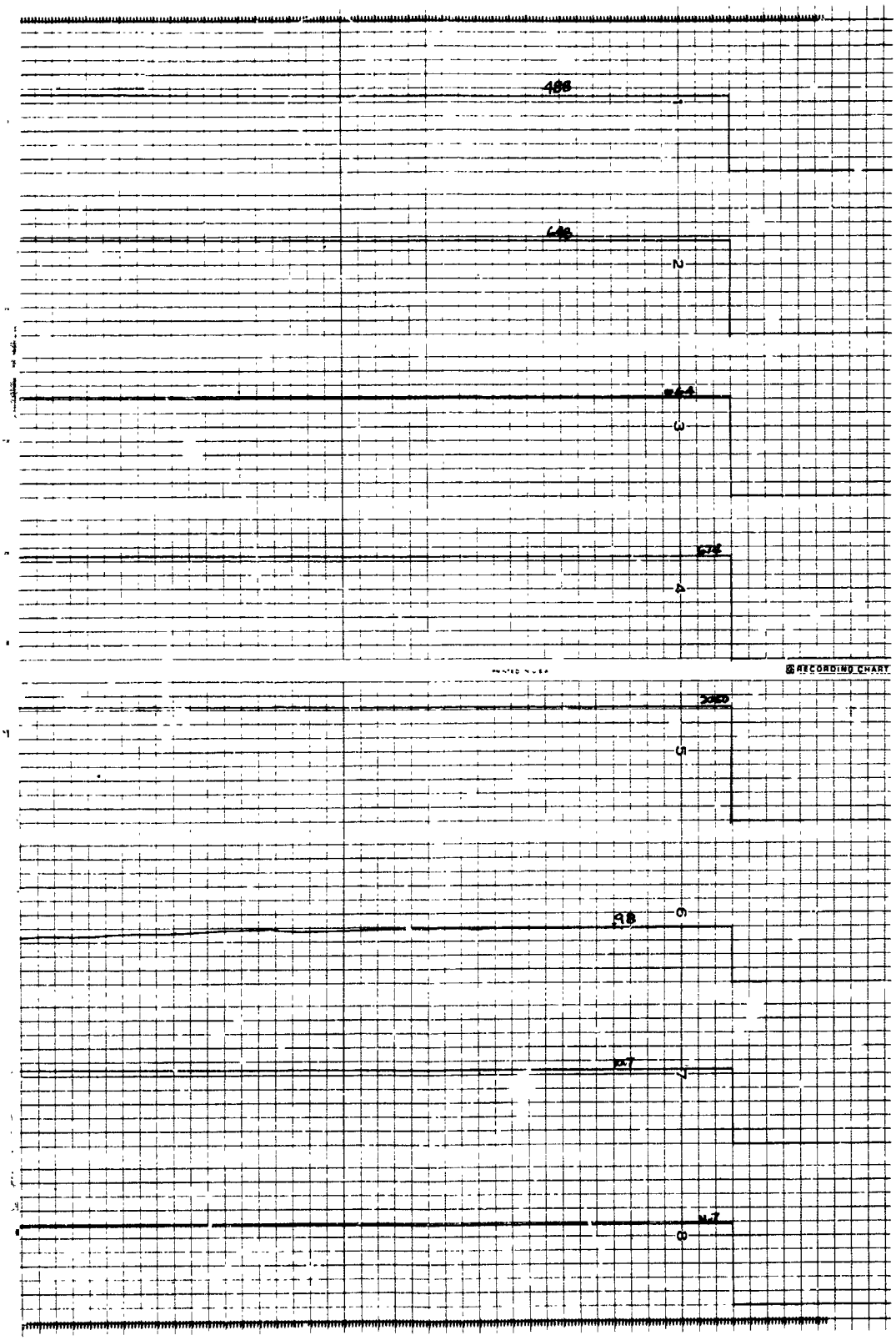

Sun-to-Shade Transient

Figure 25

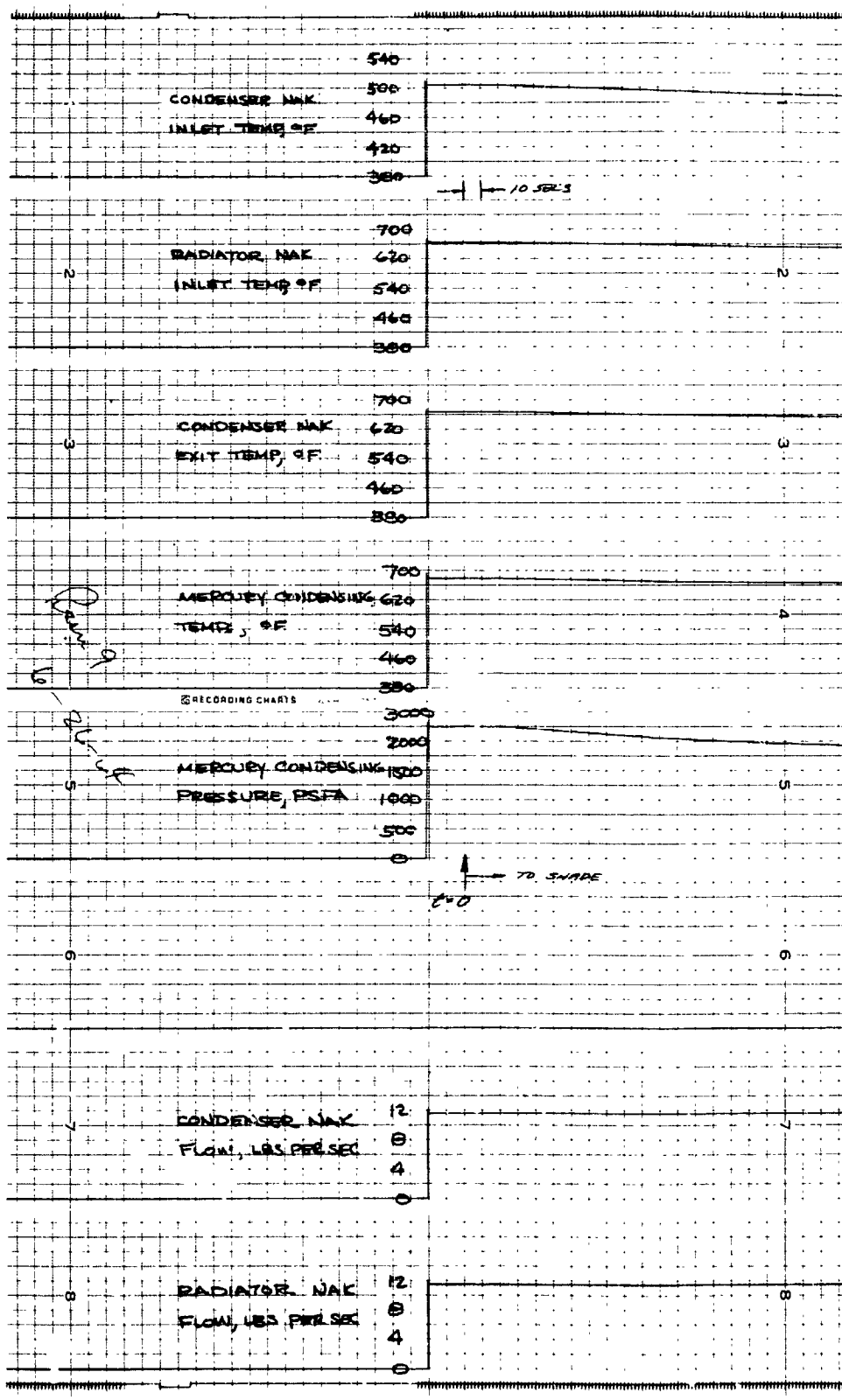

Sun-to-Shade Transi

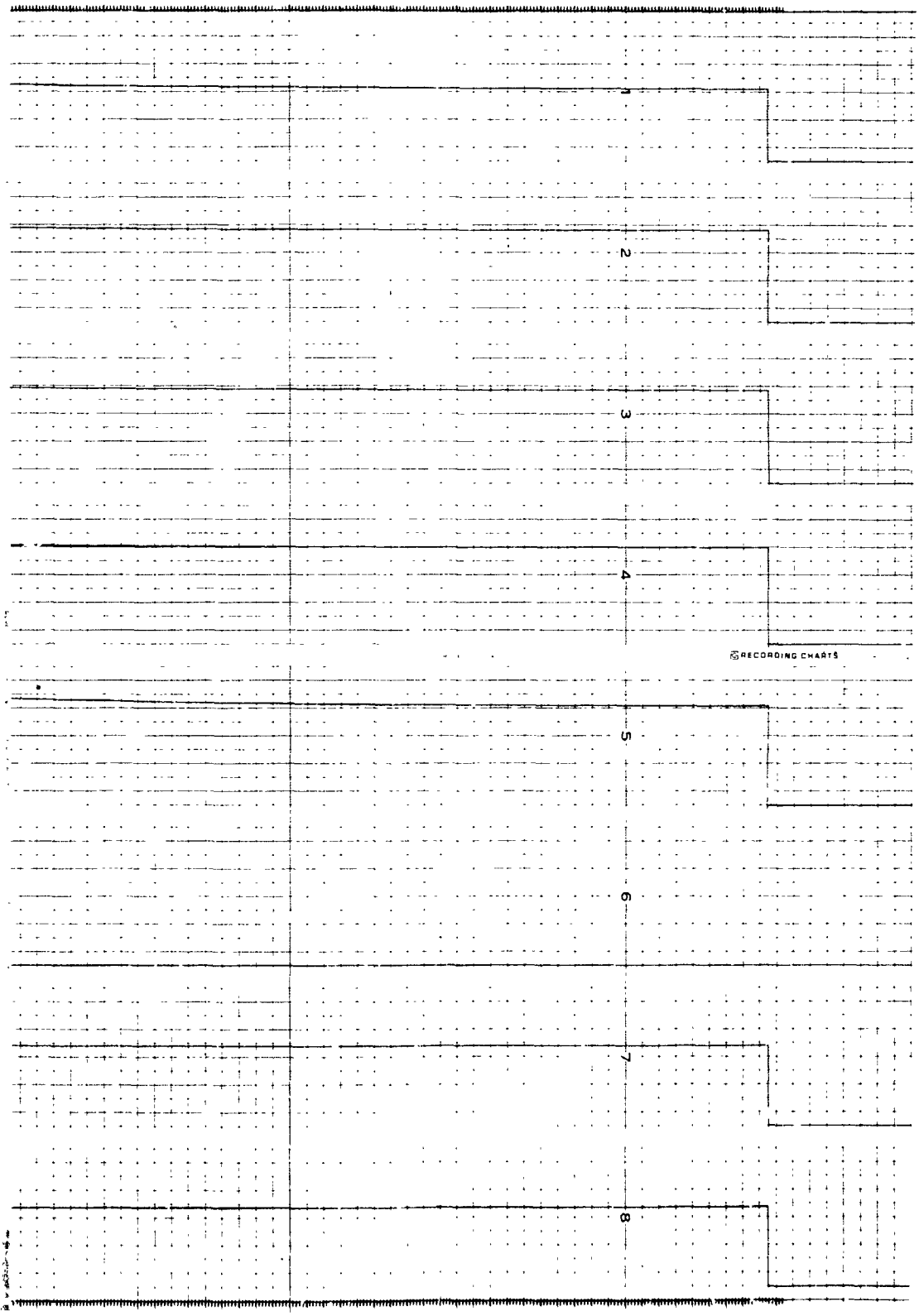

ent Without Bypass Control

Figure 5

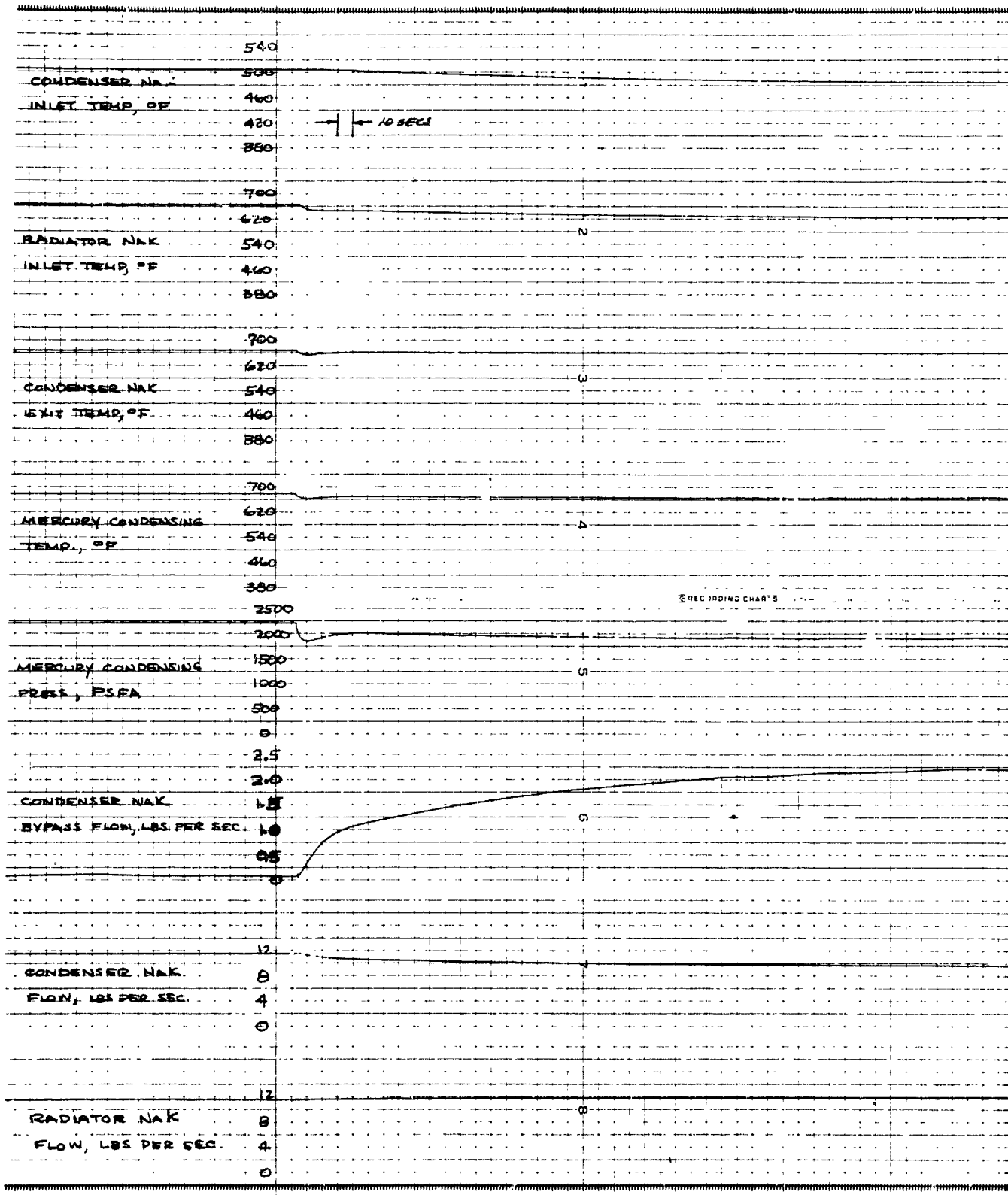

Condenser Bypass Control, -10%

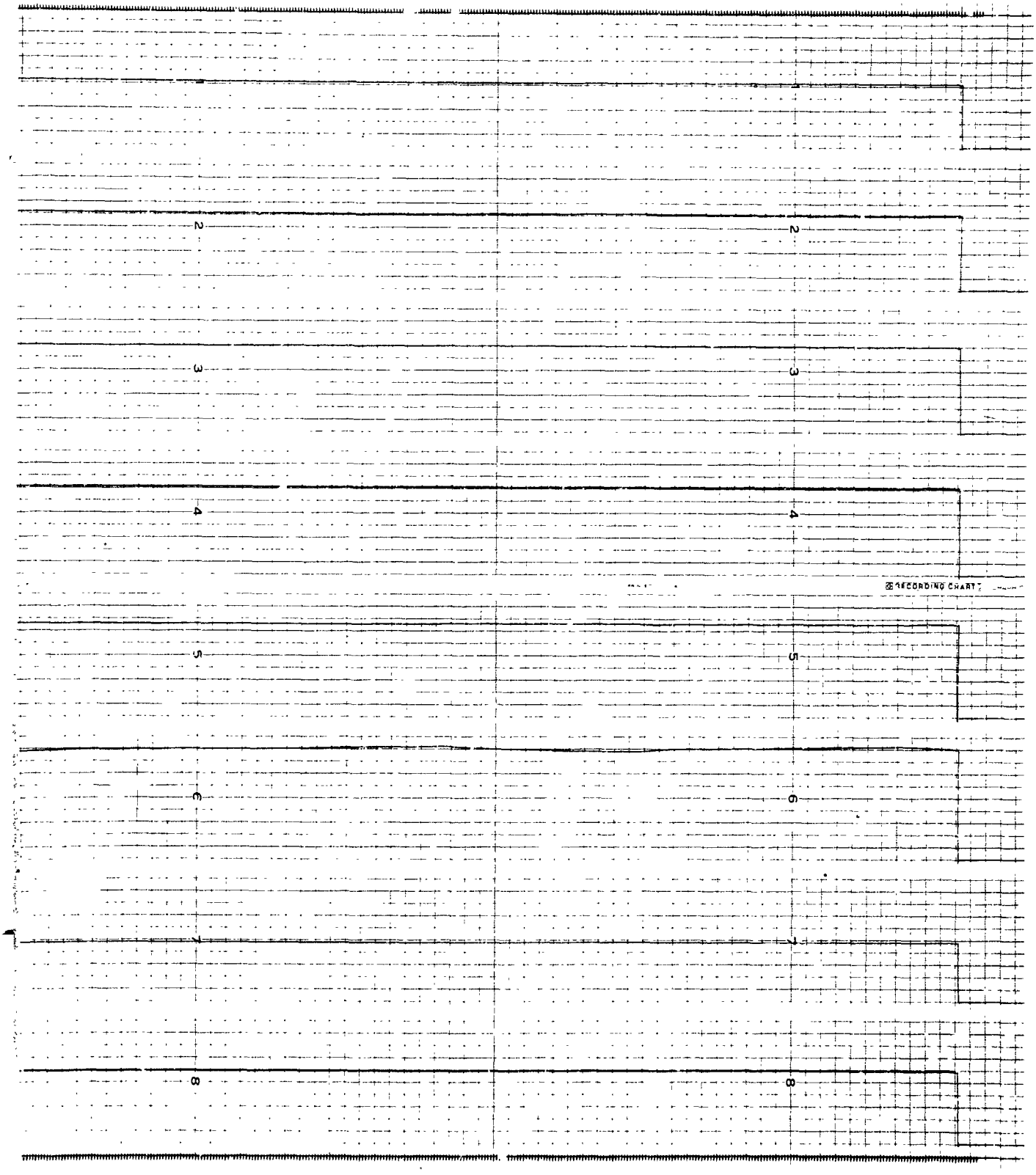

tep in Mercury Flow (3.11 to 2.8 lb/sec)

Figure 27

NOTE: K = CONTROL GAIN (LB/SEC/°F)

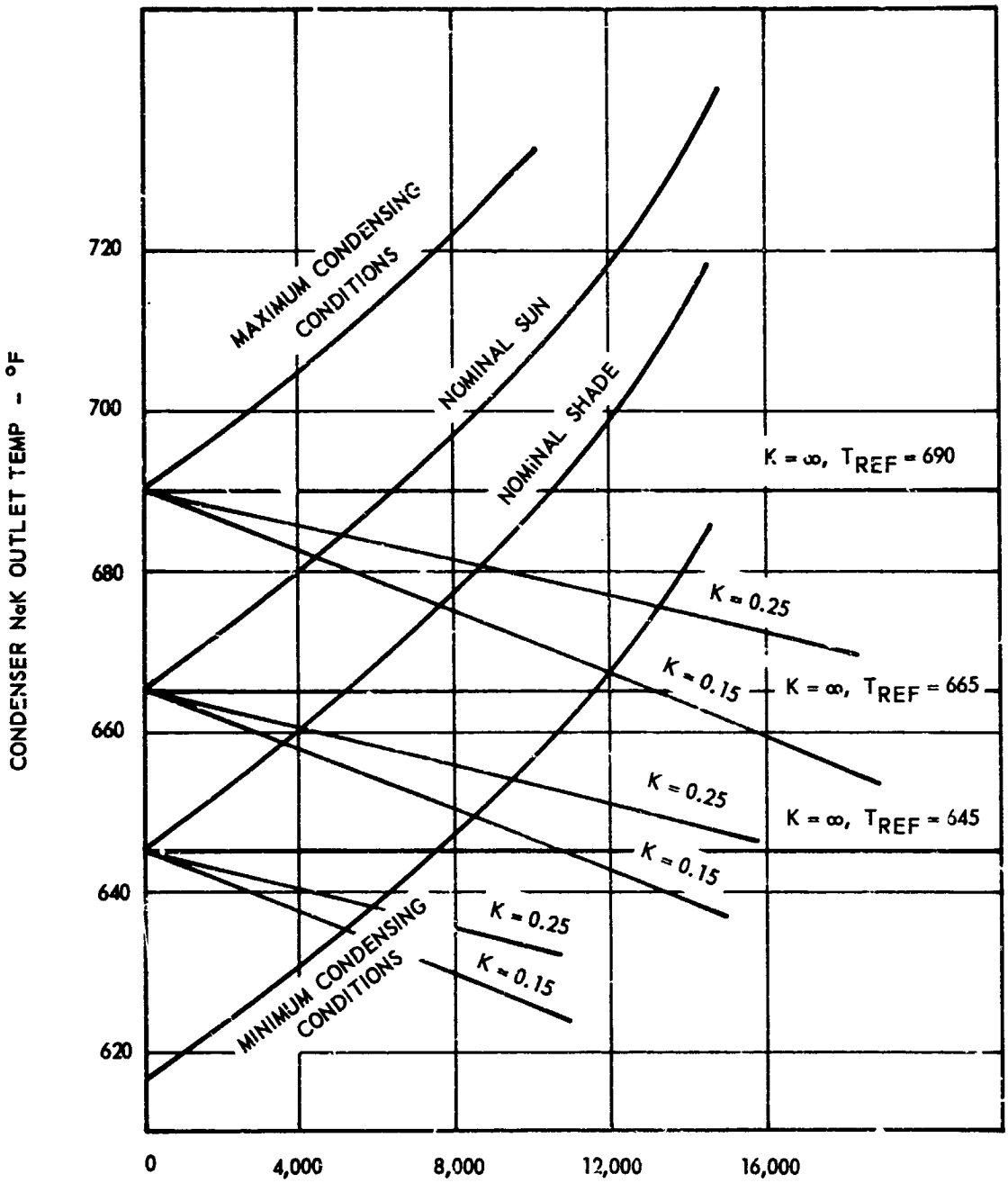

Condenser Bypass Control - NaK Exit Temperature Regulation for Varied Valve Gains

Figure 28

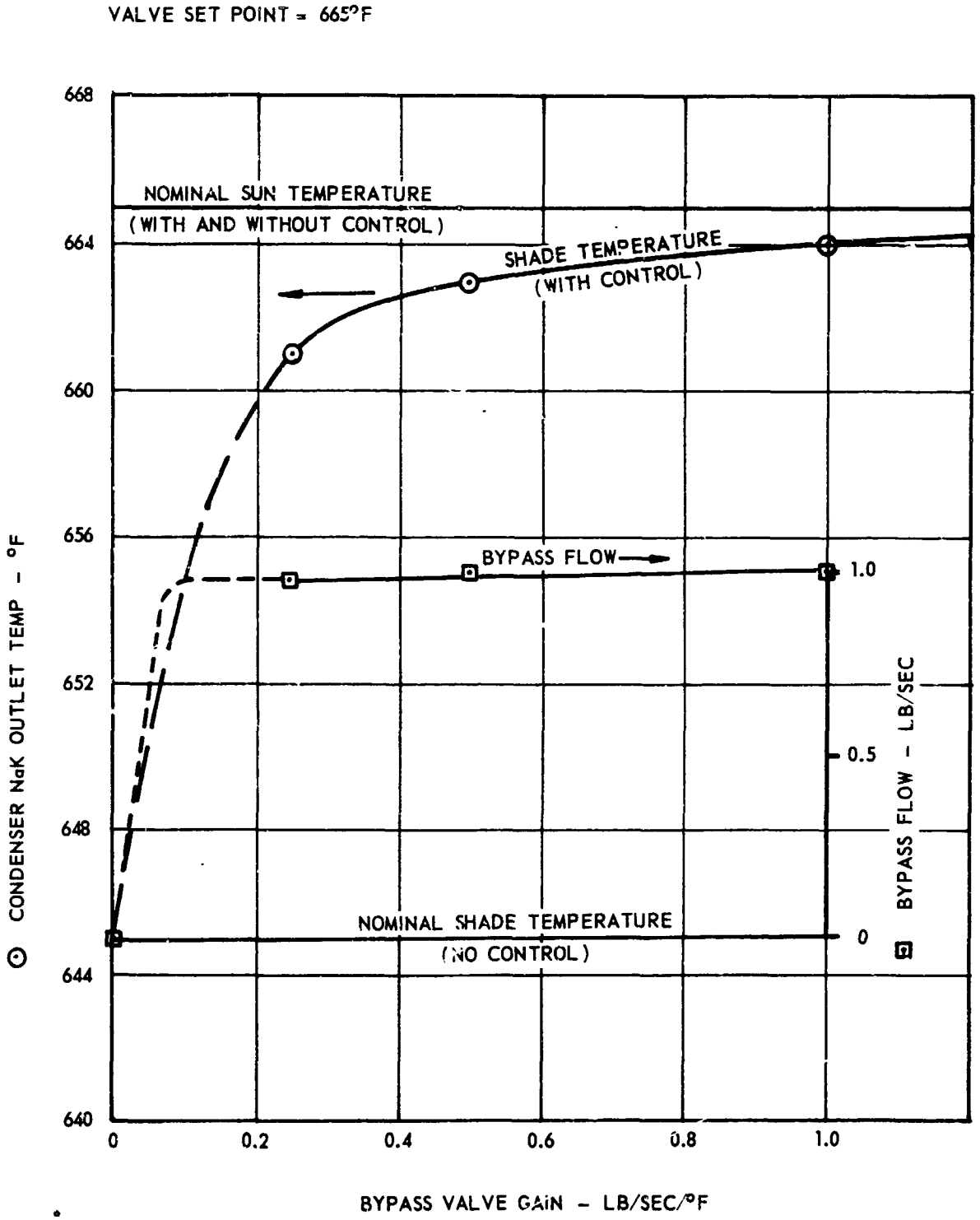

Condenser Bypass Control - Condenser NaK Outlet Temperature vs Bypass Control Gain for Radiator in Shade

Figure 29

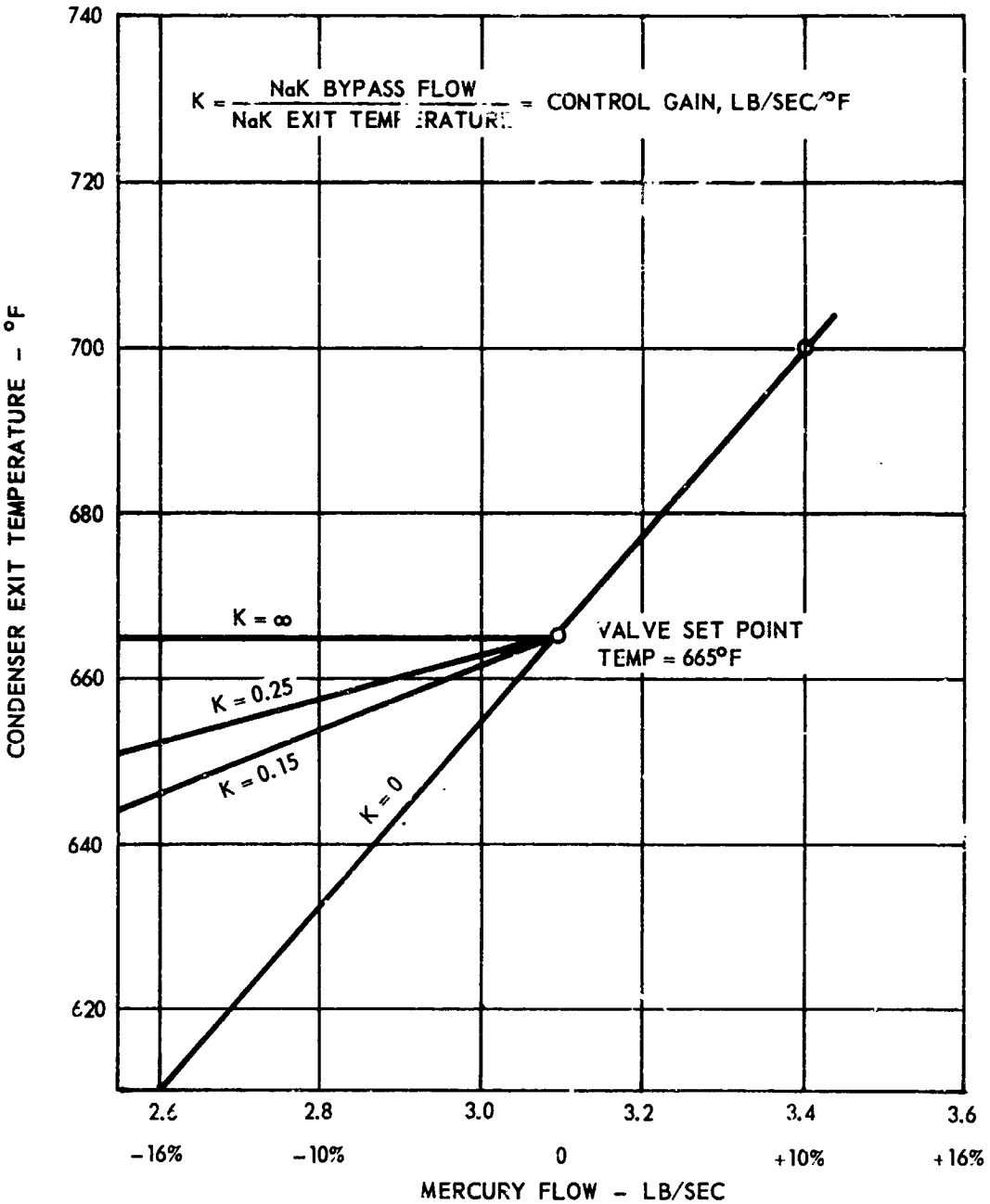

Condenser Bypass Control - Condenser NaK Exit Temperature vs Mercury Flow for Various Bypass Control Gains

Figure 30

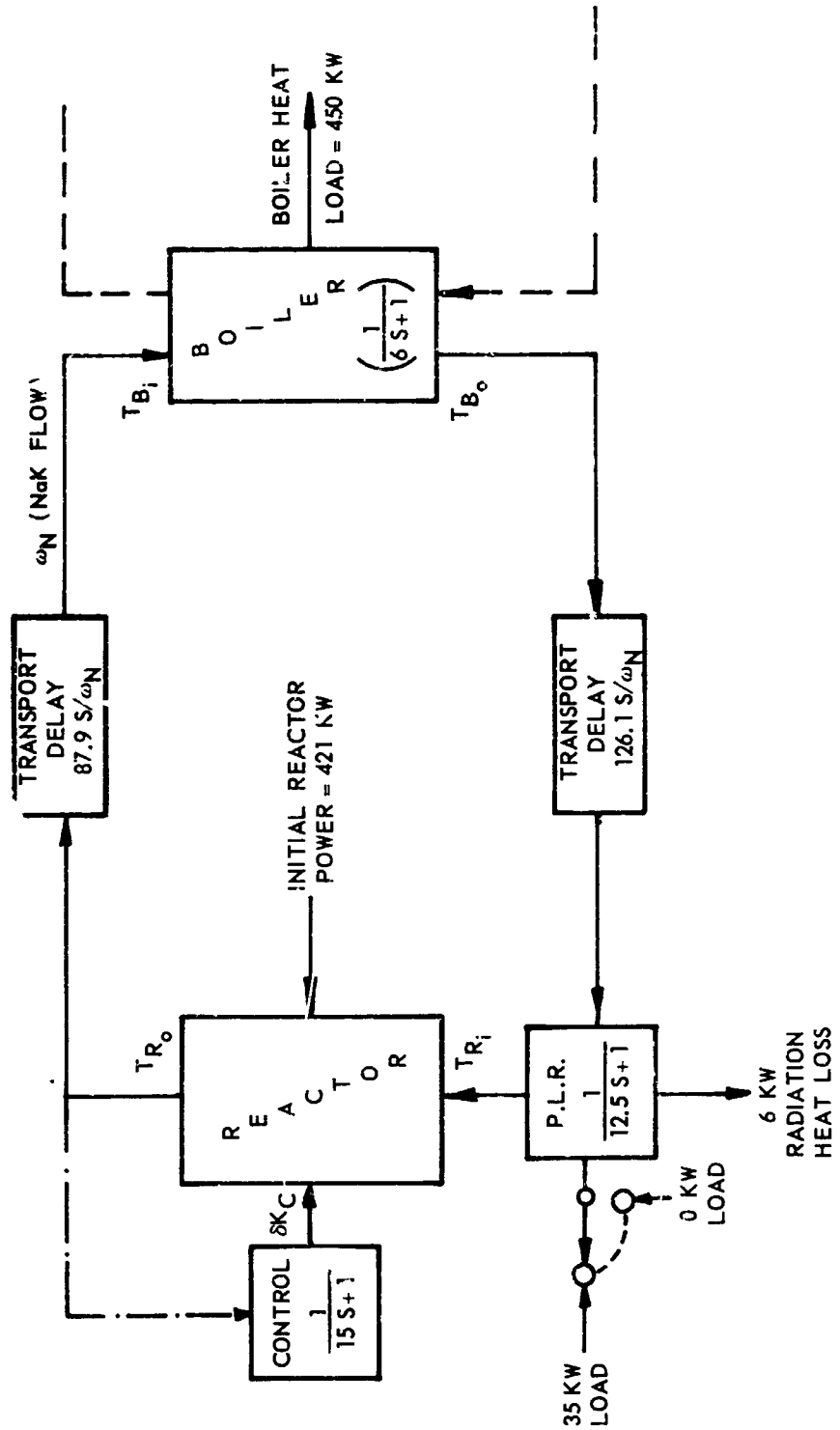

Primary Loop Simulation Schematic

Figure 31

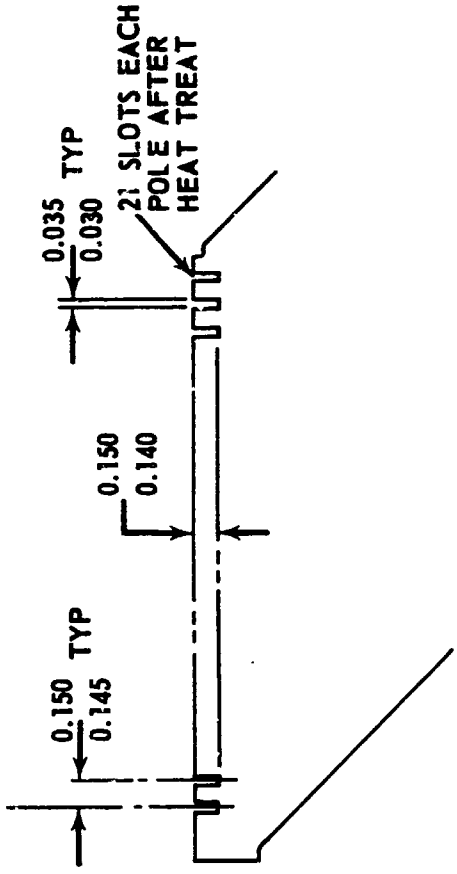

Cross Section of Slotted Alternator Pole

Figure 32

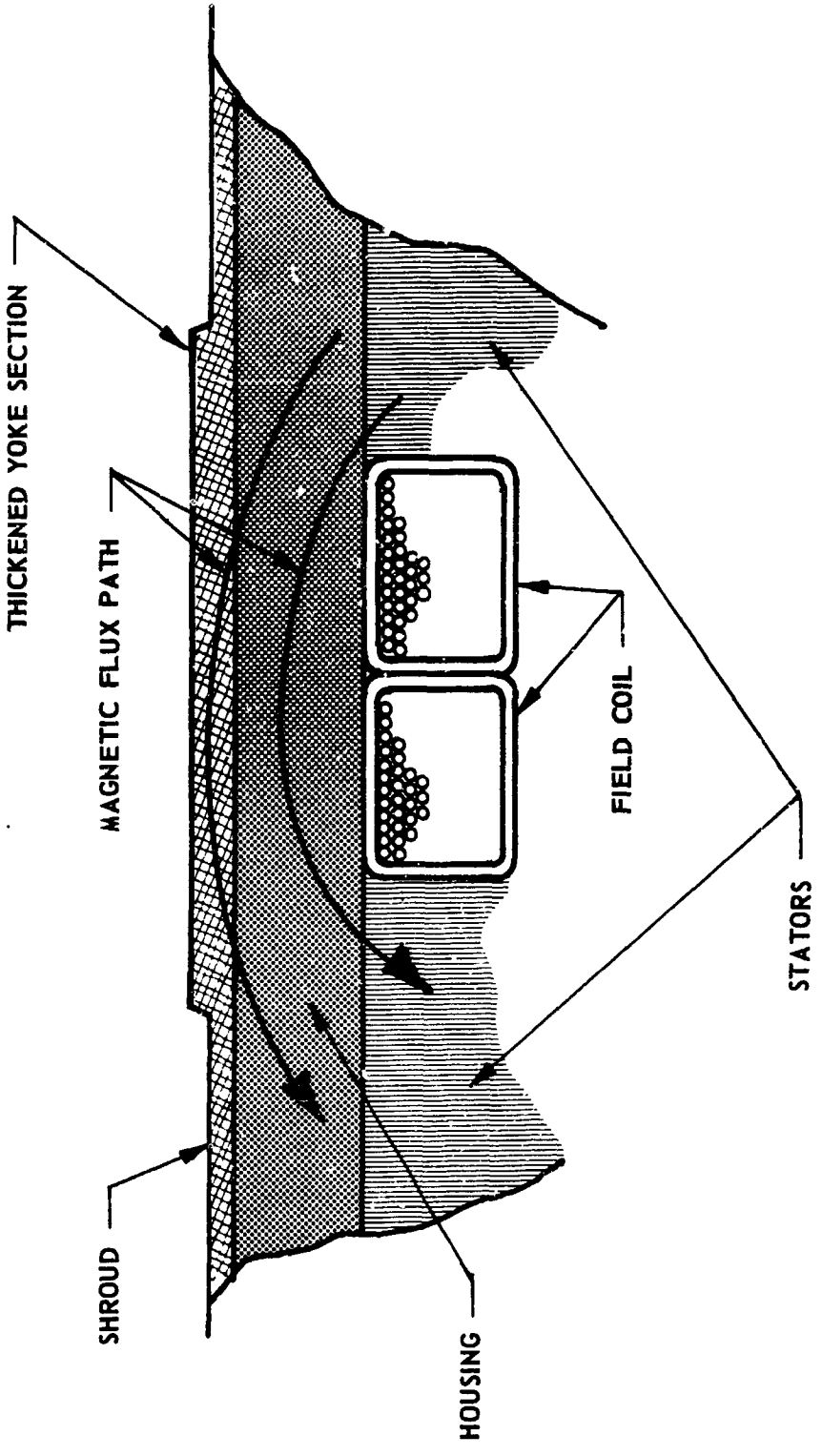

Cross Section of Alternator in Area of Yoke

Figure 33

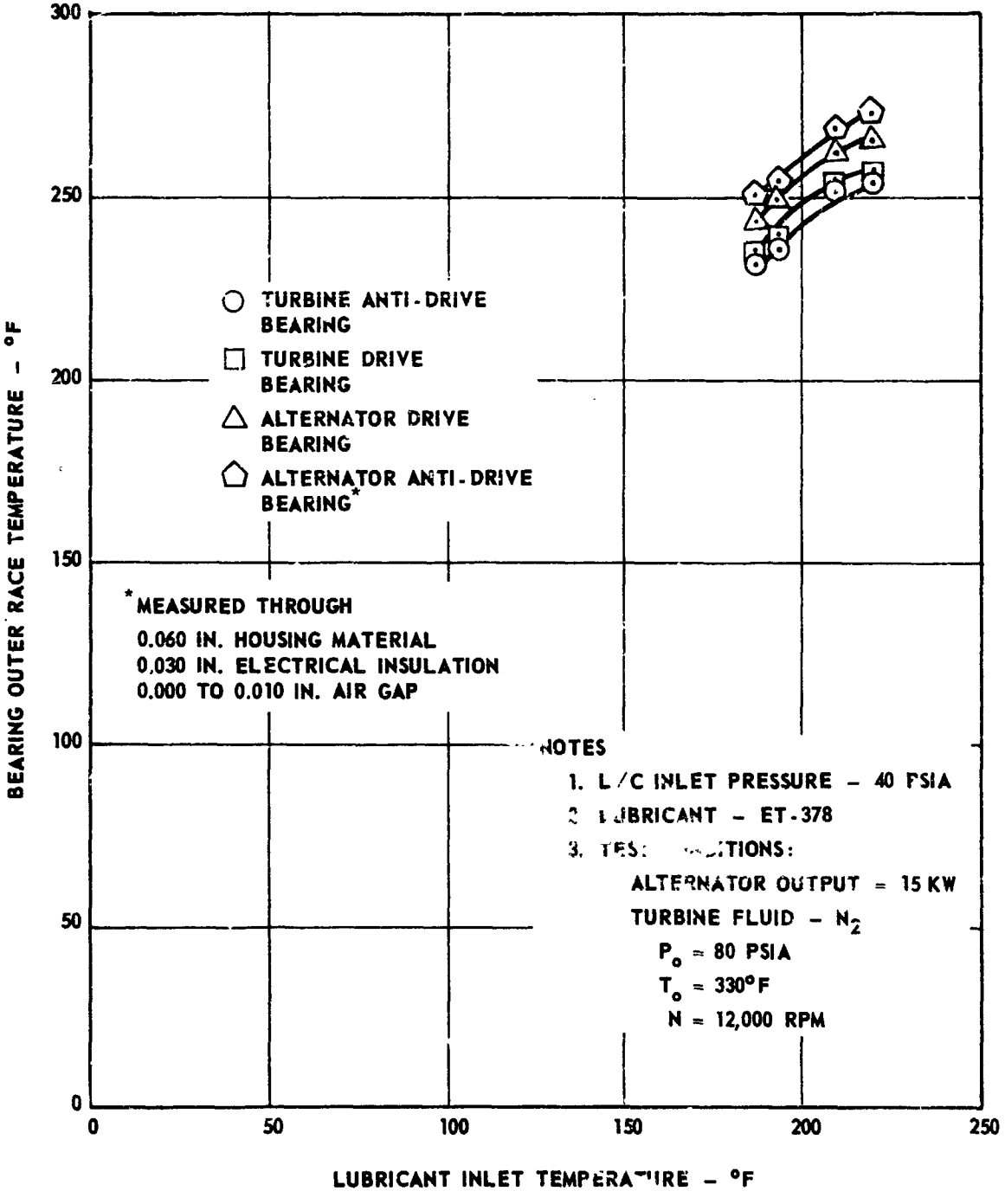

TAA Bearing Outer-Race Temperature for Different Lubricant Inlet Temperatures

Figure 34

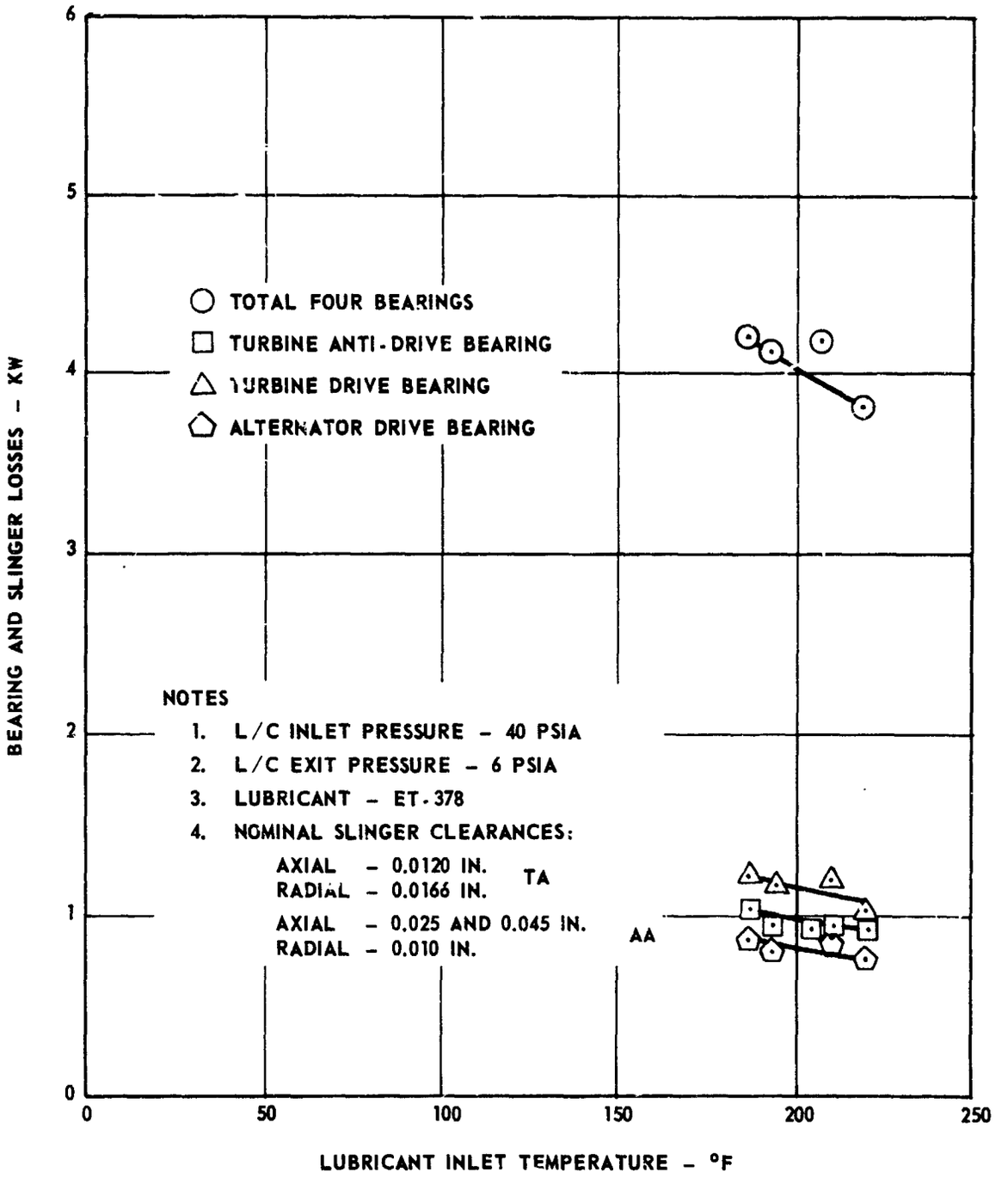

TAA Bearing and Slinger-Seal Losses for Different Lubricant Inlet Temperatures

Figure 35

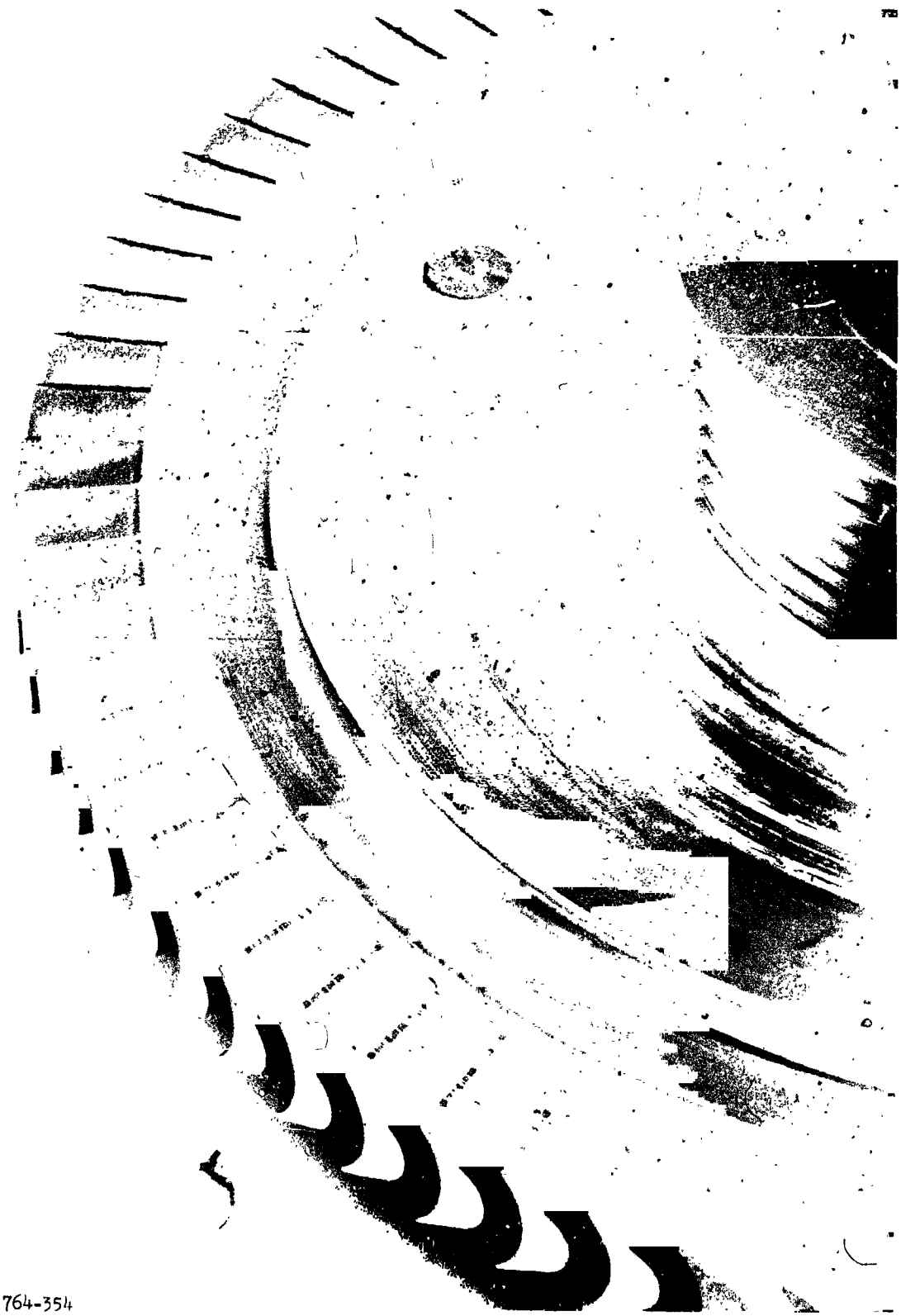

764-354

Leading Edge of TAA First-Stage Turbine Wheel Showing
Labyrinth Seal Hub Wear and Damaged Blades

Figure 36

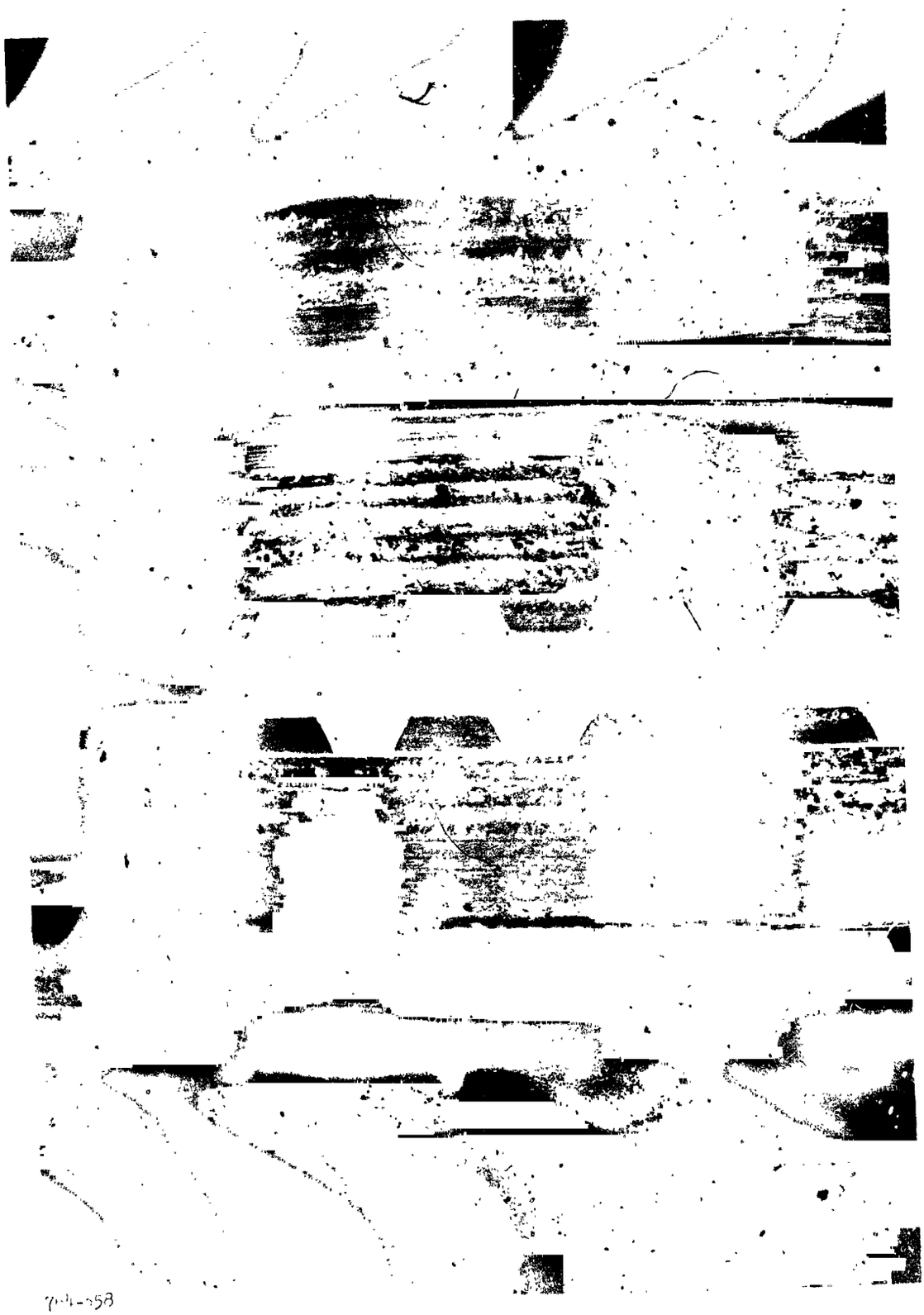

TAA First-Stage (Right) and Second-Stage (Left) Wheel Hubs
Showing Wear from Contact with Labyrinth Seal

Figure 37

TRAIL SIDE:

764-873

TRAIL SIDE:

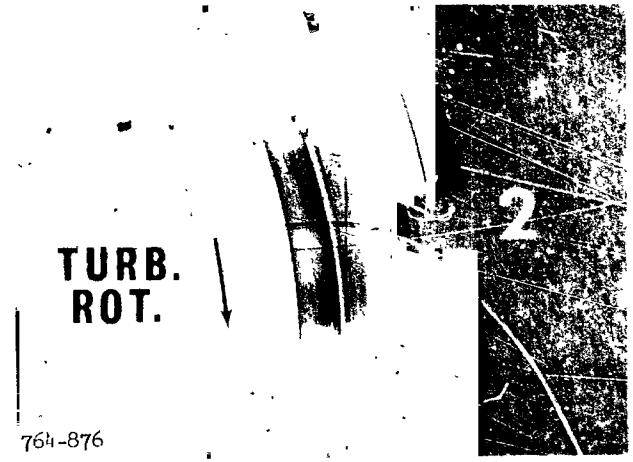

764-876

LEAD SIDE:

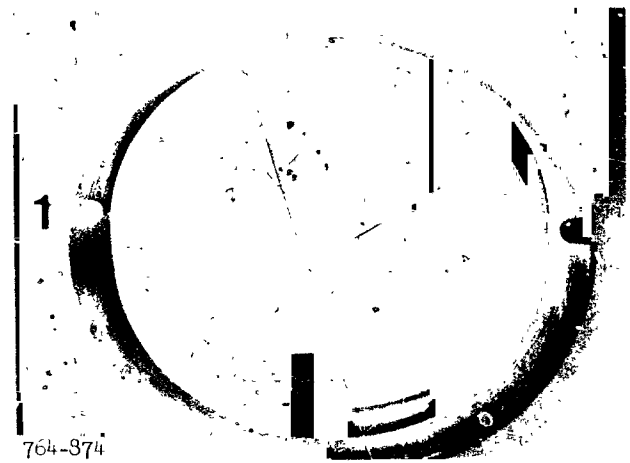

764-874

LEAD SIDE:

764-875

NOTE CRACKS AT NO. 1 AND NO. 2 SLOTS, LABYRINTH DAMAGE

2ND STAGE LABYRINTH SEAL TIME: 5 HRS, 29 MIN

Figure 38

TAA Labyrinth Seal Damage

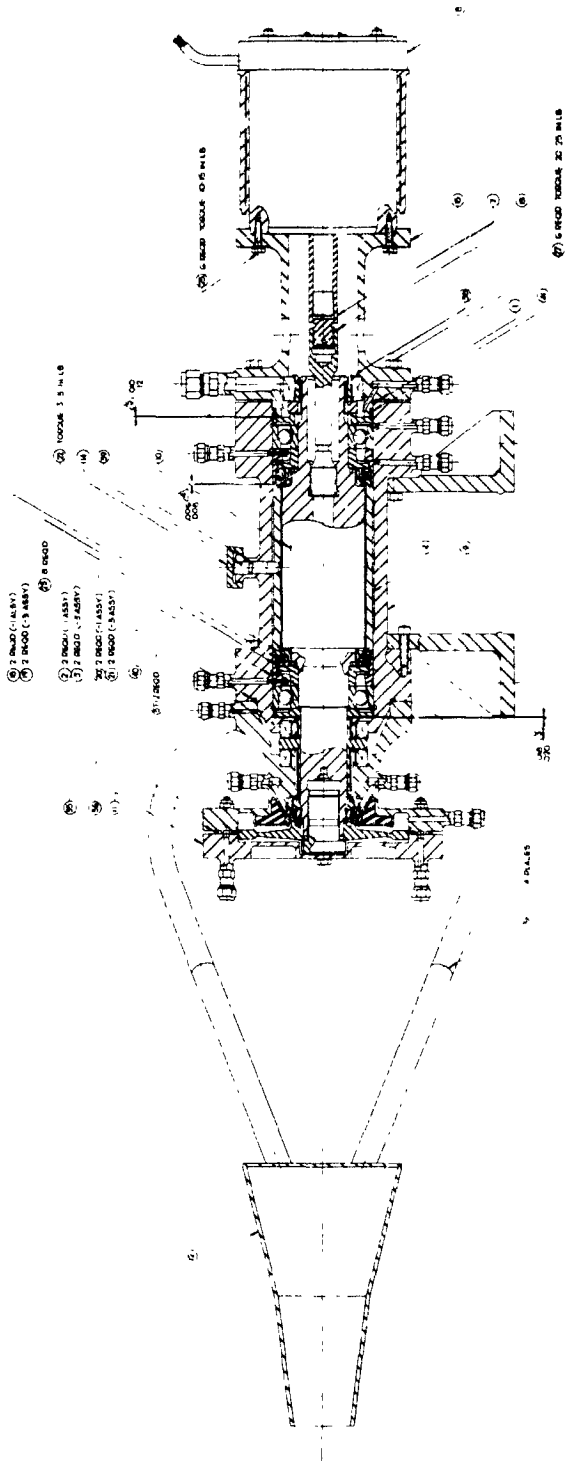

Model B Seal Simulator Assembly Drawing

Figure 39

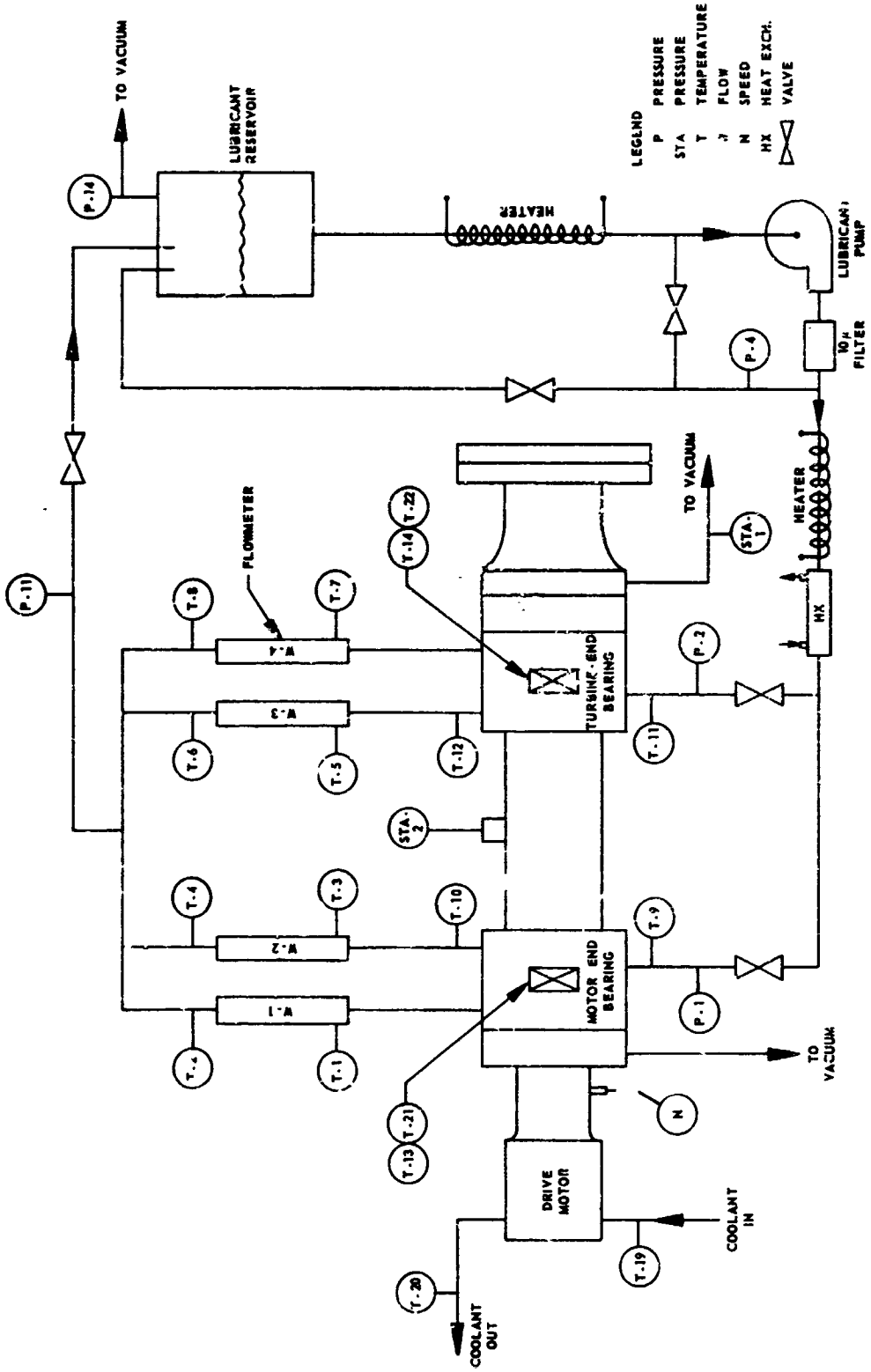

Lubrication System and Instrumentation - Model B Seal Simulator

Figure 40

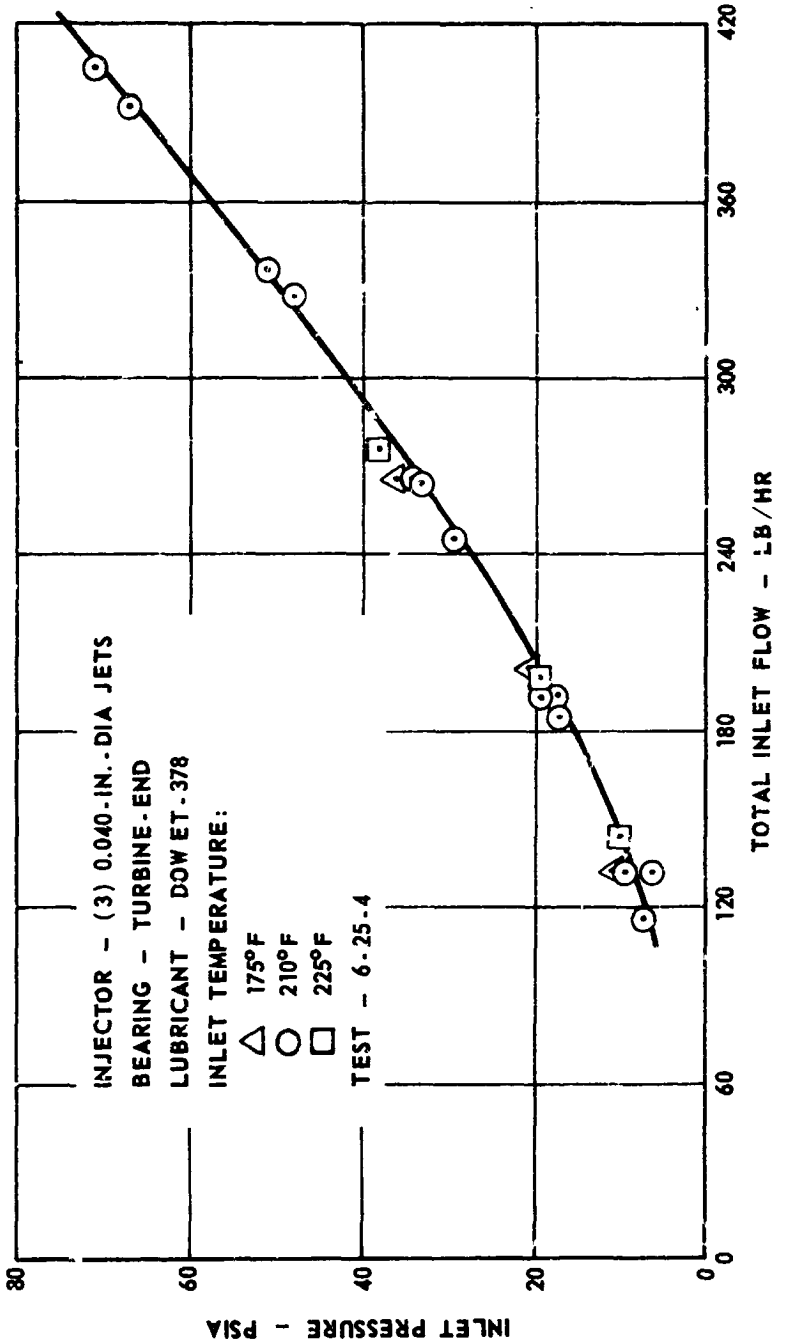

Pressure-Flow Characteristic of Lubricant Injector Ring
Model B Seal Simulator

Figure 41

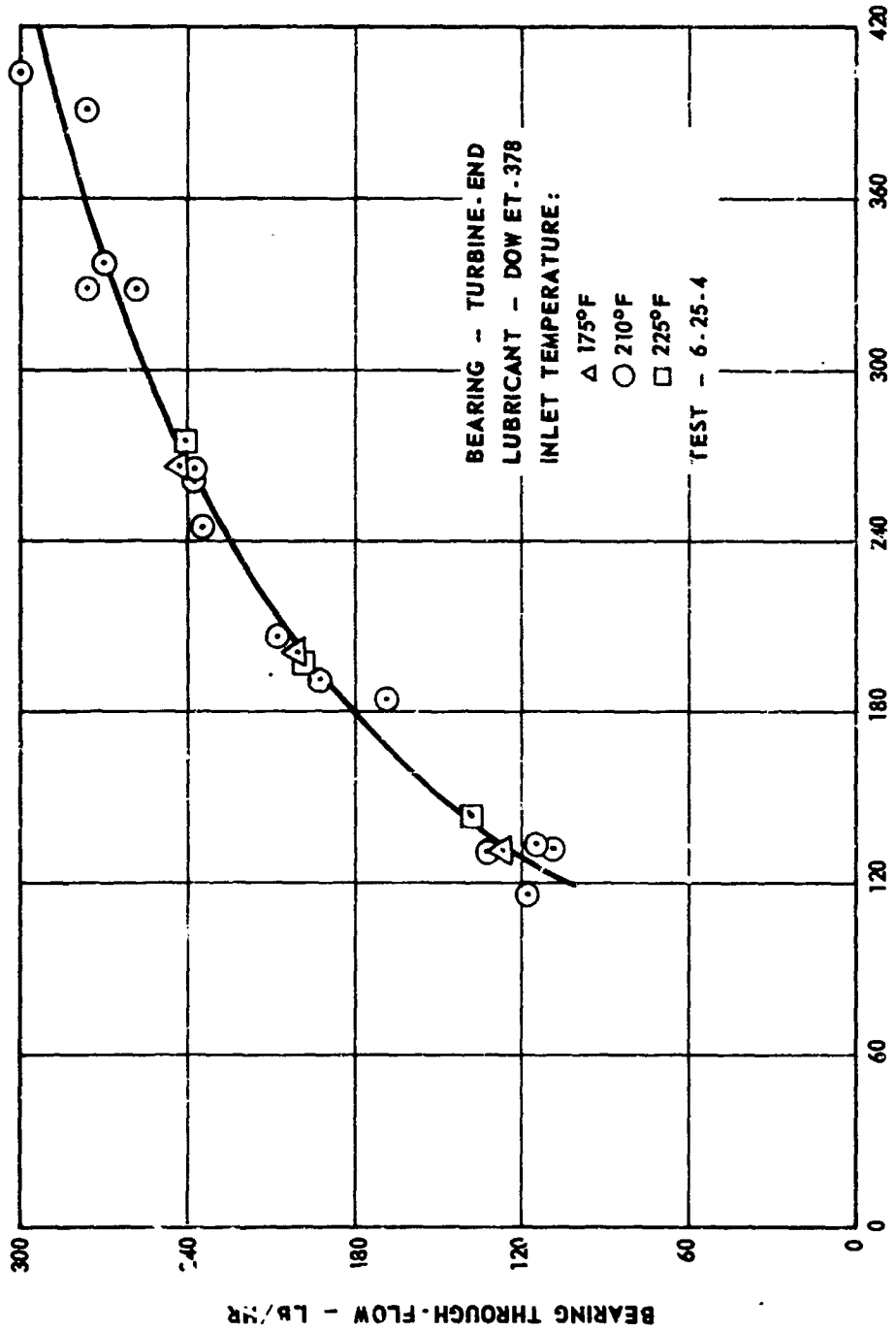

Bearing Through-Flow vs Inlet Flow - Model B Simulator Rig

Figure 42

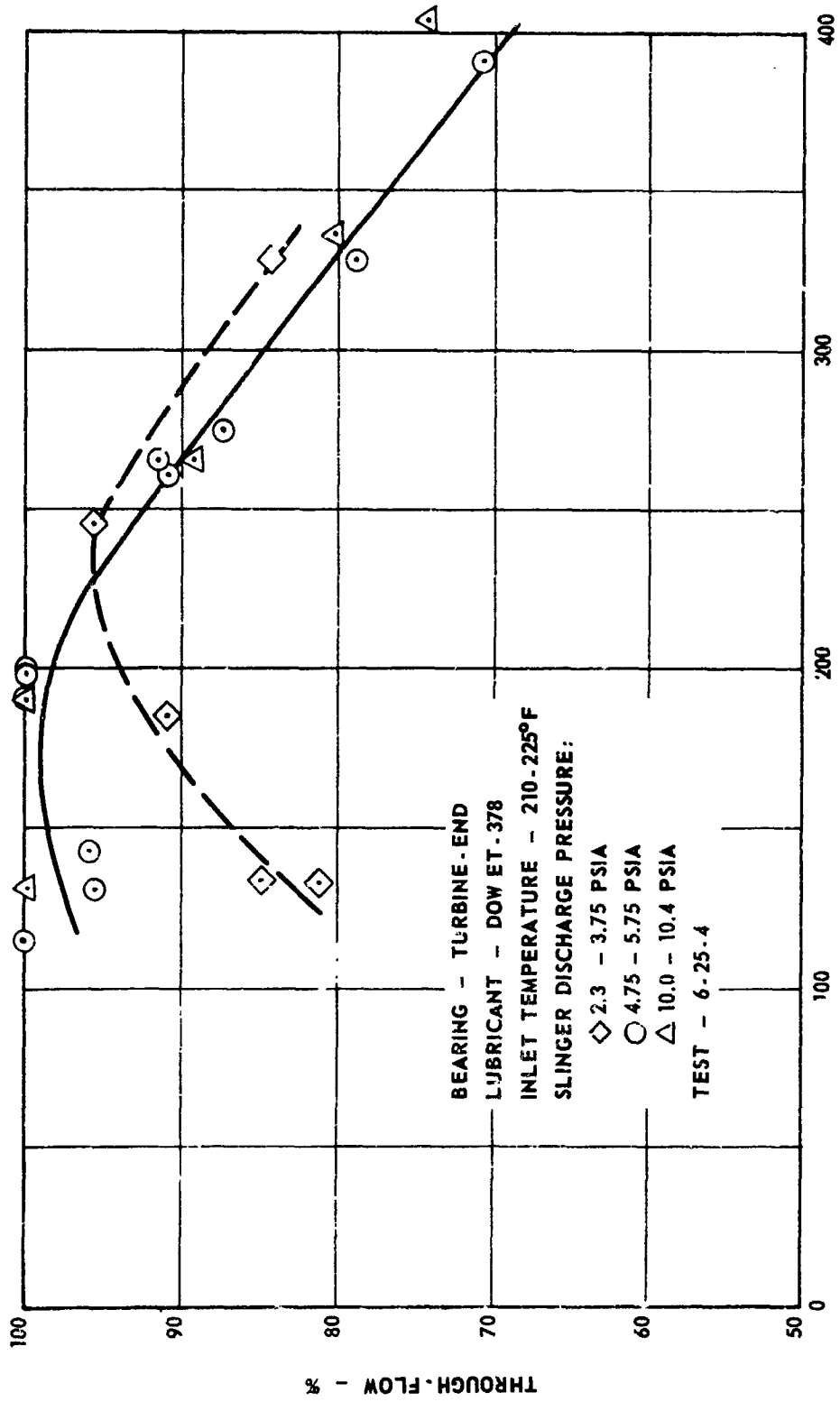

Percent Flow Through Bearing vs Total Inlet Flow
Model B Seal Simulator

Figure 43

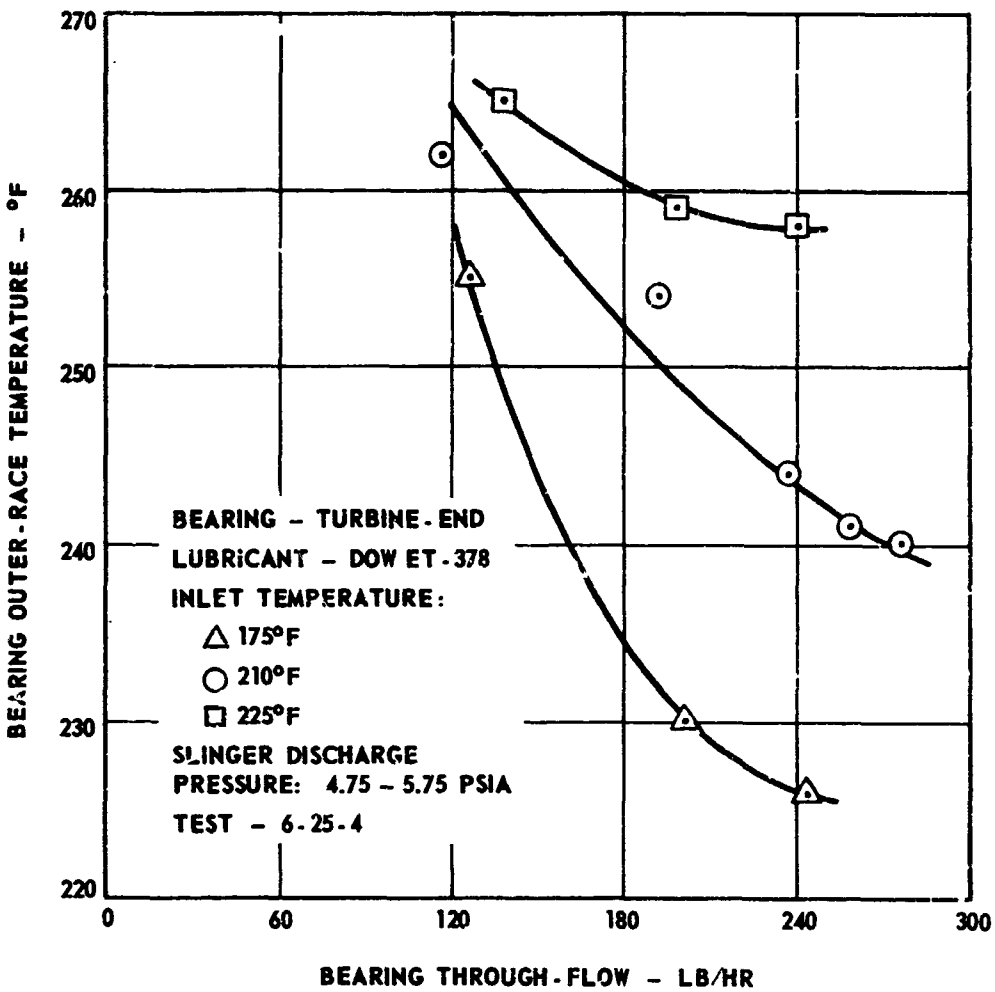

Effect of Bearing Through-Flow on Outer Race Temperature
Model B Simulator Rig

Figure 44

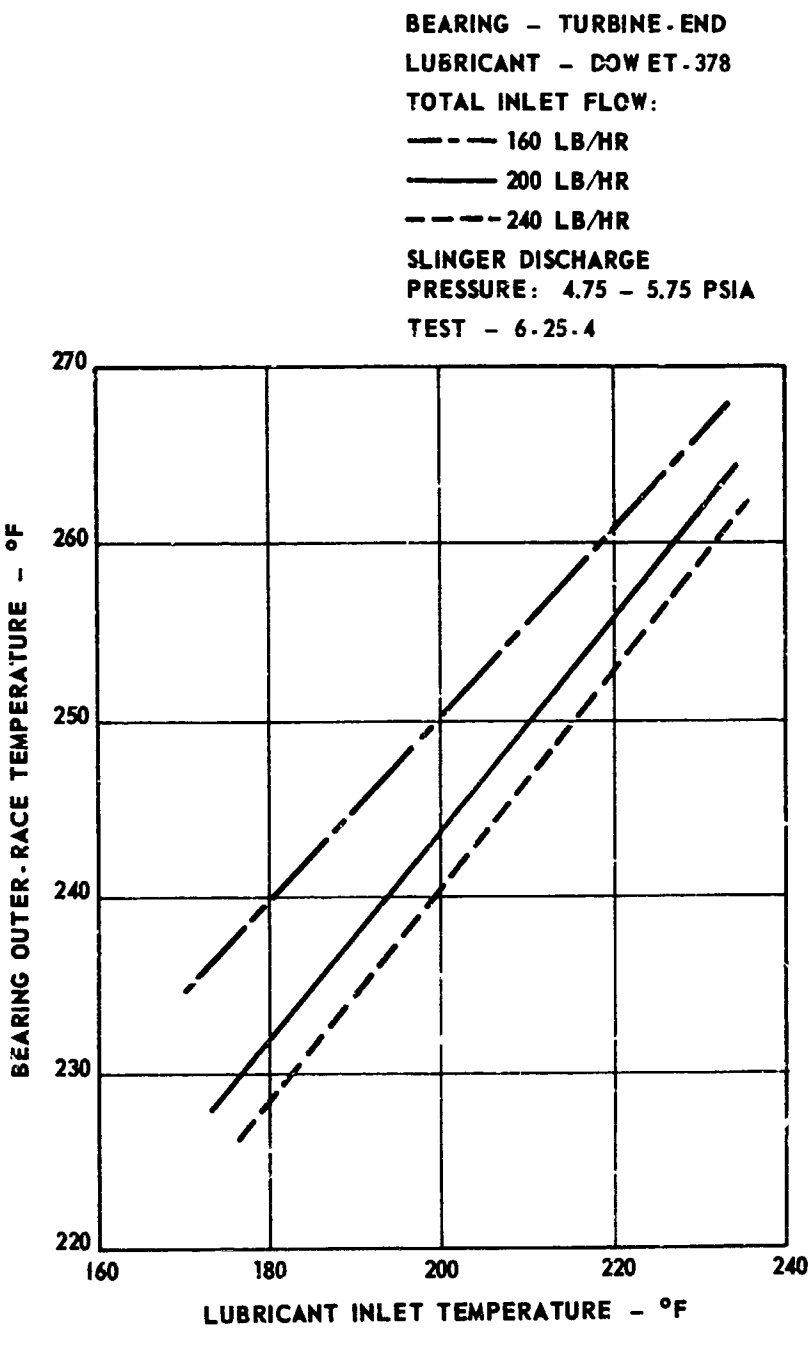

Bearing Outer-Race Temperature vs Lubricant Inlet Temperature for Various Inlet Flow Rates - Model B Simulator Rig

Figure 45

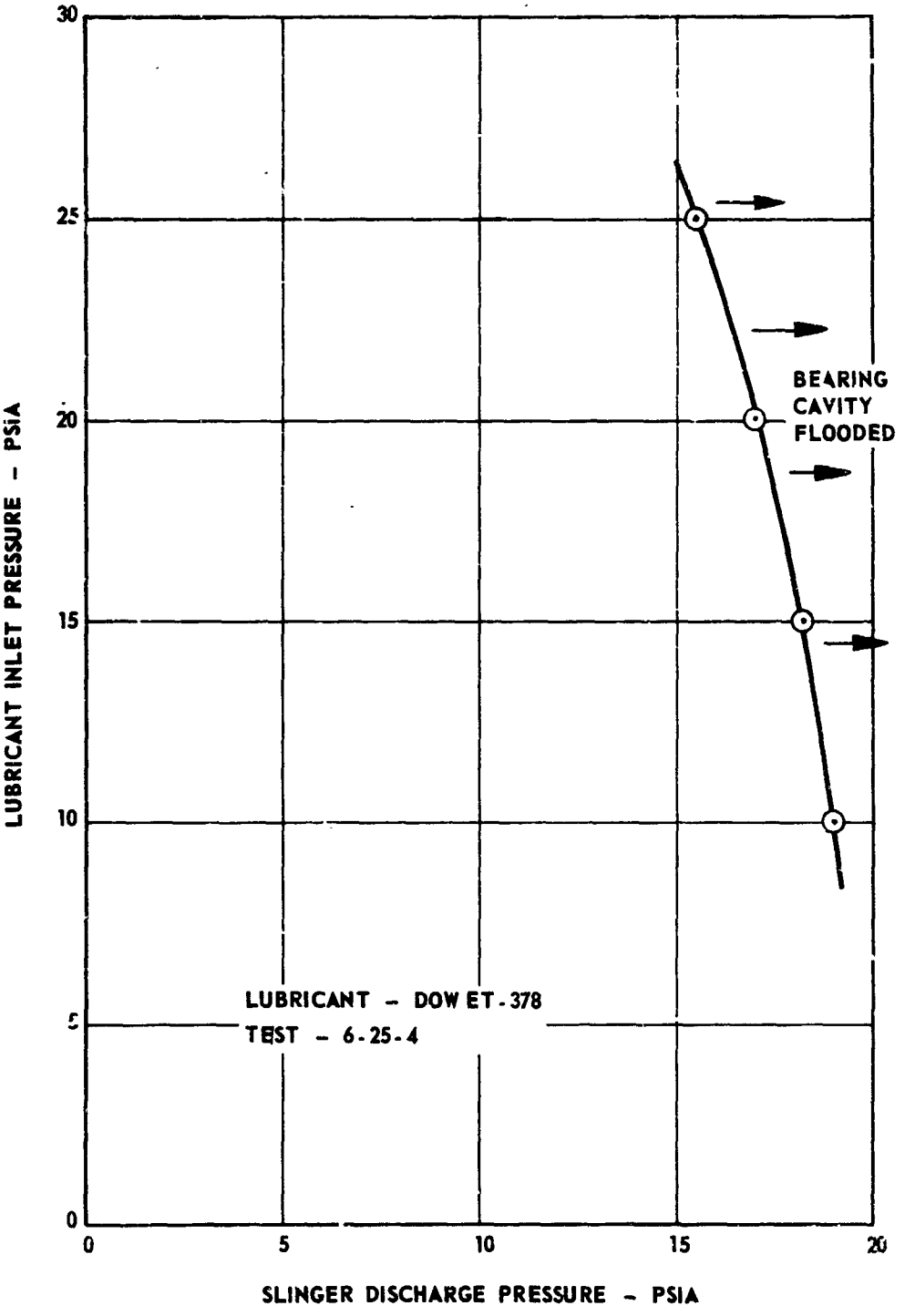

Bearing Cavity Flooding as a Function of Slinger Discharge Pressure
Model B Simulator Rig

Figure 46

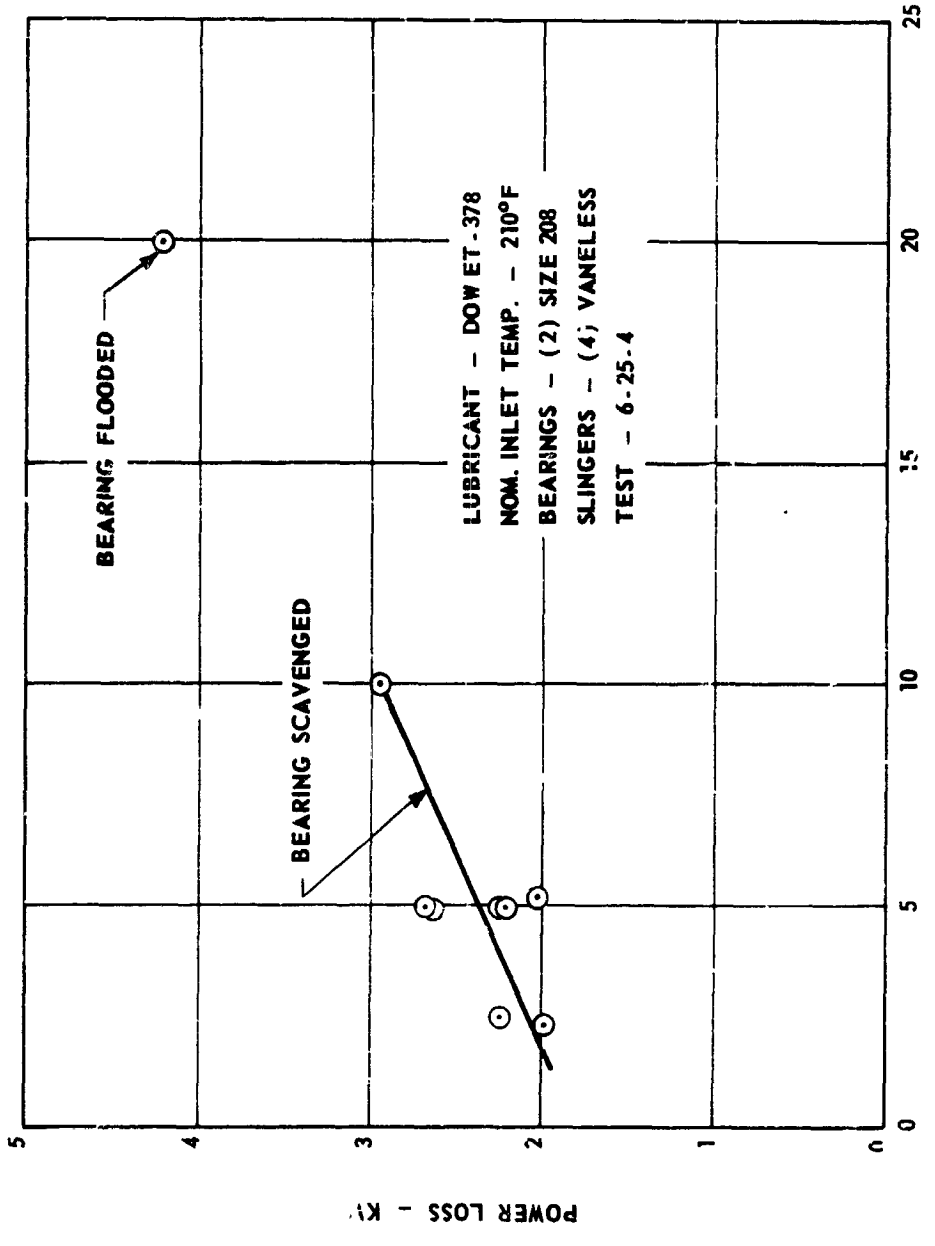

Bearing and Slinger Power Loss - Model B Seal Simulator

Figure 47

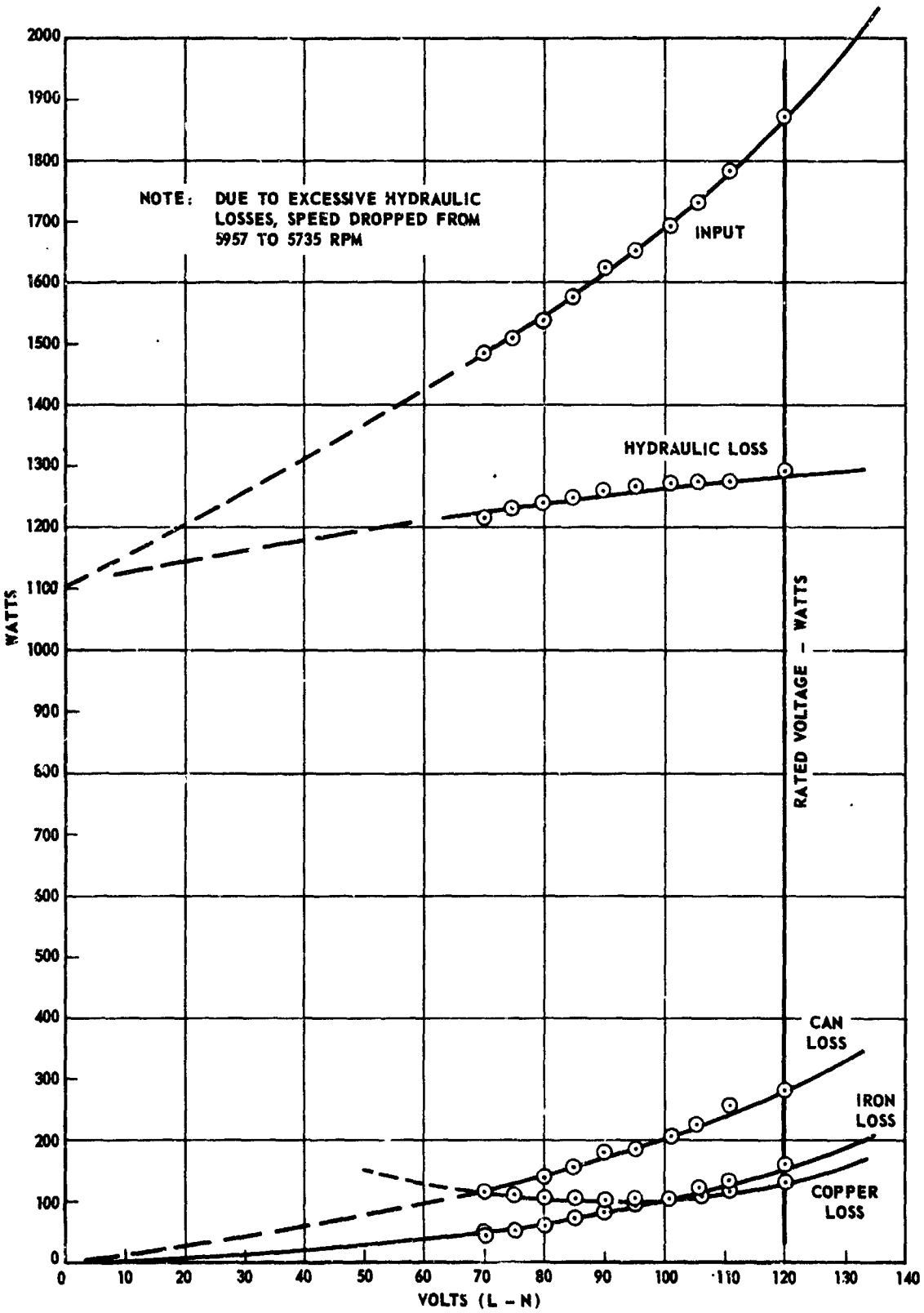

No-Load Loss Breakdown - Heat Rejection Loop Pump Motor Assembly (400 cps, 204°F)

Figure 48

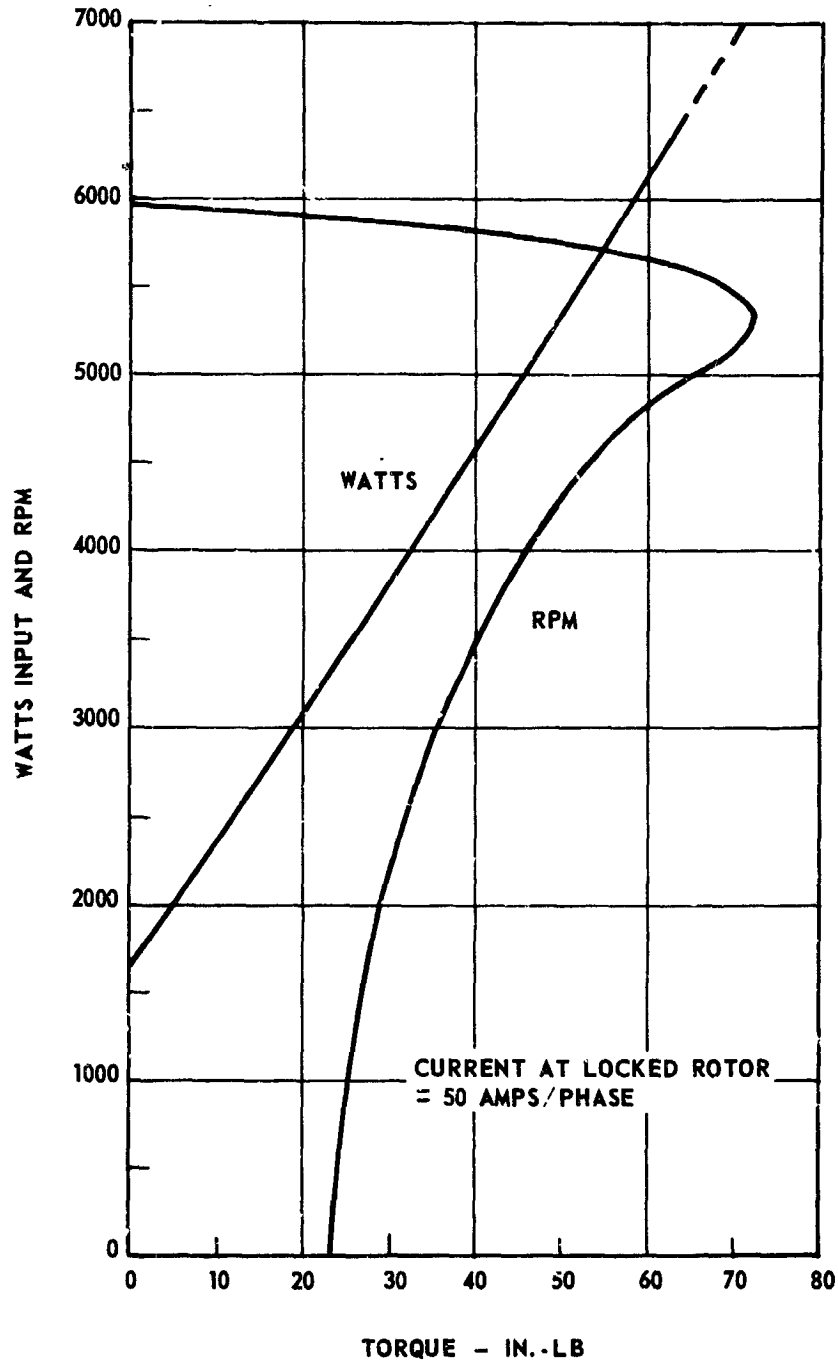

Calculated Speed-Torque - Heat Rejection Loop Pump Motor Assembly
(208 v, 400 cps, 200°C Winding Temperature)

Figure 49

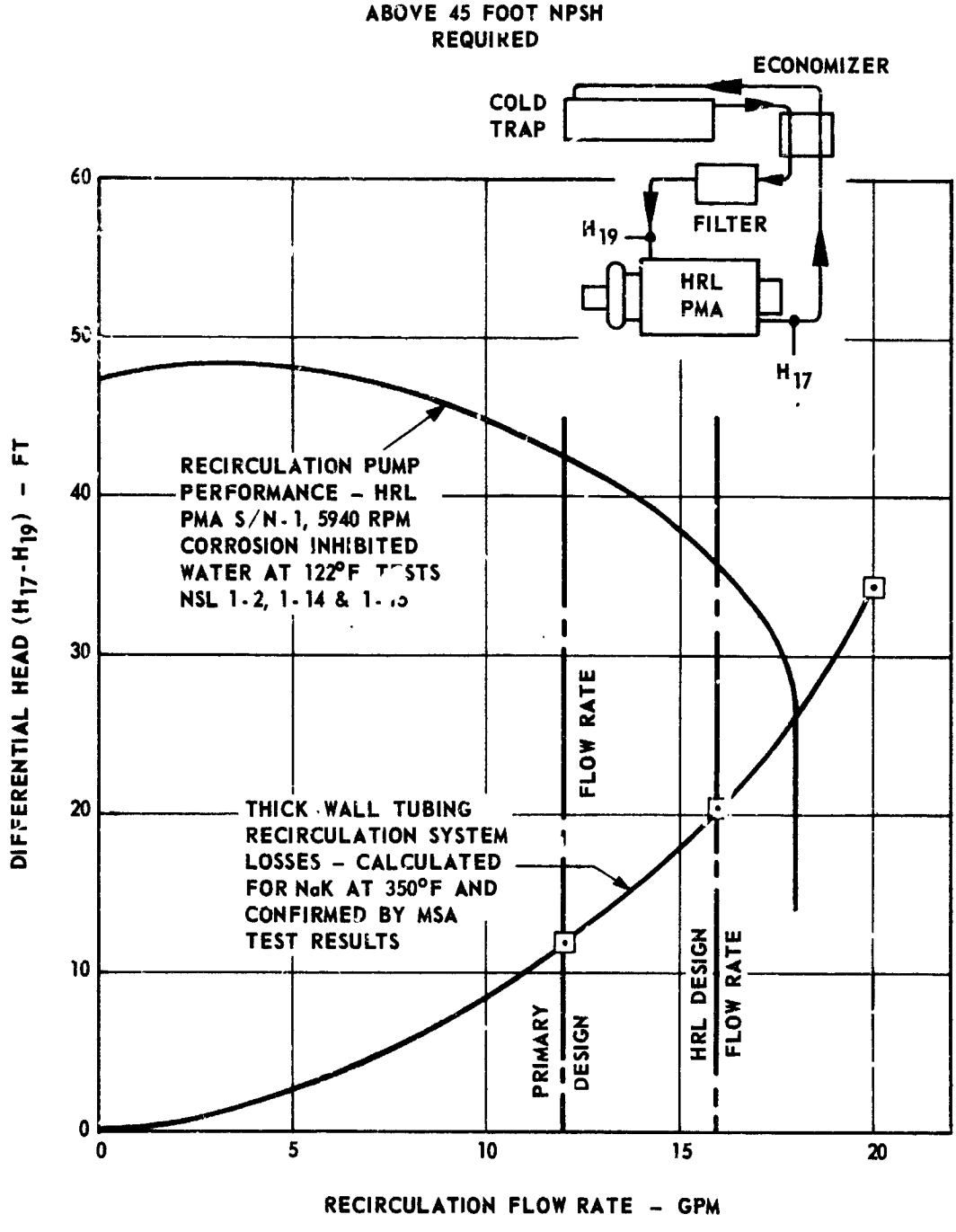

Noncavitating HRL PMA Recirculation System and Pump - Head vs Capacity

Figure 50

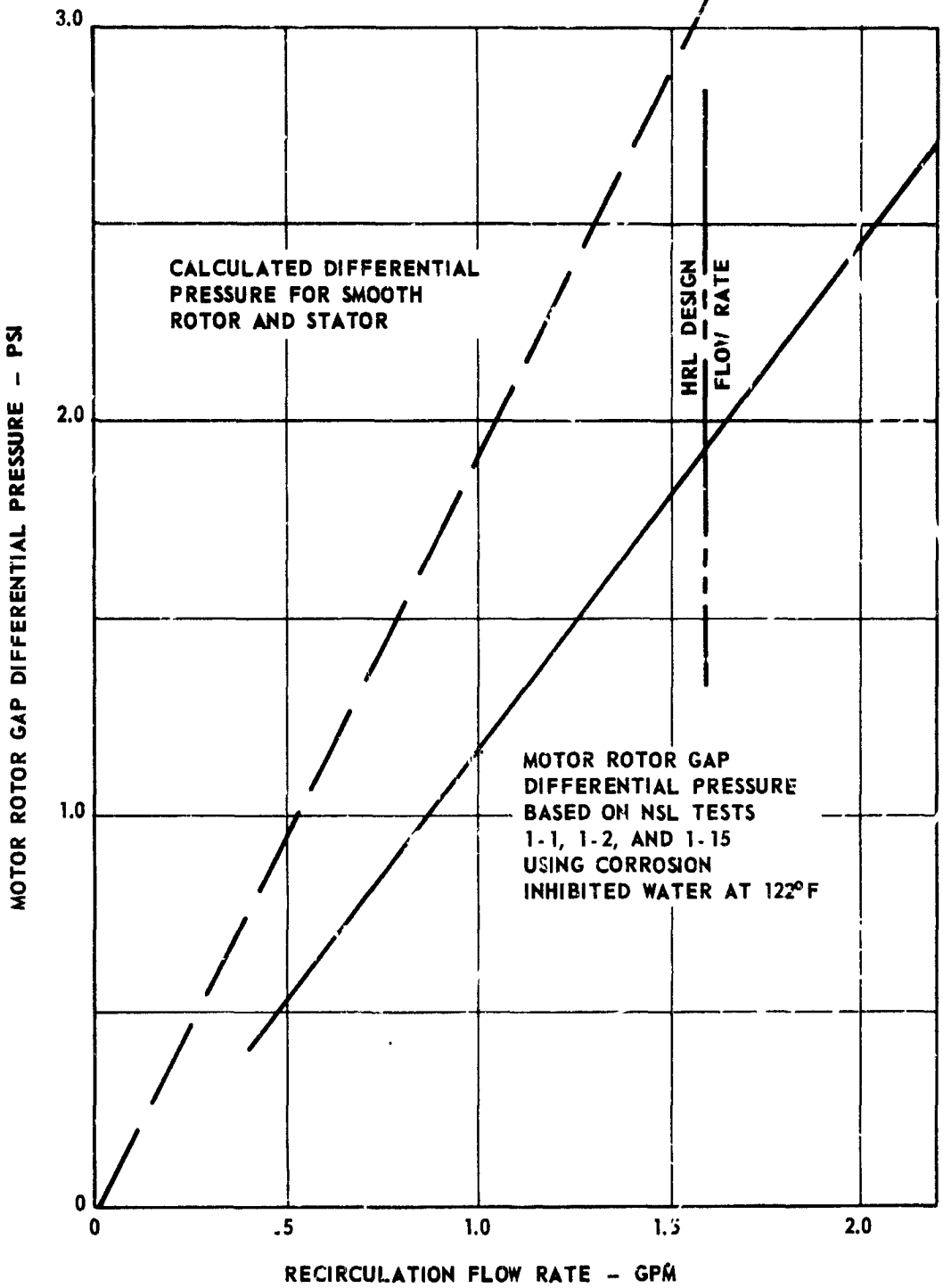

Motor Rotor Gap Pressure Drop - Noncavitating vs Recirculation Flow Rate - HRL PMA (5940 rpm, 0.015 in. Radial Clearance)

Figure 51

"C" Core Inductor for Speed Control Frequency Sensing Circuit Potted Using Fibrefra:

Figure 62

Kelsey-Hayes Coldweld Sample - Aluminum to Copper

864-691

Figure 63

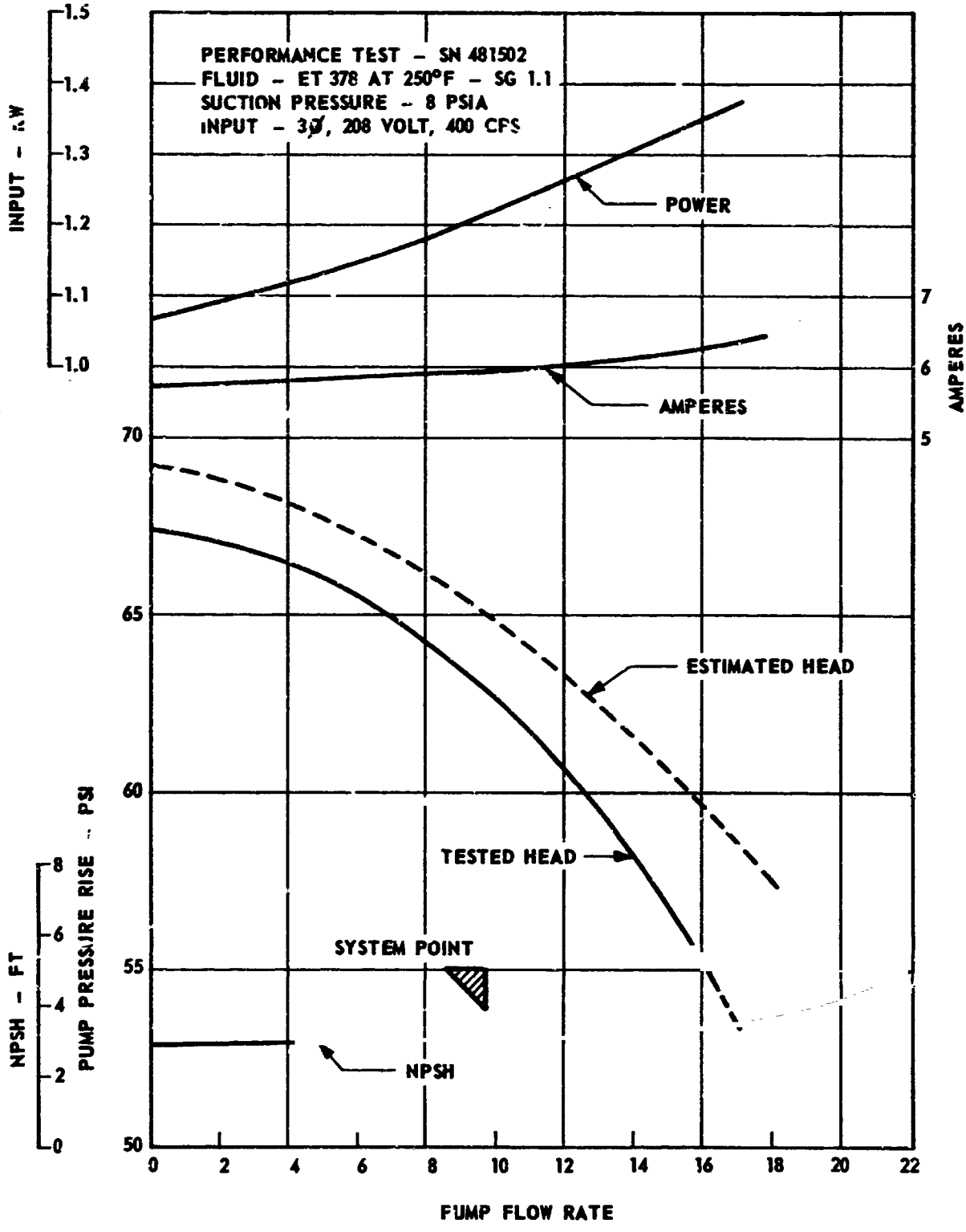

Lubricant-Coolant Pump Motor Assembly Performance Curves for First Unit

Figure 52

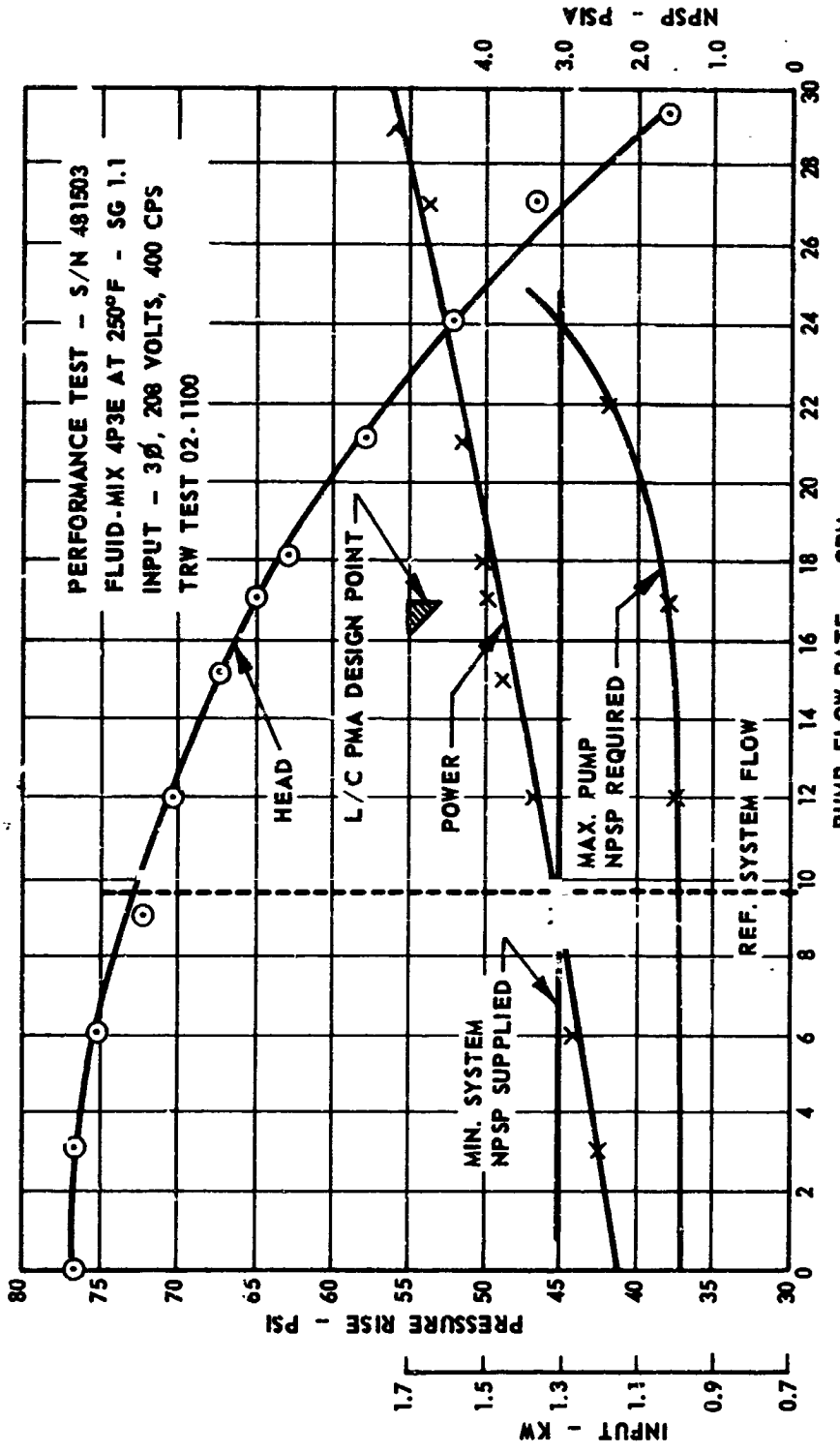

Lubricant-Coolant Pump Motor Assembly Performance Curves for Second Unit

Figure 53

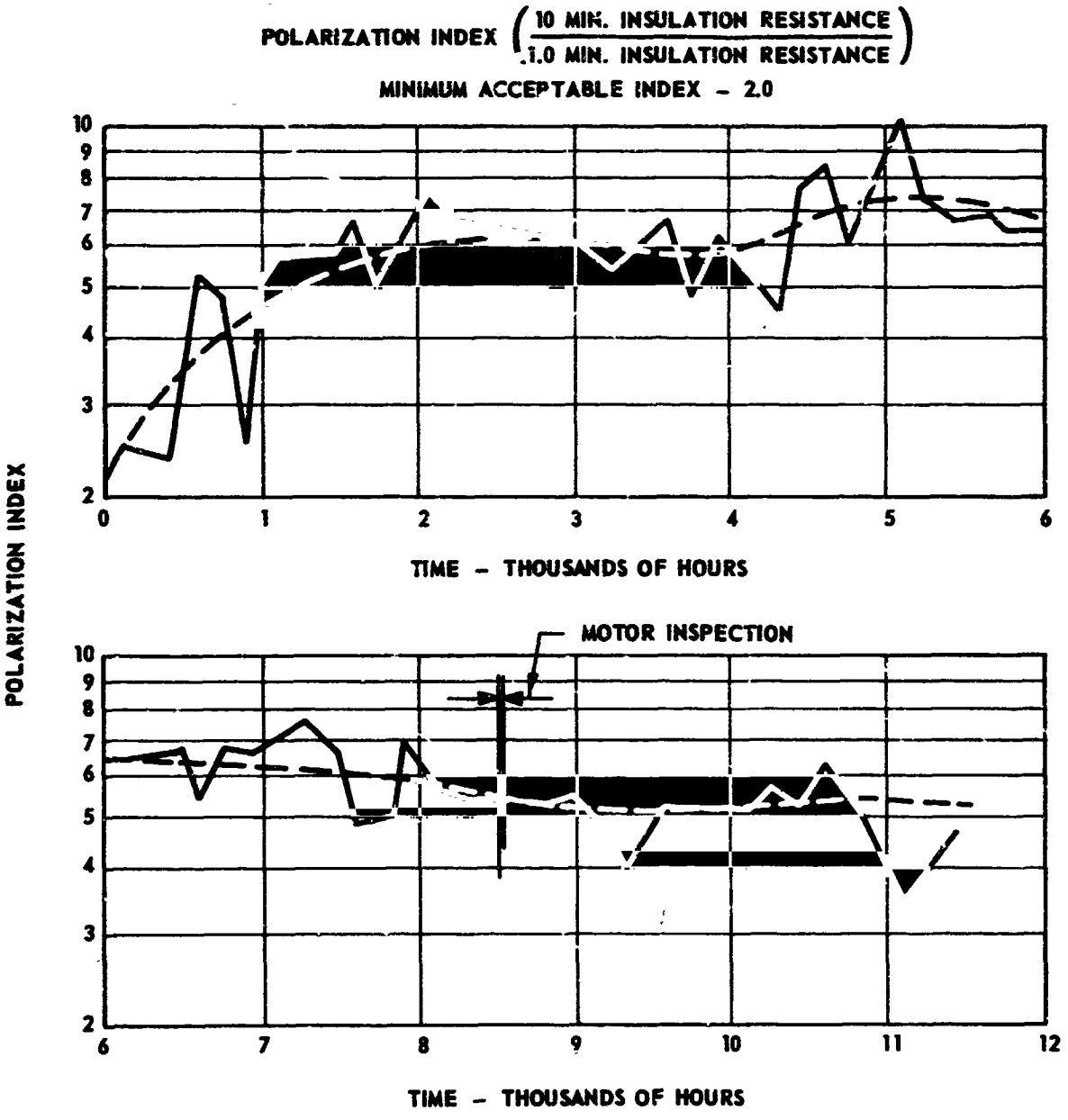

ML Insulation Resistance in Mix 4P3E Organic Fluid
Soak Temperature = 250 ± 15°F

Figure 54

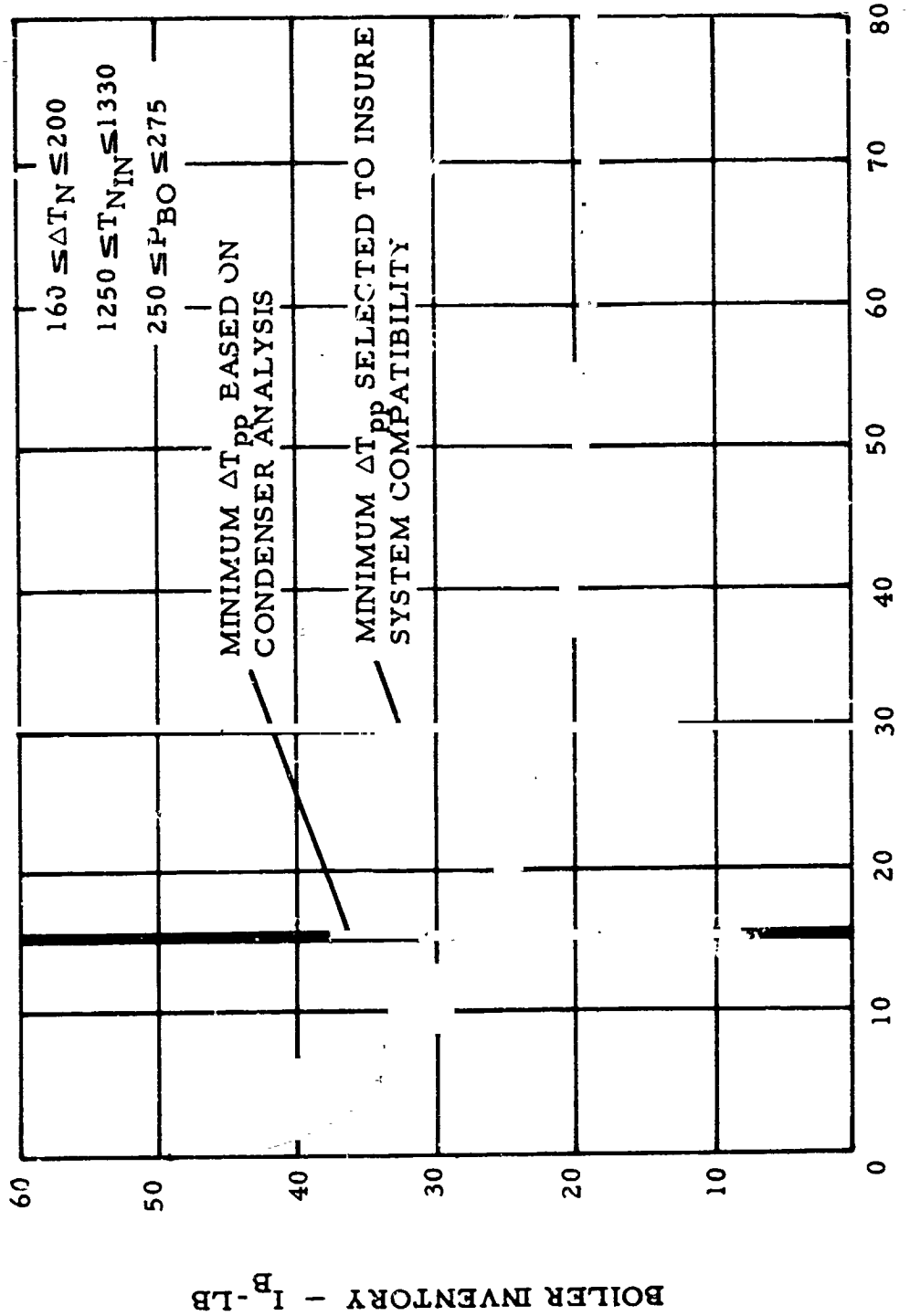

Boiler - Mercury Inventory Variation

Figure 55

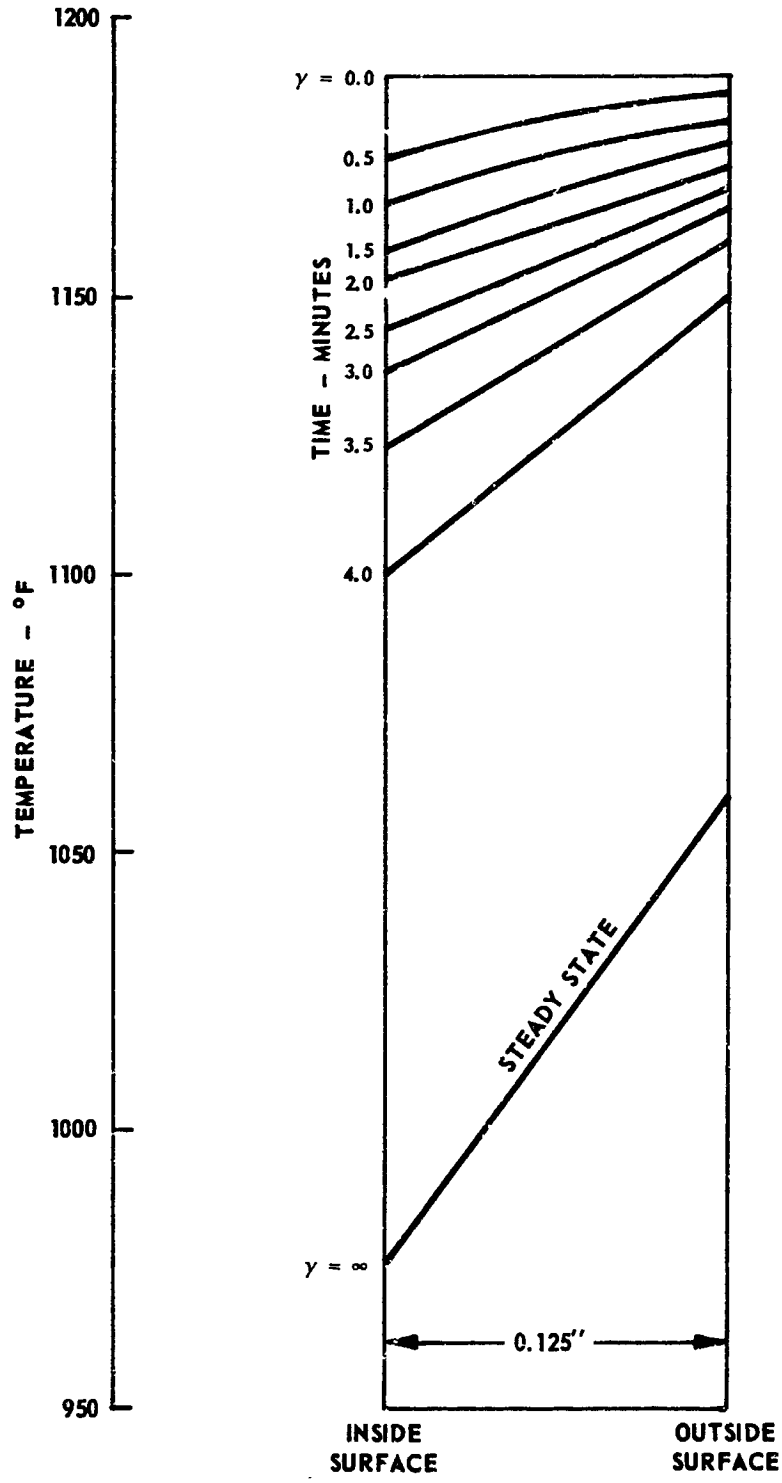

Boiler-Tube-Wall Transient Temperature Profile

Figure 56

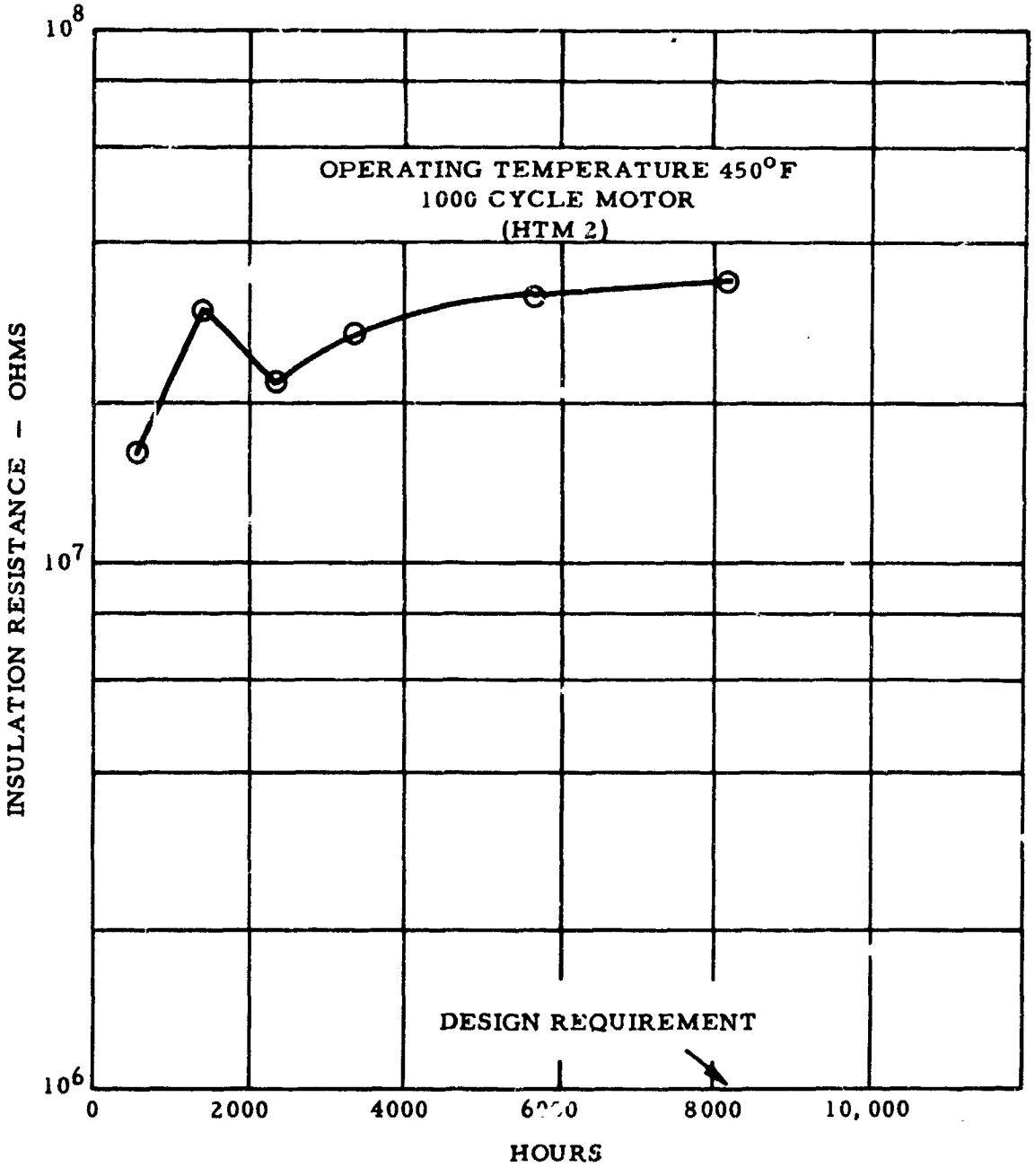

Inorganic Insulation Life Test

Figure 57

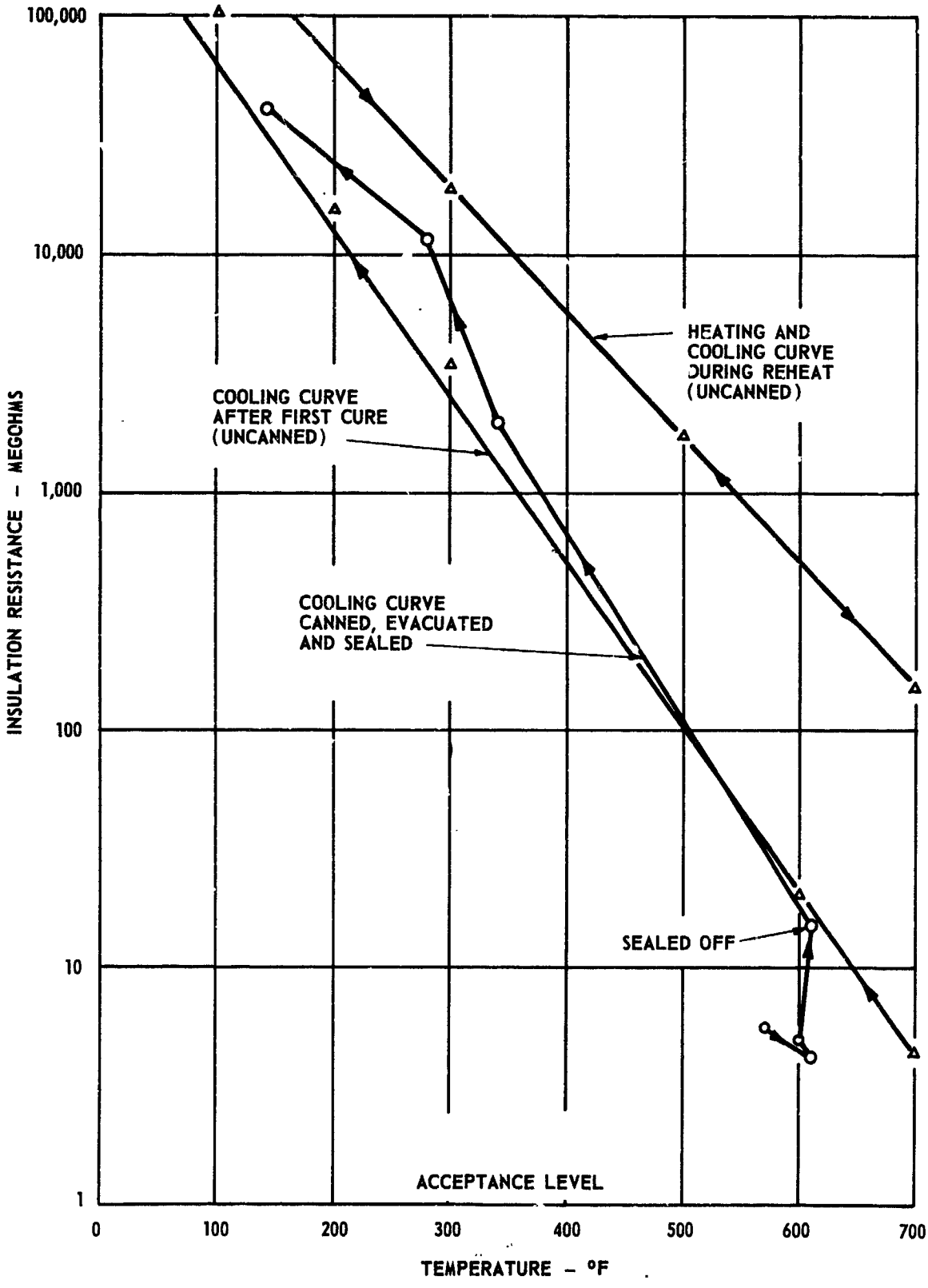

Curing Curves for HRL Motor, First Assembly Unit

Figure 58

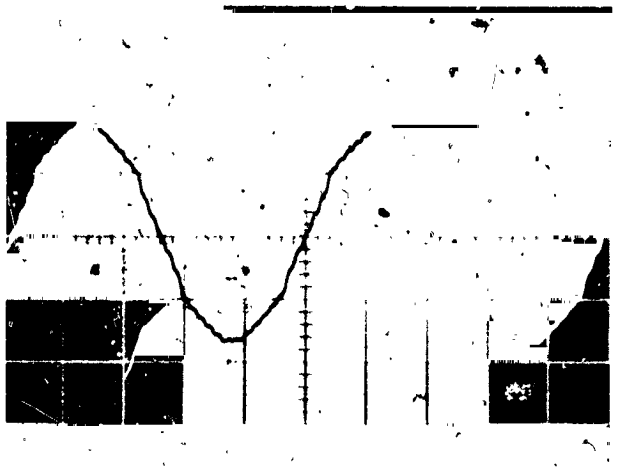

0.5 MS/CM
100 V/CM
AT NO LOAD

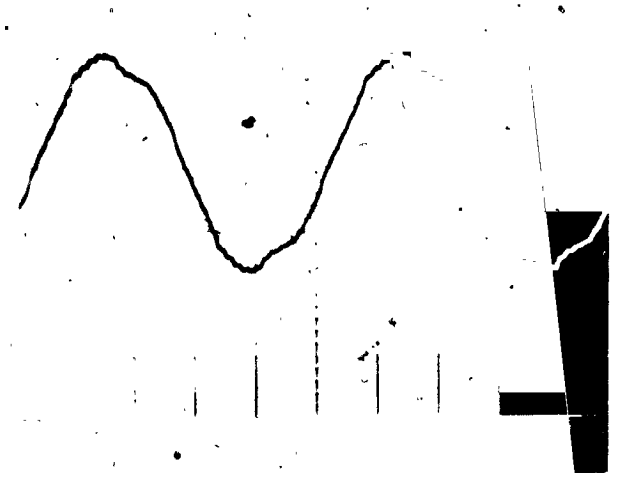

0.5 MS/CM
100 V/CM
AT 39 KW PL
NO VL

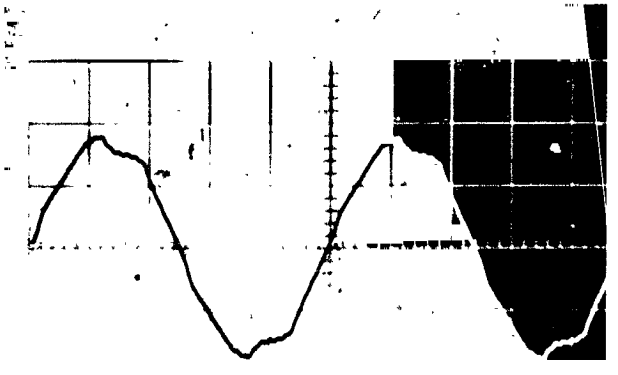

0.5 MS/CM
100 V/CM
AT 20.1 KW VL 0.9 PF
39 KW ALT 0.75 PF

Alternator Wave Forms at Alternator Terminals

Figure 59

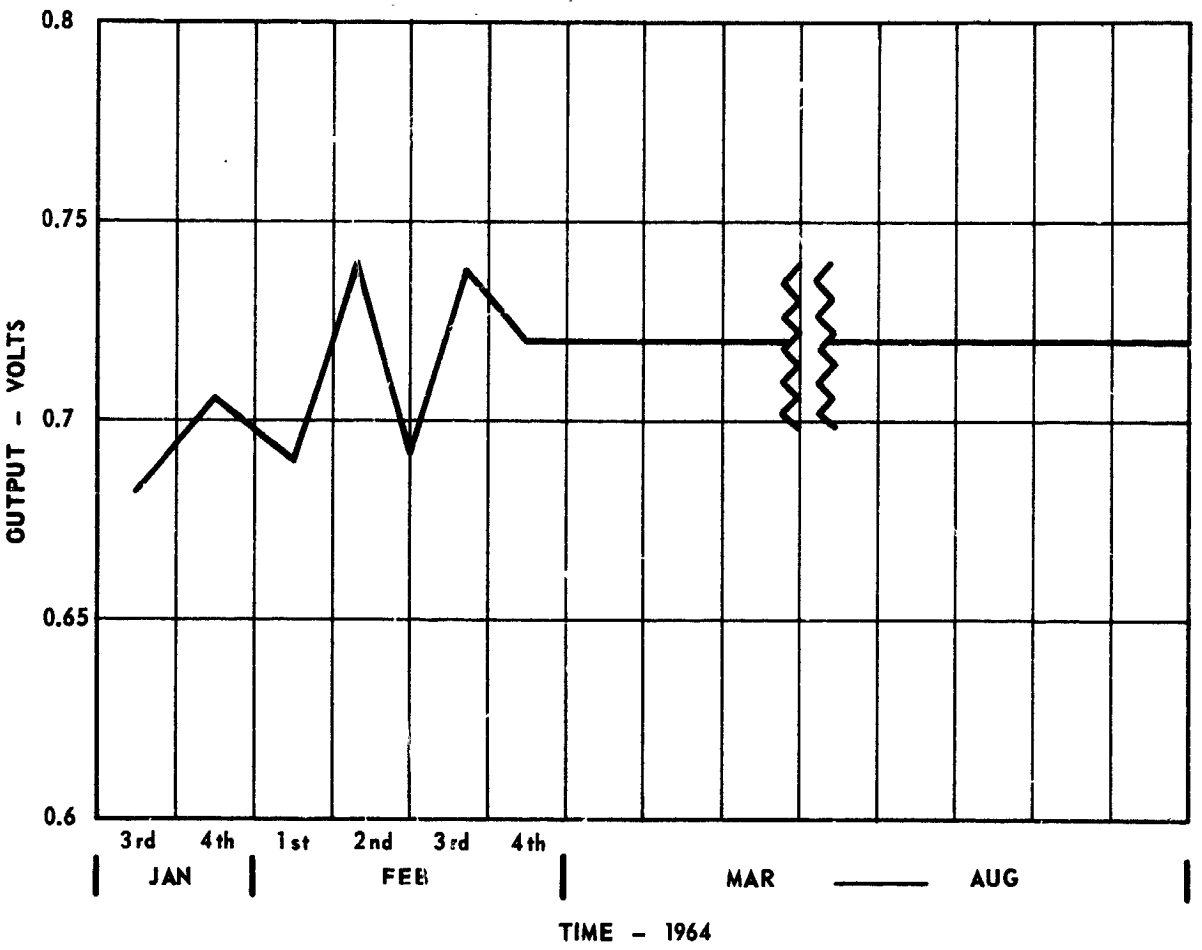

Speed Control Frequency Sensing Circuit - Output vs Time

Figure 60

"C" Core Inductor for Speed Control Frequency
Sensing Circuit Potted Using Sylgard 183

Figure 61

864-C424

"C" Core Inductor for Speed Control Frequency Sensing Circuit Potted Using Fibrefrax

Figure 62

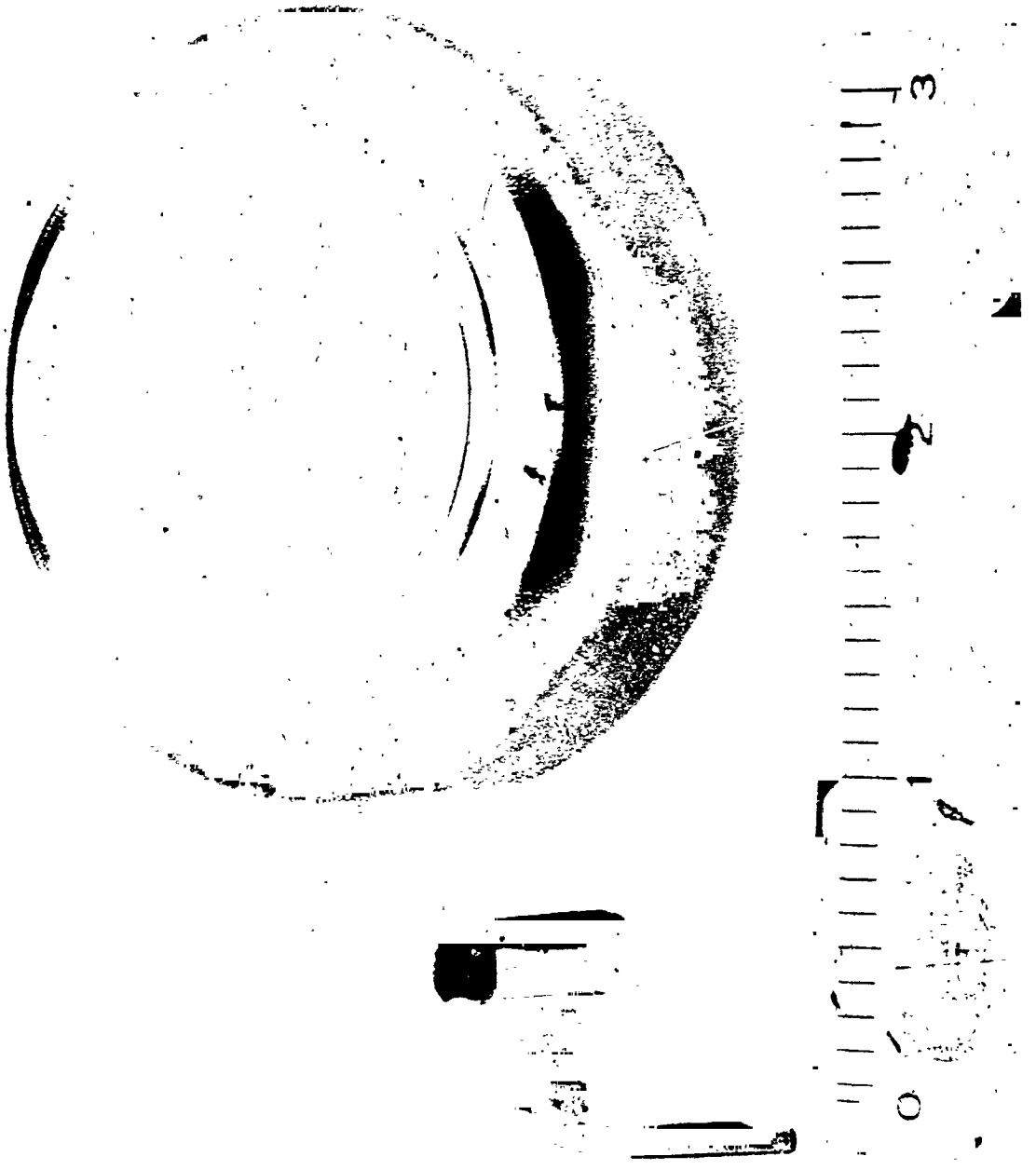

Kelsey-Hayes Coldweld Sample - Aluminum to Copper

864-691

Figure 63

Start Programer with Checkout Unit

Figure 64

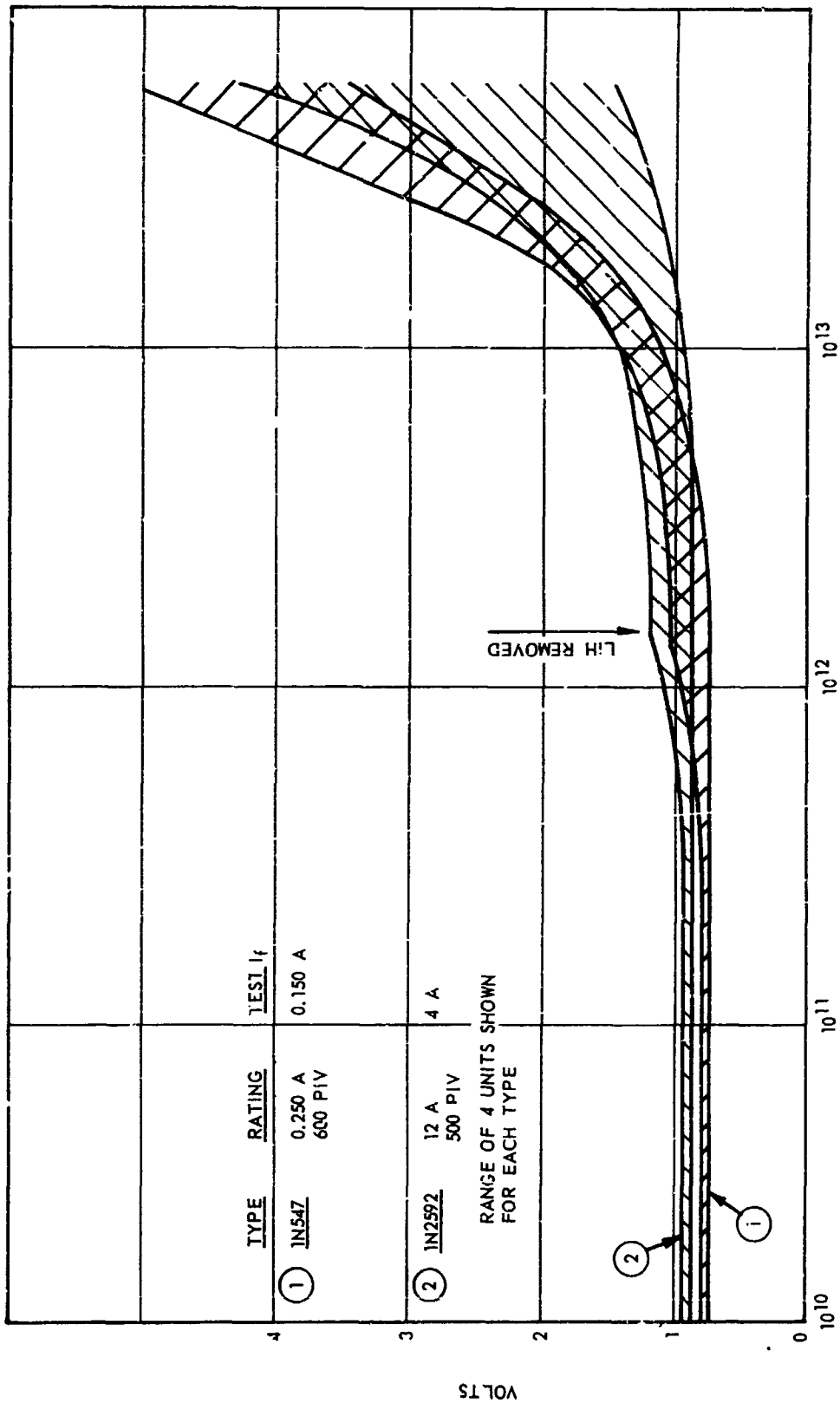

Silicon Diode Forward Voltage Drop Performance -
High and Low Current Type Comparison
vs Integrated Neutron Exposure

Figure 65

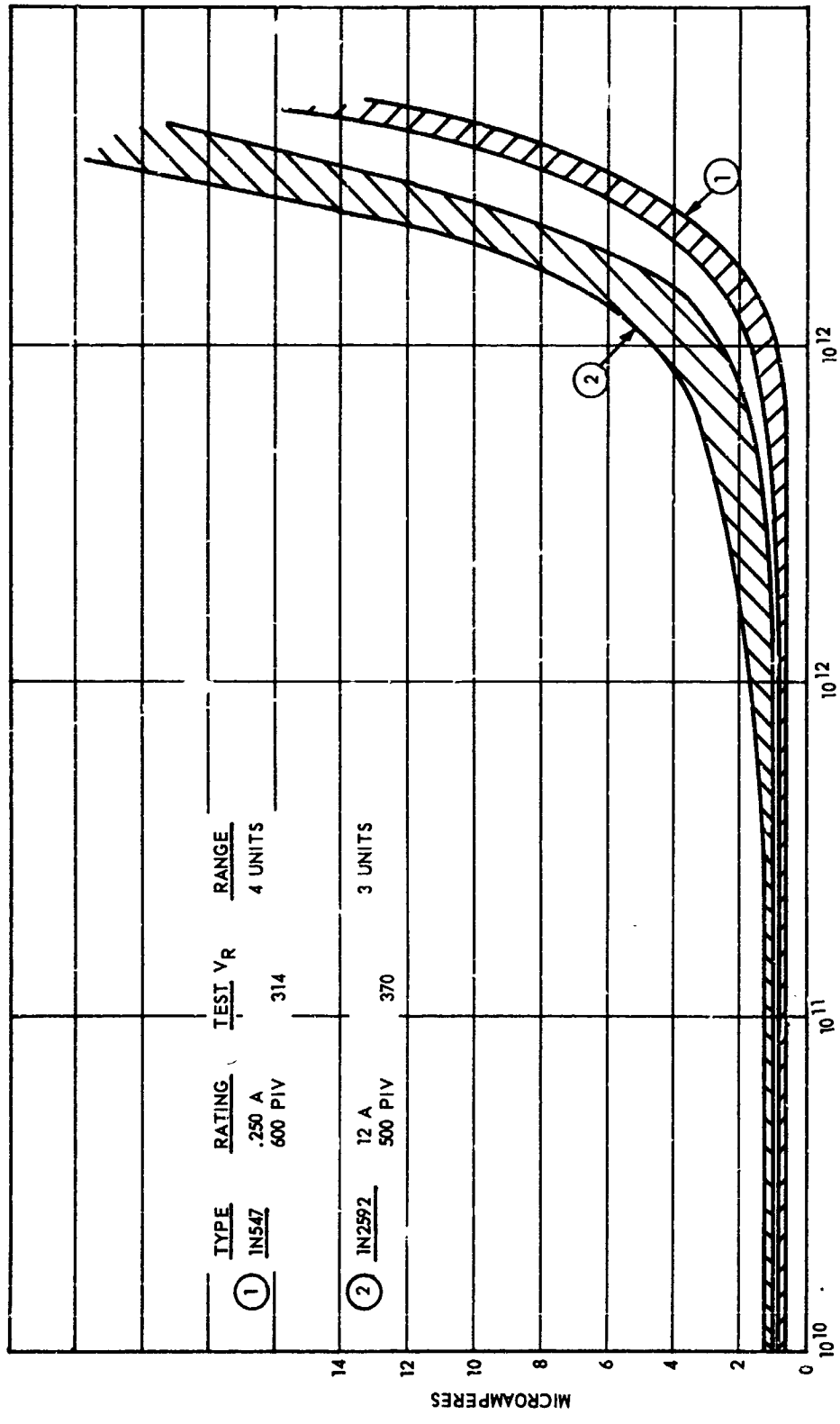

Silicon Diode Reverse Leakage Current Performance -
High and Low Current Type Comparison
vs Integrated Neutron Exposure

Figure 66

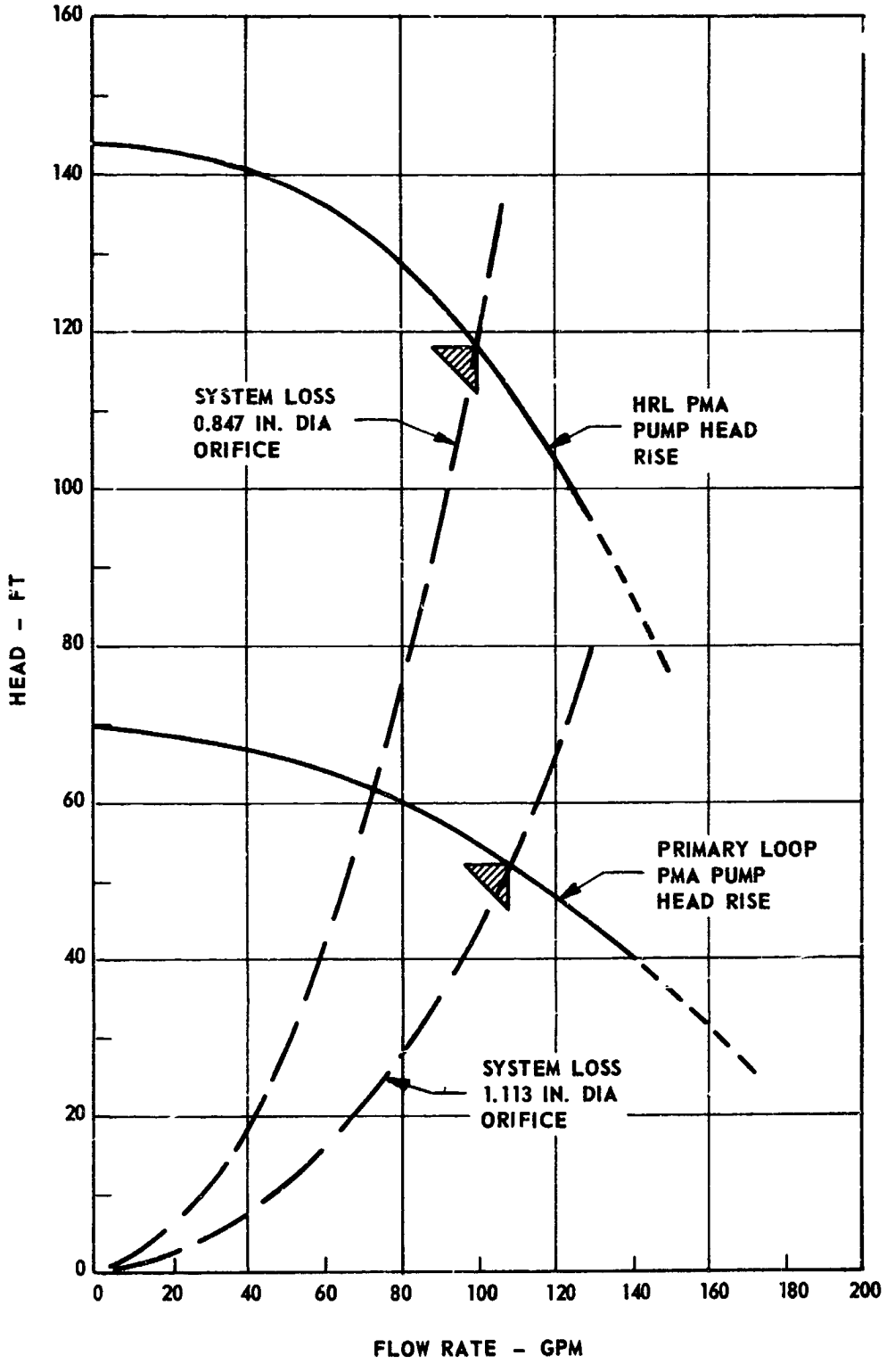

Hydraulic Design LNL-3 Required Orifice

Figure 67

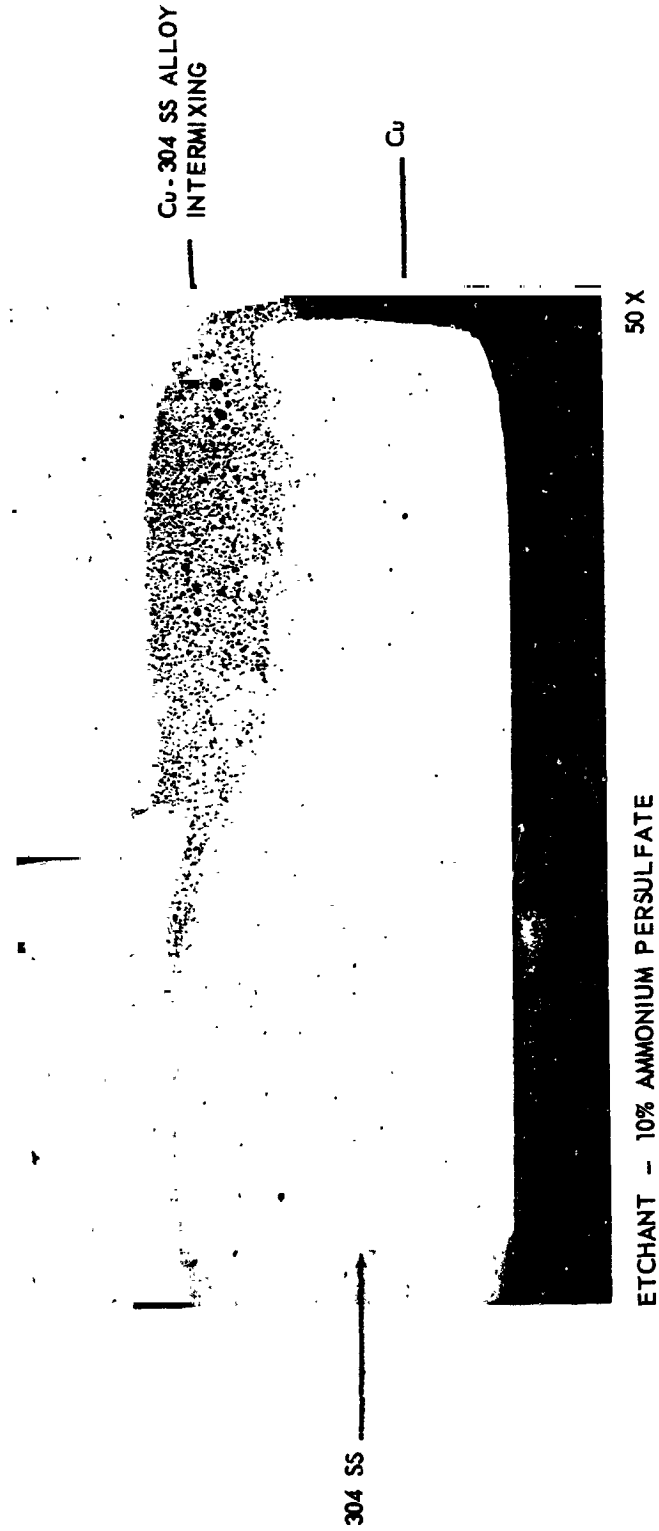

Copper-304 Stainless Steel - TIG Butt Weld

Figure 68

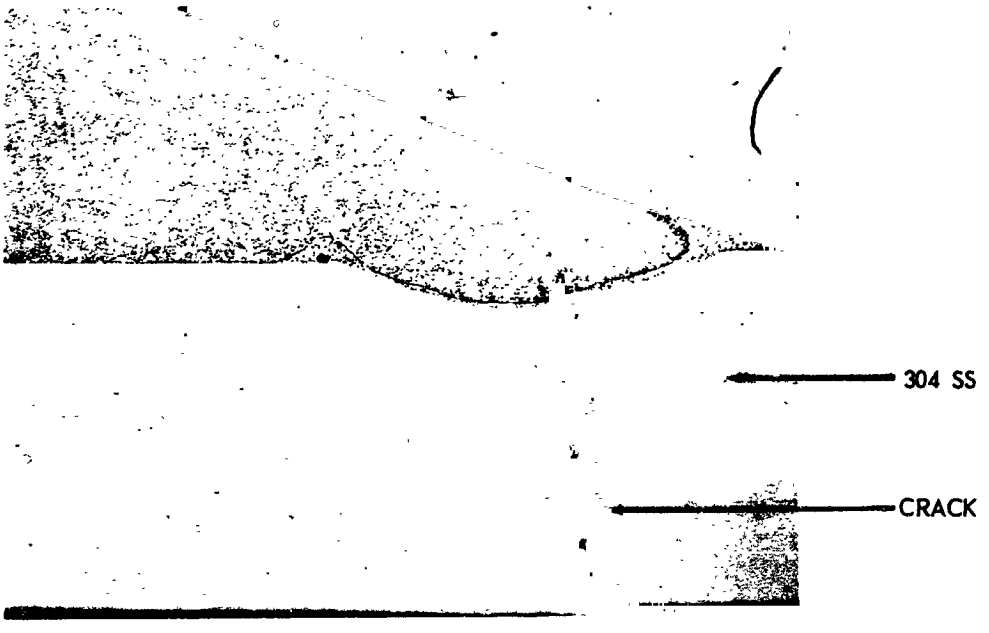

Copper-304 Stainless Steel - TIG Lap Weld

Figure 69

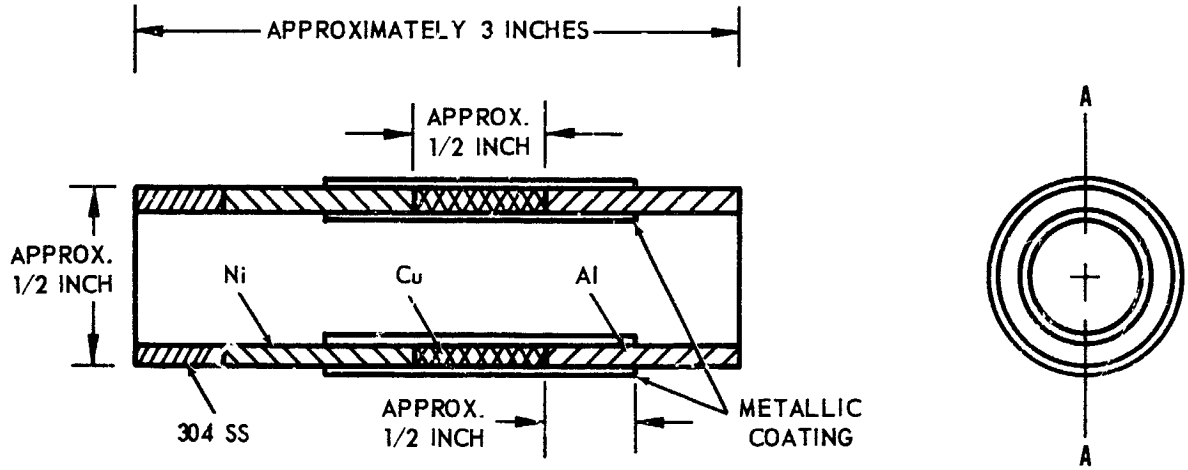

SECTION A-A
(DRAWING NOT TO SCALE)

NOTE A: METALLIC COATING TO BE ON THE OUTSIDE AND INSIDE OVER APPROXIMATE AREA SHOWN

Transition Joint - Transformer-Reactor Heat Sink to Lubricant-Coolant Loop

Figure 70

ETP COPPER
ETCHANT - HNO_3 AND
ACETIC ACID

6061 ALUMINUM ALLOY
ETCHANT - KELLER'S

L-7813 50 X

6061-T6 Aluminum/ETP Copper Interface on
Pressure Welded (Koldweld Process) Transition Joint
After 1500 Hours at 350°F

Figure 71

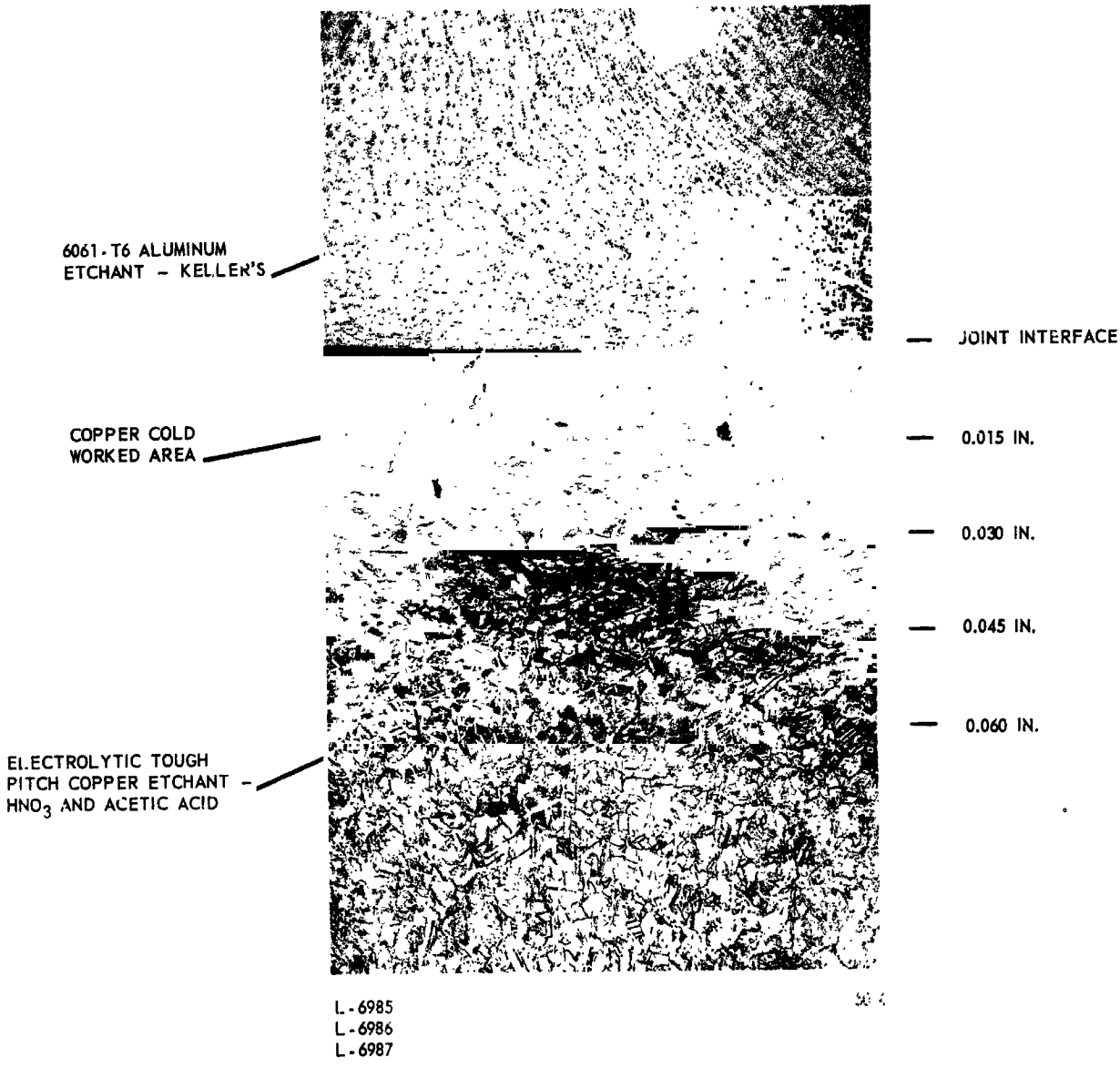

6061-T6 Aluminum/ETP Copper Interface of
Pressure Welded (Koldweld Process) Transition Joint -
Produced by Kelsey-Hayes

Figure 72

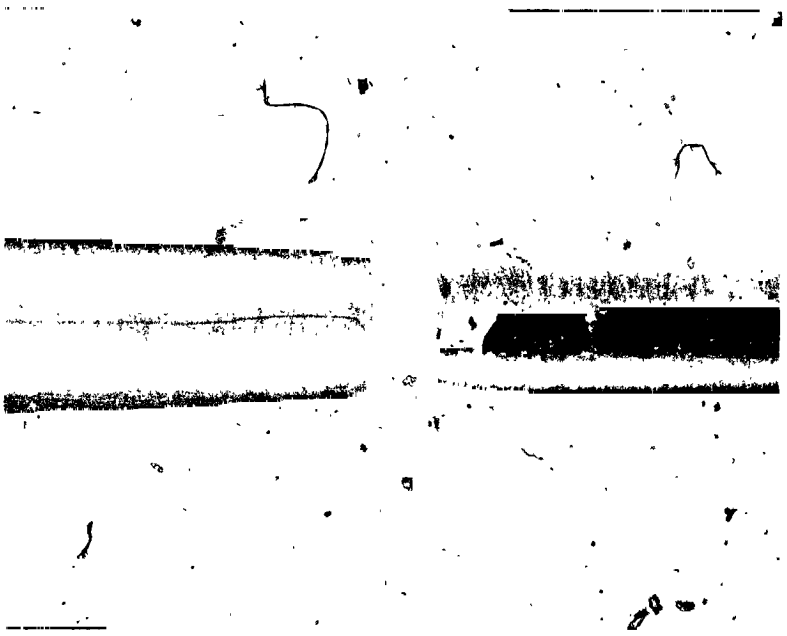

Fracture Area on Tensile Specimen of
6061-T6 Al/ETP Cu Pressure Welded (Koldweld Process)
Transition Joint. Specimen Tested at 75°F
After 1500 Hours at 350°F

Figure 73

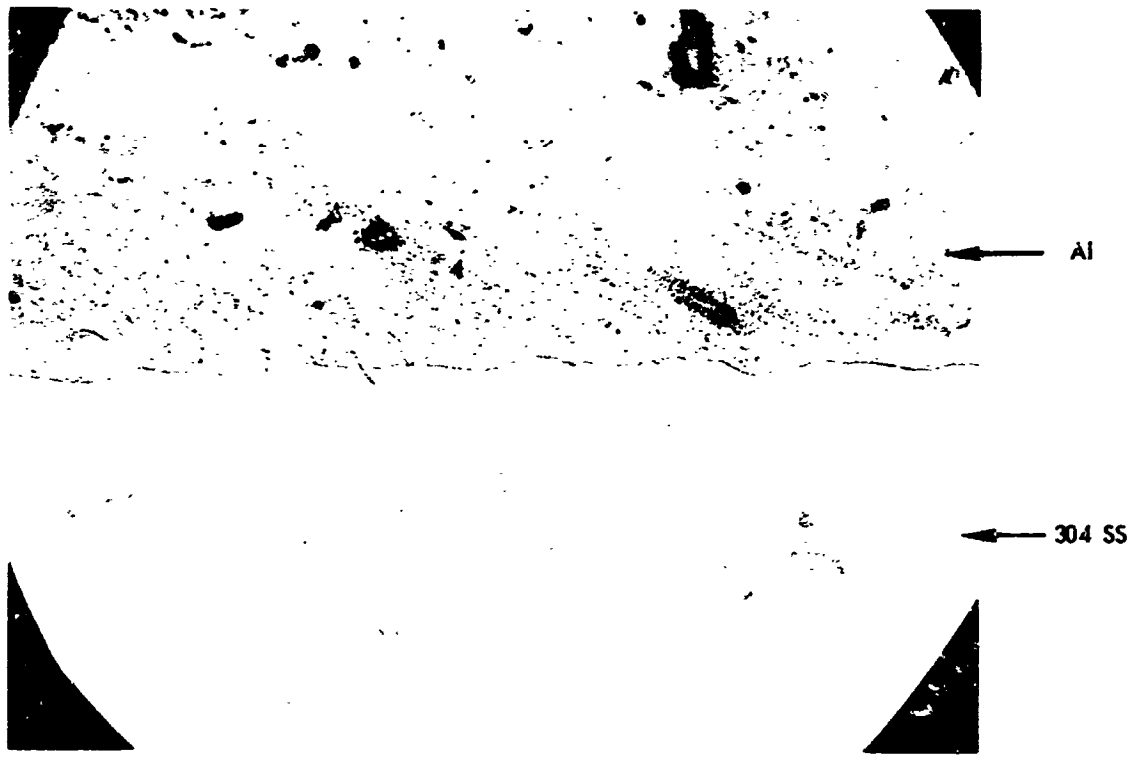

Al/304 SS Interface on Coextruded Tubular
Transition Joint - Produced by Nuclear Metals, Inc.

Figure 74

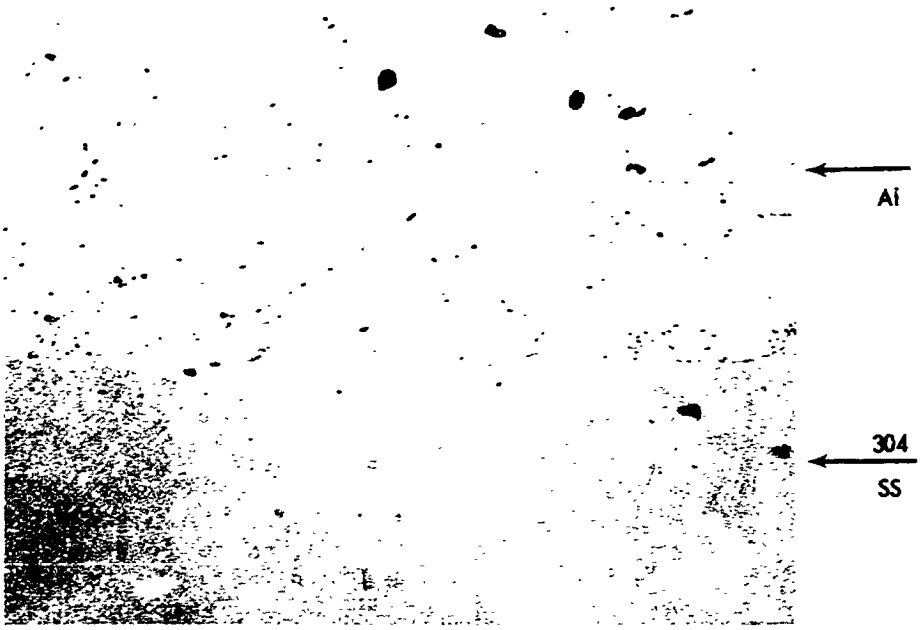

Al/304 SS Interface on Coextruded Tubular Transition Joint After 350 Hours at 275°F

Figure 75

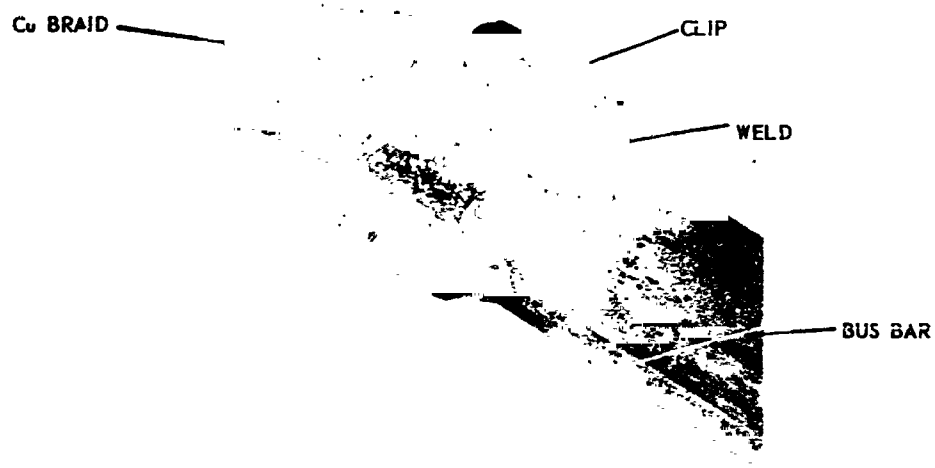

L-7807 2X

A. JOINT CONFIGURATION

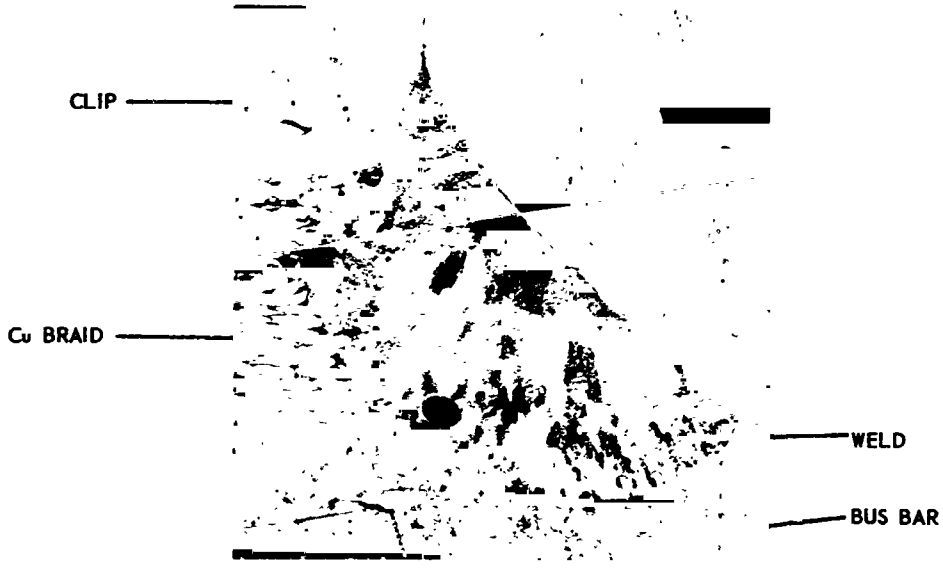

L-7809 15X

ETCHANT -
75% HNO_3 + 25% ACETIC ACID

B. JOINT CROSS-SECTION

TIG Welded Joint - Copper Braid to Terminal Strap - Configuration 1

Figure 76

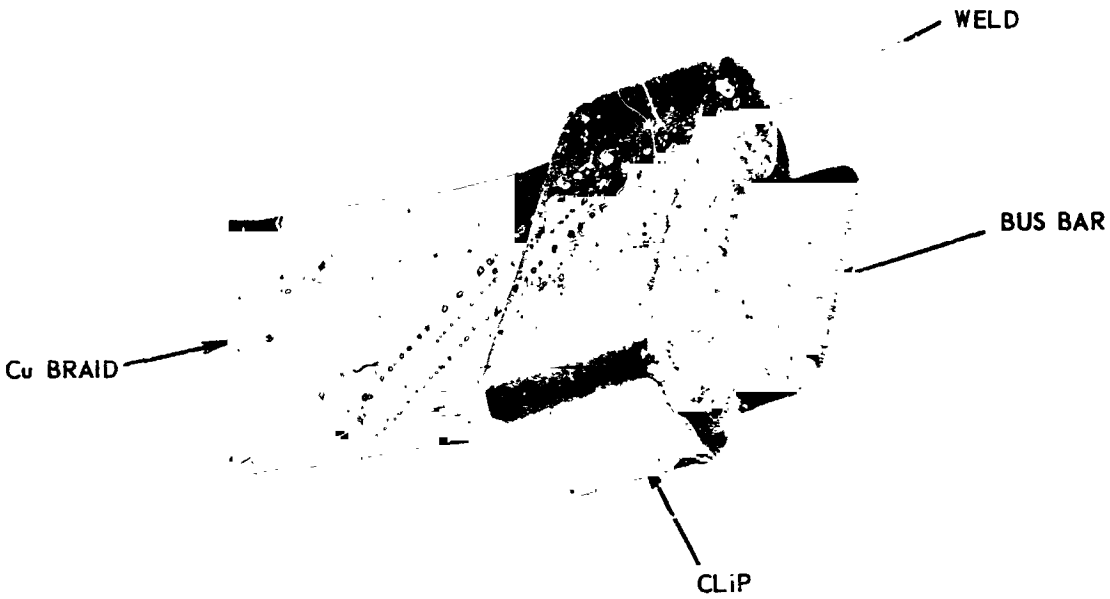

L-7723 A. JOINT CONFIGURATION 2X

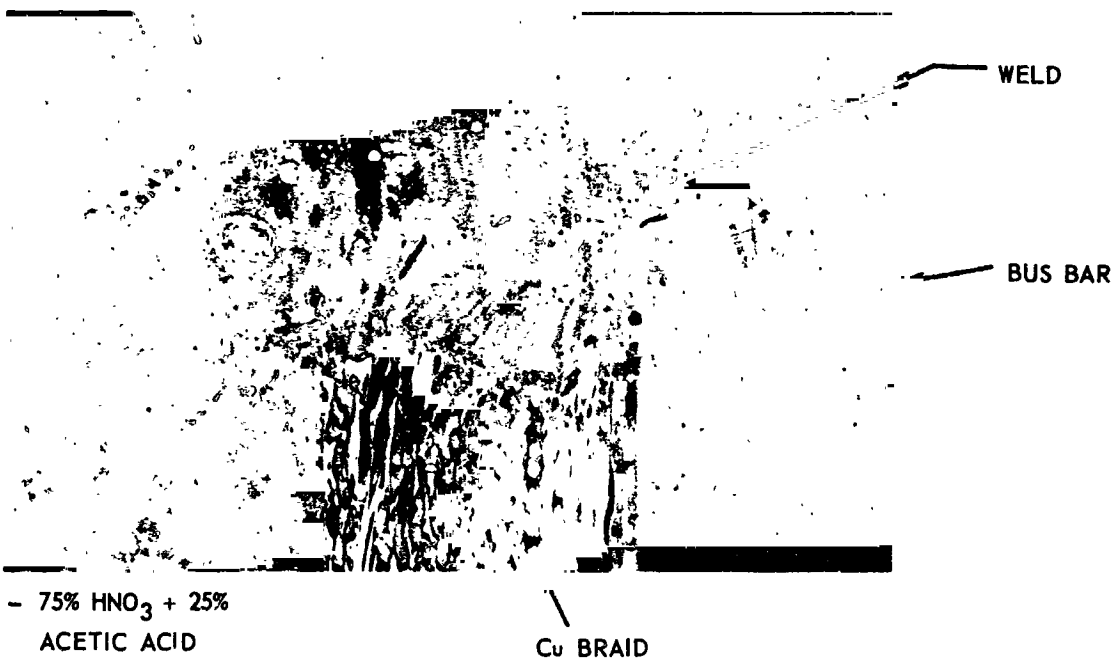

L-7724 B. JOINT CROSS-SECTION 15X

TIG Welded Joint - Copper Braid to Terminal Strap - Configuration 2

Figure 77

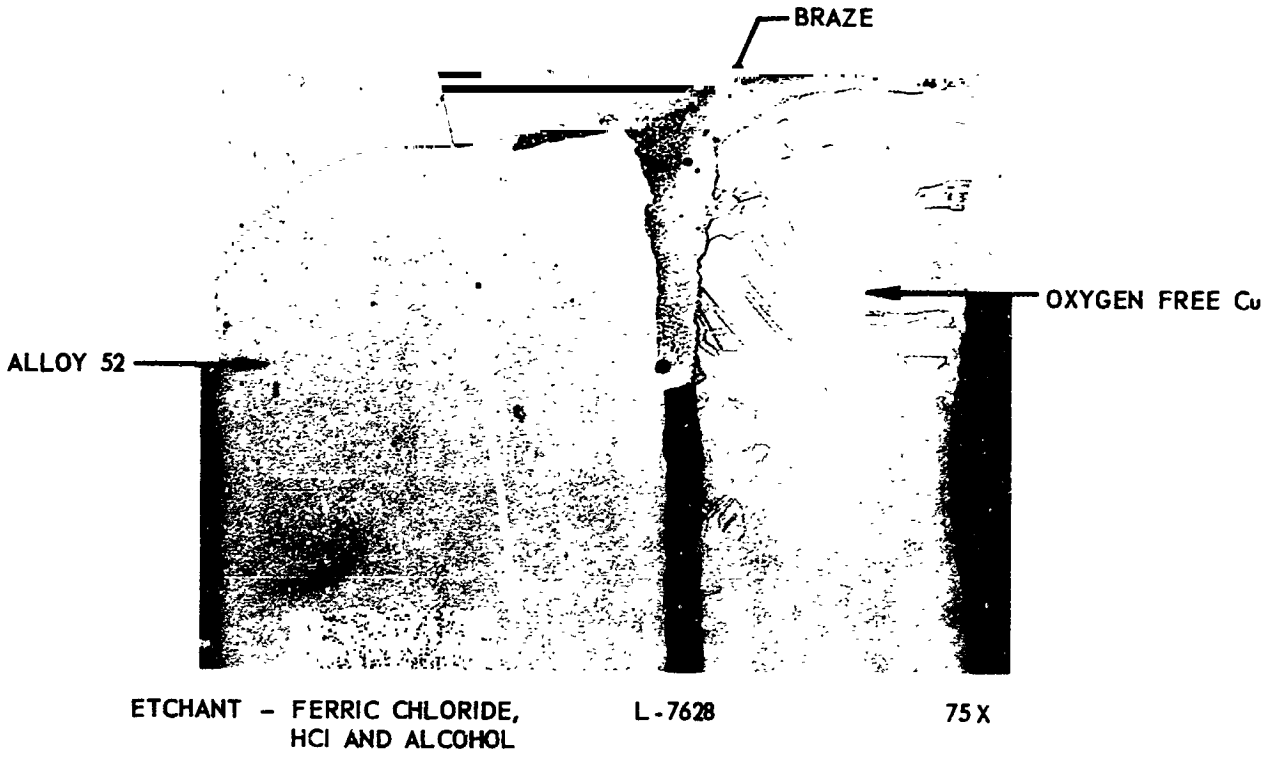

TIG Brazed Diode Terminal Joint

Figure 78

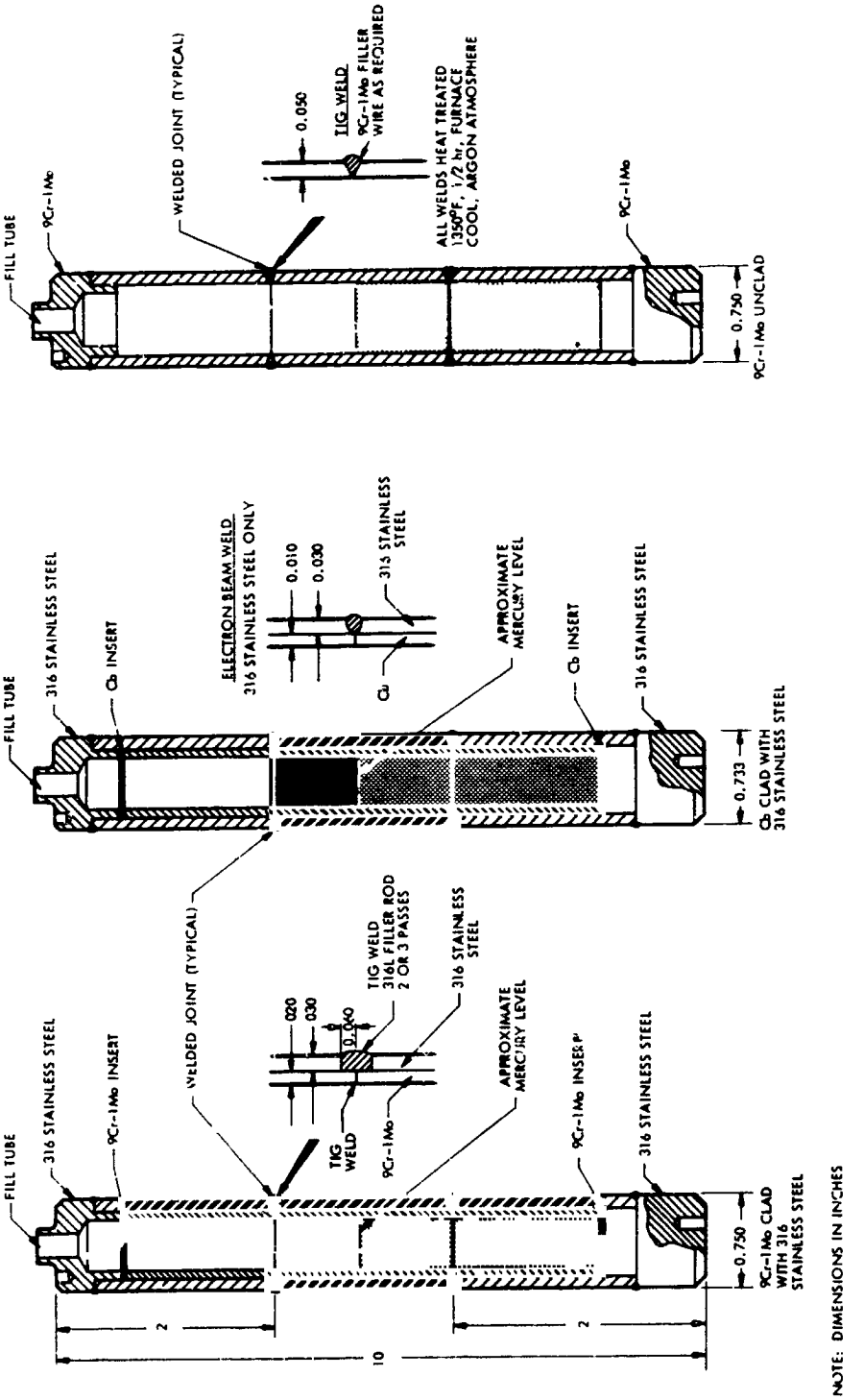

Reflux Capsules

Figure 79

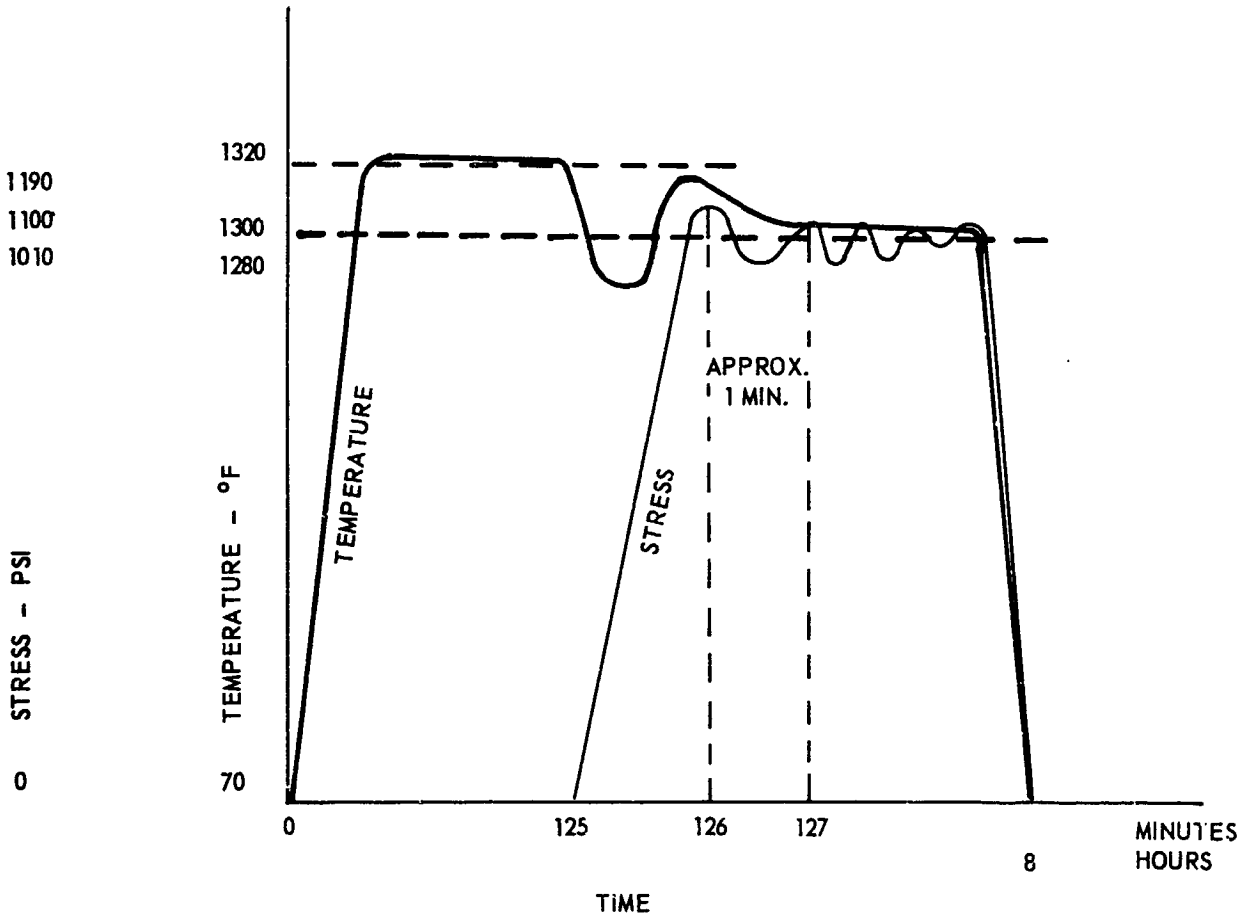

Test Conditions for Startup Phase of
9Cr-1Mo/316 SS Transition Joint Evaluation

Figure 80

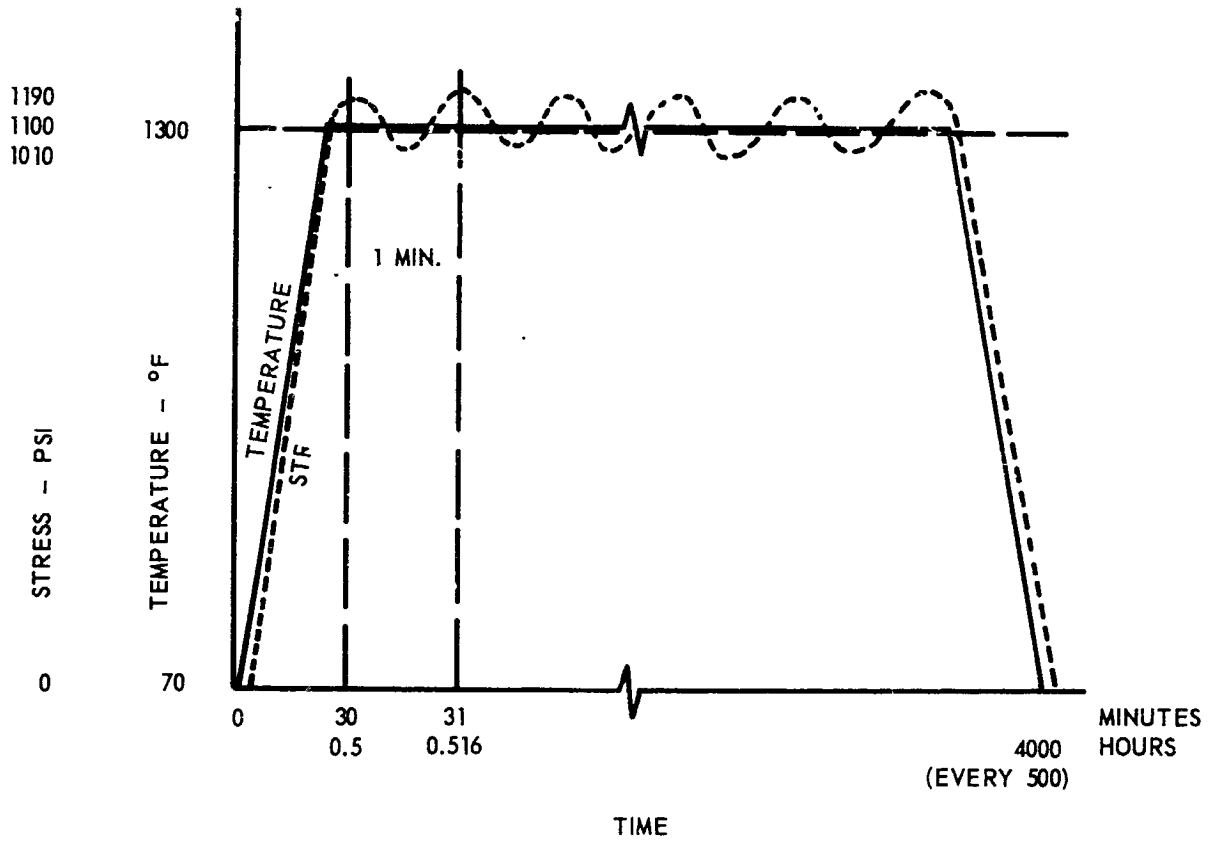

Test Conditions for Endurance Testing Phase of
9Cr-1Mo/316 SS Transition Joint Evaluation

Figure 81

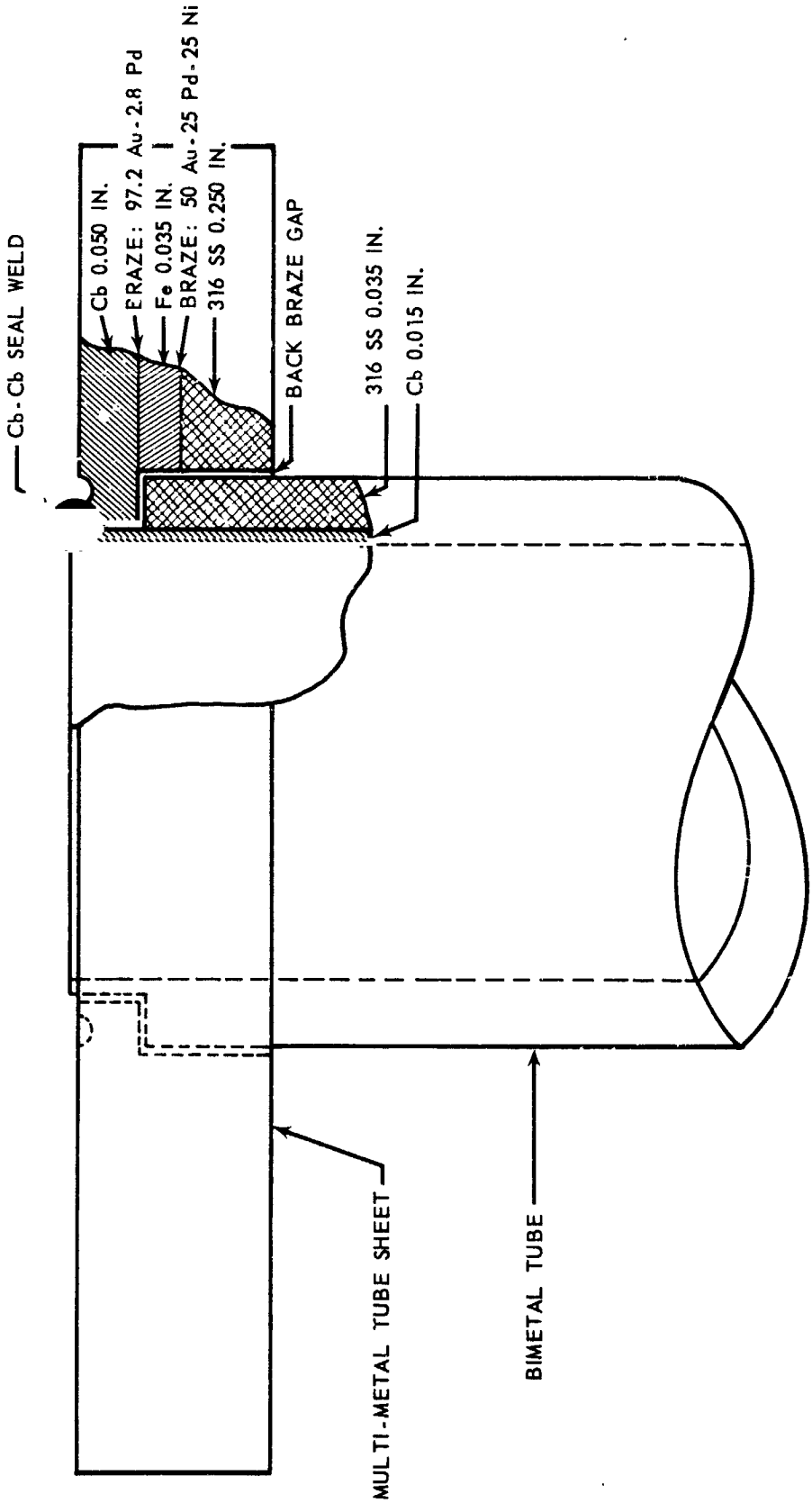

Refractor Mercury-Containment Tube-to-Tube Sheet Back-Brazed Joint

Figure 82

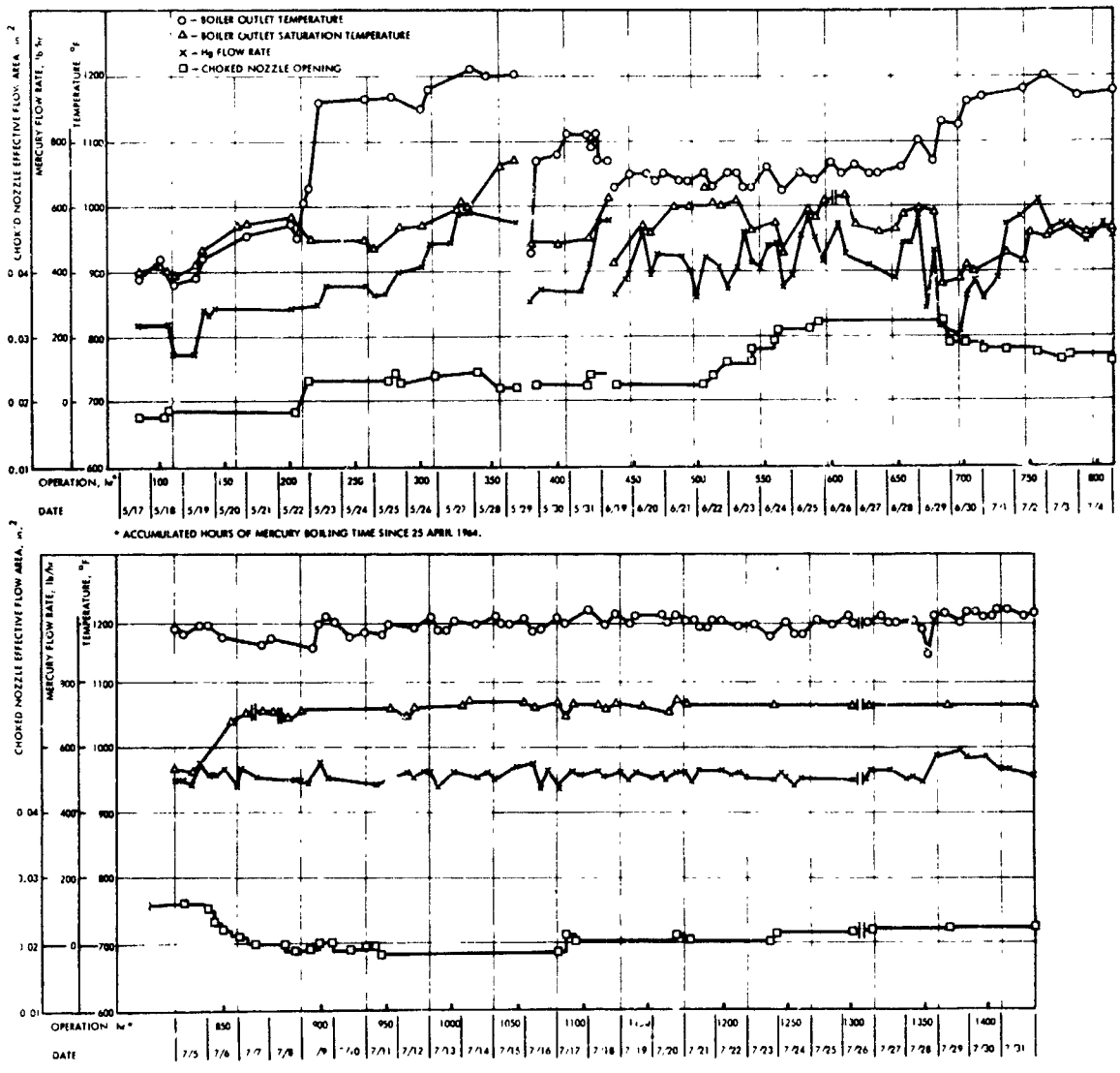

Operating Data for Corrosion Loop 3

Figure 83

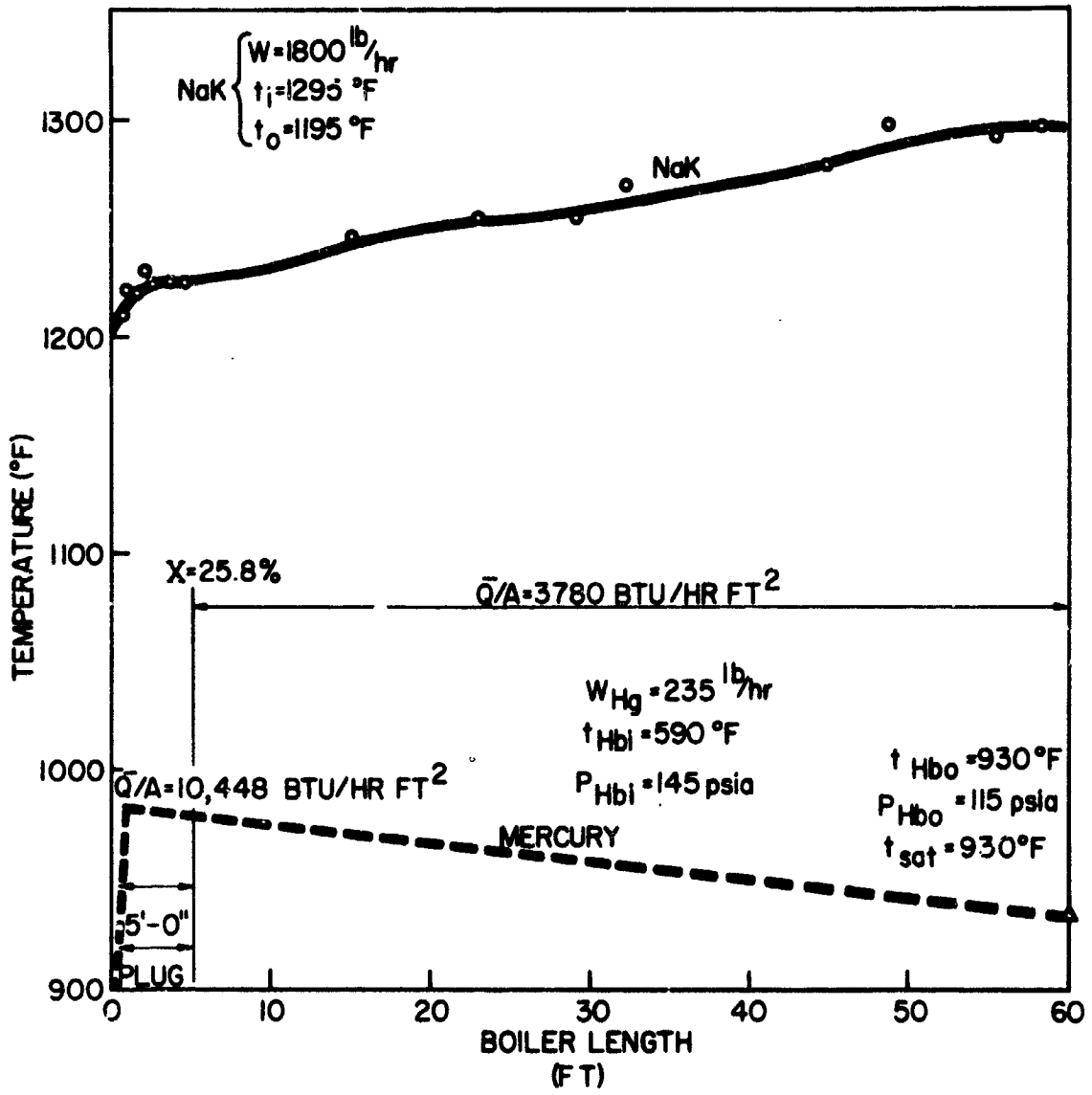

Corrosion Loop 3 Boiler Operation Data -
19 May 1964

Figure 84

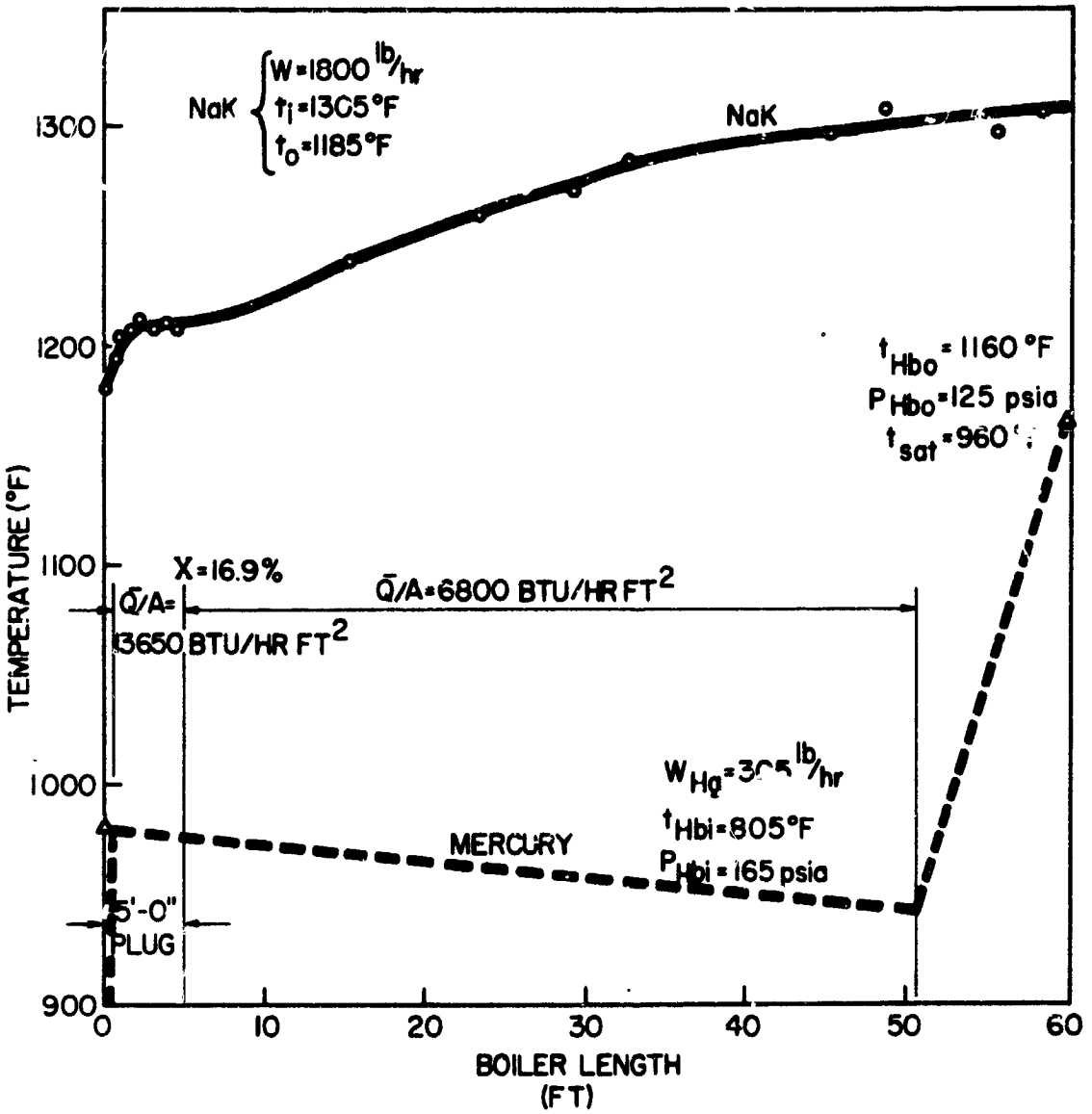

Corrosion Loop 3 Boiler Operation Data -
23 May 1964

Figure 85

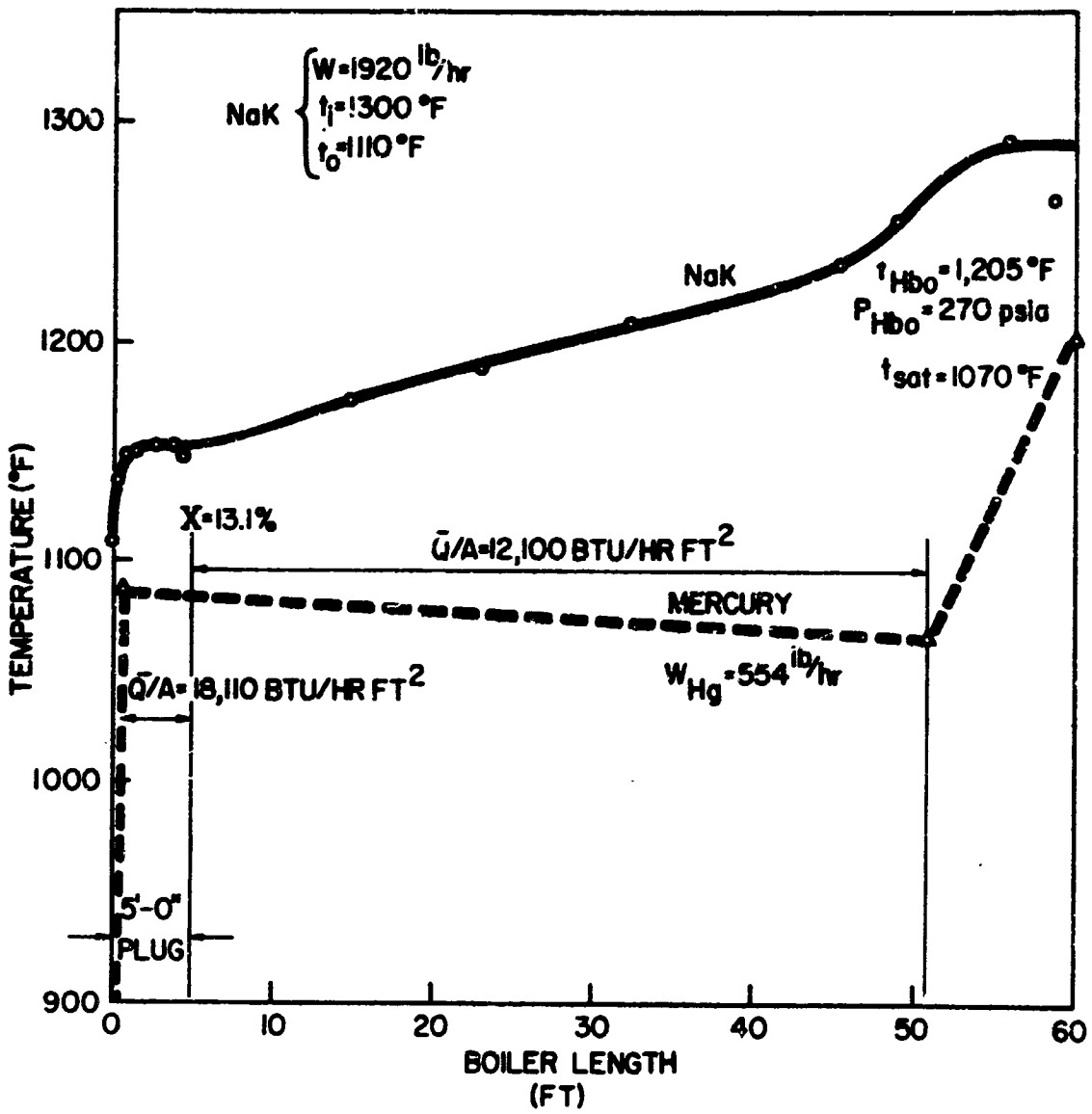

Corrosion Loop 3 Boiler Operation Data -
29 May 1964

Figure 86

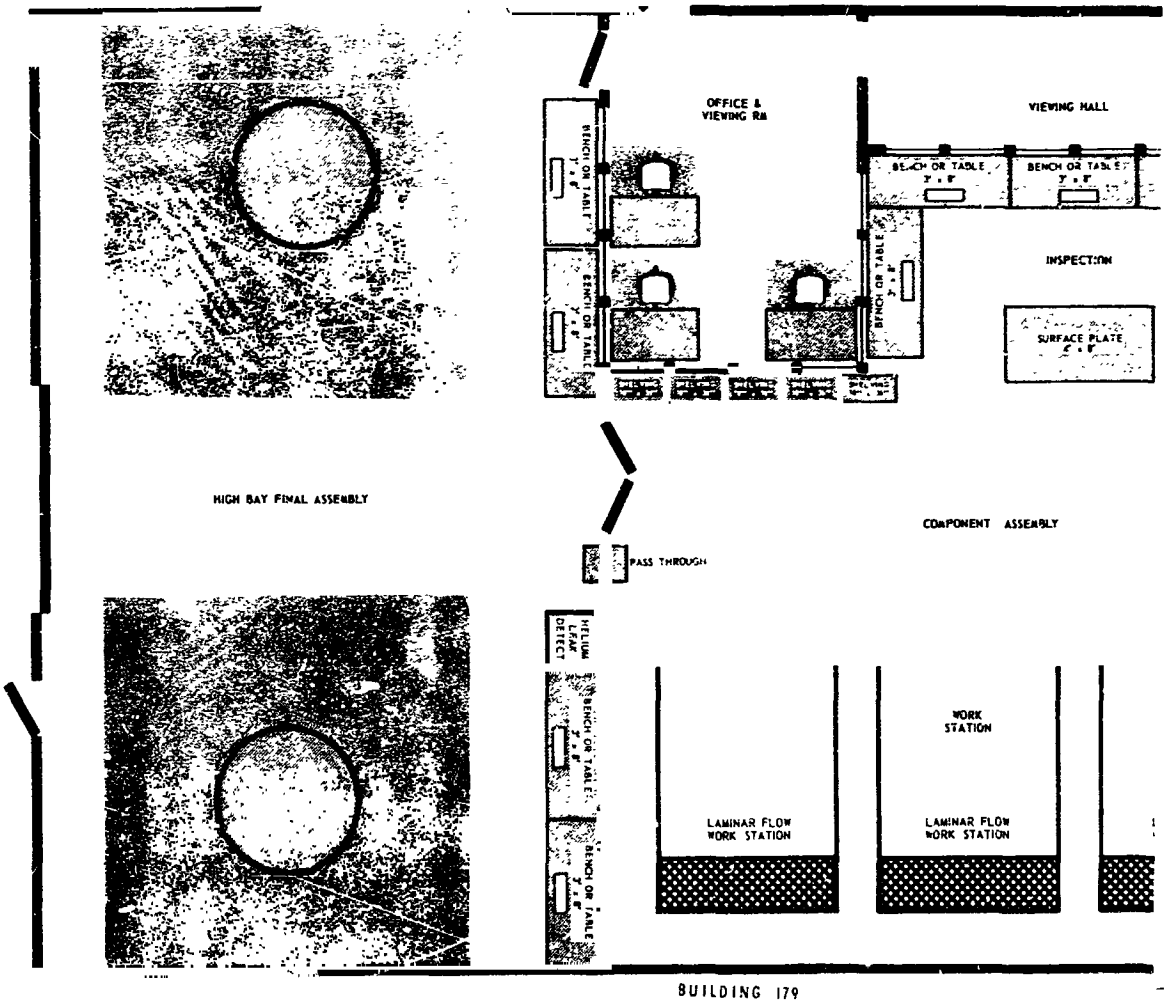

BUILDING 179

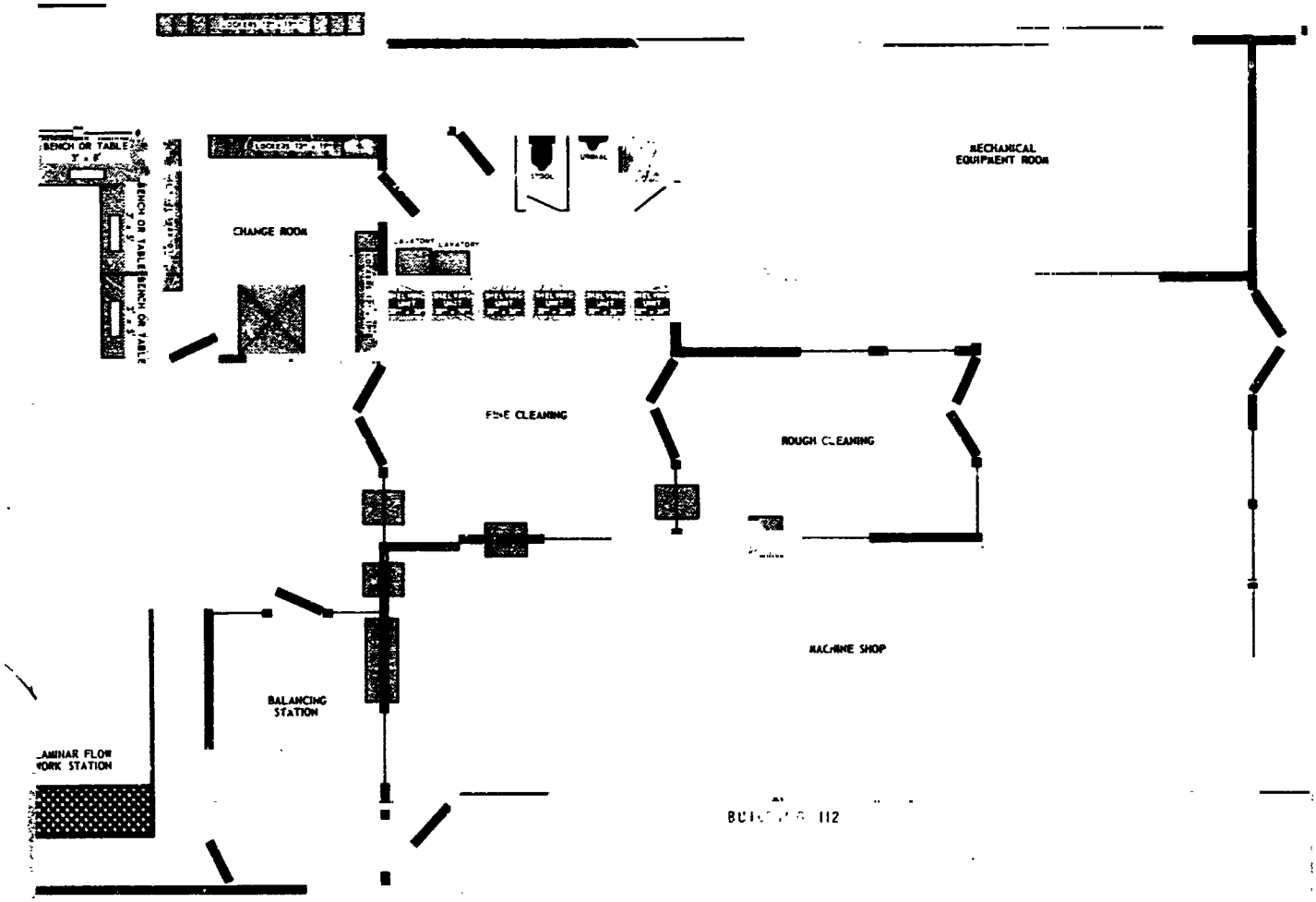

BUILDING 112

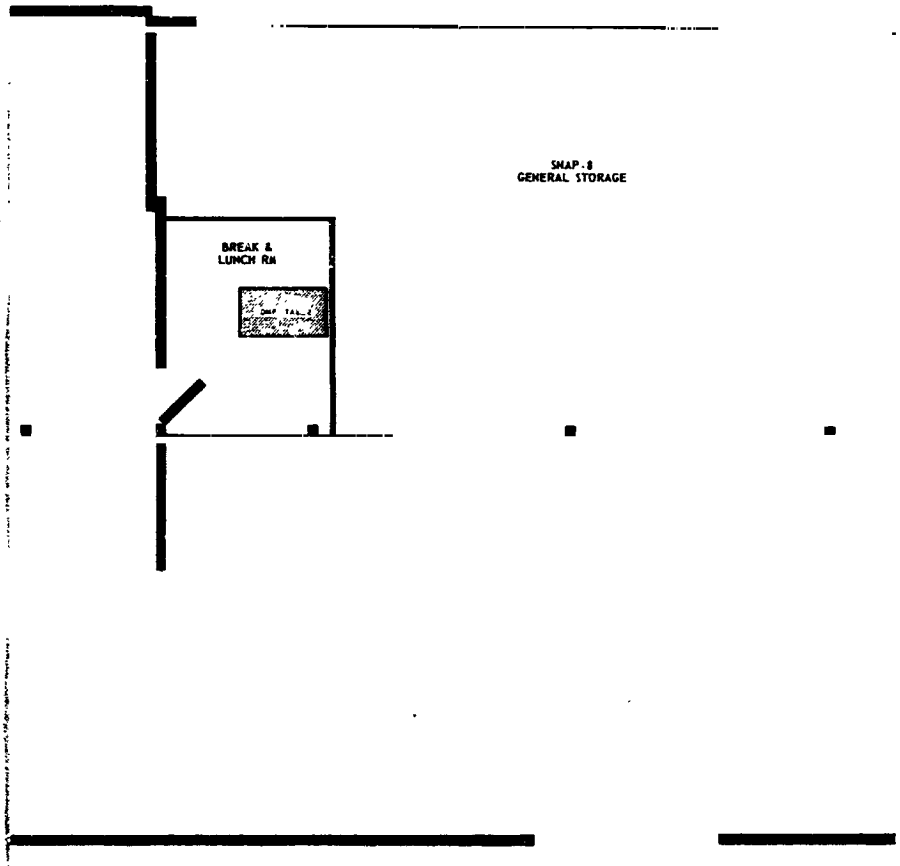

Clean Assembly and Overhaul Facility
SNAP-8 Program

Figure 87

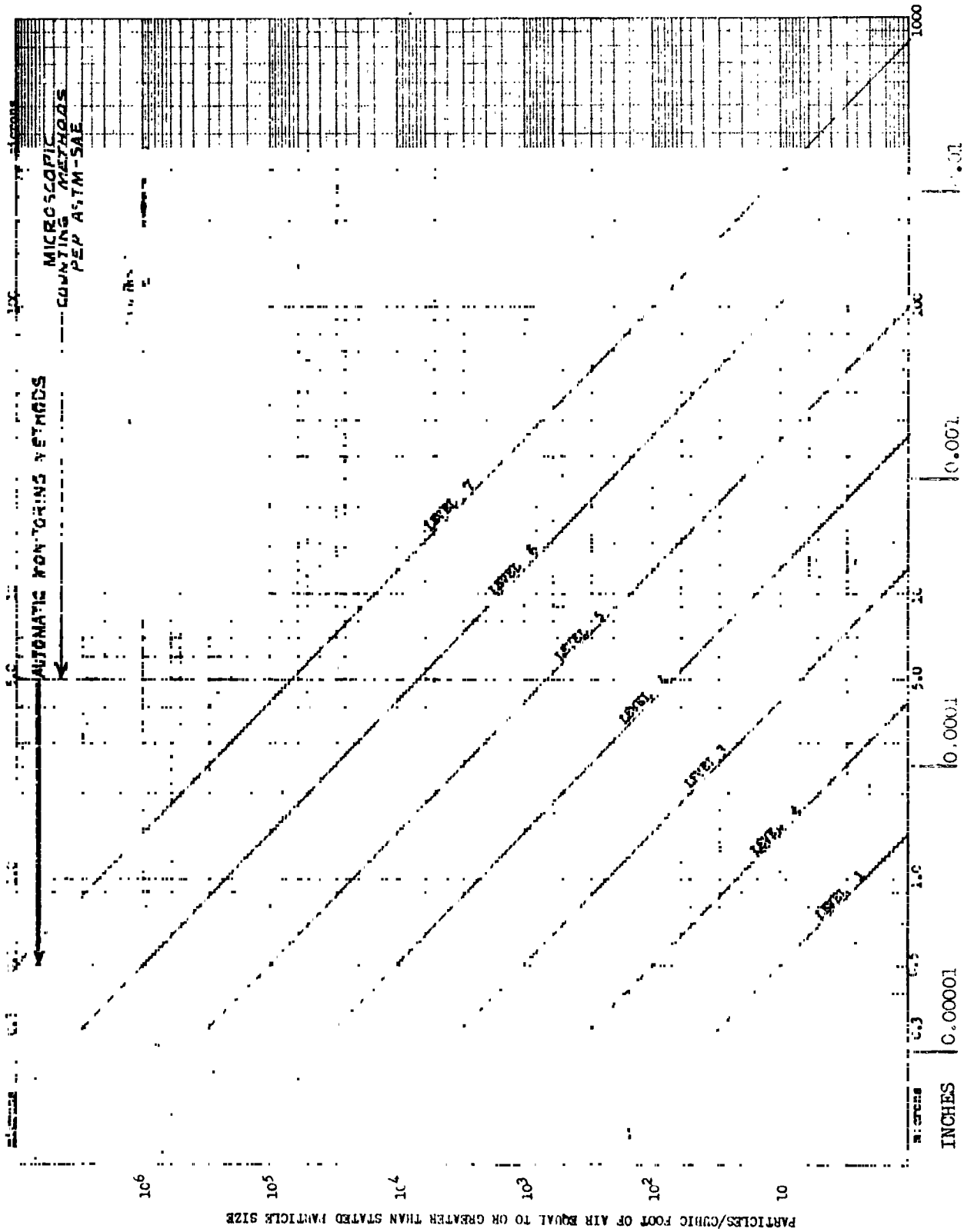

Particle Size Distribution and Cleanliness Levels

Figure 88

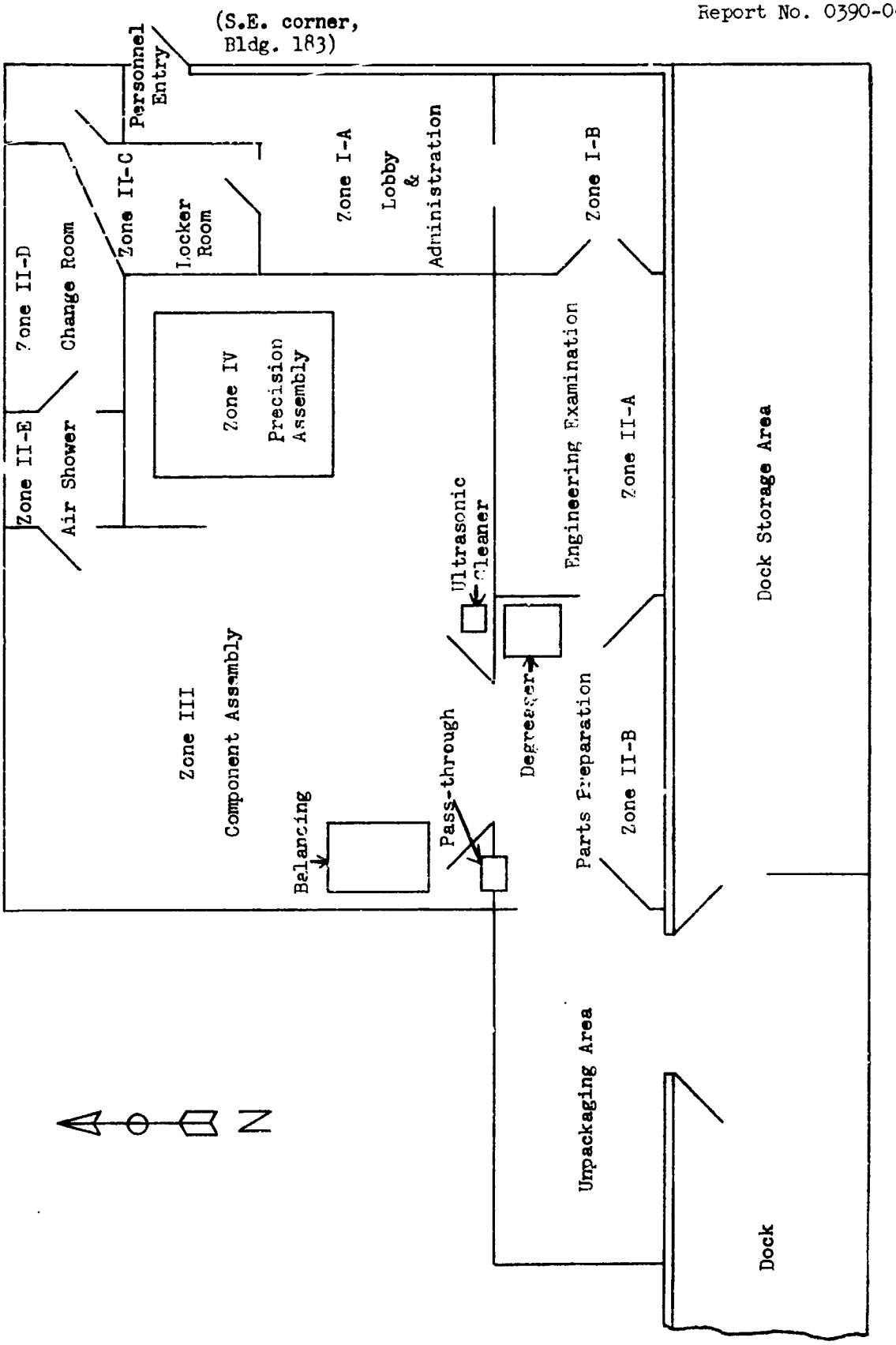

SNAP-8 Interim Clean Room

Figure 89